

Electronic Thesis and Dissertation Repository

1-21-2022 12:00 AM

Mechanisms of Diapause and Cold Tolerance in the Colorado Potato Beetle

Jacqueline E. Lebenzon, *The University of Western Ontario*

Supervisor: Sinclair, Brent J., *The University of Western Ontario*

A thesis submitted in partial fulfillment of the requirements for the Doctor of Philosophy degree in Biology

© Jacqueline E. Lebenzon 2022

Follow this and additional works at: <https://ir.lib.uwo.ca/etd>



Part of the [Comparative and Evolutionary Physiology Commons](#), and the [Systems and Integrative Physiology Commons](#)

Recommended Citation

Lebenzon, Jacqueline E., "Mechanisms of Diapause and Cold Tolerance in the Colorado Potato Beetle" (2022). *Electronic Thesis and Dissertation Repository*. 8363.
<https://ir.lib.uwo.ca/etd/8363>

This Dissertation/Thesis is brought to you for free and open access by Scholarship@Western. It has been accepted for inclusion in Electronic Thesis and Dissertation Repository by an authorized administrator of Scholarship@Western. For more information, please contact wlsadmin@uwo.ca.

Abstract

Many temperate insects enter diapause (a state of dormancy) and enhance their cold tolerance to survive the winter. During diapause, the Colorado potato beetle (CPB, *Leptinotarsa decemlineata*, Coleoptera: Chrysomelidae) stops developing, lowers its metabolism, and changes its physiology to avoid freezing. The extent to which diapause confers cold tolerance in CPB is currently unknown. In my thesis, I used CPB to improve our understanding of the mechanisms underlying metabolic suppression during diapause and cellular protection at sub-zero temperatures in insects. First, I used RNA-sequencing (RNA-seq) to compare gene expression in two metabolically important tissues (the fat body and flight muscle) of diapausing and non-diapausing CPB, and then generated testable hypotheses about diapause in CPB. Colorado potato beetles differentially modulate their fat body and flight muscle transcriptomes during diapause; fat body plays a larger role in driving hypoxia- and immune-related processes during diapause, whereas processes mediating proteostasis and mitochondrial metabolism are more important in the flight muscle. Next, I tested the hypothesis that flight muscle mitochondria modulate energy metabolism in diapausing CPB. Indeed, low metabolic rates coincided with a reduction in flight muscle mitochondrial function and density, increased expression of *Parkin* (a mitophagy-related transcript), and presence of autophagic structures inside flight muscle cells. Further, knocking down *Parkin* with RNA interference partially restored mitochondrial density and whole-animal metabolic rate suggesting that Parkin-mediated mitophagy drives metabolic suppression during CPB diapause. In anticipation of emergence from diapause, beetles reversed this mitophagy and increase mitochondrial biogenesis to re-grow their mitochondria. Finally, I used RNA-seq to explore the mechanisms underlying the acquisition of cold tolerance in diapausing CPB. The major transcriptomic shift associated with the acquisition of cold tolerance is related to chaperone protein-related expression, and cold-tolerant beetles activate the chaperone response to a greater extent than less cold-tolerant diapausing counterparts. Further, cold-tolerant beetles potentially have a greater capacity for chaperone-mediated protein repair. Together, these studies contribute to an updated framework for insect diapause and cold tolerance and improve our understanding of the mechanisms insects use to survive the winter.

Keywords

Metabolic suppression, mitochondria, insects, thermal biology, dormancy, RNAi, transcriptome, chaperone, heat shock protein

Summary for Lay Audience

Winter is a hostile season for insects because resources are scarce and freezing temperatures persist for months at a time. Many temperate insects spend most of their lives overwintering where they must survive these harsh conditions. During the winter, Colorado potato beetles (CPB) become dormant (enter diapause), where they stop developing, lower their metabolism to save energy, and enhance their ability to survive freezing temperatures. In my thesis, I used CPB to explore how overwintering insects are able to lower their metabolism and protect their tissues and cells from freezing temperatures during winter. First, I investigated patterns of gene expression during diapause in CPB in two tissues that are important for metabolism over the winter, their fat body (analogous to mammalian liver), and flight muscle. Gene expression profiles differed in each tissue; fat body expressed more genes related to surviving low oxygen environments and enhancing immunity, whereas flight muscle expressed more genes related to protein protection and mitochondrial metabolism. Next, I explored how flight muscle mitochondrial metabolism is important for diapause in overwintering CPB, and whether CPB change mitochondrial function to achieve a low metabolism over the winter. I showed that CPB do not just alter flight muscle mitochondrial metabolism to achieve a low metabolism but degrade most of their mitochondria altogether. I also showed that CPB can re-grow their flight muscle mitochondria without any cues, and in anticipation of the end of diapause. Finally, I investigated how gene expression changes in the fat body of CPB that have an enhanced ability to survive freezing temperatures (cold-tolerant CPB). Although I expected to find many genes differentially expressed in cold-tolerant CPB, I found a small number of genes responsible for cold tolerance, which were all related to the process of cellular protection by chaperone proteins. Further, cold-tolerant CPB had fewer damaged proteins in their fat body compared to less cold-tolerant CPB, which suggests that they are able to better repair proteins using the cellular chaperone response. Taken together, my thesis provides novel insights into how insects regulate their metabolism over the winter and protect their cells in the cold.

Co-Authorship Statement

Chapter 1 & Chapter 5 will be combined and prepared as a review article about the overwintering physiology of the Colorado potato beetle. I will be the first author, and co-author Brent Sinclair will contribute to writing the review article.

Chapter 2 was published in *Comparative Biochemistry and Physiology D: Genomics and Proteomics*. I am the first author, co-author Alex Torson developed the pipeline for transcriptome assembly and contributed to data visualization, and co-author Brent Sinclair contributed to experimental design and writing of the manuscript.

Chapter 3 was submitted to *Proceedings of the National Academy of Sciences of the U.S.A.* I am the first author, and Peter Denezis (PWD), Lamees Mohammad (LM), Katherine Mathers (KEM), Kurtis Turnbull (KFT), James Staples (JFS), and Brent Sinclair (BJS) are co-authors. PWD contributed to RNAi experiments, LM contributed to qPCR experiments, KM performed citrate synthase enzyme assays, KFT contributed to respirometry experiments, and JFS and BJS contributed to experimental design and writing of the manuscript.

Chapter 4 is in preparation for submission. I will be the first author with Alex Torson and Brent Sinclair as co-authors. Alex Torson developed the pipeline for transcriptome assembly and contributed to data visualization, and BJS contributed to experimental design and writing of the manuscript.

Acknowledgments

To Mom, Dad and Cara – for your love and support through grades 1-23

I would like to begin by thanking my supervisor Brent Sinclair. I would not be where I am today without your guidance, mentorship and friendship. Thank you for seeing something in me as a bright-eyed undergraduate student, trusting my potential, and lifting me up to be the best scientist I could possibly be. I will be forever grateful that you let me carve my own research path and pushed me to explore new ideas out of my (and your!) comfort zone. Your fierce mentoring and unwavering support do not go unnoticed. Thank you for creating a safe space where students from all backgrounds can succeed, and creating a lab environment that fosters scientific creativity, thrives on good humor, and successfully trains top notch scientists.

The most memorable part of my PhD has been the opportunity to learn and grow with my outstanding peers in the Sinclair Lab. From gall hunts to gongshows, I've had the greatest time with you all. To Jantina Toxopeus and Susan Anthony – You both exemplify what it means to be a successful scientist and I thank you for your invaluable support inside and outside of the lab. To Alex Torson and Kurtis Turnbull – Thank you for your shared appreciation of a good lab playlist, willingness to drive across the continent for science and fried food, and for the infinite amount of emotional and intellectual support you both provided me throughout my PhD. To Alex – Thanks for your support with my RNA-seq projects. With your teaching, wisdom, and weekly bioinformatics beers I can now proudly call myself somewhat of a bioinformatician. To Lamees Mohammad and Peter Denezis – Thanks for being dream mentees, sometimes laughing at my jokes, and always keeping me on my toes. To Meghan Duell and Yanira Jimenez-Padilla – Thank you for your friendship, encouragement, and always inspiring chats about life. To Alyssa Stephens, Tania Naseer, and Stefane Saruhashi – Thank you for your comradery as we navigated our way through an unprecedented pandemic. To other lab mates that made my time in the Sinclair lab so wonderful (and there are many because I couldn't seem to shake this place); John Ciancio, Laura Ferguson, Zander McKinnon, Lauren Des Marteaux, Sirpa Kaunisto, Raine Kortet, Adam Smith, Aisa Kuper-Psenicnik, Joanne Tang, Kevin Ong, Claire Baragar, Nasim

Amiresmaeili, Zoe Klein, Ayush Namboothiri, Arteen Torabi-Marashi, Aaron Mayordomo and Sylvia Chong, thank you!

I was lucky to have a very supportive and active advisory committee during my PhD. To Cam Donly, thank you for your molecular expertise and always wise advice about my project. To Jim Staples, thank you for your teaching both inside and outside of the lab, and for letting me use your equipment to extend the scope of my project. Your constant enthusiasm and intellectual support helped me create something far more impactful than I ever could have imagined. I also want to thank other faculty in the Department of Biology who often provided useful feedback, resources, advice (about my project and life), and smiles in the hallways of BGS; Chris Guglielmo (especially for the generous use of your rotor gene thermocycler), Natasha Mhatre, Dani Way, and Jeremy McNeil.

I could not have completed my thesis experiments without the help of a small army of undergraduate volunteers and work study students (“beetle sitters”) that helped keep my CPB populations happy and healthy. Special thanks to Aaron Hoang, Joseph Atem, Femi Adewusi, Ose Akioyamen, Ahmad Butt, Nicole Martin-Kenny, Michelle Lim, Huda Al-Sharafi, Ciji Robinson, and Danya Nguyen.

A lot of life happens in your 20s (and even more when you pursue a PhD in your 20s) and I’m grateful I had the opportunity to spend these years in grad school with a group of exceptional friends by my side. To Carlie Muir and Tim Hain – Thanks for making me laugh, supporting me through my ups and downs, and always keeping me up to date on my reality TV. To the Staples lab (Kate Mathers, Brynne Duffy, Soren Coulson and Amalie Hutchinson) – Thanks for indulging me in all of my mitochondria fantasies and providing moral support every step of the way. To my fellow BGS 2035 office mates (Joe Stinziano, Andre Duarte, Eric Dusenge, Vi Bui, and Primrose Anthony) – Thanks for keeping a smile on my face and fostering such a fun everyday work environment. Many other people that made my time in grad school so fulfilling include Lauren Rowsey, Kaylen Brzezinski, Tian Wu, Justin Croft, Katie Woolfson, Emma Churchman, Brad Bork, Kaitlyn Ludba, and Ricki Lovett. To all of you - I will always cherish our afternoons at the grad club, trivia nights, holly jolly biology parties, conference reunions, and the countless memories we made outside of the lab.

To my best friends outside of the grad school bubble – Meghan Powell, Amanda Fitzsimmons and Melissa Florence. Thanks for your support throughout undergrad and grad school and listening to my endless tales of crickets and beetles. I couldn't have asked for a better support system and personal team of cheerleaders.

I had the opportunity to be a member of several professional societies throughout my PhD. Thanks to the Entomological Society of Ontario, Society for Integrative and Comparative Biology and Canadian Society of Zoologists for lifting me up, creating useful networking opportunities, and for being my happy places in the scientific community.

I would also like to thank the Natural Sciences and Engineering Research Council (NSERC), Ontario Government, Company of Biologists, Genome Canada (especially the Biosurveillance of Alien Forest Enemies, BioSAFE, project), and Department of Biology at Western who all provided me with funding that helped support me through grad school and provided the resources I needed to complete experiments for my thesis.

My time in grad school was not only enriched by my lab, advisors and peers, but by several groups of hard-working staff in the Department of Biology at Western. To the administrative staff (Arzie Chant, Carol Curtis, Diane Gauley, Hillary Bain and Sherri Fenton) – Thanks for keeping this ship afloat and working tirelessly to make sure students like myself stay organized and happy. To the greenhouse staff (Aixia Wang and Kyle Doward) – Thanks for keeping my potato plants alive and maintaining greenhouse space that was crucial for the success of my experiments. To the Biotron microscopy staff (Karen Nygard, Reza Khazae and Richard Gardiner) – Thanks for your patience, top notch training, and sound advice on all things microscopy.

Last but certainly not least, I would like to thank my family.

To my partner Tyse – You made the last 2 marathon years of my PhD feel like a walk in the park. Thank you for cheering me on through lab days (even if that meant pretending to understand what a western blot was and why it did not work), keeping me well fed and relaxed during the later stages of my writing, being the voice of reason when I doubted myself, and most of all, thank you for your pride and encouragement. It truly means the world to me and I couldn't have finished my PhD without you by my side.

To my Mom (Darlene), Dad (Dan), and sister (Cara) – Thank you for fostering my love of science from an early age and encouraging me to pursue a career that I love and can be proud of. I am forever grateful for your steadfast support, without which I never could have finished 23 years of schooling. Even from across the country (and sometimes world!), your cheers and motivation helped push me through every stage of my PhD. You’ve always reassured me that “it will get done”, whether it was a high school essay, undergrad midterm, or tricky thesis experiment. I can finally say, that with your love and encouragement, I did indeed “get it done”.

Table of Contents

Abstract.....	ii
Summary for Lay Audience.....	iv
Co-Authorship Statement.....	v
Acknowledgments.....	vi
Table of Contents.....	x
List of Tables.....	xii
List of Figures.....	xiv
List of Abbreviations.....	xvii
List of Appendices.....	xix
Chapter 1.....	1
1 General Introduction.....	1
1.1 Physiology of insect diapause.....	3
1.2 Physiology of insect cold tolerance.....	10
1.3 Relationship between insect diapause and cold tolerance.....	15
1.4 Biology of the Colorado potato beetle.....	17
1.5 Thesis Experimental Design, Objectives and Overview.....	20
1.6 References.....	24
Chapter 2.....	37
2 Diapause differentially modulates the transcriptomes of fat body and flight muscle in the Colorado potato beetle.....	37
2.1 Introduction.....	37
2.2 Materials and Methods.....	42
2.3 Results & Discussion.....	45
2.4 Conclusions.....	68
2.5 References.....	70

Chapter 3.....	79
3 Reversible mitophagy drives metabolic suppression in a diapausing beetle	79
3.1 Introduction.....	79
3.2 Materials and Methods.....	81
3.3 Results & Discussion	89
3.4 Conclusions.....	101
3.5 References.....	102
Chapter 4.....	108
4 Activation of the chaperone response improves cold tolerance in diapausing Colorado potato beetles.....	108
4.1 Introduction.....	108
4.2 Materials and Methods.....	111
4.3 Results.....	118
4.4 Discussion.....	127
4.5 Conclusions and future directions.....	131
4.6 References.....	133
Chapter 5.....	137
5 General discussion	137
5.1 An updated framework for insect diapause: The role of mitochondrial homeostasis in metabolic suppression.....	137
5.2 An updated framework for insect cold tolerance: Defining the functional role of the chaperone response	151
5.3 Disentangling diapause from cold tolerance in CPB	155
5.4 Concluding remarks	157
5.5 References.....	159
Appendices.....	164
Curriculum Vitae	201

List of Tables

Table 2.1. Differential expression of selected developmental arrest-related transcripts in fat body (FB) and flight muscle (FM) tissues of <i>L. decemlineata</i> during diapause.....	53
Table 2.2. Differential expression of selected lipid metabolism-associated transcripts in fat body (FB) and flight muscle (FM) tissue of <i>L. decemlineata</i> during diapause.	57
Table 2.3. Differential expression of selected energy metabolism-associated transcripts in fat body (FB) and flight muscle (FM) tissue of <i>L. decemlineata</i> during diapause.	58
Table 2.4. Differential expression of selected stress tolerance-associated transcripts in fat body (FB) and flight muscle (FM) tissue of <i>L. decemlineata</i> during diapause.	60
Table 2.5. Differential expression of selected transcripts in fat body (FB) and flight muscle (FM) involved in gene regulatory processes in <i>L. decemlineata</i>	63
Table 4.1. Summary of the paired-end read libraries mapped to the <i>L. decemlineata</i> reference genome.....	120
Table 4.2. Increased expression of chaperone response, signaling, and transcriptional regulation-related transcripts in the fat body of cold-tolerant <i>L. decemlineata</i>	123
Table 4.3. All transcripts that significantly decreased in abundance in cold-tolerant <i>L. decemlineata</i> compared to diapause <i>L. decemlineata</i>	124
Table 4.4. Statistical results from a two-way ANOVA comparing protein ubiquitination in diapausing and cold-tolerant Colorado potato beetles with no prior cold shock, a cold shock, and after recovery from a cold shock.....	126
Table 5.1. Experiments that test hypothesized mechanisms underlying cell cycle arrest, changes in immunity, and antioxidant capacity in diapausing Colorado potato beetles.	150
Table A1. Summary of the paired-end read libraries mapped to the <i>Leptinotarsa decemlineata</i> reference genome.....	165

Table A2. Differential expression of selected insulin signaling-related transcripts in body (FB) and flight muscle (FM) tissue of <i>L. decemlineata</i> during diapause.	166
Table A3. Differential expression of selected juvenile hormone metabolism-related transcripts in body (FB) and flight muscle (FM) tissue of <i>L. decemlineata</i> during diapause.	168
Table A4. Differential expression of selected cell cycle arrest-related transcripts in body (FB) and flight muscle (FM) tissue of <i>L. decemlineata</i> during diapause.	170
Table A5. Differential expression of selected lipid metabolism-related transcripts in body (FB) and flight muscle (FM) tissue of <i>L. decemlineata</i> during diapause.	174
Table A6. Differential expression of selected energy metabolism-related transcripts in body (FB) and flight muscle (FM) tissue of <i>L. decemlineata</i> during diapause.	176
Table A7. Differential expression of selected stress tolerance-related transcripts in body (FB) and flight muscle (FM) tissue of <i>L. decemlineata</i> during diapause.	181
Table A8. Differential expression of selected transposable element-related transcripts in body (FB) and flight muscle (FM) tissue of <i>L. decemlineata</i> during diapause.	189
Table B1. Forward and reverse primer sequences for all genes of interest from Chapter 3 for <i>Leptinotarsa decemlineata</i>	191
Table B2. Summary of statistics for all relevant figures in Chapter 3.	192

List of Figures

Figure 1.1. Experimental design of Chapters 2-4.	23
Figure 2.1. Schematic of the predictions I make based on hypotheses of how gene expression will change during diapause in fat body and flight muscle of diapausing Colorado potato beetles.	41
Figure 2.2. Differentially expressed transcripts in (A) fat body and (B) flight muscle from diapausing beetles, compared to non-diapausing <i>L. decemlineata</i>	47
Figure 2.3. Tissue-specific patterns of gene expression in diapausing and non-diapausing <i>L. decemlineata</i>	48
Figure 2.4. Gene Ontology (GO) terms enriched in transcripts that were increased (A) and (B) decreased in abundance in both fat body and flight muscle during diapause in <i>L. decemlineata</i>	49
Figure 2.5. Gene Ontology (GO) terms enriched in transcripts that (A) increased and (B) decreased in abundance in the fat body during diapause in <i>L. decemlineata</i>	65
Figure 2.6. Gene Ontology (GO) terms enriched among transcripts that (A) increased and (B) decreased in abundance in the flight muscle during diapause in <i>L. decemlineata</i>	66
Figure 2.7. Synthesis of hypotheses on biological processes associated with diapause phenotypes in the Colorado potato beetle I evaluated (A,B,C) and generated (D,E,F).	69
Figure 3.1. Colorado potato beetles suppress their whole animal metabolic rates and mitochondrial respiration rates in the same pattern during diapause.	90
Figure 3.2. Functional mitochondria are absent from Colorado potato beetle flight muscle during diapause, but beetles reverse this mitochondrial breakdown upon diapause emergence.	92

Figure 3.3. Colorado potato beetles increase the abundance of mitophagy-related transcripts during diapause and increase the abundance of mitochondrial biogenesis-related transcripts in anticipation of emergence from diapause.	95
Figure 3.4. RNA interference knockdown of <i>Parkin</i> transcript and protein abundance in flight muscle of diapausing Colorado potato beetles.....	96
Figure 3.5. Knocking down <i>Parkin</i> transcript abundance increases flight muscle citrate synthase activity and mitochondria density.	98
Figure 3.6. Knocking down <i>Parkin</i> transcript abundance partially recovers whole animal metabolic rate, but not mitochondrial respiration rates.	99
Figure 4.1. Inducing diapausing and cold tolerance in the Colorado potato beetle.....	113
Figure 4.2. Survival at sub-zero temperatures, hemolymph osmolality, and supercooling points of control, diapausing and cold-tolerant Colorado potato beetles.....	119
Figure 4.3. Differentially expressed transcripts in the fat body of cold-tolerant Colorado potato beetles compared to diapausing Colorado potato beetles.	122
Figure 4.4. (A) Gene Ontology enrichment and (B) KEGG pathway mapping of transcripts that increased in cold-tolerant Colorado potato beetles.	125
Figure 4.5. Protein ubiquitination in diapausing and cold-tolerant Colorado potato beetles after a cold shock at $-10\text{ }^{\circ}\text{C}$ and recovery from that cold shock at $21\text{ }^{\circ}\text{C}$	127
Figure 5.1. Conceptual model of mitophagy-mediated metabolic suppression and reversal of this suppression during diapause in the Colorado potato beetle.	147
Figure 5.2. Hypothesized regulation of mitochondrial mitophagy and mitochondrial biogenesis by Parkin and AMPK in flight muscle of diapausing Colorado potato beetles. .	148
Figure 5.3. Schematic of protein protection by heat shock proteins in cold-tolerant Colorado potato beetles.	154

Figure B1. Representative respirometry traces from non-diapausing (A) and diapausing (B) Colorado potato beetles.....	193
Figure B2. Representative high-resolution respirometry traces from (A) non-diapausing (5.39 mg of tissue) and (B-C) diapausing (2.34 mg of tissue) flight muscle showing O ₂ consumption rates (blue line) of permeabilized tissue and O ₂ concentrations (red line) in the oxygraph chamber.....	194
Figure B3. State 3 (colored bars) and maximal uncoupled (black) mitochondrial respiration rates of Colorado potato beetles entering diapause (3-6), in diapause (9-15), and emerged from diapause.....	196
Figure B4. Relative normalized transcript abundance of (A) mTOR and (B) FOXO in flight muscle of control Colorado potato beetles, and beetles exposed to three, six, nine, 12, 15, and 20 weeks of diapause-inducing conditions.	197
Figure B5. (A) Successful synthesis of parkin and GFP dsRNA products at the expected size of 484 and 411 bp, respectively and (B) verification of <i>Parkin</i> transcript knockdown in flight muscle of Colorado potato beetles three- and five-days post-dsRNA injection.....	198
Figure B6. Western blot composite image of colorimetric protein ladder and Parkin protein bands confirming protein knockdown of Parkin in diapausing Colorado potato beetle flight muscle.	199
Figure C1. Western blots for data in Figure 4.5.	200

List of Abbreviations

- ADP – adenosine diphosphate
- AMP – adenosine monophosphate
- AMPK – adenosine monophosphate-activated kinase
- ANOVA – analysis of variance
- ANCOVA – analysis of covariance
- ATG – autophagy related protein
- ATP – adenosine triphosphate
- BIOPS – biopsy preservation solution
- BLAST – basic local alignment search tool
- bp – base pair
- BSA – bovine serum albumin
- CCCP – carbonyl cyanide m-chlorophenyl hydrazone
- CDK1 – cyclin dependent kinase 1
- cDNA – complementary deoxyribonucleic acid
- CPB – Colorado potato beetle
- Ct – cycle threshold
- DAPI – 4',6-diamidino-2-phenylindole
- ddH₂O – distilled, deionized water
- DNA – deoxyribonucleic acid
- DTT - dithiothreitol
- DTNB – 5,5'-dithiobis-(2-nitrobenzoid acid)
- EDTA – ethylenediaminetetraacetic acid
- EF1 α – eukaryotic translation elongation factor 1 alpha
- EGLP – entomoglyceroporin
- EGTA – ethylene glycol-bis (β -aminoethyl ether)-N,N,N',N'-tetraacetic acid
- FOXO – fork head box transcription factor
- FPKM – fragments per kilobase of transcript per million mapped reads
- FTR – fluctuating thermal regime
- dsRNA – double stranded ribonucleic acid
- GFP – green fluorescent protein
- GO – gene ontology

HEPES – 2-[4-(2-hydroxyethyl)piperazin-1-yl]ethanesulfonic acid
HSP – heat shock protein
JH – juvenile hormone
KEGG – Kyoto encyclopedia of genes and genomes
K-MES – 2-(N-Morpholino)ethanesulfonic acid potassium salt
L:D – hours of light:dark
LEA – late embryogenesis abundant
MiR05 – mitochondrial respiration buffer
mRNA – messenger ribonucleic acid
NRF1 – nuclear respiratory factor 1
PARIS – parkin interacting substrate
PCR – polymerase chain reaction
PGC1 α – peroxisome proliferator-activated receptor gamma co-activator 1-alpha
PINK1 – PTEN-induced kinase 1
PMSF – phenylmethylsulfonyl fluoride
PVDF – polyvinylidene fluoride
RNA – ribonucleic acid
RNAi – ribonucleic acid interference
ROS – reactive oxygen species
RT-qPCR – reverse transcriptase quantitative polymerase chain reaction
SCP – supercooling point
SDS – sodium dodecyl sulfate
ssRNA – single stranded ribonucleic acid
T_A – annealing temperature
TBS-T – tris buffered saline with Tween 20
TBP1 – TATA-box binding protein
TCA – tricarboxylic acid
TIM16 – mitochondrial import inner membrane translocase protein 16
Tris – trisaminomethane
UCP4 – uncoupling protein 4
 $\dot{V}CO_2$ – rate of CO₂ production

List of Appendices

Appendix A: Chapter 2 Supplementary Material	164
Appendix B: Chapter 3 Supplementary Material	191
Appendix C: Chapter 4 Supplementary Material	200

Chapter 1

1 General Introduction

Winter can be a hostile season for any organism. During winter, resources are scarce, most biologically available water is frozen, and temperatures are below most physiological thresholds for development for months at a time (Williams et al., 2015). In response to these challenges, animals that live in temperate environments have adapted complex life history strategies to survive winter. For example, many animals seek out or create microhabitats to mitigate fluctuations in temperatures (Baust, 1976) and to avoid predation (Garnham et al., 2015). Others escape winter altogether by seasonally migrating to warmer climates. Overwintering animals often enter a state of dormancy and adjust their physiology to maintain energy homeostasis during long periods of starvation (Wilsterman et al., 2021). During these dormant periods, animals will also modify their physiology to increase their capacity to survive at sub-zero temperatures (Zachariassen, 1985). This is especially important for ectotherms such as insects, whose body temperatures mirrors that of their environment.

Ectothermic insects living in temperate environments may spend over half their lives overwintering. Insects make up c. 75 % of all species, and are responsible for many important ecosystem services, including (but not limited to) pollination, seed dispersal, and nutrient cycling (Belovsky and Slade, 2000; Rader et al., 2016; Walters et al., 2006). Thus, their survival through harsh and unpredictable winter seasons is necessary to maintain balanced temperate ecosystems (Crespo-Pérez et al., 2020; Walters et al., 2006).

Several environmental challenges threaten insects during winter. Insects must endure several months without access to food and water (Hahn and Denlinger, 2011; Marshall et al., 2020; Sinclair, 2015). Low temperatures during winter will limit ectotherm movement, growth, and development (Schou et al., 2017). Cold also compromises organismal function by driving a loss of ion balance between important tissues and the hemolymph (Bayley et al., 2018; Lebenzon et al., 2020; MacMillan et al., 2015) and causing direct cold-induced damage to tissues and cells (Kukal et al., 1989; Toxopeus et al., 2019a). Furthermore, freezing at

temperatures below their supercooling point (SCP; the temperature at which body water turns to ice) can be lethal (Zachariassen, 1985).

In response to these winter challenges, insects have evolved strategies to modify their physiology and survive until spring. Insects often enter diapause in anticipation of starvation and energy drain during the winter (Hahn and Denlinger, 2007). Diapause is a pre-programmed state of dormancy characterized by developmental arrest, a low metabolic rate, and increased tolerance to general stressors such as desiccation, hypoxia if they overwinter in underground microhabitats, and low temperatures (Košťál, 2006). In addition to entering diapause, many insects have evolved the plasticity to seasonally increase their cold tolerance. In anticipation of winter, insects change their physiology to either avoid or tolerate freezing of their body fluids and survive otherwise lethal sub-zero temperatures (Lee and Denlinger, 1991).

Much of our understanding of diapause comes from studies that investigate the cues that initiate diapause, and the regulation of the shift from normal development towards diapause. In particular, there has been a heavy focus on understanding how insects perceive decreased daylength in advance of the winter, how these changes in photoperiod drive changes in developmental hormones, and consequently how changes in developmental hormones regulate entrance into diapause (see Denlinger et al., 2004). Over the past c. 30 years, advances in molecular methods (such as gene expression, ‘omics-based analyses, and genetic manipulation *via* RNA interference) have led to substantial progress in understanding the molecular basis of diapause initiation, especially in a select group of model systems (*e.g.*, adult *Culex pipiens*, Denlinger and Armbruster, 2014; pupal *Sarcophaga crassipalpis*, Lee and Denlinger 1985). However, there has been less focus on the mechanisms that contribute to the maintenance of physiological processes once insects are already in a diapause state, despite the range of molecular and physiological tools available.

Our understanding of insect cold tolerance has come from many studies that focus on 1) the incidence of cold tolerance strategies among insects and 2) whole organism temperature limits and levels of cold tolerance. Although these types of descriptive studies are important for understanding how temperatures set range limits in insects, such a broad, surface level

approach leaves a large gap in our understanding of the underlying physiology and molecular biology of cold tolerance. Furthermore, diapause and cold tolerance are often hard to tease apart and the extent to which diapause confers cold tolerance remains unknown. Some studies consider that overwintering insects enter diapause and simultaneously become cold-tolerant (*e.g.*, Michaud and Denlinger, 2007; Štětina et al., 2018), however the majority of studies do not. Thus, to tease apart which mechanisms are important for diapause, which are necessary for cold tolerance, and which are shared between the two, we must study diapause and cold tolerance in insects where these two strategies co-occur, and be able to experimentally induce diapause and cold tolerance independent of one another.

In my thesis, I take an integrative approach to further our understanding of insect diapause and cold tolerance. I use a temperate insect, the Colorado potato beetle (CPB; *Leptinotarsa decemlineata* Coleoptera: Chrysomelidae, Say), whose overwintering biology has been extensively studied for over 100 years (de Kort, 1990) yet we still know relatively little about the physiological and molecular mechanisms underlying their winter survival. Diapause and cold tolerance co-occur in overwintering CPB, and I can experimentally induce diapause and cold tolerance, which makes them an ideal system for developing an understanding of the physiological and molecular underpinnings of diapause and cold tolerance (Figure 1.1). In Chapter 2, I use RNA-seq to explore which genes, proteins, and biological processes drive diapause in CPB. I use these data to evaluate hypotheses in the latest diapause literature and form new hypotheses about the mechanisms underlying diapause in CPB. One of these hypotheses is that flight muscle mitochondria modulate energy metabolism and play a role in driving metabolic suppression (a hallmark phenotype of diapausing insects) in CPB. I test this hypothesis and demonstrate a novel mechanism for metabolic suppression in diapausing insects in Chapter 3. Finally, in Chapter 4, I use RNA-seq to explore the mechanisms underlying the acquisition of cold tolerance in CPB and determine which are responsible for driving cold tolerance independent of diapause.

1.1 Physiology of insect diapause

Diapause is a pre-programmed life history strategy that allows insects to survive harsh environments (Košťál, 2006). Diapause is used by many insects, but there is substantial

variation in diapause among species as it has likely evolved multiple times in insects (Tauber and Tauber, 1976). For example, diapause can be obligate, where regardless of environmental conditions, each individual in a generation will enter diapause (*e.g.*, *Cecropia* moths; Mansingh and Smallman, 1966). Diapause can also be facultative, where environmental conditions directly determine whether individuals in a generation enter diapause (*e.g.*, *Rhagoletis pomonella* pupae; Feder et al., 2010). Diapause can occur in any stage of insect development, and during any season. For example, beet armyworms (*Spodoptera exigua*) diapause as pupae in the winter (He et al., 2011), alfalfa weevils (*Hypera posticai*) diapause as adults in the summer (Tombes, 1966), and *Lestes sponsa* damselflies diapause both as eggs in the winter (Sawchyn and Church, 1973) and as adults in the summer (Masaki, 1980).

1.1.1 Physiological stages of insect diapause

Although diapause is a type of dormancy, it is still a dynamic process during which insects progress through defined physiological stages. Towards the end of summer and start of autumn, short photoperiods cue entrance into diapause for many species of adult temperate insects (Saunders, 2019). These changes in photoperiodic stimuli re-route direct development towards diapause (Košťál, 2006). Once insects perceive a change in photoperiod, changes in developmental hormones, such as juvenile hormone (JH), stimulate the first physiological stage of diapause, “diapause initiation”. In adult diapausing insects, a downregulation of insulin signaling after exposure to a short photoperiod leads to the cessation of juvenile hormone (JH) production by the *corpora allata*, and ultimately stimulates diapause initiation (Denlinger et al., 2004). Once diapause is initiated, adult insects halt reproductive development, many feed voraciously to increase their lipid energy stores, and slowly start to lower their metabolic rate (Hahn and Denlinger, 2007; Košťál, 2006; Sinclair, 2015; Sinclair and Marshall, 2018). During diapause initiation, insects also seek specific microhabitats, and burrow into the soil (*e.g.*, *Leptinotarsa decemlineata*; Piironen et al., 2011) or underneath tree bark (*e.g.*, *Anoplophora glabripennis*; Torson et al., 2021), that buffer the conditions they experience throughout winter.

Insects enter their “diapause maintenance” stage upon reaching maximal metabolic suppression (Košťál, 2006). During this stage, insects are more stress-tolerant than their non-diapausing counterparts as they are experiencing the worst conditions of winter. Towards the end of diapause maintenance, insects will slowly increase their sensitivity to environmental conditions in anticipation of spring (Košťál, 2006). Diapause is terminated after a specific amount of time, or after exposure to a terminating environmental condition (*i.e.*, chilling; Dong et al., 2013). The exact mechanisms driving this termination are still largely unknown, especially since diapause termination manifests differently depending on the species, life stage, and whether or not diapause is obligate or facultative (Leather et al., 1995; Tauber and Tauber, 1976). Post-diapause insects often remain quiescent, and do not resume their direct development until permissive conditions return (Poelchau et al., 2013).

Most research on the physiology of adult diapausing insects to date has focused on the upstream regulation of diapause initiation (Denlinger et al., 2004), but we know comparatively little about the mechanisms leading to changes in physiology during diapause maintenance. Although metabolic rates are lowest during diapause maintenance, insects must still maintain basal metabolism and perform biological processes that protect them from the environmental challenges of winter. Thus, focusing on developing a better understanding of diapause maintenance, and the mechanisms associated with physiological changes during maintenance, could help us better understand how diapausing insects survive the winter.

1.1.2 Physiological changes associated with diapause

Diapause is not just a pause in development but is an alternate physiological programme. Thus, insects change their physiology during diapause to achieve two main phenotypes; to maintain energy homeostasis when resources are scarce and increase their tolerance to stressors they will likely encounter during winter.

1.1.2.1 Maintaining energy homeostasis

In preparation for diapause, insects accumulate energy stores as lipids to fuel basal metabolic functions during diapause maintenance (Sinclair and Marshall, 2018). These lipids are synthesized by the fat body during preparation for diapause and stored in lipid droplets inside fat body cells (Li et al., 2019). Diapausing insects have the capacity to accumulate greater

lipid stores than their non-diapausing counterparts and do so by feeding more and re-directing those food resources away from growth and development and towards storage (Hahn and Denlinger, 2011). The propensity to store more lipids is regulated to some extent by reduced insulin and JH signaling during diapause initiation. For example, under non-diapausing conditions in *C. pipiens*, high titres of JH normally inhibit the expression of fork head transcription factors (*i.e.*, *FOXO*). During diapause initiation, decreased insulin signaling and JH levels activate *FOXO*, which stimulates the expression of downstream genes, such as *low-density lipoprotein receptor chaperone* which help drive lipid accumulation (Sim and Denlinger, 2008; Sim et al., 2015). Similarly, in diapause-destined cabbage beetles, a decrease in JH increases the expression of *Fatty acid synthase*, thereby promoting lipid synthesis and storage (Tan et al., 2017).

During diapause, most insects use lipids as their primary source of overwinter fuel (Hahn and Denlinger, 2011). Because insects do not arrest all metabolism during diapause, but rather re-configure physiological processes, some energy is still required to fuel those processes (Košťál, 2006). To mobilize stored lipids, diapausing insects increase the abundance and/or activity of lipolysis enzymes (*e.g.*, lipase) such as in diapausing *Epiblema scudderiana* (Rider et al., 2011). Some diapausing insects primarily use lipids, but also switch to using other substrates at some point during diapause. For example, diapausing *C. pipiens* and spruce budworms (*Choristoneura fumiferana*) start diapause using glycogen as their main carbohydrate fuel. *C. pipiens* switch to lipids during later diapause stages (Zhou and Miesfeld, 2009), and *C. fumiferana* metabolize carbohydrates throughout their diapause (Marshall and Roe, 2021). Diapausing *S. crassipalpis* use lipids during early diapause, and later switch to using other carbohydrate substrates (Chen et al., 2020). Regardless of patterns of lipid use during diapause, most insects require efficient storage and mobilization of fuels to sustain their basal metabolic functions. They also need energy to fuel potentially costly processes that protect them from winter stressors (*i.e.*, to protect and repair cold-damaged macromolecules).

Because the amount of stored energy is fixed at the start of diapause and cannot be replenished during the winter, diapausing insects suppress their metabolism to prevent excess energy drain and save energy to fuel post-diapause activities such as reproduction and flight

(Hahn and Denlinger, 2011). The extent of metabolic suppression varies among insects. Diapausing insects suppress their metabolic rate from as little as 40 %, such as in *Cucujus clavipes* and *E. solidaginis* larvae (Bennett et al., 2005; Irwin et al., 2001), to 90 %, such as in *Sarcophaga argyrostoma* pupae (Denlinger et al., 1972), compared to non-diapausing rates. Since insects are ectotherms, overall lower temperatures during winter drive lower rates of metabolism. However, most diapausing insects actively lower their metabolic rate independent of temperature as a strategy to maintain energy homeostasis (Wilsterman et al., 2021). Although metabolic suppression is one of the most consistent physiological changes among diapausing insects, we still do not understand the mechanisms that drive this reduced metabolism. We know relatively more about how dormant vertebrates (especially hibernating mammals) suppress their metabolism; thus, we can use strategies employed by other animals to speculate how insects might reduce their metabolic rate during diapause.

Animals can reduce energy demand and/or supply to achieve a hypometabolic state and maintain energy homeostasis in the face of starvation during the winter. To reduce energy demand, many animals reduce rates of mRNA and protein synthesis, and ATP-driven ion transport, processes which account for the majority of cellular ATP consumption (Staples and Buck, 2009; Storey and McMullen, 2004). For example, hibernating thirteen-lined ground squirrels (*Ictidomys tridecemlineatus*) suppress their metabolism by c. 95 %, arrest protein synthesis in their brain (Frerichs et al., 1998) and reduce the activity of Na⁺ K⁺-ATPase in their skeletal muscle (MacDonald and Storey, 1999). Similarly, diapausing goldenrod gall flies (*E. solidaginis*) lower the activity of Na⁺ K⁺-ATPase during the winter (Joanisse and Storey, 1994a), but a causal relationship between lower activity of ATPase enzymes in *E. solidaginis* (or other diapausing insects) and metabolic suppression has never been established.

To reduce energy supply (*i.e.*, decrease rates of ATP production), animals can reduce rates of substrate-level phosphorylation through glycolysis or the TCA cycle, or reduce rates of oxidative phosphorylation in their mitochondria, which account for the majority of cellular ATP production. For example, hibernating thirteen-lined ground squirrels and diapausing killifish (*Austrofundulus limnaeus*) embryos suppress metabolism by lowering mitochondrial respiration rates, which are regulated by altering the activity of mitochondrial electron

transport enzymes (Duerr and Podrabsky, 2010; Mathers et al., 2017). Some diapausing insects alter mitochondrial enzyme activity during winter. For example, diapausing goldenrod gall flies (*E. solidaginis*) and goldenrod gall moths (*Epiblema scudderiana*) reduce the activity of cytochrome C oxidase subunit 1 (Joanisse and Storey, 1994b), diapausing *Hyalophora cecropia* pupae reduce the content of cytochrome b (Shappirio and Williams, 1957), and diapausing boll weevils (*Anthonomus grandis*) reduce the activity of succinate cytochrome c reductase (Keeley et al., 1977). However, we do not know whether changes in mitochondrial enzyme activity in diapausing insects reflect changes in rates of oxidative phosphorylation because mitochondrial function is rarely measured in diapausing insects. To understand how diapausing insects maintain energy homeostasis, we need to investigate how insects regulate ATP-producing and consuming pathways at the cellular level, to achieve lower metabolic rates at the whole animal level.

1.1.2.2 Enhancing stress tolerance

Diapausing insects at their overwintering life stage are typically more tolerant to winter stressors than their non-diapausing counterparts (Košťál, 2006). For example, diapausing insects are more desiccation and hypoxia tolerant than their non-diapausing counterparts because winters are dry, and insects might overwinter in enclosed microhabitats where oxygen tension is low. Further, diapausing insects are exposed to sub-zero temperatures during winter, therefore they substantially increase their cold tolerance during the winter compared to non-diapausing counterparts. Here I will discuss physiological changes that drive desiccation and hypoxia tolerance in diapausing insects and will discuss the physiology of insect cold tolerance in Section 1.3.

Because losing more than 30 % of body water kills most insects (Benoit, 2010), diapausing insects must be able to mitigate water loss during diapause when water is biologically unavailable as ice. The main strategy insects use to combat desiccating conditions during diapause is to reduce water loss rates and conserve the water they already have (Danks, 2000; Benoit, 2010). Most water is lost through the insect cuticle, which is covered with lipids (mainly hydrocarbons) that form a waterproof layer between the insect and its environment (Vincent and Wegst, 2004; Chown et al. 2011). Diapausing insects reduce water loss rates by

either increasing the abundance of cuticular hydrocarbons (*e.g.*, in *Aedes albopictus* eggs; Sota and Mogi, 1992) or changing the composition of cuticular hydrocarbons towards longer, unsaturated fatty acids (*e.g.*, in *Belgica antarctica* larvae; Teets et al., 2013) to form a more effective barrier against water loss. Insects also lose a small amount of water through their spiracles during gas exchange (Chown, 2002). Some diapausing insects employ discontinuous gas exchange, a gas exchange pattern which reduces the time that spiracles are open to the environment and could help reduce respiratory water loss (White et al., 2007). Whether discontinuous gas exchange actually reduces respiratory water loss in insects remains unclear (Chown, 2011). Instead of reducing water loss rates, some insects can tolerate extreme dehydration, such as the Alaskan beetle *Cucujus clavipes* which loses c. 35 % of its body water while overwintering in diapause (Bennett et al., 2005).

Many diapausing insects overwinter in enclosed microhabitats where mixing with atmospheric oxygen is minimal, thus they likely experience hypoxia (Hahn and Denlinger, 2011). Diapausing insects therefore evolved to increase their hypoxia tolerance and can survive better in low-oxygen environments compared to their non-diapausing counterparts. For example, diapausing prepupae of the false codling moth (*Thaumatotibia leucotreta*) and alfalfa leafcutting bee (*Megachile rotundata*) survive longer in low O₂ atmospheres compared to their non-diapausing counterparts (Abdelrahman et al., 2014; Boardman et al., 2015), and diapausing *S. crassipalpis* pupae can even survive long periods in anoxia (Kukal et al., 1991). Insects survive hypoxic conditions by switching from aerobic metabolism to anaerobic metabolism in the absence of oxygen (Chen et al., 2020; Michaud and Denlinger, 2007). Furthermore, metabolic suppression that is typically associated with diapause (Section 1.2.2.3) can also help insects survive extended periods at low oxygen tension by lowering oxygen demand. Towards the end of diapause, when insects' metabolic rates increase and oxygen re-enters cells to stimulate ATP production, a large influx of oxygen can lead to the formation of reactive oxygen species (ROS). Consequently, ROS can cause oxidative damage to important macromolecules (Boardman et al., 2012). Thus, in addition to increased hypoxia tolerance, diapausing insects also tend to have an increased capacity to quench ROS by increasing the expression and/or activity of antioxidant enzymes (MacRae, 2010; Storey and Storey 2012).

Diapause phenotypes are well characterized among temperate insects, however the mechanisms that drive some of these phenotypes are less well known. Specifically, we still have a limited understanding of how insects shift to a hypometabolic state during diapause. It is unlikely that there is one mechanism or pathway responsible for the physiological changes associated with the maintenance of energy homeostasis during diapause because insects and their diapause programmes are diverse and have likely evolved multiple times (Leather et al., 1995). However, creating a basic mechanistic framework for metabolic suppression in a single species will improve our overall understanding of how insects save energy to survive the winter in a dormant state.

1.2 Physiology of insect cold tolerance

Insects are ectotherms, and thus temperature dictates their physiological performance (Huey and Berrigan, 2001). Many insects simply avoid cold exposure, and most species live in the tropics where temperatures do not decrease below 0 °C. Among insects that live in temperate ecosystems, some migrate to warmer environments in advance of the winter season, such as North American populations of the fall armyworm moth, *Spodoptera frugiperda* (Westbrook et al., 2016). Others burrow deep underground below the frost layer to buffer ambient temperatures and minimize their exposure to freezing temperatures, such as the acorn weevil, *Curculio glandium* (Udaka and Sinclair, 2014). However, many insects are unable to avoid cold exposure and have therefore evolved strategies to survive the challenges associated with low temperatures.

1.2.1 Low temperature effects on cellular and organismal function

As ectotherms, rates of physiological processes in insects are temperature sensitive and decrease alongside ambient temperatures. The activity of enzymes which mediate important metabolic reactions will slow down at low temperatures, which can impair cell function (Hochachka and Somero, 2002). Low temperatures also affect many physical and structural properties of insect cells. For example, low temperatures increase the viscosity of cellular and extracellular fluids, and reduce membrane fluidity (Longworth, 1954), which disrupts cellular permeability, prevents transport of important molecules across cell membranes, and impairs transmembrane protein function (Hochachka and Somero, 2002). Microtubules

depolymerize at low temperatures reducing the structural integrity of cells and preventing the intracellular transport of organelles and vesicles that rely on polymerized cytoskeletal elements (Des Marteaux et al., 2018; Pegoraro et al., 2017). When exposed to temperatures below 0 °C, insects' proteins can denature because low temperatures destabilize intramolecular hydrophobic interactions (Hochachka and Somero, 2002). Sub-zero temperatures can either denature proteins from their tertiary structure, or drive the dissociation of multimeric subunits, both of which render the proteins dysfunctional and unable to carry out their cellular functions (Espinosa et al., 2017). Finally, sub-zero temperatures can initiate the freezing of extracellular fluid in insects. Ice formation leads to mechanical damage of cells and macromolecules from growing ice crystals and increased osmotic pressure because freezing reduces biologically available water content in a cell. Freezing also causes membrane phase transitions which impair cellular function and can lead to both cell and whole-animal death (see Toxopeus and Sinclair 2018 for an extensive review on cellular damage associated with freezing).

The organismal function of insects is compromised at low temperatures as a result of impaired cellular function. For example, ion-motive pumps, such as Na⁺-K⁺ ATPase slow down at low temperatures and cause insects to lose extracellular ion and water homeostasis as rates of passive ion diffusion exceed active transport abilities (Overgaard and MacMillan, 2017). Loss of ion homeostasis is exacerbated at low temperature when changes in membrane fluidity reduce epithelial barrier function in the gut and Malpighian tubules (Overgaard et al., 2021). Insects that lose ion and water homeostasis face neuromuscular failure and enter a state of paralysis known as chill coma (Overgaard and MacMillan, 2017). Low temperatures also reduce the activity of enzymes involved in primary and intermediary metabolism, leading to cellular energy imbalance, the buildup of toxic end metabolites (Dollo et al., 2010; Košťál et al., 2007), and overall reduced metabolic capacity of the whole insect. Low temperatures also reduce the activity of enzymes that drive immune responses and leave insects vulnerable to pathogen infection (Ferguson et al., 2018).

Insects have evolved three main strategies in response to low temperature challenges (chill-susceptibility, freeze tolerance and freeze avoidance), and each can be categorized based on the insect's ability to survive freezing. Most insects are chill-susceptible, such as the vinegar

fly *Drosophila melanogaster* (Gilbert and Huey, 2001) and the fall field cricket *Gryllus pennsylvanicus* (Macmillan and Sinclair, 2011), and will die after exposure to low temperatures well above the point at which they freeze (the supercooling point; Overgaard and MacMillan, 2017). Chill-susceptible insects do not survive temperatures below 0 °C, thus their survival at low temperatures depends on how well they maintain ion and water balance at low temperatures above 0 °C (reviewed extensively by Overgaard and Macmillan 2017). Freeze-tolerant insects, such as the goldenrod gall fly *E. solidaginis* and spring field cricket *Gryllus veletis*, survive freezing of their body fluids (Lee et al., 1993; Toxopeus et al., 2019b). The extent to which they survive this ice formation depends on how long they remain frozen, how many times they freeze during the winter, and their ability to recover from being frozen (extensively reviewed by Toxopeus and Sinclair 2018). Freeze-avoidant insects, such as larvae of the goldenrod gall moth *E. scudderiana* and Emerald ash borer *Agrilus planipennis* survive extended periods at sub-zero temperatures, as long as they remain unfrozen (Crosthwaite et al., 2011; Rickards et al., 1987). At their supercooling point, freeze-avoidant insects will freeze and die. Thus, to survive sub-zero temperatures freeze-avoidant insects typically depress their supercooling points so body fluids remain liquid at extremely low temperatures (Zachariassen, 1985). In my thesis I study cold tolerance in a freeze-avoidant insect, thus I will focus the rest of this section on mechanisms of low temperature survival in freeze-avoidant insects.

1.2.2 Mechanisms of low temperature survival in freeze-avoidant insects

Freeze-avoidant insects can survive low temperatures by decreasing the probability that they freeze at sub-zero temperatures and preventing and/or repairing cold-induced cellular damage at non-freezing sub-zero temperatures.

Insect body water does not always freeze at 0 °C, rather it can supercool and remain as a liquid below the melting point of body fluids (Lee and Denlinger, 1991). Freeze-avoidant insects take advantage of this property and biochemically depress their supercooling point during the winter using low molecular weight cryoprotectants and antifreeze proteins.

Freeze-avoidant insects typically accumulate low molecular weight cryoprotectants such as polyhydroxy alcohols (*e.g.*, glycerol, myo-inositol), sugars (*e.g.*, trehalose), and free amino

acids (*e.g.*, proline, alanine) in their hemolymph and tissues (Storey and Storey, 1991). Insects often synthesize these metabolites in advance of winter conditions in preparation for sub-zero temperature exposure (Zachariassen, 1985). At high concentrations, low molecular weight cryoprotectants drive a concentration dependent (colligative) depression of supercooling point, allowing insects to survive extremely low temperatures in a supercooled state (Zachariassen, 1985). For example, freeze-avoidant emerald ash borer prepupae (*A. planipennis*) accumulate *c.* 4 M glycerol over the winter, which results in a *c.* 10 °C decrease in their supercooling point (Crosthwaite et al., 2011). Even in a supercooled state, ice can form in insect hemolymph. Thus, freeze-avoidant insects also use antifreeze proteins to prevent the spontaneous nucleation of ice (Zachariassen and Husby, 1982; Zachariassen and Kristiansen, 2000). Anti-freeze proteins (also referred to as thermal hysteresis proteins) bind to the growth planes of ice crystals to prevent further ice crystal growth. This stabilizes supercooled fluids in an insect by lowering their freezing point below the melting point, such as in the ribbed pine borer *Rhagium inquisitor* (Zachariassen and Husby, 1982).

Once freeze-avoidant insects are supercooled, they must protect their cells from any non-freezing damage that likely accrues when they spend extended periods at sub-zero temperatures. Low molecular weight cryoprotectants not only depress supercooling points but also non-colligatively stabilize macromolecules at lower (<1 M) concentrations. For example, the linden bug (*P. apterus*) accumulates proline and trehalose, which increases their low temperature survival but does not lower their supercooling points (Košťál et al., 2001). Because low temperatures affect many physical parameters of a cell, insects modify structural components of their cells to protect against cold-induced damage. Freeze-avoidant insects modify their cell membranes by increasing the proportion of polyunsaturated fatty acids in their membrane lipids to maintain fluidity, such as in fat body cells of *S. crassipalpis* (Lee and Denlinger, 1985) and *P. apterus* (Tomcala et al., 2006). Some insects, such as the house mosquito (*C. pipiens*) and fall field cricket (*G. pennsylvanicus*), restructure cytoskeletal elements to resist depolymerization in response to low temperatures (Kim et al., 2006; Des Marteaux et al., 2018).

Finally, to protect proteins from cold-induced denaturation, many freeze-avoidant insects will increase the expression of chaperone proteins, such as heat shock proteins (HSPs) which I will discuss in the next section.

1.2.3 The chaperone response and insect cold tolerance

Heat shock proteins (HSPs) are a large family of chaperone proteins that help maintain protein form and function in all animal cell types (Hendrick and Hartl, 1993). Heat shock proteins help preserve cellular function by preventing proteotoxicity when cells are exposed to stressors such as high temperatures, hypoxia, and desiccation. The heat shock protein 70 family (including HSP68, HSP70 and HSP72) are central proteins in the cellular chaperone response and assist in the ATP-dependent folding of denatured proteins in a cell (Rosenzweig et al., 2019). Other HSPs include those from the 20 kDa family (HSP20), 60 kDa family (HSP60), 90 kDa family (HSP90), and co-chaperones such as HSP40 (Becker and Craig, 1994).

In unstressed cells, constitutive pools of heat shock proteins (mainly HSP70) are bound to heat shock factors (HSFs; Sorger, 1991). When bound to HSP70, HSFs are inactive, but after a heat stress the proportion of denatured proteins in a cell increases and HSP70 preferentially binds to unfolded proteins. When HSP70 dissociates from HSFs, they can diffuse into the nucleus (Hochachka and Somero, 2002). Once in the nucleus, HSFs bind heat shock elements (HSEs), the promoter sequences upstream of HSP70 genes, and drive the transcription of *HSP70* mRNA and ultimately translation of HSP70 proteins (Hochachka and Somero, 2002; Rosenzweig et al., 2019). These newly synthesized HSP70 proteins repair unfolded proteins with the help of co-chaperones, such as HSP40. Co-chaperones activate the ATPase domain of HSP70 and promote binding of HSP70 to its unfolded protein substrate. HSP70 can then refold its substrate protein and release it back into the cell to resume normal functions (Laufen et al., 1999). If proteins are irreversibly damaged, HSPs will chaperone damaged proteins to the proteasome for degradation (Reeg et al., 2016). Although this current model describes heat stress as the condition which stimulates the chaperone response, sub-zero temperatures also denature proteins (Hochachka and Somero, 2002; Privalov, 1990). Thus, the chaperone response is readily activated by insect cells at low temperatures.

Most of what we understand about the cold-induced chaperone response in insects comes from overwintering patterns of gene expression of various HSPs. Many insects express HSPs in anticipation of winter, as part of their diapause programme. For example, diapausing *S. crassipalpis* increase the expression of HSP60 and HSP70 family proteins at the onset of and throughout their diapause (Rinehart et al., 2007b). Some insects, such as *P. apterus* and *G. pennsylvanicus* increase the expression of HSPs in preparation for subzero temperature exposure through processes such as cold acclimation (Tollarová-Borovanská et al., 2009; Des Marteaux et al., 2017). Other insects increase the expression of HSPs in direct response to cold shock, such as *L. decemlineata* (Yocum, 2001).

Increased HSP expression by overwintering insects is associated with increased survival at low temperature, and therefore increased levels of cold tolerance. For example, diapausing *S. crassipalpis* require HSP23 and HSP70 expression to survive low temperatures (Rinehart et al., 2007a), and adult *P. apterus* require HSP70 expression to recover from low temperature exposure (Košťál and Tollarová-Borovanská, 2009). However, despite many papers over the last 20 years that report expression of HSPs in overwintering insects, we know very little about how HSPs actually protect cells from cold-induced damage. The prevailing hypothesis is that HSPs refold proteins before they become irreversibly denatured in the cells of overwintering insects. Ultimately, HSPs could restore the function of metabolically important proteins, especially in tissues like the fat body where metabolism persists over the winter. However, there is little evidence supporting the hypothesis that HSPs protect insect proteins and cells at low temperatures. Thus, the link between HSP expression, low temperature survival, and increased cold tolerance remains unknown.

1.3 Relationship between insect diapause and cold tolerance

Diapause evolved as a response to seasonality (Leather et al., 1995) thus insects can enter diapause during seasonally unfavorable conditions even in the absence of cold winters. For example, the tropical fungus beetle (*Stenotarsus rotundus*) enters diapause to escape heat stress during dry seasons even though they never encounter temperatures below 0 °C (Tanaka et al., 1988). By contrast, some insects enhance their cold tolerance without diapause. For example, insects that live in the Southern hemisphere experience less seasonality, but still

risk unpredictable and frequent exposure to sub-zero temperatures and therefore become cold-tolerant independently of a diapause programme (Ramløv and Lee, 2000; Sinclair et al., 2003). This complex pattern of diapause and cold tolerance incidence in insects makes it difficult to disentangle the two strategies, especially in temperate overwintering insects where cold tolerance and diapause co-occur.

To understand the relationship between diapause and cold tolerance, we must identify the physiological changes that are shared or differ between diapausing and cold-tolerant insects. Diapause and cold tolerance are induced by similar cues; a short photoperiod induces diapause and cold tolerance in most temperate insects (Košťál, 2006). Diapausing and cold-tolerant insects also express similar phenotypes, such as enhanced immunity (Ferguson and Sinclair, 2017), increased desiccation tolerance (Benoit and Denlinger, 2007), and increased survival at sub-zero temperatures. Diapausing and cold-tolerant insects activate similar biological processes, such as the synthesis of low molecular weight cryoprotectants and expression of chaperone proteins. Low molecular weight cryoprotectants are produced by insects that enter diapause and become cold-tolerant (*e.g.*, *E. solidaginis*; Storey and Storey, 1983), in insects that overwinter without a diapause programme (*e.g.*, *Hemideina maori*; Ramløv and Lee, 2000), and also in insects who diapause in warm environments (*e.g.*, *S. rotundus*; Pullin and Wolda, 1993).

Similarly, chaperone proteins are expressed by insects when diapause and cold tolerance co-occur (King and Macrae, 2015), and chaperone protein expression can also be induced by exposure to low temperatures, independently of diapause (*e.g.*, HSP90 in *Chilo suppressalis*, Sonoda et al., 2006; HSP70 in *L. decemlineata*, Yocum, 2001). However, the function of chaperone proteins in overwintering insects is rarely studied and measuring the expression patterns of molecules that are shared between diapausing and cold-tolerant insects is not enough to disentangle the two strategies. Rather, we need to measure the function of these molecules to distinguish between their roles in driving diapause phenotype independently of enhancing sub-zero temperature survival.

1.4 Biology of the Colorado potato beetle

The Colorado potato beetle (CPB, *Leptinotarsa decemlineata* Say 1824; Coleoptera: Chrysomelidae) is a major pest of potato plants worldwide (Alyokhin et al., 2013). Colorado potato beetles originated in Mexico and were discovered in the western United States of America in 1824. By 1859 CPB had established populations in the U.S.A., and over the course of 15 years CPB expanded throughout the eastern U.S.A, Canada, and mainland Europe decimating potato crops and emerging as a challenging pest to control (Alyokhin et al., 2013). There are now established populations of CPB in North America, Europe, and several parts of Asia (Grapputo et al., 2005). One hypothesis for their successful invasion is their ability to adapt to a number of different stressors (Schoville et al., 2018). Indeed, CPB successfully overwinter over a wide latitudinal range, partly because of their ability to enter facultative diapause and survive harsh winter conditions.

During the summer, CPB populations exhibit one to three generations depending on latitude, environmental conditions, and availability of host potato plants (Alyokhin and Ferro, 1999). Female CPB lay eggs in clusters of c. 50 on the underside of potato plant leaves, and those eggs hatch into larvae which live and feed directly on the same host plant leaves (Alyokhin et al., 2013). Larvae progress through several instars, and upon reaching the fourth instar stage they drop from potato plants, burrow into the soil and pupate. After circa ten days, pupated beetles emerge from the soil as adults, establish on a new host plant, and reproduce to start a new generation (Ferro et al., 1999).

1.4.1 Diapause in the Colorado potato beetle

Towards late summer, decreased daylength induces diapause in CPB, and exposure to these short-day conditions from the egg stage onwards programs beetles to enter diapause as adults (De Wilde, 1960). The critical photoperiod (photoperiod which induces c. 50 % of the population to enter diapause) differs among CPB populations but is usually at or below 15 h of daylight (De Wilde et al., 1959; Senanayake et al., 2000). Upon diapause initiation in late-summer adult CPB, they feed voraciously and accumulate large lipid stores in their fat body (Güney et al., 2020; Lehmann et al., 2020; Yocum et al., 2011a). Concurrently, diapause destined CPB reduce their circulating levels of JH by lowering rates of JH biosynthesis in

their *corpora allata* and increasing JH degradation *via* JH esterase activity (De Wilde, 1960; Vermunt et al., 1998), which leads to arrested reproductive development (Guo et al., 2019).

Once CPB accumulate sufficient energy stores (after approximately three weeks under diapause-inducing conditions) they burrow into the soil where they remain for the duration of winter in their diapause maintenance stage (Lehmann et al., 2015b). CPB use their lipid stores slowly and suppress their metabolic rate during diapause until their emergence in the spring (Lehmann et al., 2015c; Lehmann et al., 2020). Upon diapause termination, CPB emerge from the soil and recover their metabolic rate. The exact timing of this metabolic rate recovery is unknown. However, we know that overwintered CPB can fly immediately to search for potato plants and mates, often before they even feed and replenish their energy stores (Ferro et al., 1999). Indeed, CPB use most of the lipid reserves they accumulated during diapause initiation, to fuel post-diapause activities (Lefevre et al., 1989). Diapausing CPB also synthesize diapause-specific hexamerin storage proteins in their fat body, which are circulated in their hemolymph and could be used as an additional source of protein fuel during diapause. However, differences in substrate use in diapausing CPB and the function of hexamerin storage proteins are currently unknown (De Kort and Koopmanschap, 1994; Yocum et al., 2011b).

Unlike diapause initiation, diapause termination in CPB is not regulated by changes in photoperiod because beetles overwinter beneath the soil where there is no light (De Kort, 1990). Once diapause is terminated, temperature is an important extrinsic factor for stimulating reproductive development; CPB only resume reproductive development at temperatures above 10 °C (Lefevre, 1989). However, the actual termination of CPB diapause and therefore the duration of their diapause programme does not appear to be regulated by temperature (de Kort, 1990). We still do not know which intrinsic physiological mechanisms lead to diapause termination and the re-establishment of non-diapausing phenotypes in CPB.

Although CPB suppress their metabolic rate during diapause, and re-establish high metabolic rates upon diapause termination, we do not understand the mechanisms that drive changes in their metabolic rate. Work in the 1960s showed that diapausing CPB degenerate their flight

muscle during diapause (Stegwee et al., 1963). Further, CPB regrow their muscle upon diapause termination. Flight muscle is one of the most energetically expensive tissues in the animal kingdom (Ellington, 1985). Around one-third of insect flight muscle wet weight is comprised of mitochondria which account for the majority of cellular ATP production (Levenbook, 1953). Thus, degrading this tissue (and therefore degrading flight muscle mitochondria) could lower cellular energy supply and therefore drive a substantial decrease in whole animal metabolic rate. However, no mechanistic link has been made between flight muscle histolysis and metabolic suppression in CPB.

Although there has been extensive research on the neuroendocrine control of diapause in CPB (see de Kort, 1990), and broader eco-physiological aspects of diapause in CPB (see Lehmann et al., 2014; Lehmann et al., 2015b), there are still several gaps in our understanding of their diapause. Mainly, we do not know the mechanisms driving physiological changes that we observe during diapause maintenance in CPB.

1.4.2 Cold tolerance in the Colorado potato beetle

Diapausing CPB are freeze-avoidant during the winter and are significantly more cold-tolerant than their non-diapausing counterparts (Salt, 1933). Diapausing CPB depress their supercooling points from c. -8°C (beetles actively feeding on plants) to c. -17°C (Boiteau and Coleman, 1996; Lehmann et al., 2015a). Diapausing CPB evacuate their guts prior to burrowing into the soil, which eliminates any potential ice nucleating bacteria thus reducing the likelihood that they will freeze and contributing to supercooling point depression (Lee et al., 1994). Although freeze-avoidance and supercooling point depression in insects is typically associated with the synthesis of polyols, diapausing CPB do not appear to accumulate these molecules in any significant quantity (Lehmann et al., 2015a). Diapausing CPB do accumulate proline (c. 40 mM, J.E. Lebenzon, unpublished data) in their hemolymph during diapause, which could be potentially cryoprotective (*cf.* Košťál et al., 2011).

Because CPB overwinter in temperate environments in Canada, Europe and Russia, where long term sub-zero temperature exposure is a risk, they should employ a variety of different molecular and biochemical mechanisms to protect their cells from low temperatures. Colorado potato beetles appear to express *HSP70* during diapause, and in response to direct

sub-zero temperature exposure (Lyytinen et al., 2012; Yocum, 2001). However, these patterns of HSP expression have not been causally linked to increased whole animal cold tolerance in CPB, and we do not know how HSPs actually protect the cells of overwintering CPB. We also do not know whether other types of chaperone proteins other than HSP70 play a role in their cold tolerance. Given that CPB do not appear to rely on classic cryoprotection by low molecular weight molecules (*e.g.*, polyols or sugars), chaperone proteins could play a large role in protecting CPB cells and protein from cold-induced damage during the winter.

1.5 Thesis Experimental Design, Objectives and Overview

In this thesis, I use the Colorado potato beetle as a model to improve our understanding of the physiological and molecular mechanisms underlying insect diapause and cold tolerance. I take a descriptive (Chapters 2 and 4) and functional hypothesis testing (Chapters 3 and 4) approach to explore how physiological changes at the whole animal, tissue, and cellular level drive diapause and cold-tolerant phenotypes in an overwintering insect. Diapause and cold tolerance co-occur in overwintering CPB under natural conditions, and I can experimentally induce them in the laboratory (Figure 1.1). To induce diapause, I rear CPB under a short photoperiod from the egg stage until adulthood, and these “diapause-destined” adults will burrow into the soil and enter diapause (Figure 1.1). By 9 weeks in diapause-inducing conditions, CPB are in their diapause maintenance stage and after c. 20 weeks they will emerge from diapause (Figure 1.1). Exposing CPB during diapause maintenance to a fluctuating temperature regime enhances their cold tolerance relative to diapausing CPB with no prior fluctuating temperature exposure (Figure 1.1). Thus, I can experimentally induce non-diapausing CPB, CPB entering diapause, CPB in their diapause maintenance stage, CPB that have emerged from diapause, and diapausing CPB with enhanced cold tolerance (Figure 1.1). This approach allows me to investigate the mechanisms underlying diapause in CPB, those underlying their acquisition of cold tolerance, and mechanisms that are shared between the two.

My first objective was to characterize tissue-specific gene expression patterns in metabolically important tissues in CPB and uncover any tissue-specific patterns in gene expression that drive diapause phenotypes. Most studies investigating patterns of gene

expression during diapause in insects do so in whole insect homogenates, which could potentially mask important inter-tissue differences. In Chapter 2 (“Diapause differentially modulates the transcriptomes of fat body and flight muscle in the Colorado potato beetle”), I address this first objective and use RNA-seq to characterize tissue-specific patterns of gene expression in fat body and flight muscle of non-diapausing and diapausing CPB. I use a combination of differential expression analysis and gene ontology enrichment analysis to determine which transcripts and biological processes are important for driving diapause phenotypes in CPB. I find that CPB differentially modulate their fat body and flight muscle transcriptomes during diapause. I also observe changes in gene expression in CPB that support longstanding hypotheses about biological processes that occur during diapause (*i.e.*, cell cycle arrest, lipid mobilization, increased antioxidant capacity). Finally, I generate novel hypotheses about the mechanisms driving metabolic suppression during diapause. One of the hypotheses that I propose is that flight muscle modulates energy metabolism during diapause, and I explore this hypothesis in Chapter 3.

My second objective was to investigate the mechanisms driving metabolic suppression, and reversal of this metabolic suppression, during diapause in CPB. There are longstanding hypotheses in the literature which posit that insects degrade metabolically important tissues such as flight muscle during diapause to lower the cost of whole organism maintenance (Hahn and Denlinger, 2011; Košťál, 2006), but this hypothesis has never been tested. Since CPB suppress their metabolism and reversibly degrade their flight muscle during diapause, they are an ideal model for identifying mechanistic links between low metabolic rate and flight muscle degradation. I demonstrate this link in Chapter 3 (“Reversible mitophagy drives metabolic suppression in diapausing Colorado potato beetles”) and show that metabolic suppression is not just a product of flight muscle degradation but is driven by the breakdown of flight muscle mitochondria. Specifically, I show that diapausing Colorado potato beetles suppress their whole-animal metabolic rate by 90 %, and that this coincides with a similar reduction in mitochondrial respiration rate and mitochondrial density in their flight muscle. Second, I show that Parkin-mediated mitophagy (mitochondrial-specific autophagy) is activated in flight muscle of diapausing CPB, as *Parkin* expression and autophagy-related structures in the flight muscle increase during diapause. Third, I test the hypothesis that

Parkin-mediated mitophagy drives metabolic suppression by knocking down *Parkin* expression in diapausing CPB using RNA interference and find that knocking down *Parkin* expression partially restores mitochondrial density and whole-animal metabolic rate. Finally, I show that CPB can reverse this mitophagy and replenish their flight muscle mitochondrial pool, in the absence of any external cues. This spontaneous resynthesis of flight muscle mitochondria is driven by the expression of mitochondrial-biogenesis related genes (*NRF1* and *PGC1 α*) in anticipation of the end of diapause.

My third objective was to explore which genes, proteins, and biological processes drive cold tolerance in CPB. Colorado potato beetles are freeze-avoidant and can survive extended periods below 0 °C, however the molecular and biochemical mechanisms that underpin CPB low temperature survival are largely unknown. Thus, in Chapter 4 (“Activation of the chaperone response improves cold tolerance in diapausing Colorado potato beetles”) I use a broad RNA-seq approach to identify biological processes that drive cold tolerance in CPB. I compare differences in fat body gene expression between diapausing and cold-tolerant CPB and find that improved cold tolerance in CPB coincides with increased abundance of chaperone-related transcripts. Further, I find that cold-tolerant CPB have slightly fewer damaged proteins in their fat body, demonstrating that increased expression of chaperone-related transcripts in cold-tolerant insects helps prevent protein damage at sub-zero temperatures.

In Chapter 5, I synthesize my findings and describe how my thesis was able to disentangle the relationship between diapause and cold tolerance in CPB. I posit a conceptual model for metabolic suppression during diapause in CPB, propose a functional role for chaperone proteins in insect cold tolerance, and demonstrate that heat shock proteins play differential roles in the diapause and cold tolerance of overwintering CPB.

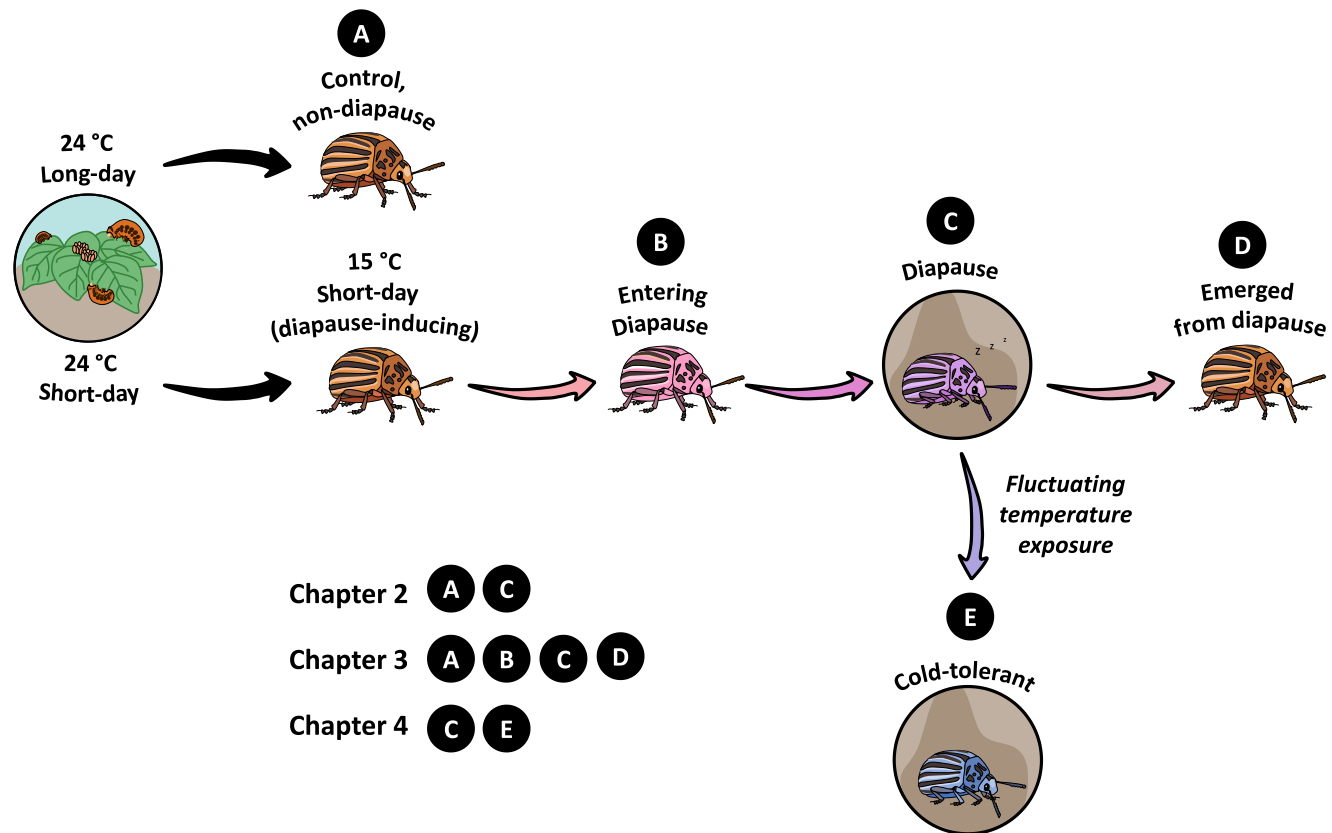


Figure 1.1. Experimental design of Chapters 2-4. In Chapter 2, I compare non-diapausing (A) and diapausing (C) CPB. In Chapter 3, I compare non-diapausing CPB (A) with beetles entering diapause (B), in diapause (C), and emerged from diapause (D). In Chapter 4 I compare diapausing (C) and cold-tolerant (E) CPB.

1.6 References

- Abdelrahman, H., Rinehart, J., Yocum, G., Greenlee, K., Helm, B., Kemp, W., Schulz, C., Bowsher, J.** (2014). Extended hypoxia in the alfalfa leafcutting bee, *Megachile rotundata*, increases survival but causes sub-lethal effects. *Journal of Insect Physiology* **64**, 81-89.
- Alyokhin, A., Udalov, M., Benkovskaya, G.** (2013). The Colorado potato beetle, In *Insect Pests of Potato*. (eds. P. Giordanengo, C. Vincent, A. Alyokhin), pp. 11-29. Elsevier.
- Alyokhin, A.V., Ferro, D.N.** (1999). Reproduction and dispersal of summer-generation Colorado potato beetle (Coleoptera: Chrysomelidae). *Environmental Entomology* **28**, 425-430.
- Baust, J.G.** (1976). Temperature buffering in an arctic microhabitat. *Annals of the Entomological Society of America* **69**, 117-119.
- Bayley, J.S., Winther, C.B., Andersen, M.K., Grønkjær, C., Nielsen, O.B., Pedersen, T.H., Overgaard, J.** (2018). Cold exposure causes cell death by depolarization-mediated Ca²⁺ overload in a chill-susceptible insect. *Proceedings of the National Academy of Sciences of the U.S.A.* **115**, E9737-E9744.
- Becker, J., Craig, E.A.** (1994). Heat-shock proteins as molecular chaperones. *European Journal of Biochemistry* **219**, 11-23.
- Belovsky, G., Slade, J.** (2000). Insect herbivory accelerates nutrient cycling and increases plant production. *Proceedings of the National Academy of Sciences of the U.S.A.* **97**, 14412-14417.
- Bennett, V.A., Sformo, T., Walters, K., Toien, O., Jeannet, K., Hochstrasser, R., Pan, Q., Serianni, A.S., Barnes, B.M., Duman, J.G.** (2005). Comparative overwintering physiology of Alaska and Indiana populations of the beetle *Cucujus clavipes* (Fabricius): roles of antifreeze proteins, polyols, dehydration and diapause. *Journal of Experimental Biology* **208**, 4467-4477.
- Benoit, J.B.** (2010). Water management by dormant insects: comparisons between dehydration resistance during summer aestivation and winter diapause. In *Aestivation*, vol. 49 (eds. C.A. Navas, J.E. Carvalho), pp 209-229. Springer.
- Benoit, J.B., Denlinger, D.L.** (2007). Suppression of water loss during adult diapause in the northern house mosquito, *Culex pipiens*. *Journal of Experimental Biology* **210**, 217-226.
- Boardman, L., Sørensen, J.G., Terblanche, J.S.** (2015). Physiological and molecular mechanisms associated with cross tolerance between hypoxia and low temperature in *Thaumatotibia leucotreta*. *Journal of Insect Physiology* **82**, 75-84.

- Boardman, L., Terblanche, J.S., Hetz, S.K., Marais, E., Chown, S.L.** (2012). Reactive oxygen species production and discontinuous gas exchange in insects. *Proceedings of the Royal Society B: Biological Sciences* **279**, 893-901.
- Boiteau, G., Coleman, W.** (1996). Cold tolerance in the Colorado potato beetle, *Leptinotarsa decemlineata* (Say) (Coleoptera: Chrysomelidae). *Canadian Entomologist* **128**, 1087-1099.
- Chen, C., Mahar, R., Merritt, M.E., Denlinger, D.L., Hahn, D.A.** (2021). ROS and hypoxia signaling regulate periodic metabolic arousal during insect dormancy to coordinate glucose, amino acid, and lipid metabolism. *Proceedings of the National Academy of Sciences of the U.S.A.* **118**, e2017603118.
- Chown, S.** (2002). Respiratory water loss in insects. *Comparative Biochemistry and Physiology Part A: Molecular & Integrative Physiology* **133**, 791-804.
- Chown, S.L.** (2011). Discontinuous gas exchange: new perspectives on evolutionary origins and ecological implications. *Functional Ecology* **25**, 1163-1168.
- Chown, S.L., Sørensen, J.G., Terblanche, J.S.** (2011). Water loss in insects: an environmental change perspective. *Journal of Insect Physiology* **8**, 1070-1084.
- Crespo-Pérez, V., Kazakou, E., Roubik, D.W., Cárdenas, R.E.** (2020). The importance of insects on land and in water: a tropical view. *Current Opinion in Insect Science* **40**, 31-38.
- Crosthwaite, J.C., Sobek, S., Lyons, D.B., Bernardis, M.A., Sinclair, B.J.** (2011). The overwintering physiology of the emerald ash borer, *Agrilus planipennis* Fairmaire (Coleoptera: Buprestidae). *Journal of Insect Physiology* **57**, 166-173.
- Danks, H.V.** (2002). Dehydration in dormant insects. *Journal of Insect Physiology* **6**, 837-852.
- De Kort, C.** (1990). Thirty-five years of diapause research with the Colorado potato beetle. *Entomologia Experimentalis et Applicata* **56**, 1-13.
- De Kort, C., Koopmanschap, A.** (1994). Nucleotide and deduced amino acid sequence of a cDNA clone encoding diapause protein 1, an arylphorin-type storage hexamer of the Colorado potato beetle. *Journal of Insect Physiology* **40**, 527-535.
- De Wilde, J., Duintjer, C., Mook, L.** (1959). Physiology of diapause in the adult Colorado beetle (*Leptinotarsa decemlineata* Say) – I The photoperiod as a controlling factor. *Journal of Insect Physiology* **3**, 75-85.
- Denlinger, D., Willis, J., Fraenkel, G.** (1972). Rates and cycles of oxygen consumption during pupal diapause in *Sarcophaga* flesh flies. *Journal of Insect Physiology* **18**, 871-882.

- Denlinger, D., Yocum, G., Rinehart, J., Gilbert, L.** (2004). Hormonal control of diapause. *Comprehensive Insect Molecular Science* **3**, 615-650.
- Denlinger, D.L., Armbruster, P.A.** (2014). Mosquito diapause. *Annual Review of Entomology* **59**, 73-93.
- Des Marteaux, L.E., McKinnon, A.H., Udaka, H., Toxopeus, J., Sinclair, B.J.** (2017). Effects of cold-acclimation on gene expression in Fall field cricket (*Gryllus pennsylvanicus*) ionoregulatory tissues. *BMC genomics* **18**, 357.
- Des Marteaux, L.E., Stinziano, J.R., Sinclair, B.J.** (2018). Effects of cold acclimation on rectal macromorphology, ultrastructure, and cytoskeletal stability in *Gryllus pennsylvanicus* crickets. *Journal of Insect Physiology* **104**, 15-24.
- Dollo, V.H., Yi, S.-X., Lee Jr, R.E.** (2010). High temperature pulses decrease indirect chilling injury and elevate ATP levels in the flesh fly, *Sarcophaga crassipalpis*. *Cryobiology* **60**, 351-353.
- Dong, Y.-C., Wang, Z.-J., Clarke, A.R., Pereira, R., Desneux, N., Niu, C.-Y.** (2013). Pupal diapause development and termination is driven by low temperature chilling in *Bactrocera minax*. *Journal of Pest Science* **86**, 429-436.
- Duerr, J.M., Podrabsky, J.E.** (2010). Mitochondrial physiology of diapausing and developing embryos of the annual killifish *Austrofundulus limnaeus*: implications for extreme anoxia tolerance. *Journal of Comparative Physiology B* **180**, 991-1003.
- Ellington, C.P.** (1985). Power and efficiency of insect flight muscle. *Journal of Experimental Biology* **115**, 293-304.
- Espinosa, Y.R., Grigera, J.R., Caffarena, E.R.** (2017). Essential dynamics of the cold denaturation: pressure and temperature effects in yeast frataxin. *Proteins: Structure, Function, and Bioinformatics* **85**, 125-136.
- Feder, J.L., Powell, T.H., Filchak, K., Leung, B.** (2010). The diapause response of *Rhagoletis pomonella* to varying environmental conditions and its significance for geographic and host plant-related adaptation. *Entomologia Experimentalis et Applicata* **136**, 31-44.
- Ferguson, L.V., Kortet, R., Sinclair, B.J.** (2018). Eco-immunology in the cold: the role of immunity in shaping the overwintering survival of ectotherms. *Journal of Experimental Biology* **221**, jeb163873.
- Ferguson, L.V., Sinclair, B.J.** (2017). Insect immunity varies idiosyncratically during overwintering. *Journal of Experimental Zoology Part A: Ecological and Integrative Physiology* **327**, 222-234.

- Ferro, D.N., Alyokhin, A.V., Tobin, D.B.** (1999). Reproductive status and flight activity of the overwintered Colorado potato beetle. *Entomologia Experimentalis et Applicata* **91**, 443-448.
- Frerichs, K.U., Smith, C.B., Brenner, M., DeGracia, D.J., Krause, G.S., Marrone, L., Dever, T.E., Hallenbeck, J.M.** (1998). Suppression of protein synthesis in brain during hibernation involves inhibition of protein initiation and elongation. *Proceedings of the National Academy of Sciences of the U.S.A.* **95**, 14511-14516.
- Garnham, J.I., Stockwell, M.P., Pollard, C.J., Pickett, E.J., Bower, D.S., Clulow, J., Mahony, M.J.** (2015). Winter microhabitat selection of a threatened pond amphibian in constructed urban wetlands. *Austral Ecology* **40**, 816-826.
- Gilbert, P., Huey, R.B.** (2002). Chill-coma temperature in *Drosophila*: effects of developmental temperature, latitude, and phylogeny. *Physiological and Biochemical Zoology* **74**, 429-434.
- Grapputo, A., Boman, S., Lindstroem, L., Lyytinen, A., Mappes, J.** (2005). The voyage of an invasive species across continents: genetic diversity of North American and European Colorado potato beetle populations. *Molecular Ecology* **14**, 4207-4219.
- Güney, G., Toprak, U., Hegedus, D.D., Bayram, Ş., Coutu, C., Bekkaoui, D., Baldwin, D., Heckel, D.G., Hänniger, S., Cedden, D.** (2020). A look into Colorado potato beetle lipid metabolism through the lens of lipid storage droplet proteins. *Insect Biochemistry and Molecular Biology* **133**, 103473.
- Guo, S., Sun, D., Tian, Z., Liu, W., Zhu, F., Wang, X.-P.** (2019). The limited regulatory roles of juvenile hormone degradation pathways in reproductive diapause preparation of the cabbage beetle, *Colaphellus bowringi*. *Journal of Insect Physiology* **119**, 103967.
- Hahn, D.A., Denlinger, D.L.** (2007). Meeting the energetic demands of insect diapause: Nutrient storage and utilization. *Journal of Insect Physiology* **53**, 760-773.
- Hahn, D.A., Denlinger, D.L.** (2011). Energetics of insect diapause. *Annual Review of Entomology* **56**, 103-121.
- He, H., Yang, H., Xiao, L., Xue, F.** (2011). Effect of temperature and photoperiod on developmental period and reproduction of *Spodoptera exigua*. *Jiangxi Plant Protection* **34**, 93.
- Hendrick, J.P., Hartl, F.-U.** (1993). Molecular chaperone functions of heat-shock proteins. *Annual Review of Biochemistry* **62**, 349-384.
- Hochachka, P.W., Somero, G.N.** (2002). Temperature. In *Biochemical adaptation: mechanism and process in physiological evolution*. pp. 290-451. Oxford university press.

- Huey, R.B., Berrigan, D.** (2001). Temperature, demography, and ectotherm fitness. *The American Naturalist* **158**, 204-210.
- Irwin, J., Bennett, V., Lee, R.** (2001). Diapause development in frozen larvae of the goldenrod gall fly, *Eurosta solidaginis* Fitch (Diptera: Tephritidae). *Journal of Comparative Physiology B* **171**, 181-188.
- Joanisse, D., Storey, K.** (1994a). Enzyme activity profiles in an overwintering population of freeze-tolerant larvae of the gall fly, *Eurosta solidaginis*. *Journal of Comparative Physiology B* **164**, 247-255.
- Joanisse, D.R., Storey, K.B.** (1994b). Mitochondrial enzymes during overwintering in two species of cold-hardy gall insects. *Insect Biochemistry and Molecular Biology* **24**, 145-150.
- Keeley, L., Moody, D., Lynn, D., Joiner, R., Vinson, S.** (1977). Succinate-cytochrome c reductase activity and lipids in diapause and non-diapause *Anthonomus grandis* from different latitudes. *Journal of Insect Physiology* **23**, 231-234.
- Kim, M., Robich, R.M., Rinehart, J.P., Denlinger, D.L.** (2006). Upregulation of two actin genes and redistribution of actin during diapause and cold stress in the northern house mosquito, *Culex pipiens*. *Journal of Insect Physiology* **52**, 1226-1233.
- Košťál, V., Šlachta, M., Šimek, P.** (2001). Cryoprotective role of polyols independent of the increase in supercooling capacity in diapausing adults of *Pyrrhocoris apterus* (Heteroptera: Insecta). *Comparative Biochemistry and Physiology Part B: Biochemistry and Molecular Biology* **130**, 365-374.
- Košťál, V.** (2006). Eco-physiological phases of insect diapause. *Journal of Insect Physiology* **52**, 113-127.
- Košťál, V., Renault, D., Mehrabianova, A., Bastl, J.** (2007). Insect cold tolerance and repair of chill-injury at fluctuating thermal regimes: role of ion homeostasis. *Comparative Biochemistry and Physiology Part A: Molecular & Integrative Physiology* **147**, 231-238.
- Košťál, V., Tollarová-Borovanská, M.** (2009). The 70 kDa heat shock protein assists during the repair of chilling injury in the insect, *Pyrrhocoris apterus*. *PloS one* **4**, e4546.
- Košťál, V., Zahradníčková, H., Šimek, P.** (2011). Hyperprolinemic larvae of the drosophilid fly, *Chymomyza costata*, survive cryopreservation in liquid nitrogen. *Proceedings of the National Academy of Sciences of the U.S.A* **108**, 13041-13046.
- Kukal, O., Denlinger, D.L., Lee, R.E.** (1991). Developmental and metabolic changes induced by anoxia in diapausing and non-diapausing flesh fly pupae. *Journal of Comparative Physiology B* **160**, 683-689.

- Kukal, O., Duman, J.G., Serianni, A.S.** (1989). Cold-induced mitochondrial degradation and cryoprotectant synthesis in freeze-tolerant arctic caterpillars. *Journal of Comparative Physiology B* **158**, 661-671.
- Laufen, T., Mayer, M.P., Beisel, C., Klostermeier, D., Mogk, A., Reinstein, J., Bukau, B.** (1999). Mechanism of regulation of hsp70 chaperones by DnaJ cochaperones. *Proceedings of the National Academy of Sciences of the U.S.A* **96**, 5452-5457.
- Leather, S.R., Walters, K.F., Bale, J.S.** (1995). The ecology of insect overwintering. Cambridge University Press.
- Lebenzon, J.E., Des Marteaux, L.E., Sinclair, B.J.** (2020). Reversing sodium differentials between the hemolymph and hindgut speeds chill coma recovery but reduces survival in the fall field cricket, *Gryllus pennsylvanicus*. *Comparative Biochemistry and Physiology Part A: Molecular & Integrative Physiology* **244**, 110699.
- Lee, R.E., Costanzo, J.P., Kaufman, P.E., Lee, M.R., Wyman, J.A.** (1994). Ice-nucleating active bacteria reduce the cold-hardiness of the freeze-intolerant Colorado potato beetle (Coleoptera: Chrysomelidae). *Journal of Economic Entomology* **87**, 377-381.
- Lee, R.E., Denlinger, D.L.** (1985). Cold tolerance in diapausing and non-diapausing stages of the flesh fly, *Sarcophaga crassipalpis*. *Physiological Entomology* **10**, 309-315.
- Lee, R.E.** (1991). Principles of insect low temperature tolerance In *Insects at Low Temperature*. (eds. R.E. Lee, D.L. Denlinger, pp. 17-46. Springer.
- Lee, R.E., McGrath, J.J., Morason, R.T., Taddeo, R.M.** (1993). Survival of intracellular freezing, lipid coalescence and osmotic fragility in fat body cells of the freeze-tolerant gall fly *Eurosta solidaginis*. *Journal of Insect Physiology* **39**, 445-450.
- Lefevere, K.** (1989). Endocrine control of diapause termination in the adult female Colorado potato beetle, *Leptinotarsa decemlineata*. *Journal of Insect Physiology* **35**, 197-203.
- Lefevere, K., Koopmanschap, A., De Kort, C.** (1989). Changes in the concentrations of metabolites in haemolymph during and after diapause in female Colorado potato beetle, *Leptinotarsa decemlineata*. *Journal of Insect Physiology* **35**, 121-128.
- Lehmann, P., Kaunisto, S., Košťál, V., Margus, A., Zahradníčková, H., Lindström, L.** (2015a). Comparative ecophysiology of cold-tolerance-related traits: assessing range expansion potential for an invasive insect at high latitude. *Physiological and Biochemical Zoology* **88**, 254-265.

- Lehmann, P., Lyytinen, A., Piironen, S., Lindström, L.** (2014). Northward range expansion requires synchronization of both overwintering behaviour and physiology with photoperiod in the invasive Colorado potato beetle (*Leptinotarsa decemlineata*). *Oecologia* **176**, 57-68.
- Lehmann, P., Lyytinen, A., Piironen, S., Lindström, L.** (2015b). Latitudinal differences in diapause related photoperiodic responses of European Colorado potato beetles (*Leptinotarsa decemlineata*). *Evolutionary ecology* **29**, 269-282.
- Lehmann, P., Piironen, S., Lyytinen, A., Lindström, L.** (2015c). Responses in metabolic rate to changes in temperature in diapausing Colorado potato beetle *Leptinotarsa decemlineata* from three European populations. *Physiological Entomology* **40**, 123-130.
- Lehmann, P., Westberg, M., Tang, P., Lindström, L., Käckelä, R.** (2020). The diapause lipidomes of three closely related beetle species reveal mechanisms for tolerating energetic and cold stress in high-latitude seasonal environments. *Frontiers in Physiology* **11**, 1219.
- Levenbook, L.** (1953). The mitochondria of insect flight muscle. *Journal of Histochemistry & Cytochemistry* **1**, 242-247.
- Li, S., Yu, X., Feng, Q.** (2019). Fat body biology in the last decade. *Annual Review of Entomology* **64**, 315-333.
- Longworth, L.** (1954). Temperature dependence of diffusion in aqueous solutions. *Journal of Physical Chemistry* **58**, 770-773.
- Lyytinen, A., Mappes, J., Lindström, L.** (2012). Variation in Hsp70 levels after cold shock: signs of evolutionary responses to thermal selection among *Leptinotarsa decemlineata* populations. *PLoS One* **7**, e31446.
- MacDonald, J.A., Storey, K.B.** (1999). Regulation of ground squirrel Na⁺ K⁺-ATPase activity by reversible phosphorylation during hibernation. *Biochemical and Biophysical Research Communications* **254**, 424-429.
- MacMillan, H.A., Sinclair, B.J.** (2011) The role of the gut in insect chilling injury: cold-induced disruption of osmoregulation in the fall field cricket, *Gryllus pennsylvanicus*. *Journal of Experimental Biology* **214**, 726-734.
- MacMillan, H.A., Baatrup, E., Overgaard, J.** (2015). Concurrent effects of cold and hyperkalaemia cause insect chilling injury. *Proceedings of the Royal Society B* **282**, 20151483.
- MacRae, T.H.** (2010). Gene expression, metabolic regulation and stress tolerance during diapause. *Cellular and Molecular Life Sciences* **67**, 2405-2424.

- Mansingh, A., Smallman, B.** (1966). Photoperiod control of an ‘obligatory’ pupal diapause. *Canadian Entomologist* **98**, 613-616.
- Marshall, K.E., Gotthard, K., Williams, C.M.** (2020). Evolutionary impacts of winter climate change on insects. *Current Opinion in Insect Science*. **41**, 54-62.
- Marshall, K.E., Roe, A.D.** (2021). Surviving in a frozen forest: the physiology of eastern spruce budworm overwintering. *Physiology* **36**, 174-182.
- Masaki, S.** (1980). Summer diapause. *Annual Review of Entomology* **25**, 1-25.
- Mathers, K.E., McFarlane, S.V., Zhao, L., Staples, J.F.** (2017). Regulation of mitochondrial metabolism during hibernation by reversible suppression of electron transport system enzymes. *Journal of Comparative Physiology B* **187**, 227-234.
- Michaud, M.R., Denlinger, D.L.** (2007). Shifts in the carbohydrate, polyol, and amino acid pools during rapid cold-hardening and diapause-associated cold-hardening in flesh flies (*Sarcophaga crassipalpis*): a metabolomic comparison. *Journal of Comparative Physiology B* **177**, 753-763.
- Overgaard, J., Gerber, L., Andersen, M.K.** (2021). Osmoregulatory capacity at low temperature is critical for insect cold tolerance. *Current Opinion in Insect Science* **47**, 38-45.
- Overgaard, J., MacMillan, H.A.** (2017). The integrative physiology of insect chill tolerance. *Annual Review of Physiology* **79**, 187-208.
- Pegoraro, A.F., Janmey, P., Weitz, D.A.** (2017). Mechanical properties of the cytoskeleton and cells. *Cold Spring Harbor Perspectives in Biology* **9**, a022038.
- Piironen, S., Ketola, T., Lyytinen, A., Lindström, L.** (2011). Energy use, diapause behaviour and northern range expansion potential in the invasive Colorado potato beetle. *Functional Ecology* **25**, 527-536.
- Poelchau, M.F., Reynolds, J.A., Elsik, C.G., Denlinger, D.L., Armbruster, P.A.** (2013). RNA-Seq reveals early distinctions and late convergence of gene expression between diapause and quiescence in the Asian tiger mosquito, *Aedes albopictus*. *Journal of Experimental Biology* **216**, 4082-4090.
- Privalov, P.L.** (1990). Cold denaturation of protein. *Critical Reviews in Biochemistry and Molecular Biology* **25**, 281-306.
- Pullin, A., Wolda, H.** (1993). Glycerol and glucose accumulation during diapause in a tropical beetle. *Physiological Entomology* **18**, 75-78.

- Rader, R., Bartomeus, I., Garibaldi, L.A., Garratt, M.P., Howlett, B.G., Winfree, R., Cunningham, S.A., Mayfield, M.M., Arthur, A.D., Andersson, G.K.** (2016). Non-bee insects are important contributors to global crop pollination. *Proceedings of the National Academy of Sciences of the U.S.A* **113**, 146-151.
- Ramløv, H., Lee, R.E.** (2000). Extreme resistance to desiccation in overwintering larvae of the gall fly *Eurosta solidaginis* (Diptera, Tephritidae). *Journal of Experimental Biology* **203**, 783-789.
- Reeg, S., Jung, T., Castro, J.P., Davies, K.J., Henze, A., Grune, T.** (2016). The molecular chaperone Hsp70 promotes the proteolytic removal of oxidatively damaged proteins by the proteasome. *Free Radical Biology and Medicine* **99**, 153-166.
- Rickards, J., Kelleher, M.J., Storey, K.B.** (1987). Strategies of freeze avoidance in larvae of the goldenrod gall moth, *Epiblema scudderiana*: winter profiles of a natural population. *Journal of Insect Physiology* **33**, 443-450.
- Rider, M.H., Hussain, N., Dilworth, S.M., Storey, J.M., Storey, K.B.** (2011). AMP-activated protein kinase and metabolic regulation in cold-hardy insects. *Journal of Insect Physiology* **57**, 1453-1462.
- Rinehart, J.P., Li, A., Yocum, G.D., Robich, R.M., Hayward, S.A., Denlinger, D.L.** (2007). Up-regulation of heat shock proteins is essential for cold survival during insect diapause. *Proceedings of the National Academy of Sciences of the U.S.A.* **104**, 11130-11137.
- Rosenzweig, R., Nillegoda, N.B., Mayer, M.P., Bukau, B.** (2019). The Hsp70 chaperone network. *Nature Reviews Molecular Cell Biology* **20**, 665-680.
- Salt, R.W.** (1933). Some experiments on the freezing and hardening of the adults of the Colorado potato beetle, *Leptinotarsa decemlineata* Say. PhD Thesis. Bozeman, Montana, U.S.A: Montana State University.
- Saunders, D.S.** (2019). Dormancy, diapause, and the role of the circadian system in insect photoperiodism. *Annual Review of Entomology* **65**, 373-389.
- Sawchyn, W., Church, N.** (1973). The effects of temperature and photoperiod on diapause development in the eggs of four species of *Lestes* (Odonata: Zygoptera). *Canadian Journal of Zoology* **51**, 1257-1265.
- Schou, M.F., Mouridsen, M.B., Sørensen, J.G., Loeschcke, V.** (2017). Linear reaction norms of thermal limits in *Drosophila*: predictable plasticity in cold but not in heat tolerance. *Functional Ecology* **31**, 934-945.

- Schoville, S.D., Chen, Y.H., Andersson, M.N., Benoit, J.B., Bhandari, A., Bowsher, J.H., Brevik, K., Cappelle, K., Chen, M.J.M., Childers, A.K., Childers, C., Christiaens, O., Clements, J., Didion, E.M., Elpidina, E.N., Engsontia, P., Friedrich, M., Garcia-Robles, I., Gibbs, R.A., Goswami, C., Grapputo, A., Gruden, K., Grynberg, M., Henrissat, B., Jennings, E.C., Jones, J.W., Kalsi, M., Khan, S.A., Kumar, A., Li, F., Lombard, V., Ma, X., Martynov, A., Miller, N.J., Mitchell, R.F., Munoz-Torres, M., Muszewska, A., Oppert, B., Palli, S.R., Panfilio, K.A., Pauchet, Y., Perkin, L.C., Petek, M., Poelchau, M.F., Record, E., Rinehart, J.P., Robertson, H.M., Rosendale, A.J., Ruiz-Arroyo, V.M., Smagghe, G., Szendrei, Z., Thomas, G.W.C., Torson, A.S., Jentzsch, I.M.V., Weirauch, M.T., Yates, A.D.T., Yocum, G.D., Yoon, J.S., Richards, S.** (2018). A model species for agricultural pest genomics: the genome of the Colorado potato beetle, *Leptinotarsa decemlineata* (Coleoptera: Chrysomelidae). *Scientific Reports* **8**, 1931.
- Senanayake, D.G., Radcliffe, E.B., Holliday, N.J.** (2000). Oviposition and diapause behavior in Colorado potato beetle (Coleoptera: Chrysomelidae) populations from East Central Minnesota and the valley of the Red River of the North. *Environmental Entomology* **29**, 1123-1132.
- Shappirio, D., Williams, C.** (1957). The cytochrome system of the *Cecropia* silkworm. II. Spectrophotometric studies of oxidative enzyme systems in the wing epithelium. *Proceedings of the Royal Society B* **147**, 233-246.
- Sim, C., Denlinger, D.L.** (2008). Insulin signaling and FOXO regulate the overwintering diapause of the mosquito *Culex pipiens*. *Proceedings of the National Academy of Sciences of the U.S.A.* **105**, 6777-6781.
- Sim, C., Kang, D.S., Kim, S., Bai, X., Denlinger, D.L.** (2015). Identification of FOXO targets that generate diverse features of the diapause phenotype in the mosquito *Culex pipiens*. *Proceedings of the National Academy of Sciences of the U.S.A.* **112**, 3811-3816.
- Sinclair, B.J.** (2015). Linking energetics and overwintering in temperate insects. *Journal of Thermal Biology* **54**, 5-11.
- Sinclair, B.J., Addo-Bediako, A., Chown, S.L.** (2003). Climatic variability and the evolution of insect freeze tolerance. *Biological Reviews* **78**, 181-195.
- Sinclair, B.J., Alvarado, L.E.C., Ferguson, L.V.** (2015). An invitation to measure insect cold tolerance: methods, approaches, and workflow. *Journal of Thermal Biology* **53**, 180-197.
- Sinclair, B.J., Marshall, K.E.** (2018). The many roles of fats in overwintering insects. *Journal of Experimental Biology* **221**, jeb161836.

- Sonoda, S., Fukumoto, K., Izumi, Y., Yoshida, H., Tsumuki, H.** (2006). Cloning of heat shock protein genes (hsp90 and hsc70) and their expression during larval diapause and cold tolerance acquisition in the rice stem borer, *Chilo suppressalis* Walker. *Archives of Insect Biochemistry and Physiology* **63**, 36-47.
- Sorger, P.K.** (1991). Heat shock factor and the heat shock response. *Cell* **65**, 363-366.
- Sota, T., Mogi, M.** (1992). Survival time and resistance to desiccation of diapause and non-diapause eggs of temperate *Aedes* (Stegomyia) mosquitoes. *Entomologia experimentalis et applicata* **63**, 155-161.
- Staples, J.F., Buck, L.T.** (2009). Matching cellular metabolic supply and demand in energy-stressed animals. *Comparative Biochemistry and Physiology Part A: Molecular & Integrative Physiology* **153**, 95-105.
- Stegwee, D., Kimmel, E., De Boer, J., Henstra, S.** (1963). Hormonal control of reversible degeneration of flight muscle in the Colorado potato beetle, *Leptinotarsa decemlineata* Say (Coleoptera). *The Journal of Cell Biology* **19**, 519-527.
- Štětina, T., Hůla, P., Moos, M., Šimek, P., Šmilauer, P., Košťál, V.** (2018). Recovery from supercooling, freezing, and cryopreservation stress in larvae of the drosophilid fly, *Chymomyza costata*. *Scientific Reports* **8**, 1-13.
- Storey, J.M., Storey, K.B.** (1983). Regulation of cryoprotectant metabolism in the overwintering gall fly larva, *Eurosta solidaginis*: temperature control of glycerol and sorbitol levels. *Journal of Comparative Physiology* **149**, 495-502.
- Storey, K.B., Storey, J.M.** (1991). Biochemistry of cryoprotectants, In *Insects at Low Temperature*. (eds. R.E. Lee, D.L. Denlinger), pp. 64-93. Springer.
- Storey, K.B., Storey, J.M.** (2012). Insect cold hardiness: metabolic, gene and protein adaptation. *Canadian Journal of Zoology* **90**, 456-475.
- Tan, Q.-Q., Liu, W., Zhu, F., Lei, C.-L., Wang, X.-P.** (2017). Fatty acid synthase 2 contributes to diapause preparation in a beetle by regulating lipid accumulation and stress tolerance genes expression. *Scientific Reports* **7**, 1-11.
- Tanaka, S., Denlinger, D.L., Wolda, H.** (1988). Seasonal changes in the photoperiodic response regulating diapause in a tropical beetle, *Stenotarsus rotundus*. *Journal of Insect Physiology* **34**, 1135-1142.
- Tauber, M.J., Tauber, C.A.** (1976). Insect seasonality: diapause maintenance, termination, and postdiapause development. *Annual Review of Entomology* **21**, 81-107.

- Teets, N.M., Kawarasaki, Y., Lee, R.E., Denlinger, D.L.** (2013). Expression of genes involved in energy mobilization and osmoprotectant synthesis during thermal and dehydration stress in the Antarctic midge, *Belgica antarctica*. *Journal of Comparative Physiology B* **183**, 189-201.
- Teets, N.M., Elnitsky, M.A., Benoit, J.B., Lopez-Martinez, G., Denlinger, D.L., Lee, R.E.** (2008). Rapid cold-hardening in larvae of the Antarctic midge *Belgica antarctica*: cellular cold-sensing and a role for calcium. *American Journal of Physiology* **294**, R1938-46.
- Tollarová-Borovanská, M., Lalouette, L., Košťál, V.** (2009). Insect cold tolerance and repair of chill-injury at fluctuating thermal regimes: Role of 70 kDa heat shock protein expression. *CryoLetters* **30**, 312-319.
- Tombes, A.S.** (1966). Aestivation (Summer Diapause) in *Hypera postica* (Coleoptera: Curculionidae). I. Effect of Aestivation, Photoperiods, and Diet on Total Fatty Acids. *Annals of the Entomological Society of America* **59**, 376-380.
- Tomcala, A., Tollarová, M., Overgaard, J., Simek, P., Košťál, V.** (2006). Seasonal acquisition of chill tolerance and restructuring of membrane glycerophospholipids in an overwintering insect: triggering by low temperature, desiccation and diapause progression. *Journal of Experimental Biology* **209**, 4102-4114.
- Torson, A.S., Zhang, M.L., Smith, A.J., Mohammad, L., Ong, K., Doucet, D., Roe, A.D., Sinclair, B.J.** (2021). Dormancy in laboratory-reared Asian longhorned beetles, *Anoplophora glabripennis*. *Journal of Insect Physiology* **130**, 104179.
- Toxopeus, J., Košťál, V., Sinclair, B.J.** (2019a). Evidence for non-colligative function of small cryoprotectants in a freeze-tolerant insect. *Proceedings of the Royal Society B* **286**, 20190050.
- Toxopeus, J., McKinnon, A.H., Štětina, T., Turnbull, K.F., Sinclair, B.J.** (2019b). Laboratory acclimation to autumn-like conditions induces freeze tolerance in the spring field cricket *Gryllus veletis* (Orthoptera: Gryllidae). *Journal of Insect Physiology* **113**, 9-16.
- Udaka, H., Sinclair, B.J.** (2014) The overwintering biology of the acorn weevil, *Curculio glandium* in southwestern Ontario. *Journal of Thermal Biology* **44**, 103-109.
- Vermunt, A., Koopmanschap, A., Vlak, J., De Kort, C.** (1998). Evidence for two juvenile hormone esterase-related genes in the Colorado potato beetle. *Insect Molecular Biology* **7**, 327-336.
- Vincent, J.F., Wegst, U.G.** (2004). Design and mechanical properties of insect cuticle. *Arthropod Structure & Development* **33**, 187-199.

- Walters, R.J., Hassall, M., Telfer, M.G., Hewitt, G.M., Palutikof, J.P.** (2006). Modelling dispersal of a temperate insect in a changing climate. *Proceedings of the Royal Society B* **273**, 2017-2023.
- Westbrook, J.K., Nagoshi, R.N., Meagher, R.L., Fleischer, S.J., Jairam, S.** (2016) Modeling seasonal migration of fall armyworm moths. *International Journal of Biometeorology* **60**, 255-267.
- White, C.R., Blackburn, T.M., Terblanche, J.S., Marais, E., Gibernau, M., Chown, S.L.** (2007). Evolutionary responses of discontinuous gas exchange in insects. *Proceedings of the National Academy of Sciences of the U.S.A.* **104**, 8357-8361.
- Williams, C.M., Henry, H.A., Sinclair, B.J.** (2015). Cold truths: how winter drives responses of terrestrial organisms to climate change. *Biological Reviews* **90**, 214-235.
- Wilsterman, K., Ballinger, M.A., Williams, C.M.** (2021). A unifying, eco-physiological framework for animal dormancy. *Functional Ecology* **35**, 11-31.
- Yocum, G.** (2001). Differential expression of two HSP70 transcripts in response to cold shock, thermoperiod, and adult diapause in the Colorado potato beetle. *Journal of Insect Physiology* **47**, 1139-1145.
- Yocum, G.D., Buckner, J.S., Fatland, C.L.** (2011a). A comparison of internal and external lipids of nondiapausing and diapause initiation phase adult Colorado potato beetles, *Leptinotarsa decemlineata*. *Comparative Biochemistry and Physiology Part B: Biochemistry and Molecular Biology* **159**, 163-170.
- Yocum, G.D., Rinehart, J.P., Larson, M.L.** (2011b). Monitoring diapause development in the Colorado potato beetle, *Leptinotarsa decemlineata*, under field conditions using molecular biomarkers. *Journal of Insect Physiology* **57**, 645-652.
- Zachariassen, K.E.** (1985). Physiology of cold tolerance in insects. *Physiological Reviews* **65**, 799-832.
- Zachariassen, K.E., Husby, J.A.** (1982). Antifreeze effect of thermal hysteresis agents protects highly supercooled insects. *Nature* **298**, 865-867.
- Zachariassen, K.E., Kristiansen, E.** (2000). Ice nucleation and antinucleation in nature. *Cryobiology* **41**, 257-279.
- Zhou, G., Miesfeld, R.L.** (2009). Energy metabolism during diapause in *Culex pipiens* mosquitoes. *Journal of insect physiology* **55**, 40-46.

Chapter 2

2 Diapause differentially modulates the transcriptomes of fat body and flight muscle in the Colorado potato beetle.

A version of this chapter was published in *Comparative Biochemistry and Physiology D: Genomics and Proteomics*. Re-print permission can be found in Appendix A.

Lebenzon, J.E., Torson, A.S., Sinclair, B.J. (2021). Diapause differentially modulates the transcriptomes of fat body and flight muscle in the Colorado potato beetle *Comparative Biochemistry and Physiology D* **40**, 100906.

2.1 Introduction

Temperate insects may spend over half their lives overwintering, during which they encounter sub-zero temperatures, low resource availability, and (in enclosed microhabitats) hypoxia (Kukal et al., 1991; Sinclair, 2015; Zachariassen, 1985). Before the onset of winter, many insects enter diapause, a preprogrammed state of developmental arrest that is often accompanied by metabolic suppression and increased stress tolerance (Hahn and Denlinger, 2007; Košťál, 2006). In adult insects, diapause is often cued when decreasing daylength initiates a neuropeptide-mediated cessation of juvenile hormone (JH) production (Denlinger et al., 2004; Košťál, 2006) and a downstream signaling cascade resulting in the initiation of diapause. Diapausing insects preferentially use lipid as a metabolic fuel (Hahn and Denlinger, 2007), can depress their metabolic rate by as much as 90 % (Denlinger, 1972), arrest their cell cycles (Košťál et al., 2009), increase their overall stress tolerance (Lee and Denlinger, 1985), and are generally unresponsive to changing environmental conditions (Denlinger, 2002). Diapause is terminated after a pre-determined amount of time has elapsed or by satisfaction of environmental exposure (*e.g.*, chilling; Dambroski and Feder, 2007; Dong et al., 2013) and post-diapause insects often remain quiescent, resuming normal development when permissive conditions return (Košťál, 2006).

Preparation for, initiation, and maintenance of diapause in adult insects is partly mediated by changes in gene expression. During diapause preparation in many adult insects, the abundance of transcripts involved in the insulin signaling pathway, such as those that encode insulin-like peptides and their receptors, decrease (Denlinger et al., 2004). Downregulation of

insulin signaling pathways change the activity of Fork head box transcription factor (FOXO) and elicits downstream transcription of genes involved in fatty acid synthesis, facilitating lipid accumulation (Sim and Denlinger, 2008, 2013). Development is arrested at species- and tissue-specific cell cycle stages, likely governed by the increased abundance of transcripts that inhibit cell cycle progression, such as *Wee-1-like protein kinase* and *Myelin transcription factor 1* (Košťál et al., 2009), and by the decreased abundance of transcripts encoding proteins that promote progression of the cell cycle, such as *proliferating cell nuclear antigen* (*PCNA*; Košťál et al., 2009; Tammariello and Denlinger, 1998). Once in diapause, transcripts encoding stress-related proteins are differentially expressed, including heat shock proteins (such as HSP70; Yocum, 2001), late embryogenesis abundant (LEA) proteins (Des Marteaux et al., 2019), and antioxidant enzymes (*e.g.*, catalase and superoxide dismutase; Sim and Denlinger, 2011). Although we broadly understand the general patterns of gene expression during diapause initiation, we know far less about the specific genes and their products that drive and maintain the diapause phenotype, especially in adult diapausing insects.

Most studies of diapausing insects to date have focused on whole animal gene expression (*e.g.*, Deng et al., 2018; Poelchau et al., 2013; Ragland et al., 2010; Sim and Denlinger, 2009; Zhou et al., 2021; Kang et al., 2016) which might mask transcriptional changes that are antagonistic between tissues and would cancel out at the whole-animal level (See Torson et al., 2020 for discussion). Some studies have focused on gene expression in the brain (*e.g.*, Tammariello and Denlinger, 1998) or reproductive tissue (*e.g.*, Poelchau et al., 2011), which identified mechanisms underlying neuroendocrine regulatory processes and reproductive arrest, respectively. Thus, there is a need to extend beyond regulation to study tissue-specific gene expression to better explore processes underlying the canonical insect diapause phenotypes (metabolic suppression and increased cellular stress tolerance).

I expect that gene expression should differ among tissues during diapause. For example, the fat body synthesizes hexamerin storage proteins during diapause, and is the main site of lipid and amino acid metabolism (Dortland, 1978, 1979; Hahn and Denlinger, 2011; Weeda et al., 1980). By contrast, flight muscle is inactive in dormant adults, and even degraded in some diapausing species (Bhakthan et al., 1970). Thus, I would predict an increase in abundance of transcripts that encode proteins involved in lipid metabolism (in insects that use lipid as fuel

throughout diapause) in the fat body during diapause. By contrast, because we do not know whether this degradation happens entirely during diapause initiation, or continues throughout diapause maintenance, I would predict increased abundance of transcripts associated with tissue degradation in the flight muscle during diapause. I also expect there to be a set of core diapause-related genes that are ubiquitously adjusted in most tissues and cell types in response to environmental stressors. For example, I expect increased expression in most tissues of heat shock proteins that promote correct folding and ensure protein quality control (Zhang and Denlinger, 2010); actin and tubulin cytoskeletal proteins which maintain cell structural integrity (Kim et al., 2006); and enzymes which mediate energy metabolism and ATP-producing and -consuming pathways.

The Colorado potato beetle (CPB; *Leptinotarsa decemlineata*; Coleoptera: Chrysomelidae) is a global pest of potato plants. Since the mid-19th Century, the range of CPB has expanded from South America to most of North America and Europe (Lehmann et al., 2014a). Colorado potato beetles overwinter in the soil as diapausing adults (De Wilde, 1960). Diapause in CPB is induced by short photoperiods, which cue a decrease in circulating juvenile hormone *via* an increase in juvenile hormone esterase activity and decrease in juvenile hormone biosynthesis by the *corpora allata* (De Kort et al., 1980; De Wilde et al., 1959; Lefevre and De Wilde, 1984). Diapause preparation in CPB is accompanied by the accumulation of triacylglycerols, and the synthesis of hexamerin storage proteins in the fat body (Yocum et al., 2011a). During diapause maintenance, CPB depress their metabolic rates, degrade their flight muscle, and increase their cold and stress tolerance (Stegwee et al. 1963; Boiteau and Coleman, 1996; Yocum et al., 2009). Despite having a broad understanding of diapause in CPB on a whole-organism level (see de Kort, 1990, for a summary) we understand less about its tissue-specific gene expression during diapause.

Several transcripts that are differentially expressed during preparation for, initiation, or maintenance of diapause have been associated with diapause in CPB (Lehmann et al., 2014b; Yocum, 2003; Yocum et al., 2009a). For example, two isoforms of *HSP70* (*HSP70a* and *HSP70b*) are differentially expressed during CPB diapause maintenance, presumably protecting cells from cold and other stress-induced damage during diapause (Yocum, 2001). Other transcripts associated with diapause in CPB are those which encode proteins involved

in immune response (*e.g.*, serine proteases), digestion (*e.g.*, digestive cysteine proteinase), and juvenile hormone metabolism (*e.g.*, juvenile hormone esterase; Lehmann et al., 2014b; Yocum, 2003). In addition, many transcripts that have been identified as “diapause-associated” in CPB are currently unannotated and therefore have unknown functions (*e.g.*, *diapause-associated transcript 1* and *diapause associated transcript 2*; Lehmann et al., 2014b; Vermunt et al., 1998; Yocum et al., 2009a; Yocum et al., 2009b). All studies to date on gene expression during diapause in CPB used RNA extracted from homogenized whole beetles and therefore do not account for any tissue-specific processes during diapause.

Here, I used RNA-seq to compare the transcriptomes of fat body and flight muscle from non-diapausing and diapausing CPB (Figure 1.1). Fat body and flight muscle should have distinct roles in metabolism, and therefore differing roles and responses to diapause. I use this dataset to evaluate several standing hypotheses (outlined in Figure 2.1) from the literature regarding how physiology is altered to produce a diapause phenotype in insects. From these hypotheses, I predict that diapausing CPB will differentially express transcripts relating to developmental arrest, lipid metabolism, metabolic suppression, and stress tolerance and that differential expression will be tissue-specific (Figure 2.1). Finally, I use this transcriptome data to generate new hypotheses about biological processes that could drive the diapause phenotype in CPB.

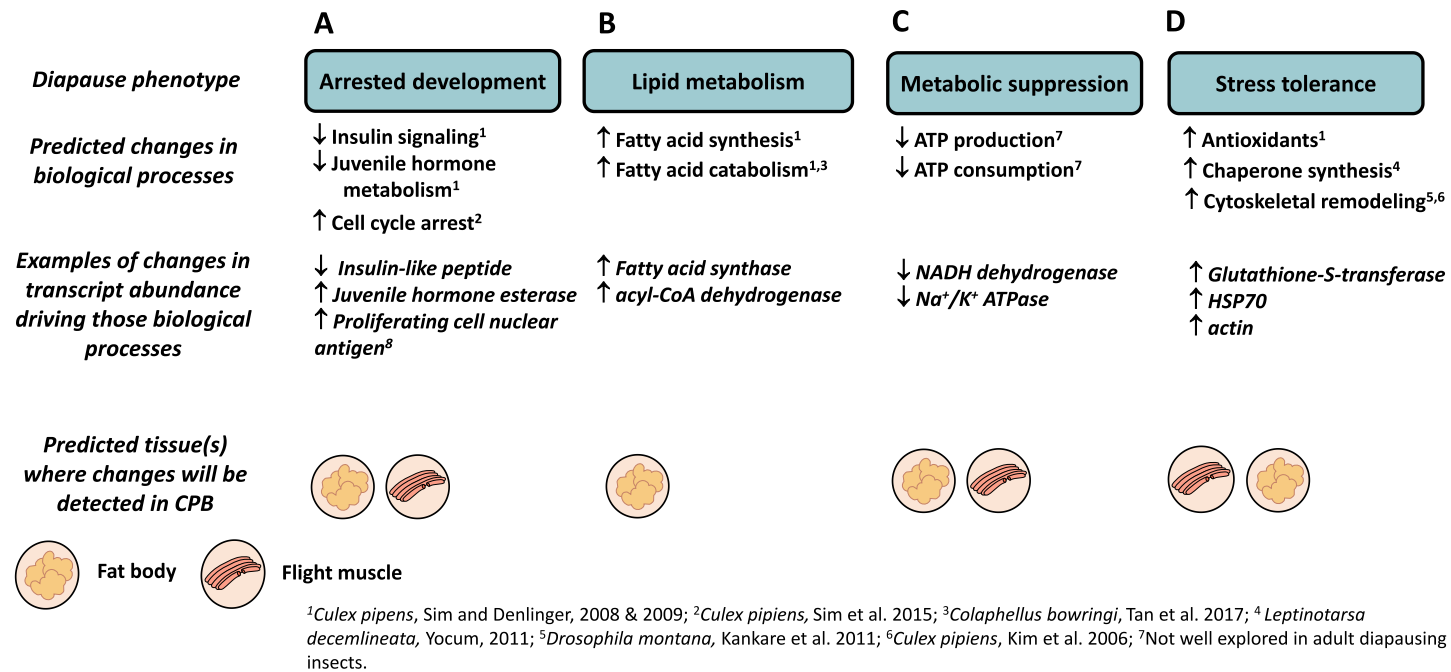


Figure 2.1. Schematic of the predictions I make based on hypotheses of how gene expression will change during diapause in fat body and flight muscle of diapausing Colorado potato beetles. (A) I predict that arrested development in diapausing CPB is driven by decreases in the abundance of transcripts involved in insulin signaling, and cell cycle arrest (or decreases in those involved in cell cycle progression), and these changes will occur in both the fat body and flight muscle. (B) I predict that lipid accumulation and use in diapausing CPB is driven by increases in abundance of transcripts involved in fatty acid synthesis and catabolism, and that I will detect these changes in the fat body, where lipid metabolism primarily occurs. (C) I predict that metabolic suppression in diapausing CPB will be driven by decreases in the abundance of transcripts involved in ATP production and consumption. I have no a priori reasons to predict which tissues this will occur in. (D) I predict that stress tolerance in diapausing CPB is driven by increases in the abundance of transcripts involved in the hypoxia response, protein chaperone synthesis, and cytoskeletal remodeling, and that I will detect these changes in both the flight muscle and fat body, as both are metabolically important tissues and would require protection during the winter. All of the above hypotheses are based on physiological and transcriptomic data on adult diapausing species from the literature and physiological and gene expression data on CPB, where cited.

2.2 Materials and Methods

2.2.1 Insect care and diapause induction

I established a colony of *L. decemlineata* with individuals originally collected from potato fields at the London Research and Development Centre in London, Ontario, Canada and maintained it in greenhouses at the University of Western Ontario. The population was first established in 2015 from a laboratory population in the research laboratories at the London Research and Development Centre and supplemented annually with c. 50 field-collected individuals to reduce inbreeding. For general rearing (control, non-diapausing beetles), I maintained eggs, larvae, and adults on fresh Kennebec potato plants in BugDorms (Megaview science, Talchung, Taiwan, W60 × D60 × H60 cm) at 24 °C under a long daylength (16:8 L:D). I allowed adults to freely mate and lay eggs on plants in the BugDorms. I induced diapause following Yocum (2001). Briefly, I reared eggs laid by control adults on excised potato leaves in petri dishes lined with moist paper towel in temperature and light-controlled incubators (Sanyo Scientific, Bensenville, IL, USA) at 24 °C and short days (8:16 L:D). I transferred newly hatched larvae to 500 mL plastic containers lined with moistened paper towels and fed them daily with fresh potato leaves. I maintained larvae in groups of c. 20 in these bins. I transferred 4th instar larvae to 14 L plastic pupation bins filled with sandy soil and provided them fresh leaves daily until larvae burrowed into the soil to pupate. Once adults emerged from the soil, I transferred them to fresh plastic bins filled with soil and kept them at 15 °C (8:16 L:D), which I refer to as diapause-inducing conditions. I kept 20-30 beetles in each diapausing bin and fed these diapause-destined adults fresh potato leaves daily for 3-4 weeks after which they stopped eating and burrowed into the soil. I did not observe any females laying eggs in these diapause-destined populations. I used adults nine weeks after emergence (*i.e.*, nine weeks after transfer to diapause-inducing conditions as adults) because I observed that these individuals are at a state of maximal metabolic suppression (Chapter 3) and therefore most likely in the maintenance stage of their diapause programme.

2.2.2 Tissue dissection, RNA extraction, cDNA library preparation and sequencing

I dissected approximately 5 mg of abdominal fat body and flight muscle tissue from age-control beetles (nine weeks old, under control conditions, *i.e.*, 24 °C, long days), and from diapausing beetles (nine weeks old, under diapause-inducing conditions, *i.e.*, 15 °C, short days). I dissected flight muscle by gently pulling off fiber bundles of dorsal longitudinal and dorsoventral muscle attached to the thorax, and fat body by gently lifting fat body from the abdominal cavity. I dissected tissues in phosphate buffered saline, blotted excess liquid, and placed the tissue into a pre-weighed 1.7 mL nuclease-free microcentrifuge tube. I flash-froze the samples in liquid nitrogen and stored the tissue at –80 °C until RNA extraction. I generated mRNA libraries from three biological replicates of each tissue (fat body and flight muscle) from control, non-diapausing, beetles, and three biological replicates of each tissue from diapausing beetles. Each biological replicate consisted of c. 5 mg of pooled tissue from each of eight individuals of mixed sex.

I homogenized each tissue sample with a plastic pestle in 500 µl of TRIzol reagent (ThermoFisher Scientific, Mississauga, Ontario, Canada), and extracted RNA according to the manufacturer's protocol. I sent samples to Génome Québec (Montreal, Quebec, Canada) where they were quality-checked (2100 Bioanalyzer, Agilent, Santa Clara, California, USA), and cDNA libraries were prepared from mRNA. Libraries were sequenced using 125 bp paired-end sequencing on the Illumina HiSeq 2500 platform (Illumina, San Diego, California, USA).

2.2.3 Transcriptome assembly and annotation

I used fastp, a program used to process RNA-seq reads produced from sequencing (version 0.19.7; Chen et al., 2018), to trim adaptor sequences from the RNA-seq reads and to filter out any sequences with a Phred score below 15. A Phred score below 15 indicates that the reads produced from sequencing are of poor quality. I used the program FastQC (version 0.11.8; Andrews, 2010) to check the quality of all my reads before and after trimming by fastp. I mapped quality-trimmed reads to the reference *L. decemlineata* genome (Schoville et al., 2018; Lepdec_OGSV1.1, Bioproject PRJNA171749, available at

<https://www.ncbi.nlm.nih.gov/bioproject/171749>) using the program Hisat2 (version 2.1.0; Kim et al., 2019), and then assembled reads using the program Stringtie (version 2.0; Pertea et al., 2015). I used the program Blast2GO (Götz et al., 2008) to obtain identities for all assembled transcripts, and provide GO (Gene Ontology) and KEGG (Kyoto Encyclopedia of Genes and Genomes) annotation information for all assembled transcripts. The transcriptome is available in the NCBI database (BioProject: PRJNA721458). I used this approach as it is a common method for transcriptome assembly and annotation for non-model organisms with a reference genome (*e.g.*, Torson et al., 2017; Kaplanoglu et al., 2017).

2.2.4 Differential gene expression and GO enrichment analysis

The program Stringtie assembled RNA-seq reads into transcripts and also provided FPKM expression values (the relative expression of a transcript proportional to the number of cDNA fragments that it originated from), but in order to use expression values in DEseq2 I transformed these FPKM expression values into read counts. To transform these FPKM expression values into read counts, I used prepDE (prepDE.py), a Python script provided by the authors of Stringtie. I then used those read counts in DEseq2 (a differential expression analysis program, version 1.24.0; Love et al., 2014) to compare transcript abundance between non-diapausing and diapausing CPB. To construct differential expression tables, I accepted transcripts as differentially expressed if the adjusted P -value was <0.05 , and the \log_2 fold change was >1.5 (I considered \log_2 fold changes below 1.5 to be less likely to be biologically relevant in the context of this study; Love et al., 2014). To compare differential expression profiles of fat body and flight muscle in diapausing CPB, I created Venn diagrams using the VennDiagram package in R (Version 1.6.20; Chen and Boutros, 2011) to identify transcripts that were differentially expressed with diapause in fat body, flight muscle, or in both tissues. I used all differentially expressed transcripts from DEseq2 to construct tissue-specific Venn diagrams. To compare expression profiles of fat body and flight muscle I also conducted a principal components analysis in R. Finally, to identify biological processes that were important in driving specific diapause phenotypes, I conducted GO enrichment analysis using the program Goseq (v3.12; Young et al., 2012) in R on full differentially expressed transcript lists (*i.e.*, not just those with a \log_2 fold change >1.5). Using full lists of differentially expressed transcripts allowed me to conduct an unbiased analysis of patterns of

gene expression. I considered GO terms to be over-represented if the P -value from the enrichment analysis was <0.05 (recommended by the goseq authors; Young et al., 2012), and if there were three or more transcripts included in a given GO term (because any GO terms with less than three transcripts would not be biologically relevant). I removed redundant GO terms using REViGO (Supek et al., 2011; <http://revigo.irb.hr/>), using the SimRel algorithm with ‘small’ similarity. I also conducted a hypergeometric test in R (using phyper) to determine the statistical significance of the overlap of differentially expressed transcripts in fat body and flight muscle during diapause. Finally, I conducted a KEGG pathway enrichment analysis using gage in R (Luo et al., 2009).

2.3 Results & Discussion

2.3.1 Transcriptome summary

I assembled a transcriptome from 12 libraries, each consisting of mRNA from pooled fat body or flight muscle ($n=8$ beetles/pooled sample) from either non-diapausing or diapausing beetles (Table A1). I obtained 57,241,508 – 111,902,498 raw reads per library (average: 78,902,296) with an average overall alignment rate of 86.8 %. 78.7 – 81.2 % of reads uniquely mapped to the reference *L. decemlineata* genome (Table A1). These values are consistent with other published Colorado potato beetle transcriptomes that report sequence mapping rates (*e.g.*, Kaplanoglu et al., 2017). Of the putative transcripts, 96 % aligned to known sequences in the UniProt database, and of those that aligned, 63 % were annotated (*i.e.*, assigned a putative sequence description), and 77 % of these aligned transcripts were assigned to GO terms. The full transcriptome assembly can be found on NCBI (BioProject: PRJNA721458).

2.3.2 Tissue-specific patterns of gene expression in diapausing CPB

In the fat body, a total of 1074 transcripts increased in abundance and 873 transcripts decreased in abundance during diapause (Figure 2.2). In the flight muscle, a total of 1165 transcripts were increased in abundance, and 664 decreased in abundance during diapause (Figure 2.2). To address my hypothesis that differential expression during diapause would be tissue specific, I compared the transcripts that were differentially expressed during diapause between fat body and flight muscle. Diapausing and non-diapausing CPB each had their own

distinct patterns of gene expression in their fat body and flight muscle according to my PCA analysis (Figure 2.2). Among the transcripts that increased in abundance during diapause, 40 % were uniquely expressed in the fat body (n=767), and 44 % (n=858) were uniquely expressed in the flight muscle. The remaining 16 % of transcripts that increased in abundance were expressed in both tissues (Figure 2.3). Among transcripts that decreased in abundance during diapause, 40 % were uniquely expressed in the fat body (n=444), and 26 % were uniquely expressed in the flight muscle (n=285). The remaining 34 % of transcripts that decreased in abundance were differentially expressed in both tissues during diapause (Figure 2.3). Based on a hypergeometric test, the overlap of increased and decreased transcripts in fat body and flight muscle during diapause that I observed was more than expected by chance ($p < 0.001$ for both increased and decreased abundance).

I conducted a GO enrichment analysis on transcripts that were differentially expressed in both tissues during diapause to identify biological processes that were ubiquitously important to both tissues during diapause. Among transcripts that increased in abundance, I observed an enrichment of GO terms related to epigenetic regulation, ubiquitination, metal ion binding and transport, tRNA metabolism, and extracellular matrix organization (Figure 2.4). Among transcripts that decreased in abundance, I observed an enrichment of GO terms related to fatty acid metabolism, protein metabolism, and membrane transport. I discuss the biological significance of these categories in the relevant sections below. Although I conducted a KEGG pathway enrichment analysis, I did not find any KEGG pathways that were significantly enriched during diapause in either tissue. I speculate that there were too many differentially expressed transcripts from a broad range of categories to enrich any specific KEGG pathway.

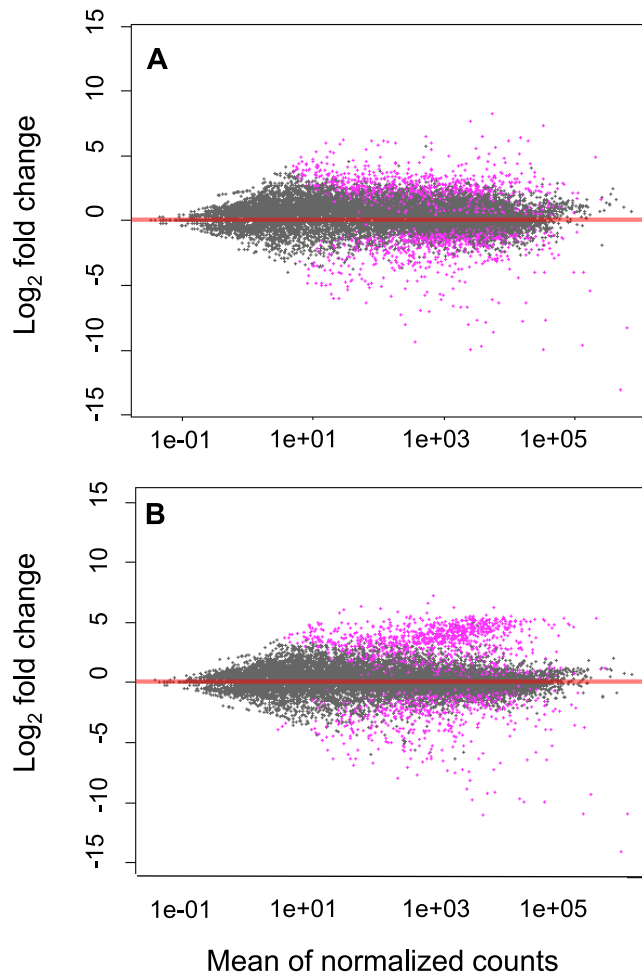
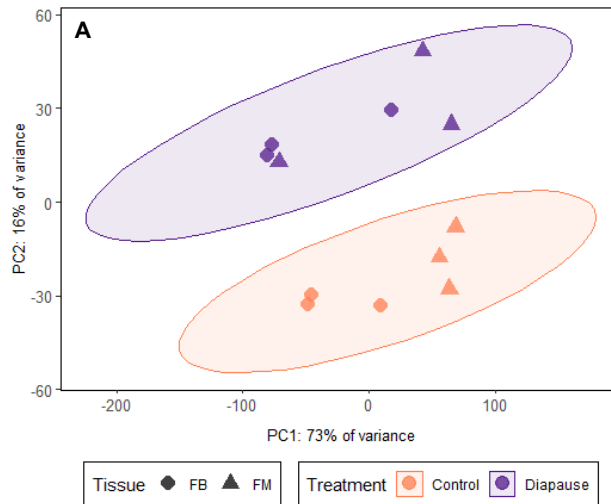
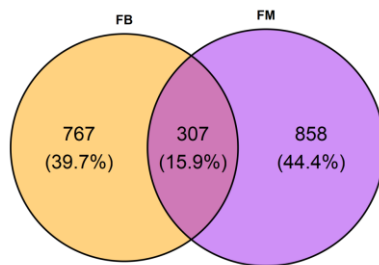


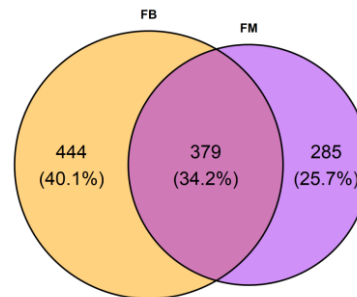
Figure 2.2. Differentially expressed transcripts in (A) fat body and (B) flight muscle from diapausing beetles, compared to non-diapausing *L.decemlineata*. All data points represent differentially expressed transcripts based on \log_2 fold change expression values. Grey points are non-significantly differentially expressed, and purple points are significantly differentially expressed based on differential expression analysis with DEseq2 ($p < 0.05$). The red line represents transcripts with no change in transcript abundance between diapausing and non-diapausing beetles. Points above and below the red line represent transcripts increased and decreased in abundance, respectively, in diapausing beetles compared to non-diapausing beetles.



B: Transcripts with increased abundance during diapause

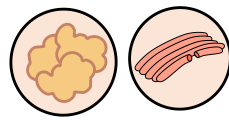


C: Transcripts with decreased abundance during diapause

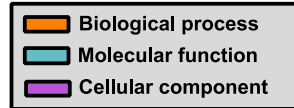


- Transcripts expressed exclusively in fat body during diapause
- Transcripts expressed exclusively in flight muscle during diapause
- Transcripts expressed in both fat body and flight muscle during diapause

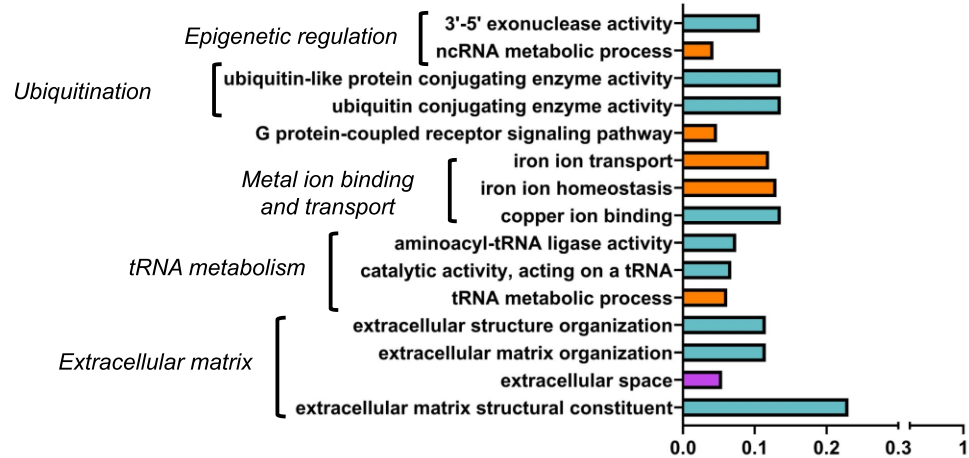
Figure 2.3. Tissue-specific patterns of gene expression in diapausing and non-diapausing *L. decemlineata*. (A) Principal components analysis (PCA) based on fat body (circle) and flight muscle (triangle) transcript abundance in diapausing (purple ellipse) and non-diapausing (orange ellipse) CPB. Each point represents expression values from one biological sample of eight pooled individuals. Ellipses represent the 95 % confidence intervals of each group. (B) Number of transcripts significantly upregulated in fat body (FB), flight muscle (FM), and upregulated in both tissues. (C) Number of transcripts significantly decreased in abundance in fat body (FB), flight muscle (FM), and in both tissues.



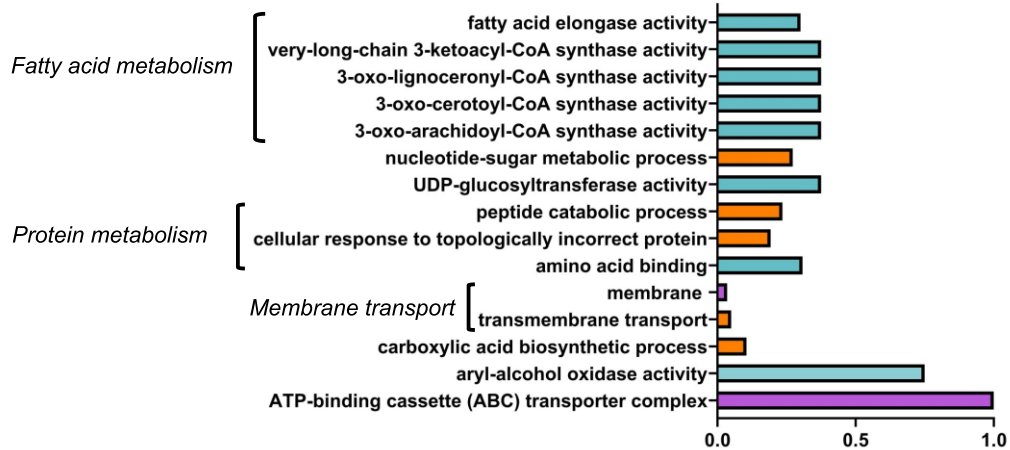
Tissue overlap



A: Increased abundance



B: Decreased abundance



Proportion of differentially expressed transcripts

Figure 2.4. Gene Ontology (GO) terms enriched in transcripts that were increased (A) and (B) decreased in abundance in both fat body and flight muscle during diapause in *L. decemlineata*. Bars represent the proportion of differentially expressed transcripts annotated with that specific GO term to total number of genes in that GO category. I further categorized the GO terms manually into functional groups, indicated by terms next to the brackets. I reduced full enriched GO term lists produced by Goseq in REVIGO, and then chose to represent the top 15 GO terms with the highest proportion.

2.3.3 Diapausing CPB express transcripts related to juvenile hormone metabolism and cell cycle arrest

I hypothesized that diapausing CPB would express transcripts related to arrested development, such as those involved in insulin-signaling, juvenile hormone (JH) metabolism, and cell cycle progression (Figure 2.1). Although I identified transcripts encoding proteins involved in the insulin signaling pathway in both the fat body and flight muscle transcriptomes, none of these transcripts were significantly differentially expressed during diapause in either tissue (Table A2).

There were several differentially expressed transcripts encoding proteins involved in JH metabolism in both tissues (Table 2.1). Diapausing CPB have low hemolymph JH titres, driven by the breakdown of hemolymph JH by JH esterases (De Kort et al., 1982; Kramer and De Kort, 1976). In diapausing fat body, I observed differential expression of transcripts involved in the JH synthesis pathway (Table 2.1), which implies a subtle regulation of these circulating levels to modulate the diapause phenotype, and is consistent with previous studies on diapausing CPB (*e.g.*, Lehmann et al., 2014b). Diapausing CPB also differentially expressed several JH metabolism-related transcripts in their flight muscle (Table 2.1). In particular, I note a decrease in transcript abundance of *juvenile hormone binding protein*, which likely promotes JH breakdown during diapause, as it normally protects JH from degradation *via* JH esterases (Hammock et al., 1975). Although there are few data exploring JH metabolism in tissues other than the hemolymph in CPB, other insects express JH-related transcripts and proteins in other tissues, including flight muscle (Kobayashi and Ishikawa, 1994; Zhang et al., 2020). Thus, I speculate that a decrease in *JH binding protein* in the flight muscle is involved in maintaining a low overall hemolymph JH titre throughout diapause. Transcripts encoding a nuclear hormone receptor (FTZ-F1) were decreased in diapausing fat body which led to an enrichment of the GO term “Steroid hormone receptor activity” (Figure 2.5). In other insects, FTZ-F1 receptor activity is directly modulated by circulating JH to regulate gene expression related to development progression (Mello et al., 2019). Overall, I interpret these results to suggest that circulating JH and its cellular actions are regulated to maintain diapause in CPB, which supports many previous studies on JH metabolism during diapause in CPB (De Kort, 1990).

Cell cycle arrest is key to arrested whole-animal development during diapause (Košťál et al., 2009). Several cell cycle-related transcripts were differentially expressed in fat body of diapausing CPB, including increased abundance of *cyclin dependent kinase 1 (CDK1)*, which encodes a kinase that phosphorylates hundreds of downstream proteins that regulate cell cycle transitions (Ubersax et al., 2003), and a decrease in *G2/mitotic specific cyclin A (cyclin A)* abundance. *Cyclin A* encodes a protein that promotes the transition of cells from G2 through to mitosis (Vigneron et al., 2018; Table 1), and which I interpret to indicate that diapausing CPB arrest their cell cycle at G2. This contrasts with other diapausing insects which appear to arrest cell cycles at the G0-G1 transition (Košťál et al., 2009; Tammariello and Denlinger, 1998). Normal cell cycle progression is arrested at the G2 checkpoint when DNA damage is detected (and subsequently repaired) by the cell *via* homologous recombination (Elledge 1996). I hypothesize that a G2 arrest in diapausing CPB fat body cells would allow repair of any environmental stressor-induced DNA damage accrued over winter (Fleck and Carey, 2005). Indeed, *Rad51* (which encodes a protein pivotal in G2 arrest DNA repair) is increased in abundance in the fat body of diapausing CPB (Table 2.1).

In contrast to the fat body, diapausing CPB flight muscle did not differentially express any cell cycle progression-related transcripts, such as *CDK1* or *Cyclin A*. Those annotated with the GO term “negative regulation of cell proliferation” were over-represented among transcripts with increased abundance during diapause (Figure 2.6). Increased abundance of *apoptosis stimulation of p53 protein* in diapausing flight muscle (Table 2.1) could imply arrest at the G2/mitosis transition, similar to fat body. However, this transcript can also stimulate apoptosis. Although apoptosis is generally inhibited during diapause (MacRae, 2010), CPB flight muscle degrades during winter (Stegwee et al., 1963), so I speculate that apoptosis could provide quality control to maintain the integrity of remaining flight muscle tissue before the tissue is regenerated in the spring. If this were the case, I would predict higher rates of apoptosis in diapausing CPB flight muscle, compared to other diapausing CPB tissues and their non-diapausing counterparts.

Among transcripts that increased in both tissues, those annotated with GO terms related to tRNA (transfer RNA) metabolism were enriched (Figure 2.4). tRNAs can promote cell cycle

arrest, such as in diapause formation in *Artemia* embryos (Chen et al., 2016), thus I speculate that diapausing CPB are regulating the cell cycle in both fat body and flight muscle.

2.3.4 Diapausing CPB differentially express transcripts related to lipid and energy metabolism

During diapause preparation, CPB synthesize lipids which they mobilize and metabolize during diapause (Güney et al., 2020; Yocum et al., 2011a). I observed that diapausing CPB increased the abundance of transcripts encoding fatty acid synthase, fatty acid binding protein (FABP), lipase, and apolipoprotein III precursor (Table 2.2). These are all consistent with enhanced lipid synthesis, catabolism, and transport during diapause in insects (Sinclair and Marshall, 2018). Flight muscle is largely inactive during the winter, and I observed a correspondingly decreased abundance of *Triacylglycerol lipase* in diapausing flight muscle (Table 2.2).

Because diapausing insects suppress their metabolic rate, I hypothesized that transcripts involved in ATP production (*e.g.*, glycolysis, TCA cycle, electron transport and oxidative phosphorylation) and ATP consumption (*e.g.*, ion transport) would decrease in abundance in both tissues during diapause (Figure 2.1). Among decreased transcripts in both tissues, I observed the enrichment of GO terms related to fatty acid metabolism, protein metabolism, and membrane transport (Figure 2.4), all biological processes I would expect to decrease as a result of low metabolic rate during diapause. Despite this, the abundance of transcripts involved in energy metabolism did not appear to decrease in either the flight muscle or fat body (Table A2). However, I did see consistent increases in abundance of transcripts involved in energy metabolism in the flight muscle only (Table 2.3). Diapausing beetles do not fly, and their flight muscle appears to be degraded (Stegwee et al., 1963). Thus, although the flight muscle is inactive, there appears to be some metabolic activity during diapause.

Table 2.1. Differential expression of selected developmental arrest-related transcripts in fat body (FB) and flight muscle (FM) tissues of *L. decemlineata* during diapause. Fold change values represent increased or decreased abundance of transcripts (adjusted *p*-value of <0.05) during diapause compared to a non-diapausing control. ns indicates where expression values were deemed non-significant according to differential gene expression analysis in DEseq2. All transcript IDs that follow a sequence description are variants of the same transcript.

Sequence Description	Transcript ID(s)	log ₂ Fold Change	
		FB	FM
Juvenile hormone metabolism			
<i>Juvenile hormone esterase-like</i>	LDEC006810-RA	2.7	ns
<i>Juvenile hormone acid O-methyltransferase-like</i>	LDEC020565-RA	2.3	ns
	LDEC023596-RA	4.1	ns
	LDEC020564-RA	-1.8	ns
<i>Juvenile hormone binding protein</i>	LDEC009488-RA	ns	-4.5
<i>Putative juvenile hormone-inducible protein</i>	LDEC004293-RA	ns	-2.5
<i>Juvenile hormone acid O-methyltransferase-like</i>			
Cell cycle arrest			
<i>Cyclin-dependent kinase 1</i>	LDEC008989-RA	2.2	1.7
<i>Apoptosis-stimulation of p53 protein 1</i>	LDEC001725-RA	ns	5.8
<i>G2/mitotic-specific cyclin-A</i>	LDEC003103-RA	-1.5	ns
	LDEC003104-RA	-1.8	ns

Of the transcripts involved in energy metabolism that CPB increased in abundance during diapause, many were involved in the TCA cycle and mitochondrial electron transport (Table 2.3). I speculate that a change in redox state (*e.g.*, increase in cellular NAD^+/NADH) caused by energy deprivation during diapause could increase the expression of TCA cycle and electron transport-related transcripts in the flight muscle (Sarbasov and Sabatini, 2005). Despite an increase in mitochondrial metabolism-related transcripts in flight muscle, diapausing CPB increased the abundance of several transcripts involved in mitochondrial breakdown and quality control, particularly those involved in mitochondrion-specific autophagy (mitophagy; Table 2.3). I hypothesize that the breakdown of flight muscle mitochondria could modulate energy metabolism and yield metabolic suppression during diapause in CPB. Indeed, *Citrate synthase* (an enzyme often used as a proxy for mitochondrial abundance) decreased in abundance during diapause (Table 2.3), suggesting a decrease in mitochondrial abundance in the flight muscle of diapausing CPB.

2.3.5 Diapausing CPB differentially express transcripts related to stress tolerance

I predicted differential expression of stress tolerance-related transcripts in both the fat body and flight muscle during diapause. In particular, the environmental stresses associated with diapause led me to expect increased abundance of transcripts encoding proteins in the hypoxia response, chaperone response, and cell structure (Figure 2.1).

Diapausing insects may experience oxidative stress during diapause as a result of low metabolic rates (Zhang et al., 2017). I found that GO terms associated with oxidative stress were enriched among transcripts with increased abundance in the fat body (Figure 2.5), and that diapausing CPB increased the abundance of transcripts encoding antioxidant enzymes (*e.g.*, *superoxide dismutase*) in both tissues (Table 2.4). Furthermore, diapausing CPB increased abundance of *mitochondrial uncoupling protein 4 (UCP4)* in flight muscle, which plays a role in reducing reactive oxygen species (ROS) in other insect species (Table 2.3; Alves-Bezerra et al., 2014). Taken together, I hypothesize that increased antioxidant enzyme and *UCP4* expression during diapause in CPB could increase cellular capacity to quench ROS produced as a byproduct of low metabolism or upon resumption of higher metabolic

rates upon diapause emergence (Brown et al., 2012). However, ROS such as H₂O₂ can also regulate metabolism during diapause (Chen et al., 2020; Reczek and Chandel, 2015), so I cannot rule out that changes I see in antioxidant capacity reflect broader regulatory processes that maintain diapause in CPB. For example, ROS can activate the hypoxia inducible factor (HIF) pathway (Lee et al., 2010b). I found that diapausing CPB decreased *HIF1α inhibitor* abundance in their fat body, which implies activation of the HIF1α pathway, supporting at least some regulatory role for ROS during diapause in this species.

Heat shock protein 70 (HSP70) transcript abundance is well-known to be increased during diapause in CPB (e.g., Lyytinen et al., 2012; Yocum, 2001). These previous studies have used whole-body homogenates, and I only observed an increase in *HSP70* in the flight muscle, whereas other chaperone-related transcripts such as *HSP68* decreased in abundance in both tissues (Table 2.4). Given that there is already evidence that flight muscle is degraded during diapause in CPB, this 5.2-fold increase in *HSP70* abundance is surprising (Table 2.4). I speculate that either 1) flight muscle breakdown does not involve complete tissue histolysis and *HSP70* chaperones important proteins that are not degraded or 2) *HSP70* is promoting degradation itself by stabilizing the 20S proteasome (Grune et al., 2011). These hypotheses are readily distinguished: If *HSP70* is chaperoning proteins, then knocking down *HSP70* with RNAi should result in more tissue histolysis in diapausing flight muscle. If *HSP70* promotes degradation, then knocking down *HSP70* with RNAi would decrease overall rates of proteasomal protein degradation in diapausing flight muscle.

A dynamic cytoskeleton is more able to maintain cell structure in response to stress, and other diapausing and cold-tolerant insects often remodel their cytoskeleton for protection (Des Marteaux et al., 2018; Kim et al., 2006). I predicted that diapausing CPB would differentially express cytoskeleton-related transcripts. In diapausing CPB, I observed increased abundance of actin-related transcripts in the fat body and an increase in tubulin-related transcripts in the flight muscle (Table 2.4), alongside an enrichment of GO terms associated with cytoskeletal structure and dynein-related movement in both tissues (Figure 2.4). This suggests that diapausing CPB are remodeling the cytoskeleton (in different ways) in both tissues. I speculate that the increased tubulin and dynein could be associated with clearing autophagic waste in flight muscle, as muscle cells rely on these molecules to

transport organelles around the cell (Lee et al., 2010a; Vives-Bauza and Przedborski, 2011). Furthermore, among transcripts with overlapped expression in both fat body and flight muscle I observed an enrichment of GO terms related to the extracellular matrix (Figure 2.4), providing further evidence that maintaining cell structure is important for both tissues during diapause.

Alongside abiotic stressors such as temperature and desiccation, overwintering insects likely experience biotic stressors such as pathogens (Ferguson et al., 2018). Although I did not predict a change in immune-related gene expression *a priori*, I found that diapausing CPB differentially expressed several serine protease transcripts in both the fat body and flight muscle (Table 2.4), and GO terms related to immunity were enriched among differentially expressed transcripts in the fat body (Figure 2.5). Insects can still respond to pathogens during dormancy (Nakamura et al., 2011), and immune responses change in complex ways over winter (Ferguson and Sinclair, 2017). Thus, I speculate that CPB enhance their immune function during diapause, likely enhancing survival in the face of pathogen pressure over winter.

Increased stress tolerance is an integral component of the diapause programme (Košťál, 2006). In CPB, transcripts associated with the hypoxia response in fat body could be integral to whole animal responses to hypoxia, as insect fat body can sense hypoxia and coordinate whole animal responses (Lee et al., 2019). Furthermore, increased immunity appears to be prioritized in CPB fat body; indeed, most immunity-related genes are constitutively expressed in the fat body (Gorman and Paskewitz, 2001). By contrast, protein quality control appears to be prioritized in flight muscle, with more significant expression of chaperone-related transcripts, perhaps maintaining cellular integrity during environmental stresses. The expression of antioxidants and cytoskeletal proteins in both tissues suggest that protection from ROS and maintenance of cell structure are important processes for many tissue and cell types during diapause.

Table 2.2. Differential expression of selected lipid metabolism-associated transcripts in fat body (FB) and flight muscle (FM) tissue of *L. decemlineata* during diapause. Fold change values represent increased or decreased abundance of transcripts (adjusted *p*-value of <0.05) during diapause compared to a non-diapausing control. ns indicates where expression values were deemed non-significant according to differential gene expression analysis in DEseq2. All transcript IDs that follow a sequence description are variants of the same transcript.

Sequence Description	Transcript ID(s)	log ₂ Fold Change	
		FB	FM
Fatty acid biosynthesis			
<i>Elongation of very long chain fatty acids protein AAEL008004-like</i>	LDEC011862-RA	2.7	ns
	LDEC010496-RA	-2.6	-2.5
	LDEC016593-RA	-1.7	-1.7
<i>Elongation of very long chain fatty acids protein 4-like</i>	LDEC022762-RA	-4.7	-4.9
<i>Fatty acid synthase</i>	LDEC020615-RA	2.5	ns
Fatty acid catabolism			
<i>Lipase 3</i>	LDEC017075-RA	3.3	ns
<i>Lipase 3-like</i>	LDEC005771-RA	3.1	ns
	LDEC010801-RA	2.9	2.7
	LDEC024623-RA	1.7	ns
	LDEC005772-RA	1.6	1.5
	LDEC005773-RA	ns	2.0
<i>Lipase member H-A</i>	LDEC012490-RA	3.1	ns
<i>Triacylglycerol lipase</i>	LDEC006931-RA	2.2	-2.0
<i>Lipase-related protein 2-like</i>	LDEC010492-RA	ns	2.9
Fatty Acid transport			
<i>Fatty acid binding protein-like</i>	LDEC004342-RA	3.2	ns
<i>Apolipoprotein III precursor</i>	LDEC016750-RA	2.1	ns

Table 2.3. Differential expression of selected energy metabolism-associated transcripts in fat body (FB) and flight muscle (FM) tissue of *L. decemlineata* during diapause. Fold change values represent increased or decreased abundance of transcripts (adjusted *p*-value of <0.05) during diapause compared to a non-diapausing control. ns indicates where expression values were deemed non-significant according to differential gene expression analysis in DEseq2. All transcript IDs that follow a sequence description are variants of the same transcript.

Sequence Description	Transcript ID(s)	log ₂ Fold Change	
		FB	FM
Glycolysis			
<i>Phosphoglycerate kinase</i>	LDEC010565-RA	ns	2.8
<i>Enolase</i>	LDEC003977-RA	ns	4.5
TCA Cycle			
<i>Malate dehydrogenase, mitochondrial-like</i>	LDEC017289-RA	ns	5.2
	LDEC002299-RA	ns	4.9
	LDEC023960-RA	ns	2.5
<i>Probable pyruvate dehydrogenase E1 component subunit alpha, mitochondrial</i>	LDEC014842-RA	ns	3.3
<i>Pyruvate dehydrogenase E1 component, alpha subunit</i>	LDEC014843-RA	ns	3.7
<i>ATP-Citrate synthase isoform XI</i>	LDEC009047-RA	ns	-1.4
Oxidative phosphorylation			
<i>Cytochrome c oxidase subunit 6A1, mitochondrial</i>	LDEC000603-RA	ns	3.7
<i>Succinate dehydrogenase [ubiquinone] flavoprotein subunit, mitochondrial</i>	LDEC001800-RA	ns	4.7
<i>Succinate dehydrogenase assembly factor 3, mitochondrial</i>	LDEC022565-RA	1.5	ns
<i>ATP synthase subunit e, mitochondrial</i>	LDEC002395-RA	ns	4.8
<i>ATP synthase subunit b, mitochondrial</i>	LDEC004794-RA	ns	4.3
<i>NADH dehydrogenase [ubiquinone] iron-sulfur protein 3, mitochondrial</i>	LDEC006874-RA	ns	3.9
<i>NADH dehydrogenase [ubiquinone] iron-sulfur protein 4, mitochondrial</i>	LDEC024041-RA	ns	4.3

Sequence Description	Transcript ID(s)	log ₂ Fold Change	
		FB	FM
<i>Table 3 cont'd.</i>			
<i>NADH dehydrogenase subunit 4 (mitochondrion)</i>	LDEC024748-RA	3.0	ns
<i>Cytochrome b-c1 complex subunit Rieske, mitochondrial</i>	LDEC010568-RA	ns	4.7
<i>ATP synthase subunit epsilon, mitochondrial-like isoform X2</i>	LDEC016085-RA	ns	2.6
<i>Cytochrome c oxidase subunit 5A, mitochondrial</i>	LDEC018071-RA	ns	4.4
<i>Mitochondrial uncoupling protein 4 isoform X1</i>	LDEC014589-RA	ns	5.2
Mitochondrial homeostasis and quality control			
<i>Mitochondrial import inner membrane translocase subunit TIM16</i>	LDEC021138-RA	ns	3.9
<i>Biogenesis of lysosome-related organelles complex 1 subunit 2</i>	LDEC009682-RA	ns	3.2
<i>Ubiquitin-conjugating-like enzyme ATG10</i>	LDEC017552-RA	1.6	1.6
<i>Mitochondrial uncoupling protein 4-like</i>	LDEC014589-RA	ns	5.2

Table 2.4. Differential expression of selected stress tolerance-associated transcripts in fat body (FB) and flight muscle (FM) tissue of *L. decemlineata* during diapause. Fold change values represent increased or decreased abundance of transcripts (adjusted *p*-value of <0.05) during diapause compared to a non-diapausing control. ns indicates where expression values were deemed non-significant according to differential gene expression analysis in DEseq2. All transcript IDs that follow a sequence description are variants of the same transcript.

Sequence Description	Transcript ID(s)	log ₂ Fold Change	
		FB	FM
Hypoxia response			
<i>Thioredoxin-domain-containing protein 17</i>	LDEC017665-RA	ns	4.7
<i>Superoxide dismutase</i>	LDEC013236-RA	1.5	1.6
<i>Glutathione S-transferase 1-like</i>	LDEC001116-RA	2.2	ns
<i>Catalase</i>	LDEC012452-RA	Ns	-1.8
<i>Glutathione S-transferase 1</i>	LDEC015216-RA	-2.8	ns
	LDEC020265-RA	-2.0	-1.8
<i>Hypoxia-inducible factor 1-alpha inhibitor-like</i>	LDEC024414-RA	-1.7	ns
Chaperone response			
<i>Heat shock protein 70</i>	LDEC000250-RA	ns	5.2
<i>Heat shock protein 68-like</i>	LDEC001137-RA	-4.0	-3.8
	LDEC001140-RA	-4.0	-3.9
	LDEC001138-RA	-4.0	-3.6
<i>Heat shock cognate 71 kDa protein-like</i>	LDEC000251-RA	ns	-1.5
Immunity			
<i>Serine protease P153</i>	LDEC000866-RA	2.3	ns
	LDEC000867-RA	2.1	ns
<i>Serine protease 7-like</i>	LDEC018941-RA	2.9	ns
<i>Serine protease H57</i>	LDEC010088-RA	2.6	3.6
	LDEC009783-RA	-3.0	ns
<i>Serine protease Persephone</i>	LDEC020484-RA	2.0	ns
<i>Serine protease easter-like</i>	LDEC021025-RA	2.5	3.4
<i>Serine protease nudel</i>	LDEC008820-RA	-2.7	-2.4
	LDEC008818-RA	-3.7	-3.5
<i>Serine protease gd-like</i>	LDEC024229-RA	-1.7	ns

Sequence Description	Transcript ID(s)	log ₂ Fold Change	
		FB	FM
Cell structure and integrity			
<i>Phosphatase and actin regulator 2</i>	LDEC004147-RA	4.6	ns
<i>Activity-regulated cytoskeleton associated protein 1-like</i>	LDEC017756-RA	2.4	ns
<i>Tubulin alpha-8 chain-like</i>	LDEC016447-RA	ns	4.5
<i>Tubulin alpha-1 chain</i>	LDEC016448-RA	ns	4.2
<i>Actin, alpha skeletal muscle-like</i>	LDEC000503-RA	ns	-1.7
<i>Actin-binding Rho-activating protein-like</i>	LDEC012542-RA	-2.4	-1.3

2.3.6 Diapausing CPB express transcripts related to epigenetic regulation and transposable elements

Diapause phenotypes can be driven directly by changes in gene expression, but also indirectly *via* epigenetic processes that regulate gene expression (Reynolds, 2017). Among transcripts whose expression overlapped between fat body and flight muscle, I observed an enrichment of GO terms directly related to epigenetic regulation (Figure 2.4). Furthermore, diapausing CPB increased the abundance of one and decreased the abundance of two transcripts encoding a histone methyltransferase (Table 2.5). I hypothesize that CPB could be differentially methylating genes to either repress or activate genes required to drive diapause phenotypes such as metabolic suppression, cell cycle arrest, or photoperiodic responses, as seen in some insects and other dormant animals (Dai et al., 2017; Pegoraro et al., 2016; Tessier et al., 2017).

Transposable elements comprise 17 % of the CPB genome (Schoville et al., 2018), and several diapause-associated transcripts in CPB contain transposable elements (Yocum et al., 2011b). Thus, it is not surprising that I observed differential expression of transcripts encoding several putative transposase enzymes (Table 2.5). Transposases can induce changes in gene expression through the insertion of DNA into promoters or enhancers and ultimately drive phenotypic changes at the whole animal level (Bonchev and Parisod, 2013; McCart and French-Constant, 2008). I speculate that the expression of transposase enzymes during diapause in CPB suggest that diapause phenotypes could be, in part, mediated by the regulation of transposable elements. To my knowledge, the role of transposable elements in diapause regulation and maintenance has not been explored.

Table 2.5. Differential expression of selected transcripts in fat body (FB) and flight muscle (FM) involved in gene regulatory processes in *L. decemlineata*. Fold change values represent increased or decreased abundance of transcripts (adjusted *p*-value of <0.05) during diapause compared to a non-diapausing control. ns indicates where expression values were deemed non-significant according to differential gene expression analysis in DEseq2. All transcript IDs that follow a sequence description are variants of the same transcript.

Sequence Description	Transcript ID(s)	log ₂ Fold Change	
		FB	FM
Epigenetic regulation			
<i>Histone-lysine N-methyltransferase SETMAR-like</i>	LDEC000993-RA	-3.3	-2.5
	LDEC001789-RA	2.7	ns
<i>Histone-lysine N-methyltransferase ASHR1-like isoform X2</i>	LDEC009890-RA	-1.5	ns
Transposable element regulation			
<i>piggyBac transposable element-derived protein 2-like</i>	LDEC011452-RA	4.6	ns
<i>Tigger transposable element-derived protein 6-like isoform X4</i>	LDEC011331-RA	4.1	ns
<i>Tigger transposable element-derived protein 6-like protein</i>	LDEC006892-RA	-1.67	ns
<i>piggyBac transposable element-derived protein 3-like</i>	LDEC009727-RA	3.9	ns
	LDEC010331-RA	3.7	ns
	LDEC002328-RA	2.8	ns
	LDEC011630-RA	2.4	ns
	LDEC001649-RA	2.5	ns
	LDEC020990-RA	2.1	1.8
	LDEC020065-RA	1.9	2.0
	LDEC024288-RA	1.8	ns
	LDEC002190-RA	1.7	ns
LDEC016603-RA	1.6	ns	

Sequence Description	Transcript ID(s)	log ₂ Fold Change	
		FB	FM
	LDEC001191-RA	1.6	ns
	LDEC005258-RA	ns	4.6
	LDEC022021-RA	-2.0	-1.6
<i>Table 5 cont'd</i>			
<i>piggyBac transposable element-derived protein 4-like</i>	LDEC022668-RA	3.6	3.8
	LDEC017961-RA	2.6	1.8
	LDEC010475-RA	1.7	ns
	LDEC014811-RA	1.7	ns
	LDEC023604-RA	ns	-3.9
<i>Transposable element P transposase</i>	LDEC021965-RA	2.2	ns
<i>piggyBac transposable element-derived protein 1-like</i>	LDEC022696-RA	ns	4.4
	LDEC008607-RA	ns	1.7
<i>Putative RNA-directed DNA polymerase from transposon BS-like protein</i>	LDEC021446-RA	-5.31	ns

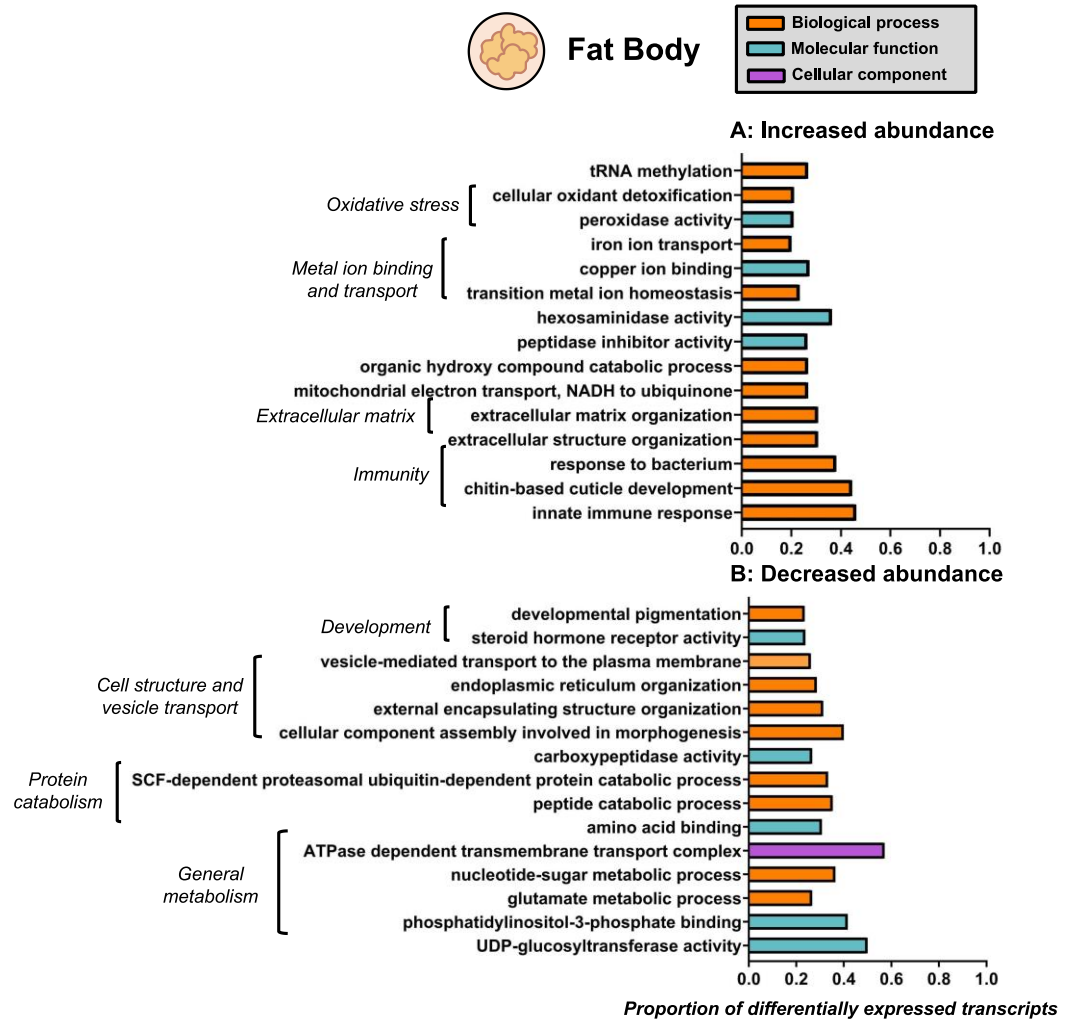


Figure 2.5. Gene Ontology (GO) terms enriched in transcripts that (A) increased and (B) decreased in abundance in the fat body during diapause in *L. decemlineata*. Bars represent the proportion of differentially expressed transcripts annotated with that specific GO term to total number of genes in that GO category. I further categorized the GO terms manually into functional groups, indicated by terms next to the brackets. I reduced full enriched GO term lists produced by Goseq in REVIGO, and then chose to represent the top 15 GO terms with the highest proportion.

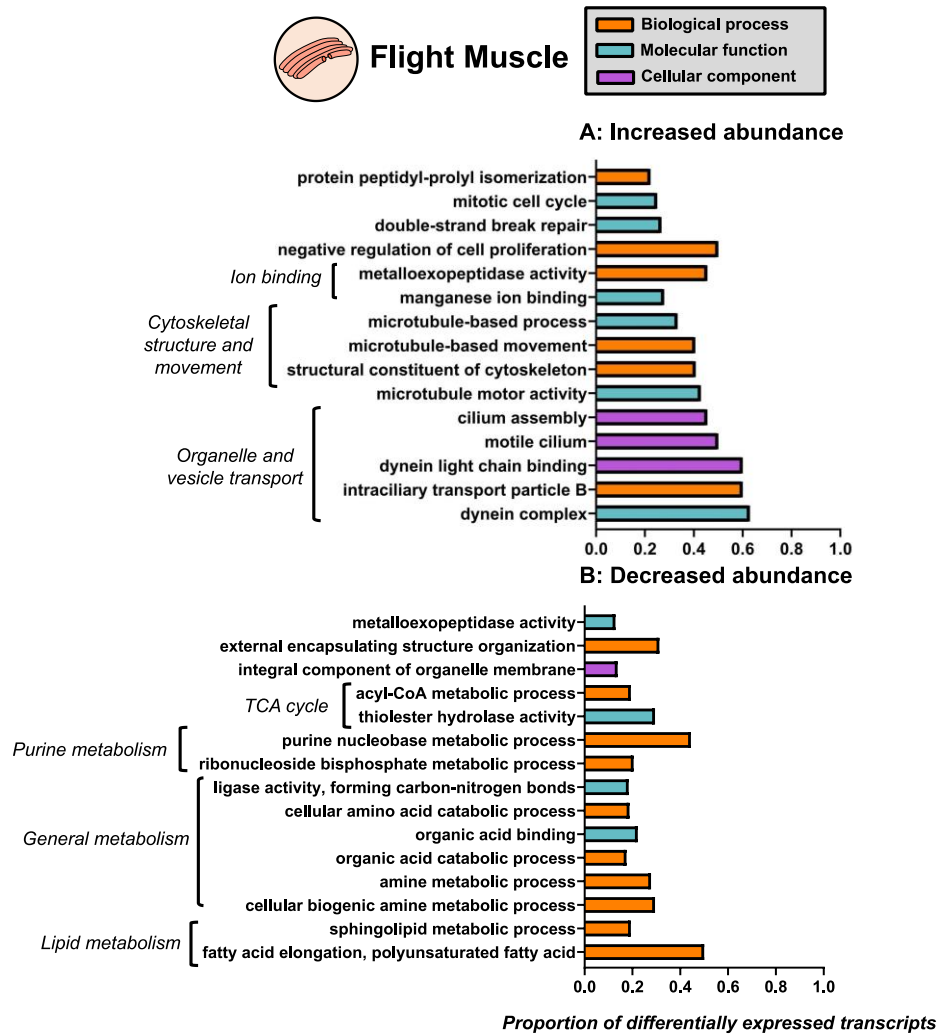


Figure 2.6. Gene Ontology (GO) terms enriched among transcripts that (A) increased and (B) decreased in abundance in the flight muscle during diapause in *L. decemlineata*. Bars represent the proportion of differentially expressed transcripts annotated with that specific GO term to total number of genes in that GO category. I manually categorized the GO terms into functional groups, indicated by terms adjacent to the brackets. I reduced full enriched GO term lists produced by Goseq in REVIGO, and then chose to represent the top 15 GO terms with the highest proportion.

2.3.7 Effects of temperature and photoperiod on diapause-related changes in gene expression

Because diapausing beetles experienced a lower temperature than non-diapausing controls (15 °C versus 24 °C), it is possible that some changes in gene expression I observed are driven by the difference in temperature rather than the photoperiod-initiated diapause programme. Indeed, some changes in gene expression I observed in diapausing CPB mirror changes in gene expression during cold acclimation in other insects. Specifically, transcripts related to cytoskeletal remodeling (*e.g.*, Des Marteaux et al., 2017; MacMillan et al., 2016b), antioxidants (*e.g.*, Des Marteaux et al., 2017), the chaperone response (*e.g.*, Des Marteaux et al., 2019; Des Marteaux et al., 2017; Enriquez and Colinet, 2019; MacMillan et al., 2016b), immunity (*e.g.*, MacMillan et al., 2016a) and lipid transport (*e.g.*, Enriquez and Colinet, 2019; MacMillan et al., 2016a) are differentially expressed in some non-diapausing, cold-acclimated insects. However, 15 °C is warmer than usually used to initiate a cold acclimation response in most temperate insects (*i.e.*, the studies referenced above use temperatures below 10 °C), and many of the changes in gene expression that I observed (including those just listed) overlap with observations from other studies where diapause was induced solely *via* changes in photoperiod. For example, genes related to the chaperone response (*e.g.*, Des Marteaux et al., 2019), lipid metabolism (*e.g.*, Poelchau et al., 2013; Qi et al., 2015; Santos et al., 2018), cell cycle arrest (*e.g.*, Deng et al., 2018; Košťál et al., 2009; Santos et al., 2018), epigenetic regulation (*e.g.*, Santos et al., 2018) and immunity (*e.g.*, Poelchau et al., 2013; Santos et al., 2018) are all differentially expressed in some diapausing insects independent of temperature. Thus, although I manipulated both temperature and photoperiod to induce diapause in CPB, the changes in gene expression I observed can still be interpreted as changes derived from a diapause phenotype.

2.4 Conclusions

In this study I used an RNA-seq data set to evaluate hypotheses from the literature regarding the physiological mechanisms driving diapause in adult insects, and specifically in CPB (Figure 2.1). My data support many of my initial hypotheses (see Figure 2.7). In diapausing CPB, arrested development appears to be driven by the expression of transcripts related to cell cycle arrest at the G2/M transition and juvenile hormone catabolism in both the fat body and flight muscle. Energy metabolism appears to be modulated primarily by changes in transcripts related to mitochondrial homeostasis in the flight muscle. The hypoxia response and enhanced immunity appear to be driven by changes in transcript abundance in the fat body, and whole animal hypoxia tolerance and immunity-related changes during diapause require further exploration in this species. Transcriptional changes in the flight muscle likely regulate proteostasis and the chaperone response. Both tissues prioritize increasing antioxidant capacity and cytoskeletal remodeling during diapause. Finally, I propose that epigenetic modifications *via* histone methylation, and transposable element regulation may regulate gene expression and ultimately diapause phenotypes during diapause in CPB. In total, I identified over 1000 differentially expressed transcripts associated with diapause in both the fat body and flight muscle, which is a high number of transcripts when compared to similar RNA-seq experiments using whole body homogenates (*e.g.*, <100 transcripts in Kang et al., 2016 and Poelchau et al., 2013). This suggests that whole body RNA-seq studies mask important inter-tissue differences in gene expression, and that studies using whole body homogenates may generate extremely conservative, or even spurious, results.

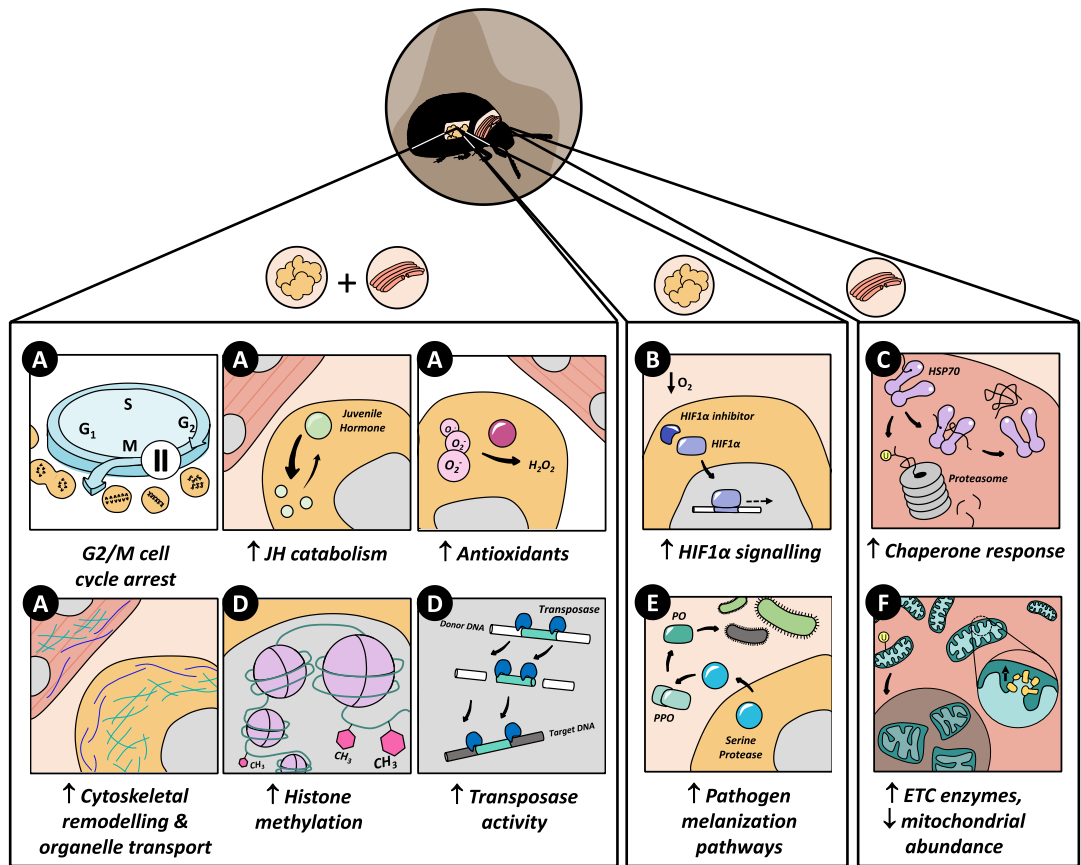


Figure 2.7. Synthesis of hypotheses on biological processes associated with diapause phenotypes in the Colorado potato beetle I evaluated (A,B,C) and generated (D,E,F). My data support the hypotheses that diapausing beetles (A) arrest cell cycles, increase juvenile hormone catabolism, increase antioxidant metabolism, and remodel cytoskeleton in both fat body and flight muscle, (B) increase HIF1 α signaling in just the fat body, and (C) increase chaperone responses in just the flight muscle. From these data I also generated new hypotheses that diapausing beetles increase (D) histone methylation and transposase activity in fat body and flight muscle, (E) increase pathogen melanization pathways in just the fat body, and (F) increase transcription of electron transport chain (ETC) enzyme and decrease mitochondrial abundance in flight muscle.

2.5 References

- Alves-Bezerra, M., Cosentino-Gomes, D., Vieira, L.P., Rocco-Machado, N., Gondim, K.C., and Meyer-Fernandes, J.R.** (2014). Identification of uncoupling protein 4 from the blood-sucking insect *Rhodnius prolixus* and its possible role on protection against oxidative stress. *Insect Biochemistry and Molecular Biology* **50**, 24-33.
- Andrews, S.** (2010) FastQC: a quality control tool for high throughput sequence data. [Online]. Available online at: <http://www.bioinformatics.babraham.ac.uk/projects/fastqc/>
- Bhakthan, N., Borden, J., Nair, K.** (1970). Fine Structure of Degenerating and Regenerating Flight Muscles in a Bark Beetle, *Ips confusus*: I. Degeneration. *Journal of Cell Science* **6**, 807-819.
- Boiteau, G., Coleman, W.** (1996). Cold tolerance in the Colorado potato beetle, *Leptinotarsa decemlineata* (Say) (Coleoptera: Chrysomelidae). *Canadian Entomologist* **128**, 1087-1099.
- Bonchev, G., Parisod, C.** (2013). Transposable elements and microevolutionary changes in natural populations. *Molecular Ecology Resources* **13**, 765-775.
- Brown, J.C., Chung, D.J., Belgrave, K.R., Staples, J.F.** (2012). Mitochondrial metabolic suppression and reactive oxygen species production in liver and skeletal muscle of hibernating thirteen-lined ground squirrels. *American Journal of Physiology* **302**, R15-R28.
- Chen, D.-F., Lin, C., Wang, H.-L., Zhang, L., Dai, L., Jia, S.-N., Zhou, R., Li, R., Yang, J.-S., Yang, F.** (2016). An La-related protein controls cell cycle arrest by nuclear retrograde transport of tRNAs during diapause formation in *Artemia*. *BMC Biology* **14**, 1-13.
- Chen, C., Mahar, R., Merritt, M.E., Denlinger, D.L., Hahn, D.A.** (2020). ROS and hypoxia signaling regulate periodic metabolic arousal during insect dormancy to coordinate glucose, amino acid, and lipid metabolism. *Proceedings of the National Academy of Sciences of the U.S.A.* **118**, e2017603118.
- Chen, H., Boutros, P.C.** (2011). VennDiagram: a package for the generation of highly-customizable Venn and Euler diagrams in R. *BMC Bioinformatics* **12**, 35.
- Chen, S., Zhou, Y., Chen, Y., Gu, J.** (2018). fastp: an ultra-fast all-in-one FASTQ preprocessor. *Bioinformatics* **34**, i884-i890.
- Dai, L., Ye, S., Li, H.-W., Chen, D.-F., Wang, H.-L., Jia, S.-N., Lin, C., Yang, J.-S., Yang, F., Nagasawa, H.** (2017). SETD4 regulates cell quiescence and catalyzes the trimethylation of H4K20 during diapause formation in *Artemia*. *Molecular Cell Biology* **37**, e00453-16.

- Dambroski, H., Feder, J.** (2007). Host plant and latitude-related diapause variation in *Rhagoletis pomonella*: a test for multifaceted life history adaptation on different stages of diapause development. *Journal of Evolutionary Biology* **20**, 2101-2112.
- De Kort, C.** (1990). Thirty-five years of diapause research with the Colorado potato beetle. *Entomology Experimental Applications* **56**, 1-13.
- De Kort, C., Bergot, B., Schooley, D.** (1982). The nature and titre of juvenile hormone in the Colorado potato beetle, *Leptinotarsa decemlineata*. *Journal of Insect Physiology* **28**, 471-474.
- De Kort, C., Schooneveld, H., De Wilde, J.** (1980). Endocrine regulation of seasonal states in the Colorado potato beetle, *Leptinotarsa decemlineata*. In *Integrated control of insect pests in the Netherlands*, ed. C. De Kort, H. Schooneveld, J. De Wilde. 233-240.
- De Wilde, J.** (1960). Diapause in the Colorado beetle (*Leptinotarsa decemlineata*, Say) as an endocrine deficiency syndrome of the *corpora allata*. In *Ontogeny of Insects*, ed. I. Hrdy: Palala Press.
- De Wilde, J., Duintjer, C., Mook, L.** (1959). Physiology of diapause in the adult Colorado beetle (*Leptinotarsa decemlineata*, Say) – I The photoperiod as a controlling factor. *Journal of Insect Physiology* **3**, 75-85.
- Deng, Y., Li, F., Rieske, L.K., Sun, L.-L., Sun, S.-H.** (2018). Transcriptome sequencing for identification of diapause-associated genes in fall webworm, *Hyphantria cunea* Drury. *Gene* **668**, 229-236.
- Denlinger, D.L., Yocum, G., Rinehart, J., Gilbert, L.** (2004). Hormonal control of diapause. *Comprehensive Molecular Insect Science* **3**, 615-650.
- Denlinger, D.L.** (1972). Seasonal phenology of diapause in the flesh fly *Sarcophaga bullata*. *Annals of the Entomological Society of America* **65**, 410-414.
- Denlinger, D.L.** (2002). Regulation of diapause. *Annual Reviews of Entomology* **47**, 93-122.
- Des Marteaux, L.E., McKinnon, A.H., Udaka, H., Toxopeus, J., Sinclair, B.J.** (2017). Effects of cold-acclimation on gene expression in Fall field cricket (*Gryllus pennsylvanicus*) ionoregulatory tissues. *BMC Genomics* **18**, 357.
- Des Marteaux, L.E., Hůla, P., Košťál, V.** (2019). Transcriptional analysis of insect extreme freeze tolerance. *Proceedings of the Royal Society B* **286**, 20192019.
- Des Marteaux, L.E., Stinziano, J.R., Sinclair, B.J.** (2018). Effects of cold acclimation on rectal macromorphology, ultrastructure, and cytoskeletal stability in *Gryllus pennsylvanicus* crickets. *Journal of Insect Physiology* **104**, 15-24.

- Dong, Y.-C., Wang, Z.-J., Clarke, A.R., Pereira, R., Desneux, N., Niu, C.-Y.** (2013). Pupal diapause development and termination is driven by low temperature chilling in *Bactrocera minax*. *Journal of Pest Science* **86**, 429-436.
- Dortland, J.** (1978). Synthesis of vitellogenins and diapause proteins by the fat body of *Leptinotarsa decemlineata*, as a function of photoperiod. *Physiological Entomology* **3**, 281-288.
- Dortland, J.** (1979). The hormonal control of vitellogenin synthesis in the fat body of the female Colorado potato beetle. *General and Comparative Endocrinology* **38**, 332-344.
- Enriquez, T., Colinet, H.** (2019). Cold acclimation triggers major transcriptional changes in *Drosophila suzukii*. *BMC Genomics* **20**, 1-17.
- Ferguson, L.V., Kortet, R., Sinclair, B.J.** (2018). Eco-immunology in the cold: the role of immunity in shaping the overwintering survival of ectotherms. *Journal of Experimental Biology* **221**, jeb163873.
- Ferguson, L.V., Sinclair, B.J.** (2017). Insect immunity varies idiosyncratically during overwintering. *Journal of Experimental Zoology* **327**, 222-234.
- Gorman, M.J., Paskewitz, S.M.** (2001). Serine proteases as mediators of mosquito immune responses. *Insect Biochemistry and Molecular Biology* **31**, 257-262.
- Götz, S., García-Gómez, J.M., Terol, J., Williams, T.D., Nagaraj, S.H., Nueda, M.J., Robles, M., Talón, M., Dopazo, J., Conesa, A.** (2008). High-throughput functional annotation and data mining with the Blast2GO suite. *Nucleic Acids Research* **36**, 3420-3435.
- Grune, T., Catalgol, B., Licht, A., Ermak, G., Pickering, A.M., Ngo, J.K., Davies, K.J.** (2011). HSP70 mediates dissociation and reassociation of the 26S proteasome during adaptation to oxidative stress. *Free Radical Biology Medicine* **51**, 1355-1364.
- Güney, G., Toprak, U., Hegedus, D.D., Bayram, Ş., Coutu, C., Bekkaoui, D., Baldwin, D., Heckel, D.G., Hänniger, S., Cedden, D.** (2020). A look into Colorado potato beetle lipid metabolism through the lens of lipid storage droplet proteins. *Insect Biochemistry and Molecular Biology* **133**, 103473.
- Hahn, D.A., Denlinger, D.L.** (2007). Meeting the energetic demands of insect diapause: Nutrient storage and utilization. *Journal of Insect Physiology* **53**, 760-773.
- Hahn, D.A., Denlinger, D.L.** (2011). Energetics of insect diapause. *Annual Reviews of Entomology* **56**, 103-121.

- Hammock, B., Nowock, J., Gooddman, W., Stamoudis, V., Gilbert, L.I.** (1975). The influence of hemolymph-binding protein on juvenile hormone stability and distribution in *Manduca sexta* fat body and imaginal discs *in vitro*. *Molecular and Cellular Endocrinology* **3**, 167-184.
- Kang, D.S., Cotten, M.A., Denlinger, D.L., Sim, C.** (2016). Comparative transcriptomics reveals key gene expression differences between diapausing and non-diapausing adults of *Culex pipiens*. *PLoS One* **11**, e0154892.
- Kaplanoglu, E., Chapman, P., Scott, I.M., Donly, C.** (2017). Overexpression of a cytochrome P450 and a UDP-glycosyltransferase is associated with imidacloprid resistance in the Colorado potato beetle, *Leptinotarsa decemlineata*. *Scientific Reports* **7**, 1-10.
- Kim, D., Paggi, J.M., Park, C., Bennett, C., Salzberg, S.L.** (2019). Graph-based genome alignment and genotyping with HISAT2 and HISAT-genotype. *Nature Biotechnology* **37**, 907-915.
- Kim, M., Robich, R.M., Rinehart, J.P., Denlinger, D.L.** (2006). Upregulation of two actin genes and redistribution of actin during diapause and cold stress in the northern house mosquito, *Culex pipiens*. *Journal of Insect Physiology* **52**, 1226-1233.
- Kobayashi, M., Ishikawa, H.** (1994). Involvement of juvenile hormone and ubiquitin-dependent proteolysis in flight muscle breakdown of alate aphid (*Acyrtosiphon pisum*). *Journal of Insect Physiology* **40**, 107-111.
- Košťál, V.** (2006). Eco-physiological phases of insect diapause. *Journal of Insect Physiology* **52**, 113-127.
- Košťál, V., Šimůnková, P., Kobelková, A., Shimada, K.** (2009). Cell cycle arrest as a hallmark of insect diapause: changes in gene transcription during diapause induction in the drosophilid fly, *Chymomyza costata*. *Insect Biochemistry and Molecular Biology* **39**, 875-883.
- Kramer, S., De Kort, C.** (1976). Age-dependent changes in juvenile hormone esterase and general carboxyesterase activity in the hemolymph of the Colorado potato beetle, *Leptinotarsa decemlineata*. *Molecular and Cellular Endocrinology* **4**, 43-53.
- Kukal, O., Denlinger, D.L., Lee, R.E.** (1991). Developmental and metabolic changes induced by anoxia in diapausing and non-diapausing flesh fly pupae. *Journal of Comparative Physiology B* **160**, 683-689.
- Lee, B., Barretto, E.C., Grewal, S.S.** (2019). TORC1 modulation in adipose tissue is required for organismal adaptation to hypoxia in *Drosophila*. *Nature Communications* **10**, 1878.

- Lee, J.-Y., Nagano, Y., Taylor, J.P., Lim, K.L., Yao, T.-P.** (2010a). Disease-causing mutations in parkin impair mitochondrial ubiquitination, aggregation, and HDAC6-dependent mitophagy. *Journal of Cell Biology* **189**, 671-679.
- Lee, R.E., Denlinger, D.L.** (1985). Cold tolerance in diapausing and non-diapausing stages of the flesh fly, *Sarcophaga crassipalpis*. *Physiological Entomology* **10**, 309-315.
- Lee, S.-J., Hwang, A.B., Kenyon, C.** (2010b). Inhibition of respiration extends *C. elegans* life span via reactive oxygen species that increase HIF-1 activity. *Current Biology* **20**, 2131-2136.
- Lefevre, K., De Wilde, J.** (1984). Effect of photoperiod and allatectomy on reproduction and (second) diapause induction in post-diapause adult females of the Colorado potato beetle, *Leptinotarsa decemlineata* Say. *International Journal of Invertebrate Reproductive Development* **7**, 69-72.
- Lehmann, P., Lyytinen, A., Piironen, S., Lindström, L.** (2014a). Northward range expansion requires synchronization of both overwintering behaviour and physiology with photoperiod in the invasive Colorado potato beetle (*Leptinotarsa decemlineata*). *Oecologia* **176**, 57-68.
- Lehmann, P., Piironen, S., Kankare, M., Lyytinen, A., Paljakka, M., Lindström, L.** (2014b) Photoperiodic effects on diapause-associated gene expression trajectories in European *Leptinotarsa decemlineata* populations. *Insect Molecular Biology* **23**, 566-578.
- Love, M.I., Huber, W., Anders, S.** (2014). Moderated estimation of fold change and dispersion for RNA-seq data with DESeq2. *Genome Biology* **15**, 550.
- Luo, W., Friedman, M.S., Shedden, K., Hankenson, K.D., Woolf, P.J.** (2009). GAGE: generally applicable gene set enrichment for pathway analysis. *BMC Bioinformatics* **10**, 1-17.
- Lyytinen, A., Mappes, J., Lindström, L.** (2012). Variation in Hsp70 levels after cold shock: signs of evolutionary responses to thermal selection among *Leptinotarsa decemlineata* populations. *PLoS One* **7**, e31446.
- MacMillan, H.A., Knee, J.M., Dennis, A.B., Udaka, H., Marshall, K.E., Merritt, T.J., Sinclair, B.J.** (2016a). Cold acclimation wholly reorganizes the *Drosophila melanogaster* transcriptome and metabolome. *Scientific Reports* **6**, 28999.
- MacRae, T.H.** (2010). Gene expression, metabolic regulation and stress tolerance during diapause. *Cellular and Molecular Life Sciences* **67**, 2405-2424.
- McCart, C., French-Constant, R.H.** (2008). Dissecting the insecticide-resistance-associated cytochrome P450 gene Cyp6g1. *Pest Management Science* **64**, 639-645.

- Mello, T., Aleixo, A., Pinheiro, D., Nunes, F., Cristino, A., Bitondi, M., Barchuk, A., Simões, Z.** (2019). Hormonal control and target genes of ftz-fl expression in the honeybee *Apis mellifera*: a positive loop linking juvenile hormone, ftz-fl, and vitellogenin. *Insect Molecular Biology* **28**, 145-159.
- Nakamura, A., Miyado, K., Takezawa, Y., Ohnami, N., Sato, M., Ono, C., Harada, Y., Yoshida, K., Kawano, N., Kanai, S.** (2011). Innate immune system still works at diapause, a physiological state of dormancy in insects. *Biochemical and Biophysical Research Communications* **410**, 351-357.
- Pegoraro, M., Bafna, A., Davies, N.J., Shuker, D.M., Tauber, E.** (2016). DNA methylation changes induced by long and short photoperiods in *Nasonia*. *Genome Research* **26**, 203-210.
- Pertea, M., Pertea, G.M., Antonescu, C.M., Chang, T.-C., Mendell, J.T., Salzberg, S.L.** (2015). StringTie enables improved reconstruction of a transcriptome from RNA-seq reads. *Nature Biotechnology* **33**, 290.
- Poelchau, M.F., Reynolds, J.A., Denlinger, D.L., Elsik, C.G., Armbruster, P.A.** (2011). A *de novo* transcriptome of the Asian tiger mosquito, *Aedes albopictus*, to identify candidate transcripts for diapause preparation. *BMC Genomics* **12**, 619.
- Poelchau, M.F., Reynolds, J.A., Elsik, C.G., Denlinger, D.L., Armbruster, P.A.** (2013). RNA-Seq reveals early distinctions and late convergence of gene expression between diapause and quiescence in the Asian tiger mosquito, *Aedes albopictus*. *Journal of Experimental Biology* **216**, 4082-4090.
- Qi, X., Zhang, L., Han, Y., Ren, X., Huang, J., Chen, H.** (2015). *De novo* transcriptome sequencing and analysis of *Coccinella septempunctata* L. in non-diapause, diapause and diapause-terminated states to identify diapause-associated genes. *BMC Genomics* **16**, 1.
- Ragland, G.J., Denlinger, D.L., Hahn, D.A.** (2010). Mechanisms of suspended animation are revealed by transcript profiling of diapause in the flesh fly. *Proceedings of the National Academy of Sciences of the U.S.A.* **107**, 14909-14914.
- Reczek, C.R., Chandel, N.S.** (2015). ROS-dependent signal transduction. *Current Opinions in Cell Biology* **33**, 8-13.
- Reynolds, J.A.** (2017). Epigenetic influences on diapause. *Advances in Insect Physiology* **53**, 115-144.
- Santos, P.K.F., de Souza Araujo, N., Françoso, E., Zuntini, A.R., Arias, M.C.** (2018). Diapause in a tropical oil-collecting bee: molecular basis unveiled by RNA-Seq. *BMC Genomics* **19**, 1-11.

- Sarbasov, D.D., Sabatini, D.M.** (2005). Redox regulation of the nutrient-sensitive raptor-mTOR pathway and complex. *Journal of Biological Chemistry* **280**, 39505-39509.
- Schoville, S.D., Chen, Y.H., Andersson, M.N., Benoit, J.B., Bhandari, A., Bowsher, J.H., Brevik, K., Cappelle, K., Chen, M.J.M., Childers, A.K., Childers, C., Christiaens, O., Clements, J., Didion, E.M., Elpidina, E.N., Engsontia, P., Friedrich, M., Garcia-Robles, I., Gibbs, R.A., Goswami, C., Grapputo, A., Gruden, K., Grynberg, M., Henrissat, B., Jennings, E.C., Jones, J.W., Kalsi, M., Khan, S.A., Kumar, A., Li, F., Lombard, V., Ma, X., Martynov, A., Miller, N.J., Mitchell, R.F., Munoz-Torres, M., Muszewska, A., Oppert, B., Palli, S.R., Panfilio, K.A., Pauchet, Y., Perkin, L.C., Petek, M., Poelchau, M.F., Record, E., Rinehart, J.P., Robertson, H.M., Rosendale, A.J., Ruiz-Arroyo, V.M., Smagghe, G., Szendrei, Z., Thomas, G.W.C., Torson, A.S., Jentzsch, I.M.V., Weirauch, M.T., Yates, A.D.T., Yocum, G.D., Yoon, J.S., Richards, S.** (2018). A model species for agricultural pest genomics: the genome of the Colorado potato beetle, *Leptinotarsa decemlineata* (Coleoptera: Chrysomelidae). *Scientific Reports* **8**, 1931.
- Sim, C., Denlinger, D.L.** (2008). Insulin signaling and FOXO regulate the overwintering diapause of the mosquito *Culex pipiens*. *Proceedings of the National Academy of Sciences of the U.S.A.* **105**, 6777-6781.
- Sim, C., Denlinger, D.L.** (2009). Transcription profiling and regulation of fat metabolism genes in diapausing adults of the mosquito *Culex pipiens*. *Physiological Genomics* **39**, 202-209.
- Sim, C., Denlinger, D.L.** (2011). Catalase and superoxide dismutase-2 enhance survival and protect ovaries during overwintering diapause in the mosquito *Culex pipiens*. *Journal of Insect Physiology* **57**, 628-634.
- Sim, C., Denlinger, D.L.** (2013). Insulin signaling and the regulation of insect diapause. *Frontiers in Physiology* **4**, 189.
- Sinclair, B.J.** (2015). Linking energetics and overwintering in temperate insects. *Journal of Thermal Biology* **54**, 5-11.
- Sinclair, B.J., Marshall, K.E.** (2018). The many roles of fats in overwintering insects. *Journal of Experimental Biology* **221**, jeb.161836.
- Stegwee, D., Kimmel, E., De Boer, J., Henstra, S.** (1963). Hormonal control of reversible degeneration of flight muscle in the Colorado potato beetle, *Leptinotarsa decemlineata* Say (Coleoptera). *Journal of Cell Biology* **19**, 519-527.
- Supek, F., Bošnjak, M., Škunca, N., Šmuc, T.** (2011). REVIGO summarizes and visualizes long lists of gene ontology terms. *PloS One* **6**, e21800.

- Tammariello, S.P., Denlinger, D.L.** (1998). G0/G1 cell cycle arrest in the brain of *Sarcophaga crassipalpis* during pupal diapause and the expression pattern of the cell cycle regulator, proliferating cell nuclear antigen. *Insect Biochemistry and Molecular Biology* **28**, 83-89.
- Tessier, S.N., Luu, B.E., Smith, J.C., Storey, K.B.** (2017). The role of global histone post-translational modifications during mammalian hibernation. *Cryobiology* **75**, 28-36.
- Torson, A.S., Yocum, G.D., Rinehart, J.P., Nash, S.A., Kvidera, K.M., Bowsher, J.H.** (2017). Physiological responses to fluctuating temperatures are characterized by distinct transcriptional profiles in a solitary bee. *Journal of Experimental Biology* **220**, 3372-3380.
- Torson, A.S., Dong, Y.-W., Sinclair, B.J.** (2020). Help, there are 'omics' in my comparative physiology! *Journal of Experimental Biology* **223**, jeb.191262.
- Ubersax, J.A., Woodbury, E.L., Quang, P.N., Paraz, M., Blethrow, J.D., Shah, K., Shokat, K.M., Morgan, D.O.** (2003). Targets of the cyclin-dependent kinase Cdk1. *Nature* **425**, 859-864.
- Vermunt, A., Koopmanschap, A., Vlak, J., De Kort, C.** (1998). Evidence for two juvenile hormone esterase-related genes in the Colorado potato beetle. *Insect Molecular Biology* **7**, 327-336.
- Vigneron, S., Sundermann, L., Labbé, J.-C., Pintard, L., Radulescu, O., Castro, A., Lorca, T.** (2018). Cyclin A-cdk1-dependent phosphorylation of Bora is the triggering factor promoting mitotic entry. *Developmental Cell* **45**, 637-650.
- Vives-Bauza, C., Przedborski, S.** (2011). Mitophagy: the latest problem for Parkinson's disease. *Trends in Molecular Medicine* **17**, 158-165.
- Weeda, E., Koopmanschap, A., De Kort, C., Beenackers, A.T.** (1980). Proline synthesis in fat body of *Leptinotarsa decemlineata*. *Insect Biochemistry* **10**, 631-636.
- Yocum, G.** (2001). Differential expression of two HSP70 transcripts in response to cold shock, thermoperiod, and adult diapause in the Colorado potato beetle. *Journal of Insect Physiology* **47**, 1139-1145.
- Yocum, G.** (2003). Isolation and characterization of three diapause-associated transcripts from the Colorado potato beetle, *Leptinotarsa decemlineata*. *Journal of Insect Physiology* **49**, 161-169.
- Yocum, G.D., Buckner, J.S., Fatland, C.L.** (2011a). A comparison of internal and external lipids of nondiapausing and diapause initiation phase adult Colorado potato beetles, *Leptinotarsa decemlineata*. *Comparative Biochemistry and Physiology B* **159**, 163-170.

- Yocum, G.D., Rinehart, J.P., Chirumamilla-Chapara, A., Larson, M.L.** (2009a). Characterization of gene expression patterns during the initiation and maintenance phases of diapause in the Colorado potato beetle, *Leptinotarsa decemlineata*. *Journal of Insect Physiology* **55**, 32-39.
- Yocum, G.D., Rinehart, J.P., Larson, M.L.** (2009b). Down-regulation of gene expression between the diapause initiation and maintenance phases of the Colorado potato beetle, *Leptinotarsa decemlineata* (Coleoptera: Chrysomelidae). *European Journal of Entomology* **106**, 471-476.
- Yocum, G.D., Toutges, M.J., Roehrdanz, R.L., Dihle, P.J.** (2011b). Insertion of miniature subterminal inverted repeat-like elements in diapause-regulated genes in the Colorado potato beetle, *Leptinotarsa decemlineata* (Coleoptera: Chrysomelidae). *European Journal of Entomology* **108**, 197-203.
- Young, M.D., Wakefield, M.J., Smyth, G.K., Oshlack, A.** (2012). goseq: Gene Ontology testing for RNA-seq datasets. *R Bioconductor* **8**, 1-25.
- Zachariassen, K.E.** (1985). Physiology of cold tolerance in insects. *Physiological Reviews* **65**, 799-832.
- Zhang, Q., Denlinger, D.L.** (2010). Molecular characterization of heat shock protein 90, 70 and 70 cognate cDNAs and their expression patterns during thermal stress and pupal diapause in the corn earworm. *Journal of Insect Physiology* **56**, 138-150.
- Zhang, L., Cheng, L., Chapman, J.W., Sappington, T.W., Liu, J., Cheng, Y., Jiang, X.** (2020). Juvenile hormone regulates the shift from migrants to residents in adult oriental armyworm, *Mythimna separata*. *Scientific Reports* **10**, 1-12.
- Zhou, Z.-X., Dong, X.-L., Li, C.-R.** (2021). Comparative transcriptome analysis of different developmental stage of *Bactrocera minax* (Diptera: Tephritidae): Implication of the molecular basis of its obligatory diapause induction. *Comparative Biochemistry and Physiology D* **38**, 1008.

Chapter 3

3 Reversible mitophagy drives metabolic suppression in a diapausing beetle

A version of this chapter was submitted for publication to *Proceedings of the National Academy of Sciences of the U.S.A.*

3.1 Introduction

When resources are limited during the winter, animals face energetic stress (Sinclair, 2015; Williams et al., 2015). To save energy during these periods, many animals become dormant and suppress their metabolic rate (Wilsterman et al., 2021). Metabolic suppression is widespread in dormant animals and is facilitated by reducing rates of ATP production in the mitochondria, thereby allowing animals to consume less stored food energy (Staples and Buck, 2009). Many dormant vertebrates, such as hibernating ground squirrels and diapausing killifish embryos, reduce ATP production by lowering the activity of mitochondrial electron transport system enzymes (Duerr and Podrabsky, 2010; Mathers et al., 2017). Insects also suppress their metabolic rate during diapause, a hypometabolic dormant state that insects enter before the onset of harsh environmental conditions (Košťál, 2006). However, we know less about the mechanisms that underpin metabolic suppression in insects than in vertebrates. Further, we do not know how insects reverse this suppression and increase their metabolic rate in the spring to power energy costly activities such as flight and reproduction.

The Colorado potato beetle (CPB; *Leptinotarsa decemlineata*) is a pest of potato plants and lives in temperate areas across North America, Europe, and Asia (Boiteau et al., 2003; Grapputo et al., 2005). In late summer and early autumn, short daylengths cue decreased levels of circulating developmental hormones (especially juvenile hormone) which initiate diapause in adult beetles (De Kort et al., 1982; De Wilde et al., 1959). During this stage of diapause initiation, adult beetles feed voraciously, arrest their reproductive development, accumulate lipid energy stores, and eventually burrow into the soil where they overwinter in diapause (Yocum et al., 2011). Diapausing Colorado potato beetles suppress their metabolic rates (Lehmann et al., 2015) and increase their tolerance to stresses such as low temperatures

and desiccation (Boiteau and Coleman, 1996). In the spring, beetles terminate their diapause, emerge from the soil and immediately disperse to fly to search for food and a mate (Ferro et al., 1999).

During diapause, CPB degrade their flight muscle, and rapidly regrow it post-winter (Stegwee et al., 1963). In Chapter 2, I found that Colorado potato beetle flight muscle differentially expresses transcripts associated with protein turnover and mitochondrial homeostasis during diapause, including mitochondrial import inner membrane translocase protein (*TIM16*), autophagy-related protein 10 (*ATG10*), and biogenesis of lysosome-related organelles complex 1 subunit 2. From these changes in transcript abundance, I hypothesized that flight muscle is not just degraded, but could play a role in modulating mitochondria-dependent energy metabolism during diapause. Mitochondria make up one third of an insect's flight muscle wet weight (Levenbook, 1953). Thus, flight muscle degradation is a good candidate for exploring the mechanisms underlying substantial decreases in whole-animal metabolic rate. Further, we know that CPB regrow their flight muscle and recover high metabolic rates in the spring, but a mechanistic link between flight muscle regeneration and re-establishment of metabolism in diapausing insects has not been made.

Here I show that whole-animal metabolic suppression in a diapausing insect, the Colorado potato beetle, is driven by tissue-specific mitochondrial breakdown (mitophagy). During diapause, CPB activate Parkin-mediated mitophagy in their flight muscle, which remodels mitochondrial homeostasis and results in a lower metabolic rate. Furthermore, CPB can reverse this mitophagy just before diapause ends without any external cues. In anticipation of their emergence from diapause, CPB use transcriptionally mediated mitochondrial biogenesis to regrow their flight muscle mitochondrial pool and concomitantly recover a high metabolic rate. My results provide insight into the diversity of adaptations animals use to save energy in resource-limited environments and provide potential mechanisms to activate mitochondrial proliferation in diseased states.

3.2 Materials and Methods

3.2.1 Insect care and diapause induction

I established a colony of *Leptinotarsa decemlineata* with individuals originally collected from potato fields at the London Research and Development Centre in London, Ontario, Canada and maintained the colony in greenhouses at the University of Western Ontario. The population was supplemented annually with c. 50 field-collected individuals to reduce inbreeding. For general rearing (control, non-diapausing CPB), I maintained eggs, larvae, and adults on fresh Kennebec potato plants in BugDorms (Megaview science, Talchung, Taiwan, W60 × D60 × H60 cm) at 24 °C under a long daylength (16:8 L:D). I allowed adults to freely mate and lay eggs on plants in the BugDorms.

I induced diapause following the same protocols as Chapter 2 (Figure 1.1). Briefly, I reared eggs laid by control adults on excised potato leaves in petri dishes lined with moist paper towel in temperature and light-controlled incubators (Sanyo Scientific, Bensenville, IL, USA) at 24 °C and short days (8:16 L:D). I transferred newly hatched larvae to 500 mL plastic containers lined with moistened paper towels and fed them daily with fresh potato leaves. I maintained larvae in groups of c. 20 in these containers until they reached the 4th instar stage. I transferred 4th instar larvae to 14 L plastic pupation bins filled with soil and provided them fresh leaves daily until the larvae burrowed into the soil to pupate. Once adults emerged from the soil, I transferred them to fresh plastic bins filled with soil and kept them at 15 °C (8:16 L:D), which I refer to as diapause-inducing conditions (Figure 1.1). I kept 20-30 beetles in each bin and fed these diapause-destined adults fresh potato leaves daily for 3-4 weeks after which they stopped eating and burrowed into the soil. I did not observe any females laying eggs in these diapause-destined populations. After nine weeks in diapause-inducing conditions, all beetles had burrowed into the soil. After 15-20 weeks in diapause-inducing conditions, beetles spontaneously emerged from the soil (Figure 1.1).

3.2.2 Whole animal respirometry

I tracked whole-animal metabolic rate in control CPB and in CPB exposed to diapause-inducing conditions throughout their diapause programme using Sable Systems flow-through respirometry (Sable Systems International, Las Vegas, NV, USA). I included CPB from the

following groups: non-diapause (control), exposed to diapause-inducing conditions for three, six, nine, 12, 15, and 20 weeks (emerged). I measured CO₂ production as a proxy for metabolic rate at 15 °C according to Williams et al. (2012). Briefly, I passed dry CO₂-free air through chambers at 80 mL min⁻¹ using mass-flow valves (Sierra Instruments, Monterey, California, USA) and a mass-flow controller (Super Systems Inc., Cincinnati, OH, USA). I recorded CO₂ release for 30 min per individual using a Li7000 infrared gas analyzer (LiCor, Lincoln, Nebraska, USA). I recorded data on Expedata software using a UI2 interface (Super Systems Inc., Cincinnati, OH, USA), and corrected CO₂ release to baseline recordings of an empty chamber made for 5 min before and after each run. I calculated $\dot{V}CO_2$ for three consecutive cycles of discontinuous gas exchange using the equation:

$$\dot{V}CO_2 = \left(\frac{CO_2}{1000000} \right) \times FR$$

where FR is the incurrent flow rate of CO₂-free air (mL min⁻¹) and CO₂ is the CO₂ concentration leaving the chamber (ppm). I weighed individuals before and after each run, and corrected $\dot{V}CO_2$ for body mass by dividing $\dot{V}CO_2$ by the average mass of each individual. I fasted non-diapausing CPB 24 h before measurements to ensure steady state resting metabolic rates, however I did not fast diapausing CPB because they were no longer actively feeding. I compared $\dot{V}CO_2$ measurements using a one-way ANCOVA, with CPB mass (averaged between the start and end of each run for each individual) as a co-variate, and analysed differences among treatment groups using a Tukey's HSD in R (R, version 3.3.2, R Core Team, Vienna, Austria).

3.2.3 High-resolution respirometry

I measured mitochondrial respiration rates in saponin-permeabilized CPB flight muscle using high-resolution respirometry. I included CPB from the following groups: non-diapause (control), exposed to diapause-inducing conditions for three, six, nine, 12, 15, and 20 weeks (Emerged). From each group, I dissected thorax flight muscle of CPB directly into a 500 µl aliquot of ice-cold BIOPS permeabilization buffer (50 mM K-MES, 7.23 mM EGTA, 2.77 mM Ca₃K₂EGTA, 20 mM imidazole, 20 mM taurine, 5.7 mM ATP, 14.3 mM phosphocreatine, 6.56 mM MgCl₂, pH 7.1; Eigentler et al., 2012) to preserve the energetic state of the tissue. I removed any adhering fat body tissue while the tissue was submerged in

BIOPS and placed the remaining flight muscle into 2 mL of fresh ice cold BIOPS containing 50 µg/mL of saponin (Sigma). I incubated the samples in saponin for 30 minutes on a shaker under constant agitation (300 rpm) to permeabilize the muscle fibers, and then gently transferred the permeabilized fibers to 2 mL of ice-cold mitochondrial respiration buffer (MiR05; 105 mM K-MES, 30 mM KCl, 1 mM EGTA, 10 mM KH₂PO₄, 5 mM MgCl₂, 5 mg/mL BSA, pH 7.1; Kuznetsov et al., 2008), and incubated the fibers on a shaker under constant agitation for 5 minutes (300 rpm). I repeated this step twice to remove any residual saponin. Immediately after the second wash in MiR05, I gently blotted the flight muscle samples twice with a cotton swab to remove excess buffer, and weighed them on a microbalance (MX5, Mettler Toledo).

Immediately after weighing the permeabilized tissue, I gently transferred it to chambers of an Oxygraph-2k high resolution respirometer (Oroboros Instruments, Austria), containing 2 mL of MiR05 under constant stirring (750 rpm) at 15 °C (the same temperature used in whole-animal flow-through respirometry measurements). First, I assessed stable State 2 mitochondrial respiration rates stimulated with L-proline (10 mM). I used L-proline as a substrate because it was the only fuel that stimulated measurable O₂ consumption rates in tissue from both non-diapausing and diapausing beetles (J.E. Lebenzon, unpublished data). After stable State 2 respiration rates were reached with the addition of L-proline, I added ADP (2 mM) and Mg²⁺ (5 mM) to stimulate State 3 respiration. I then added oligomycin (1 mg/mL in ethanol) to inhibit ATP synthase and estimate State 4 respiration followed by CCCP (1 mM) to uncouple electron transfer from O₂ consumption and measure Maximal Uncoupled mitochondrial respiration rates (Figure S2). I compared State 3 respiration rates using a one-way ANCOVA, with fresh flight muscle mass as a co-variate, and analysed differences among treatment groups using a Tukey's HSD in R (R, version 3.3.2, R Core Team, Vienna, Austria).

3.2.4 Citrate synthase activity

I measured citrate synthase activity in flight muscle of CPB, as citrate synthase activity is often used as a proxy for mitochondrial abundance (Larsen et al., 2012). I included CPB from the following groups: non-diapause (control), exposed to diapause-inducing conditions for

three, six, nine, 12, 15, and 20 weeks (emerged). I dissected flight muscle from beetles in each group directly into Ringer's solution (160 mM NaCl, 11 mM KCl, 8.4 mM CaCl₂, 5.9 mM MgCl₂, 5 mM HEPES, pH=7.0), then placed tissue into pre-weighed 1.7 mL microcentrifuge tubes which I flash-froze in liquid nitrogen vapor and stored at -80 °C until use in enzyme assays. On the day of enzyme assays, I added ice-cold homogenization buffer (20 mM Tris, 1 mM EDTA, 0.1 % Triton X-100, pH 7.2; 20:1, buffer volume to tissue mass) to each sample, and homogenized the tissue using a handheld electric homogenizer (VWR Pellet Mixer). I then centrifuged the homogenate for 5 min at 2000 × g at 4 °C and transferred the supernatant to two new tubes; one aliquot was used for citrate synthase enzyme activity, and the other for protein quantification.

I performed citrate synthase enzyme assays according to Mathers and Staples (2015). Briefly, I combined 2.5 µl of supernatant with 294.5 µl of citrate synthase reaction mixture (50 mM Tris pH 8.0, 1.5 mM Acetyl Coenzyme A, 1.5 mM DTNB) in wells of a 96-well assay plate and ran parallel reactions with and without the addition of 33 mM oxaloacetate. I measured absorbance at 412 nm at 10 s intervals for 5 min at 21 °C for each reaction on a Spectromax plate spectrophotometer (Molecular Devices, Sunnyvale, CA), and calculated citrate synthase enzyme activity from the difference between rates with and without oxaloacetate. I ran samples in triplicate, and calculated citrate synthase activity from the mean of triplicates. I standardized citrate synthase enzyme activity to total protein concentration in each sample, which I measured using a bicinchoninic acid assay (ThermoFisher Scientific, Massachusetts, USA). I compared citrate synthase enzyme activities among groups using a one-way ANCOVA using protein content as a co-variate and compared differences among each treatment group using Tukey's HSD in R (R, version 3.3.2, R Core Team Vienna, Austria).

3.2.5 Fluorescence and electron microscopy

I used fluorescence microscopy to image nuclei in the flight muscle of control CPB and CPB exposed to nine weeks of diapause-inducing conditions (during diapause maintenance). I dissected flight muscle from CPB in each treatment into ice-cold 4 % paraformaldehyde and incubated overnight at 4 °C. I then embedded tissues into paraffin, cross-sectioned the

paraffin blocks, and mounted the paraffinized flight muscle sections on slides. I deparaffinized tissue sections in xylene, rehydrated them in 70 % ethanol, and stained for nuclei using DAPI (4',6-diamidino-2-phenylindole; 0.6 μ M). I imaged slides with a Zeiss LSM 5 Duo Vario confocal microscope and ZEN Pro software (Carl Zeiss Microscopy GmbH, Jena, Germany).

I used transmission electron microscopy to visualize the structure and presence of mitochondria in flight muscle cells. I included CPB from the following groups: non-diapause (control), exposed to diapause-inducing conditions for six, nine, 12, 15, and 20 weeks. I dissected flight muscle from beetles in each group straight into ice-cold fixative (2 % glutaraldehyde, 2.5 % paraformaldehyde in 0.2 M sodium phosphate buffer, pH=7.4) and incubated the samples overnight at 4 °C. I washed tissues (1 \times 5 min, 5 \times 30 min) in double distilled water to ensure the removal of residual fixative, and stained tissue with 1 % osmium tetroxide on ice and in the dark for 45 min. Directly following osmium tetroxide staining, I washed tissues (1 \times 5 min, 5 \times 30 min) in double distilled water to ensure the removal of residual osmium tetroxide, and stained with 2 % uranyl acetate in the dark, overnight. I washed tissues again (1 \times 5 min, 5 \times 30 min) in double distilled water, and then serially dehydrated the tissue in acetone, and embedded tissues in Epon-Araldite resin (Electron Microscopy Sciences, Fort Washington, PA, USA), which I then polymerized at 60 °C for four days. I cut 0.5 μ m sections and stained each section with 2 % uranyl acetate (20 min per section), immediately followed by Reynold's lead citrate (1 minute per section). I imaged sections at 19000 \times magnification with a Philips CM10 Transmission Microscope (Philips Electron Optics, Eindhoven, The Netherlands) equipped with an AMT Advantage digital imaging system and Hamamatsu Orca 2 MPx HRL Camera (Advanced Microscopy Techniques, Woburn, MA).

3.2.6 mRNA abundance quantification

I used quantitative real time PCR (qPCR) to measure changes in abundance of mitophagy and mitochondrial biogenesis-related transcripts. I included CPB from the following groups: non-diapause (control), exposed to diapause-inducing conditions for six, nine, 12, 15, and 20 weeks. I dissected c. 5 mg of flight muscle from CPB in each treatment group directly into

Ringer's solution (160 mM NaCl, 11 mM KCl, 8.4 mM CaCl₂, 5.9 mM MgCl₂, 5 mM HEPES, pH=7.0), placed tissue into pre-weighed 1.7 mL microcentrifuge tubes, flash froze tissues in liquid nitrogen vapor, and stored them at -80 °C until RNA extractions.

I extracted RNA using TRIzol (ThermoFisher Scientific, Mississauga, ON, Canada) according to the manufacturer's instructions, removed residual genomic DNA from the sample using DNase (Quantabio, Beverly, Massachusetts, USA), and measured absorbance at 260 nm to determine the RNA concentration using a Nanodrop spectrophotometer (ThermoFisher scientific, Mississauga, ON, Canada). The A₂₆₀/A₂₈₀ of all RNA samples after DNase reactions was between 1.8-2.0, indicating high quality RNA. I synthesized cDNA from 1000 ng of RNA using the iScript cDNA synthesis kit (Bio-Rad, Mississauga, ON, Canada), and stored the cDNA in -20 °C until use. I diluted all cDNA to the same concentration prior to use in qPCR reactions. To amplify cDNA, I used SsoAdvanced Universal SYBR Green supermix (Bio-Rad, Mississauga, ON, Canada) according to the manufacturer's instructions. Each qPCR reaction included 10 mM of forward and 10 mM reverse primer, and 1000 ng cDNA, and I ran each reaction in triplicate using a Rotor-Gene Q real-time PCR cycler (Qiagen, Hilden, Germany). Primer sequence information for mitophagy and mitochondrial biogenesis-related genes can be found in Table B1.

I normalized transcript abundance in two ways; to two validated reference genes (*TBP1* and *EF1α*; See Table B1 for primer sequence information), and to internal calibrator samples consisting of cDNA synthesized from RNA extracted from fat body tissue in control beetles. I used these internal calibrator samples in each run to control for any inconsistencies among different qPCR runs. Finally, I calculated relative normalized transcript abundance using the comparative C_T method ($2^{-\Delta\Delta C_T}$), which compared treated samples (those under diapause-inducing conditions) against the non-diapausing control (Livak and Schmittgen, 2001). I compared comparative C_T values using a one-way ANOVA and compared differences among treatment groups using a Tukey's HSD test in R (R, version 3.3.2, R Core Team 2017 Vienna, Austria).

3.2.7 RNA interference knockdown of *Parkin*

I designed and synthesized a dsRNA construct to target *Parkin*, and also synthesized a dsRNA construct complementary to *green fluorescent protein (GFP)*, to inject as a negative control for off-target effects that should not target any endogenous insect mRNAs. I used E-RNAi (Horn and Boutros, 2010; <https://www.dkfz.de/signaling/e-rnai3/>) to design primers which could amplify either *Parkin* (NCBI: XM_023174278.1) from beetle cDNA or *GFP* (Genbank: U55762.1) from a pEGFP-N1 plasmid. Each primer contained a T7 promoter sequence on the 5' end, which is required for downstream dsRNA synthesis by a T7 RNA polymerase. I used these primers to generate templates for dsRNA synthesis from beetle cDNA and the pEGFP-N1 plasmid *via* PCR (GeneDirex Taq DNA polymerase; FroggaBio, Toronto, ON, Canada), according to the manufacturer's instructions.

I synthesized dsRNA using the MEGAScript RNAi kit (ThermoFisher Scientific, Waltham Massachusetts, USA) according to the manufacturer's protocols. Briefly, I transcribed *Parkin* and *GFP* amplicons from both 5' ends to single stranded RNA (ssRNA), annealed the complementary ssRNA molecules by heating them to 75 °C and allowing them to cool to room temperature and thus anneal to dsRNA, and performed a final nuclease digestion to remove residual DNA and ssRNA. I confirmed successful dsRNA synthesis by performing gel electrophoresis and observing bands at 484 bp and 411 bp for *Parkin* and *GFP*, respectively (Figure B5).

I reduced the transcript abundance in diapausing CPB by injecting diapausing beetles with *dsParkin* and injected a second group with *dsGFP* as a negative control. I injected beetles with a 10 µl Hamilton syringe (Hamilton Company, Reno, Nevada, USA) fitted with a 30 G needle, filled with 1 µg of dsRNA complementary to *Parkin* or *GFP* in 5 µL phosphate-buffered saline. To ensure I injected beetles with dsRNA prior to the peak expression of *Parkin* during diapause (nine weeks), I injected beetles that had been in diapause-inducing conditions for seven weeks. I used qPCR to verify transcript knockdown and western blot analysis to verify protein knockdown (as described below). I used the same individuals for qPCR and western blot analysis. After injection I waited five days before dissecting c. 5 mg flight muscle directly into Ringer's solution. Five days was the amount of time to reach

maximal transcript knockdown in beetle flight muscle (Figure B5). I then measured whole-animal metabolic rate, flight muscle mitochondrial respiration rate, citrate synthase enzyme activity and mitochondrial abundance in knockdown beetles five days post-injection (as described in sections above).

3.2.8 Protein quantification by western Blotting

To extract protein from flight muscle, I placed 200 μ l of lysis buffer (2 % SDS, 50 mM Tris, 1 mM PMSF, protease inhibitor cocktail [Sigma Aldrich, St. Louis, Missouri, USA]) into tubes with tissue, sonicated samples 2×20 s with a handheld sonication probe (LabX, Ontario, Canada), and centrifuged them $5000 \times g$ at 4 °C for 10 min. I reserved a 10 μ l aliquot (diluted 10X in 90 μ l lysis buffer) for protein quantification using a BCA protein assay kit (Thermo Scientific, Waltham, MA, USA) to determine the volume of extract containing 20 μ g of protein.

I denatured protein extracts in 4X Laemmli Sample buffer at 100 °C for 5 min prior to loading (20 μ g of protein/ well) in a 4-20 % polyacrylamide TGX Stain-Free Gel (Bio-Rad, Mississauga, ON, Canada) I separated protein by electrophoresis at 120 V for 1.5 h in Tris-glycine-SDS running buffer (25 mM Tris, 192 mM glycine, 0.1 % SDS). After electrophoresis, I activated gels on a ChemiDoc imaging system (Bio-Rad, Mississauga, ON, Canada) using UV light which allowed for total protein visualization for eventual standardization of Parkin protein abundance to total protein abundance. After gel activation, I immediately transferred proteins to a low fluorescence polyvinylidene fluoride (PVDF) membrane (Bio-Rad, Mississauga, ON, Canada) at 100 V for 2 h at 4 °C. Immediately after transferring, I imaged the blot for total protein on a ChemiDoc imaging systems, washed the membranes 3×5 min in $1 \times$ Tris-buffered Saline (TBS-T; 20 mM Tris, 143 mM NaCl, 0.05 % Tween-20), and then blocked membranes at room temperature for 2 h with 5 % bovine serum albumin (BSA) in $1 \times$ TBS-T under constant agitation (300 rpm). After blocking, I washed each membrane 3×5 mins with $1 \times$ TBS-T, and probed membranes with a custom *Leptinotarsa decemlineata* Parkin primary antibody (Life Tein Labs, 1:1000 in 0.05 % BSA in TBS-T, antibody raised against *L. decemlineata* Parkin sequence Accession ID: XP_0230300053.1) for 15 h at 4 °C under constant agitation (300 rpm). After primary

antibody incubation, I washed membranes 3×5 mins in $1 \times$ TBS-T, and then incubated membranes with a secondary antibody (mouse anti-rabbit, 1:10000 in 5 % BSA in TBS-T; Santa Cruz Biotechnology, California, USA) for 1.5 h at room temperature under constant agitation (300 rpm). Finally, I imaged membranes using the Biorad ChemiDoc system after incubating membranes in Pierce ECL Western blot substrate (Bio-Rad, Mississauga, ON, Canada).

3.3 Results & Discussion

3.3.1 Diapausing CPB reduce their metabolism and break down their flight muscle mitochondria

Laboratory-cultured CPB enter diapause when reared from egg to adult under short daylength (24 °C 8 h: 16 h, L:D) and transferred to diapause-inducing conditions (15 °C 8 h: 16 h, L:D; same conditions used to induce diapause in Chapter 2). After c. nine weeks in these diapause-inducing conditions, CPB suppress their metabolic rates and burrow into the soil. At this point, whole-animal metabolic rate reaches a nadir approximately 90 % lower than that of non-diapausing CPB (Figure 3.1). Diapausing CPB maintain this low metabolic rate for approximately nine more weeks (Figure 3.1). After 17-20 weeks in these constant, diapause-inducing conditions, CPB spontaneously break diapause and rapidly increase their metabolic rates to levels higher than pre-diapause values (Figure 3.1).

I hypothesized that the reduced metabolic rate I observed in diapausing CPB was driven by reduced mitochondrial respiratory capacity. I focused on flight muscle because CPB appear to histolyze this metabolically costly tissue during diapause (Stegwee et al., 1963), and the extent to which histolysis contributes to whole-organism metabolic suppression is not clear. Using high-resolution respirometry, I found that the mitochondrial respiration rates of saponin-permeabilized flight muscle in diapausing CPB (State 3, saturating proline and ADP) decline in the same temporal pattern as whole-animal metabolic rate, and to the same extent compared with non-diapausing beetles (Figure 3.1). Respiration rates did not increase after the addition of the uncoupler CCCP (Maximal Uncoupled Rates; Figure B2, B3), suggesting that any decreases during diapause were due to reduced ETS oxidative capacities rather than active suppression of ATP synthase (a strategy used by other diapausing ectotherms, *e.g.*,

Duerr and Podrabsky, 2010). Such a decrease could result from either a change in mitochondrial abundance or changes in flux through the electron transport system.

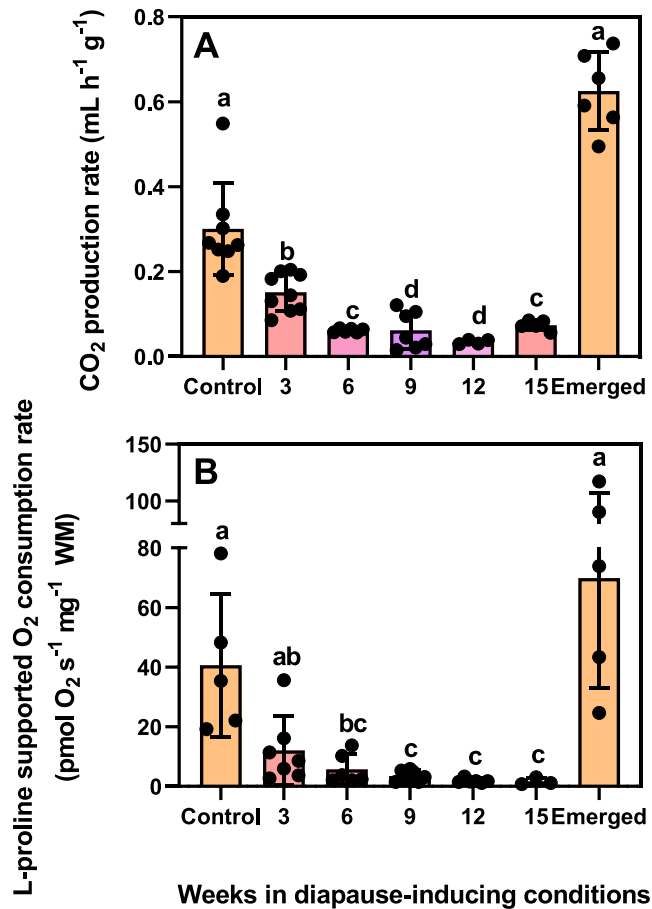


Figure 3.1. Colorado potato beetles suppress their whole animal metabolic rates and mitochondrial respiration rates in the same pattern during diapause. (A) Mean \pm S.D. CO₂ production rate measured using flow-through respirometry in CPB entering diapause (3-9 weeks), during diapause (9-15 weeks), and upon emergence from diapause (emerged, after 17-20 weeks). (B) Mean \pm S.D. proline-supported mitochondrial O₂ consumption in saponin-permeabilized flight muscle fibers (standardized to wet tissue mass, WM) measured using high-resolution respirometry in the same treatment groups as (A). Each point represents an individual beetle (A) or beetle's flight muscle (B). Groups were compared using a one-way ANCOVA with beetle mass (A) and flight muscle wet mass (WM; B) used as co-variates. Different letters denote significant differences among treatment groups ($p < 0.05$, Table B2).

Two lines of evidence support decreased mitochondrial abundance as the cause of suppressed flight muscle metabolism in CPB. First, citrate synthase activity (a proxy for mitochondrial abundance; Larsen et al., 2012) decreased concurrently with, and to the same extent as, mitochondrial respiration rates (Figure 3.2). I also observed a decrease in *citrate synthase* transcript abundance in the flight muscle of diapausing CPB in Chapter 2 (Table 2.3). Second, transmission electron microscopy revealed that mitochondria in the flight muscle of diapausing CPB are virtually absent (Figure 3.2). This corroborates early work suggesting that diapause coincides with degeneration of flight muscle sarcosomes in this species (Stegwee, 1964). However, I found that diapausing CPB degrade flight muscle mitochondria without a concomitant decrease in the number of nuclei (and presumably cells; Figure 3.2). Thus, beetles appear to selectively degrade metabolically costly mitochondria *via* mitophagy (mitochondrion-specific autophagy), without entirely degrading the flight muscle cells themselves.

Many insects irreversibly histolyze their flight muscle to redirect those resources to other processes such as reproduction (Edwards, 1969; Gunn and Gatehouse, 1993; Sun et al., 2020). However, those insects lose flight capability permanently, whereas Colorado potato beetles, like other insects that diapause as adults, fly in early spring. Therefore, I propose that CPB selectively degrade mitochondria during diapause rather than incur the cost of regrowing their muscle altogether. Such a strategy should be advantageous because it reduces muscle metabolic demands by avoiding even costlier hyperplasia at the end of diapause.

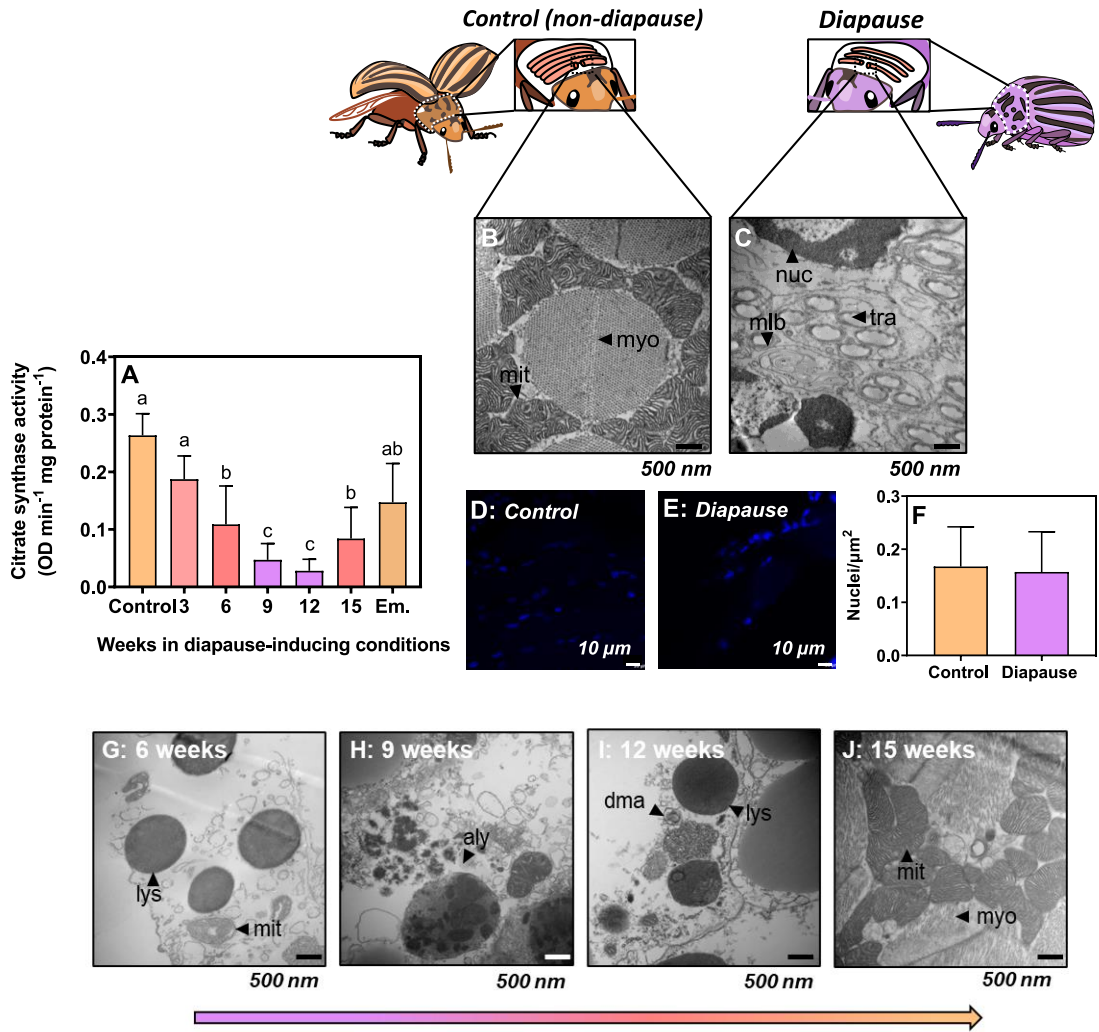


Figure 3.2. Functional mitochondria are absent from Colorado potato beetle flight muscle during diapause, but beetles reverse this mitochondrial breakdown upon diapause emergence. (A) Mean \pm S.D. citrate synthase activity as a proxy for mitochondrial abundance in flight muscle of CPB as they enter diapause (3-9 weeks), during diapause (9-15 weeks), and upon emergence (Em.). Groups were compared using a one-way ANCOVA with protein content as a covariate, and different letters denote significant differences among treatments ($p < 0.05$, Table B2). (B-C) Representative transmission electron micrographs of flight muscle cross sections from (B) non-diapausing and (C) diapausing CPB (19000 \times magnification). Mit=mitochondria, myo=myofibril, nuc=nucleus, tra=trachea, mlb=multilamellar body. (D-F) DAPI nuclei staining of flight muscle nuclei in non-diapausing (D) and diapausing (E) CPB. (G-J) Representative transmission electron micrographs of flight muscle cross sections from CPB entering diapause (G-H), and emerged CPB (J). Control CPB flight muscle has densely packed mitochondria (mit) surrounding large muscle myofibrils (myo), while diapausing CPB flight muscle lack mitochondria, but still have nuclei (nuc) and trachea (tra). As CPB enter diapause, autophagy machinery is assembled. At six weeks in diapause-inducing conditions (G) there are lysosomes in flight muscle cells (lys), at 12 weeks in diapause-inducing conditions (H) autolysosomes (aly), with broken-down mitochondria inside, form, and at 15 weeks in diapause-inducing conditions (I) double membrane autophagosomes (dma) appear. When CPB emerge from diapause, their flight muscle mitochondrial abundance is recovered (J).

3.3.2 Parkin-mediated mitophagy is active in diapausing flight muscle

To maintain mitochondrial and metabolic homeostasis, cells of active animals balance the selective removal of dysfunctional mitochondria (mitophagy), with the synthesis of new mitochondria (mitochondrial biogenesis; Palikaras and Tavernarakis, 2014). I hypothesized that a shift towards mitophagy during diapause drives the decline in mitochondrial abundance (and consequently mitochondrial metabolism) that I observed in flight muscle.

Mitophagy can be driven by the PTEN-induced putative kinase protein 1 (PINK1)/Parkin pathway (Jin and Youle, 2012; Figure 3.3). The decreased mitochondrial membrane potential of a dysfunctional or damaged mitochondrion induces PINK1 to stabilize to the outer mitochondrial membrane. PINK1 then recruits the E3-ubiquitin ligase Parkin which ubiquitinates proteins on the outer membrane of the damaged mitochondrion and tags it for autophagic removal (Narendra et al., 2008; Narendra et al., 2010). When cells require more mitochondria, for example during prolonged exercise or exercise training when energy demand is high, mitochondrial biogenesis is initiated *via* the transcription factor peroxisome proliferator activated receptor gamma coactivator 1 alpha (PGC1 α ; Gureev et al., 2019). PGC1 α forms a heterodimer with nuclear respiratory factors (NRF1 and 2) which initiate transcription and translation of mitochondrial proteins and coordinate the synthesis of new mitochondria (Scarpulla et al., 2012; Figure 3.3).

I assessed the potential for Parkin-mediated mitophagy to drive decreased abundance of flight muscle mitochondria during diapause by measuring mitophagy markers using microscopy and quantitative real-time PCR (qPCR). I observed a range of autophagic structures inside diapausing CPB flight muscle including multilamellar bodies, lysosomes, autolysosomes containing degraded mitochondrial contents, and double membrane autophagosomes (Figure 3.2). The development of these structures is consistent with activated Parkin-mediated mitophagy in *Drosophila* flight muscle (Cornelissen et al., 2018; Si et al., 2019) and mammalian skeletal muscle (Rogers et al., 2017; Vainshtein et al., 2015). I measured the mRNA abundance of *PINK1*, *Parkin* and *ATG5*, all of which are crucial to the initiation and execution of mitophagy (Figure 3.3). mRNA abundance of *PINK1*, *Parkin* and *ATG5* remained stable and low in early diapause (Figure 3.3). However, after nine weeks of

the 20-week diapause period, *Parkin* abundance doubled, and remained high throughout the diapause period (Figure 3.3). *ATG5* abundance peaked after 12-weeks in diapause-inducing conditions (Figure 3.3), and *PINK1* abundance was highest upon emergence from diapause (Figure 3.3). In Chapter 2, I found increased abundance of several additional mitophagy markers in diapausing flight muscle, including *TIM16* (involved in stabilizing *PINK1* to the inner mitochondrial membrane; Jin et al., 2010), *Biogenesis of lysosome-related organelles complex 1 subunit 2* (involved in lysosome assembly; Zhang et al., 2014), and *ATG10* (which forms a complex with *ATG5* and initiates autophagosome formation; Han et al., 2019). Taken together, these results suggest that Parkin-mediated mitophagy is activated in flight muscle early in diapause, leading to the mitochondrial degradation that I observed.

Mitophagy is normally activated when mitochondria are damaged and their mitochondrial membrane potential decreases, yet I have no evidence to suggest that mitochondria in CPB entering diapause are unhealthy. Thus, mitophagy appears to be selectively degrading otherwise healthy mitochondria in diapausing CPB. When activated, uncoupling proteins (UCPs) can decrease mitochondrial membrane potential in the absence of damage (Wu et al., 2014), and overexpression of UCPs can stimulate mitophagy and rescue ageing defects in mice (Bakula and Scheibye-Knudsen, 2020) and *C. elegans* (Cho et al., 2017). Indeed, *UCP4* is overexpressed at nine weeks in diapausing CPB flight muscle (Chapter 2). Thus, I speculate that increased *UCP4* abundance drives a decrease in membrane potential of flight muscle mitochondria and activates Parkin-mediated mitophagy during diapause in CPB.

In the first nine weeks of diapause, CPB appear to shift mitochondrial homeostasis towards mitophagy. Transcript abundance of *PGC1 α* and *NRF1* (which drive mitochondrial biogenesis) are low and stable in the first nine weeks of diapause (Figure 3.3) suggesting that mitophagy has increased without altering mitochondrial biogenesis. My RNA-seq data in Chapter 2 also showed no significant changes in the transcript abundance of *PGC1 α* and *NRF1* in the flight muscle of diapausing CPB (Chapter 2). This imbalance in mitochondrial homeostasis is analogous to some mammalian disease phenotypes. For example, amyotrophic lateral sclerosis is associated with enhanced mitophagy (Evans and Holzbaur, 2019), and sarcopenia is associated with deficient mitochondrial biogenesis (Jiao and Demontis, 2017; Joseph et al., 2013). The excessive muscle atrophy in disease states associated with this

increased mitophagy is irreversible. By contrast, the enhanced mitophagy I observed in diapausing CPB is spontaneously reversed.

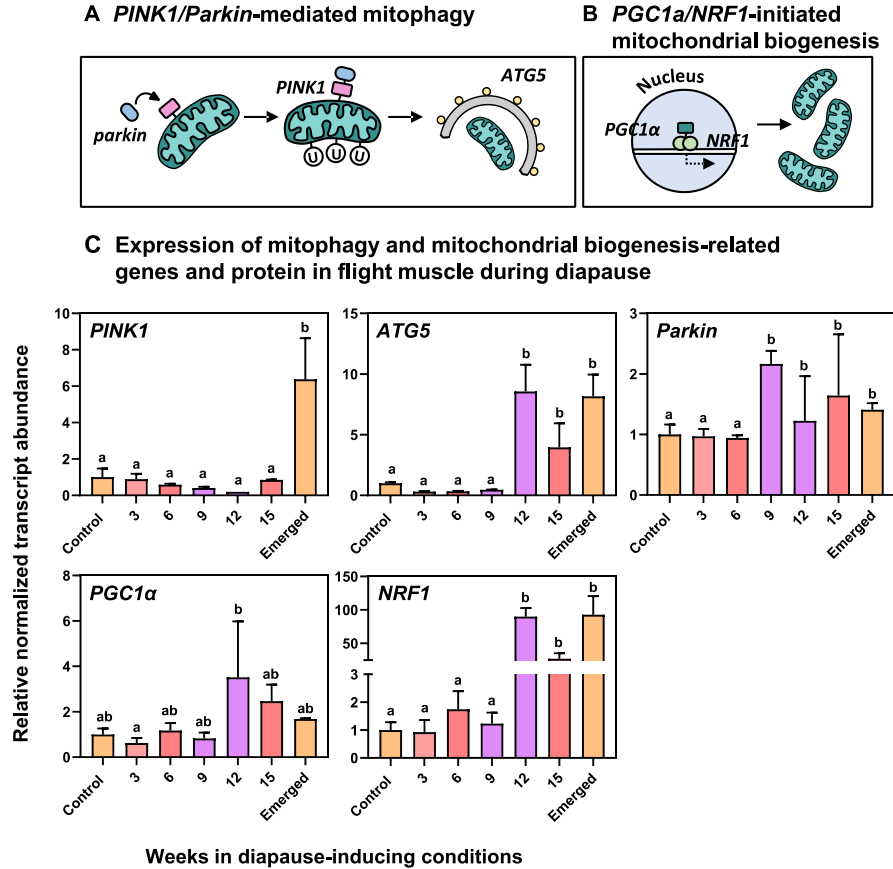


Figure 3.3. Colorado potato beetles increase the abundance of mitophagy-related transcripts during diapause and increase the abundance of mitochondrial biogenesis-related transcripts in anticipation of emergence from diapause. (A) A schematic of PINK1/Parkin-mediated mitophagy. (B) A schematic of PGC1 α /NRF1-initiated mitochondrial biogenesis. (C) Mean \pm S.D. normalized abundance of selected mitophagy and mitochondrial biogenesis-related transcripts in CPB as they enter diapause (3-9 weeks), during diapause (9-15 weeks), and upon emergence from diapause. Expression values are normalized to control values and two reference genes according to the $\Delta\Delta C_t$ method. Groups were analyzed with a one-way ANOVA and different letters denote significant differences among treatment groups ($p < 0.05$, Table B2).

3.3.3 Parkin-mediated mitophagy drives whole-animal metabolic suppression during diapause

Mitochondrial ATP production accounts for the vast majority of an animal's oxygen consumption (White and Kearney, 2013), so I hypothesized that Parkin-mediated mitophagy drives the metabolic suppression I observed in diapausing CPB. I predicted that knocking down *Parkin* transcript abundance in CPB entering diapause would inhibit mitophagy and prevent metabolic rate suppression. I used RNA interference (RNAi) to knock down *Parkin* mRNA and reduce protein abundance in CPB (referred to as ds*Parkin* beetles) after seven weeks in diapause-inducing conditions, two weeks before peak *Parkin* expression. ds*Parkin* injection knocked down 80 % of *Parkin* mRNA and protein (compared to ds*GFP* controls) in CPB flight muscle after five days (Figure 3.4).

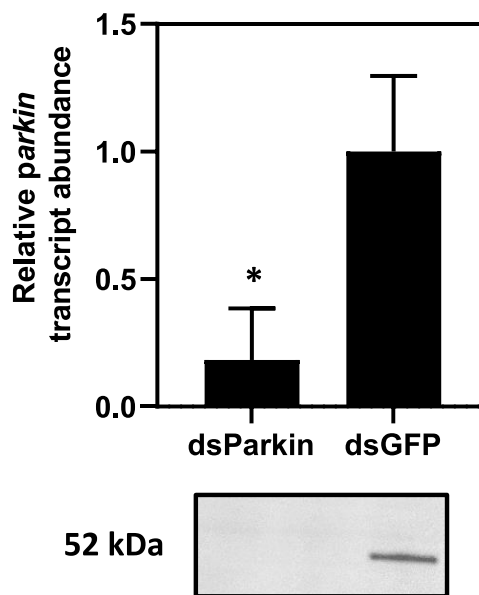


Figure 3.4. RNA interference knockdown of *Parkin* transcript and protein abundance in flight muscle of diapausing Colorado potato beetles. Verification of transcript and protein knockdown *via* qPCR and western blot, respectively in beetles injected with ds*Parkin* compared to beetles injected with a negative control dsRNA construct, ds*GFP*. All values are represented as \pm S.D. Asterisks denote significant differences between treatments according to a Welch's T-test ($p < 0.05$, Table B2).

Knocking down *Parkin* increased CPB flight muscle citrate synthase activity three-fold compared to control diapausing CPB (Figure 3.5) which suggests an increase in mitochondrial abundance in *dsParkin* beetles relative to diapausing beetles. Using transmission electron microscopy, I found that mitochondrial density in flight muscle of *dsParkin* beetles was 9.4-fold higher than in control diapausing beetles, but mitochondrial density in *dsParkin* beetles remained lower than in active, non-diapausing beetles (Figure 3.5). Thus, an 80 % reduction in *Parkin* partially inhibited mitophagy during the early stages of diapause. *Parkin* knockdown also prevented a decline in whole-animal metabolic rate. *dsParkin* beetles had CO₂ production 40 % higher than that of diapausing controls (Figure 3.6). Although these *dsParkin* beetles had higher metabolic rates, they did not fully return to non-diapausing levels (Figure 3.6) or restore continuous gas exchange (Figure B1), which suggests that the *dsParkin* beetles remained in diapause.

Knocking down *Parkin* rescued citrate synthase activity in diapausing beetles (Figure 3.5) but did not restore mitochondrial oxidative capacity (Figure 3.6). I suggest that *Parkin* modulates the TCA cycle independent of its role in mitophagy. *Parkin* has many potential substrates (Hattori and Mizuno, 2017) and can inhibit the activity of some glycolytic enzymes such as pyruvate kinase, thereby decreasing rates of glycolysis (Liu et al., 2016). I speculate that knocking down *Parkin* activated glycolysis in diapausing flight muscle, feeding substrates into the TCA cycle and activating citrate synthase and other enzymes.

However, *dsParkin* did not fully restore mitochondrial density or whole organism metabolic rate, mitochondrial respiration remained low, and these beetles appear to remain in diapause. The beetles were already committed to diapause when I injected *dsParkin*, so I conclude that *Parkin*-mediated mitophagy is necessary for metabolic suppression during diapause, but not for maintaining dormancy. This suggests there are regulatory molecules upstream of *Parkin* that maintain diapause phenotypes, such as reactive oxygen species (ROS) which regulate metabolic rate in diapausing flesh fly pupae (Chen et al., 2020). Furthermore, *FOXO* (fork head-box O) transcription factors are well-established central regulators of diapause in insects (Sim and Denlinger, 2008), and energy metabolism in most animal systems (Webb and Brunet, 2014). *FOXO* can activate the expression of mitophagy related genes (Kim and

Koh, 2017; Mei et al., 2009), and could thus play an important role upstream of Parkin in regulating mitochondrial degradation and metabolic rate in diapausing CPB.

The disconnect between a moderate increase in mitochondrial abundance and unchanged mitochondrial respiration implies that CPB either 1) have additional mechanisms to suppress respiration in the few mitochondria that remain intact during diapause or 2) leftover mitochondria are non-functional to begin with, thus reversing mitophagy might not result in enhanced mitochondrial respiration. Furthermore, there are Parkin-independent mitophagy pathways that could be playing a compensatory role in mitophagy activation in *dsParkin* beetles. For example, some mitophagy still occurs in Parkin-deficient *Drosophila* mutants (Villa et al., 2018), suggesting the presence of other Parkin-independent pathways capable of degrading mitochondria, and this merits further investigation. I also expect that respiration in tissues other than flight muscle (*i.e.*, brain, fat body) likely contributes to whole-animal metabolic suppression which could explain why metabolic rate was only partially rescued in *dsParkin* beetles.

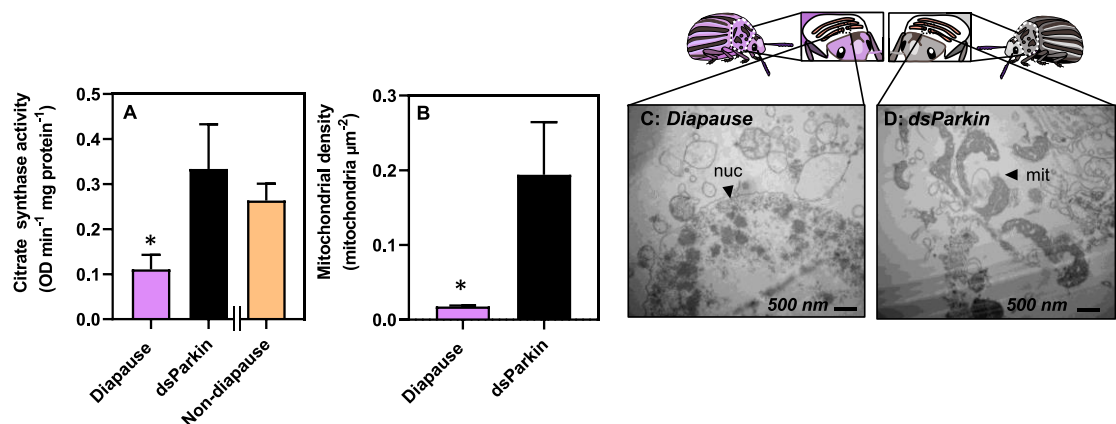


Figure 3.5. Knocking down *Parkin* transcript abundance increases flight muscle citrate synthase activity and mitochondria density. Mean \pm S.D. citrate synthase as a proxy for mitochondrial abundance (A) and mean \pm S.D. mitochondrial density measured with transmission electron microscopy (B-D) in diapausing CPB and diapausing CPB injected with *dsParkin*. Asterisks denote significant differences between diapause and *dsParkin* knockdown CPB according to a Welch's t-test ($p < 0.05$, Table B2). X-axis breaks separate out the non-diapause data which was collected in previous experiments (Figures 3.1-3.3) to show the extent of the knockdown phenotype.

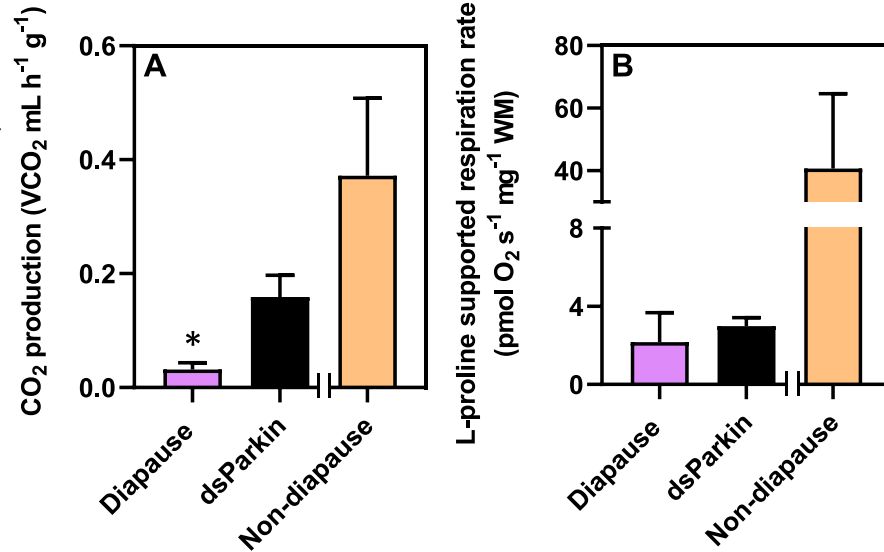


Figure 3.6. Knocking down *Parkin* transcript abundance partially recovers whole animal metabolic rate, but not mitochondrial respiration rates. Mean \pm S.D. CO₂ production rate (A) and mean \pm S.D. mitochondrial respiration rates (B) in diapausing CPB and diapausing CPB injected with *dsParkin*. Asterisks denote significant differences between diapause and *dsParkin* knockdown CPB according to a Welch's t-test ($p < 0.05$, Table B2). X-axis breaks separate out the non-diapause data which was collected in previous experiments (Figures 3.1-3.3) to show the extent of the knockdown phenotype.

3.3.4 Mitochondrial biogenesis drives metabolic recovery after diapause

After diapause, CPB metabolic rates return to pre-diapause levels as CPB search for food, resume reproductive development, and find a mate. After 17-20 weeks in diapause-inducing conditions, laboratory-reared CPB spontaneously emerge from diapause and increase their metabolic rates (Figure 3.1). I hypothesized that the reversal of metabolic suppression after diapause was driven by the recovery of flight muscle mitochondrial abundance *via* mitochondrial biogenesis. Beetles emerging from diapause recovered their flight muscle mitochondrial respiration rates in the same pattern as their whole-animal metabolic rates; by 17-20 weeks in diapause-inducing conditions proline-supported mitochondrial respiration (State 2 respiration) in permeabilized flight muscle increased to rates that surpassed pre-diapause values (Figure 3.1), indicating that mitochondrial respiration is no longer suppressed. Indeed, citrate synthase activity in flight muscle increased to non-diapause levels

(Figure 3.2), and the flight muscle of emerged CPB contained newly synthesized mitochondria (Figure 3.2). This concordance of increased mitochondrial respiration rates, TCA cycle enzymes, and mitochondrial abundance in emerged, post-diapause beetles mirrored whole-animal metabolic rates (Figures 3.1-3.2). Thus, the re-proliferation of mitochondria appears to drive increased metabolic rate upon diapause emergence.

Because mitochondrial homeostasis shifted towards mitophagy during diapause, I hypothesized that the proliferation of mitochondria results from a shift back to mitochondrial biogenesis as spontaneous diapause emergence approaches. At 12 weeks in diapause-inducing conditions (during the diapause maintenance period), CPB increased the abundance of *PGC1 α* and *NRF1* by c. 2- and 100-fold, respectively, driving mitochondrial proliferation (Figure 3.3). Mitochondrial homeostasis appears to be maintained towards the end of diapause and upon diapause emergence: beetles not only activated mitochondrial biogenesis, but also maintained a level of mitophagy (both *Parkin* and *PINK1* expression remained high; Figure 3.3). Maintenance of mitochondrial homeostasis by balancing mitophagy and mitochondrial biogenesis is crucial for healthy cell function (Palikaras and Tavernarakis, 2014). Imbalances in mitochondrial homeostasis are normally irreversible and are associated with ageing-related diseases such as sarcopenia (Rygiel et al., 2016). Diapausing beetles can readily reverse this damaging phenotype and re-establish mitochondrial homeostasis while concomitantly recovering their metabolic rates toward the end of diapause. Thus, these beetles could provide insight into mitigating the adverse effects of aging on mitochondrial homeostasis.

Colorado potato beetles activated mitochondrial biogenesis even though conditions remained constant throughout their diapause, suggesting that mitochondrial homeostasis (and ultimately metabolic rate) are regulated by an endogenous rhythm in this species. *PGC1 α* expression also increases during hibernation in ground squirrels (Xu et al., 2013) and bats (Eddy and Storey, 2003), when these animals are otherwise immobile and in overwintering microhabitats with constant conditions. However, mammals that usually maintain muscle mass keep all their mitochondria (Cotton, 2016), whereas I show that CPB degrade mitochondria during diapause. Thus, in contrast to hibernating mammals, CPB endogenously activate mitochondrial biogenesis in atrophied and mitochondria-deficient muscle, without

external stimuli, and in anticipation of an increased energy demand in the spring. Early work on CPB showed that flight muscle degeneration during diapause is hormonally regulated (Stegwee et al., 1963), but the mechanisms linking seasonal rhythms of hormone production and recovery of mitochondria to emergence from diapause merit further investigation.

3.4 Conclusions

Insects from at least two orders degenerate and re-generate flight muscle during the winter (Edwards, 1969; Kaitala and Huldén, 1990; Unnithan and Nair, 1977), and here I reveal a role for Parkin-mediated mitophagy in this process. While other dormant animals suppress their metabolic rates by reducing mitochondrial respiration, diapausing Colorado potato beetles remove mitochondria altogether. Possibly, the cost to insects of degrading and re-growing mitochondria is lower than the cost of maintaining mitochondrial function over the winter. Furthermore, this mitophagy is reversible; beetles activate transcriptionally mediated mitochondrial biogenesis to recover metabolic rate and re-establish mitochondrial homeostasis in their flight muscle in anticipation of emergence from diapause. My study establishes a mechanistic link between mitochondrial degradation in insect tissues over the winter and metabolic suppression. Further, it provides insight into the diversity of adaptations that animals use to save energy in resource-limited environments.

3.5 References

- Bakula, D., Scheibye-Knudsen, M.** (2020). MitophAging: Mitophagy in aging and disease. *Frontiers in Cell and Developmental Biology* **8**, 239.
- Boiteau, G., Alyokhin, A., Ferro, D.** (2003). The Colorado potato beetle in movement. *Canadian Entomologist* **135**, 1-22.
- Boiteau, G., Coleman, W.** (1996). Cold tolerance in the Colorado potato beetle, *Leptinotarsa decemlineata* (Say)(Coleoptera: Chrysomelidae). *Canadian Entomologist* **128**, 1087-1099.
- Chen, C., Mahar, R., Merritt, M.E., Denlinger, D.L., Hahn, D.A.** (2020). ROS and hypoxia signaling regulate periodic metabolic arousal during insect dormancy to coordinate glucose, amino acid, and lipid metabolism. *Proceedings of the National Academy of Sciences of the U.S.A.* **118**, e2017603118.
- Cho, I., Song, H.-O., Cho, J.H.** (2017). Mitochondrial uncoupling attenuates age-dependent neurodegeneration in *C. elegans*. *Molecules and Cells* **40**, 864.
- Cornelissen, T., Vilain, S., Vints, K., Gounko, N., Verstreken, P., Vandenberghe, W.** (2018). Deficiency of parkin and PINK1 impairs age-dependent mitophagy in *Drosophila*. *eLife* **7**, e35878.
- Cotton, C.J.** (2016). Skeletal muscle mass and composition during mammalian hibernation. *Journal of Experimental Biology* **219**, 226-234.
- De Kort, C., Bergot, B., Schooley, D.** (1982). The nature and titre of juvenile hormone in the Colorado potato beetle, *Leptinotarsa decemlineata*. *Journal of Insect Physiology* **28**, 471-474.
- De Wilde, J., Duintjer, C., Mook, L.** (1959). Physiology of diapause in the adult Colorado beetle (*Leptinotarsa decemlineata* Say) – I The photoperiod as a controlling factor. *Journal of Insect Physiology* **3**, 75-85.
- Duerr, J.M., Podrabsky, J.E.** (2010). Mitochondrial physiology of diapausing and developing embryos of the annual killifish *Austrofundulus limnaeus*: implications for extreme anoxia tolerance. *Journal of Comparative Physiology B* **180**, 991-1003.
- Eddy, S.F., Storey, K.B.** (2003). Differential expression of Akt, PPAR γ , and PGC-1 during hibernation in bats. *Biochemistry and Cell Biology* **81**, 269-274.
- Edwards, F.** (1969). Environmental control of flight muscle histolysis in the bug *Dysdercus intermedius*. *Journal of Insect Physiology* **15**, 2013-2020.

- Eigentler, A., Fontana-Ayoub, M., Fasching, M., Lassnig, B., Stadlmann, S., Rieger, G., Haffner, B., Lemieux, H., Gnaiger, E.** (2012). Selected media and chemicals for respirometry with mitochondria and permeabilized cells. *Mitochondrial Physiology Network* **3**, 1-9.
- Evans, C.S., Holzbaur, E.L.** (2019). Autophagy and mitophagy in ALS. *Neurobiology of Disease* **122**, 35-40.
- Ferro, D.N., Alyokhin, A.V., Tobin, D.B.** (1999). Reproductive status and flight activity of the overwintered Colorado potato beetle. *Entomologia Experimentalis et Applicata* **91**, 443-448.
- Grapputo, A., Boman, S., Lindstroem, L., Lyytinen, A., Mappes, J.** (2005). The voyage of an invasive species across continents: genetic diversity of North American and European Colorado potato beetle populations. *Molecular Ecology* **14**, 4207-4219.
- Gunn, A., Gatehouse, A.** (1993). The migration syndrome in the African armyworm moth, *Spodoptera exempta*: allocation of resources to flight and reproduction. *Physiological Entomology* **18**, 149-159.
- Gureev, A.P., Shaforostova, E.A., Popov, V.N.** (2019). Regulation of mitochondrial biogenesis as a way for active longevity: interaction between the Nrf2 and PGC-1 α signaling pathways. *Frontiers in Genetics* **10**, 435.
- Han, Z., Wang, W., Lv, X., Zong, Y., Liu, S., Liu, Z., Wang, L., Song, L.** (2019). ATG10 (autophagy-related 10) regulates the formation of autophagosome in the anti-virus immune response of pacific oyster (*Crassostrea gigas*). *Fish & Shellfish Immunology* **91**, 325-332.
- Hattori, N., Mizuno, Y.** (2017). Twenty years since the discovery of the parkin gene. *Journal of Neural Transmission* **124**, 1037-1054.
- Livak, K.J., Schmittgen, T.D.** (2001). Analysis of relative gene expression data using real-time quantitative PCR and the $2^{-\Delta\Delta CT}$ method. *Methods* **25**, 402-408.
- Jiao, J., Demontis, F.** (2017). Skeletal muscle autophagy and its role in sarcopenia and organismal aging. *Current Opinion in Pharmacology* **34**, 1-6.
- Jin, S.M., Lazarou, M., Wang, C., Kane, L.A., Narendra, D.P., Youle, R.J.** (2010). Mitochondrial membrane potential regulates PINK1 import and proteolytic destabilization by PARL. *Journal of Cell Biology* **191**, 933-942.
- Jin, S.M., Youle, R.J.** (2012). PINK1-and Parkin-mediated mitophagy at a glance. *Journal of Cell Science* **125**, 795-799.

- Joseph, A.-M., Adhietty, P.J., Wawrzyniak, N.R., Wohlgemuth, S.E., Picca, A., Kujoth, G.C., Prolla, T.A., Leeuwenburgh, C.** (2013). Dysregulation of mitochondrial quality control processes contribute to sarcopenia in a mouse model of premature aging. *PLoS One* **8**, e69327.
- Kaitala, A., Huldén, L.** (1990). Significance of spring migration and flexibility in flight-muscle histolysis in waterstriders (Heteroptera, Gerridae). *Ecological Entomology* **15**, 409-418.
- Kim, S., Koh, H.** (2017). Role of FOXO transcription factors in crosstalk between mitochondria and the nucleus. *Journal of Bioenergetics and Biomembranes* **49**, 335-341.
- Košťál, V.** (2006). Eco-physiological phases of insect diapause. *Journal of Insect Physiology* **52**, 113-127.
- Kuznetsov, A.V., Veksler, V., Gellerich, F.N., Saks, V., Margreiter, R., Kunz, W.S.** (2008). Analysis of mitochondrial function in situ in permeabilized muscle fibers, tissues and cells. *Nature Protocols* **3**, 965.
- Larsen, S., Nielsen, J., Hansen, C.N., Nielsen, L.B., Wibrand, F., Stride, N., Schroder, H.D., Boushel, R., Helge, J.W., Dela, F.** (2012). Biomarkers of mitochondrial content in skeletal muscle of healthy young human subjects. *Journal of Physiology* **590**, 3349-3360.
- Lehmann, P., Piironen, S., Lyytinen, A., Lindström, L.** (2015). Responses in metabolic rate to changes in temperature in diapausing Colorado potato beetle *Leptinotarsa decemlineata* from three European populations. *Physiological Entomology* **40**, 123-130.
- Levenbook, L.** (1953). The mitochondria of insect flight muscle. *Journal of Histochemistry & Cytochemistry* **1**, 242-247.
- Liu, K., Li, F., Han, H., Chen, Y., Mao, Z., Luo, J., Zhao, Y., Zheng, B., Gu, W., Zhao, W.** (2016). Parkin regulates the activity of pyruvate kinase M2. *Journal of Biological Chemistry* **291**, 10307-10317.
- Livak, K.J., Schmittgen, T.D.** (2001). Analysis of relative gene expression data using real-time quantitative PCR and the $2^{-\Delta\Delta CT}$ method. *Methods* **25**, 402-408.
- Mathers, K.E., McFarlane, S.V., Zhao, L., Staples, J.F.** (2017). Regulation of mitochondrial metabolism during hibernation by reversible suppression of electron transport system enzymes. *Journal of Comparative Physiology B* **187**, 227-234.
- Mathers, K.E., Staples, J.F.** (2015). Saponin-permeabilization is not a viable alternative to isolated mitochondria for assessing oxidative metabolism in hibernation. *Biology Open* **4**, 858-864.

- Mei, Y., Zhang, Y., Yamamoto, K., Xie, W., Mak, T.W., You, H.** (2009). FOXO3a-dependent regulation of Pink1 (Park6) mediates survival signaling in response to cytokine deprivation. *Proceedings of the National Academy of Sciences of the U.S.A.* **106**, 5153-5158.
- Narendra, D., Tanaka, A., Suen, D.-F., Youle, R.J.** (2008). Parkin is recruited selectively to impaired mitochondria and promotes their autophagy. *Journal of Cell Biology* **183**, 795-803.
- Narendra, D.P., Jin, S.M., Tanaka, A., Suen, D.-F., Gautier, C.A., Shen, J., Cookson, M.R., Youle, R.J.** (2010). PINK1 is selectively stabilized on impaired mitochondria to activate Parkin. *PLoS Biology* **8**, e1000298.
- Palikaras, K., Tavernarakis, N.** (2014). Mitochondrial homeostasis: the interplay between mitophagy and mitochondrial biogenesis. *Experimental Gerontology* **56**, 182-188.
- Rogers, R.S., Tungtur, S., Tanaka, T., Nadeau, L.L., Badawi, Y., Wang, H., Ni, H.-M., Ding, W.-X., Nishimune, H.** (2017). Impaired mitophagy plays a role in denervation of neuromuscular junctions in ALS mice. *Frontiers in Neuroscience* **11**, 473.
- Rygiel, K.A., Picard, M., Turnbull, D.M.** (2016). The ageing neuromuscular system and sarcopenia: a mitochondrial perspective. *Journal of Physiology* **594**, 4499-4512.
- Scarpulla, R.C., Vega, R.B., Kelly, D.P.** (2012). Transcriptional integration of mitochondrial biogenesis. *Trends in Endocrinology & Metabolism* **23**, 459-466.
- Si, H., Ma, P., Liang, Q., Yin, Y., Wang, P., Zhang, Q., Wang, S., Deng, H.** (2019). Overexpression of pink1 or parkin in indirect flight muscles promotes mitochondrial proteostasis and extends lifespan in *Drosophila melanogaster*. *PloS One* **14**, e0225214.
- Sim, C., Denlinger, D.L.** (2008). Insulin signaling and FOXO regulate the overwintering diapause of the mosquito *Culex pipiens*. *Proceedings of the National Academy of Sciences of the U.S.A.* **105**, 6777-6781.
- Sinclair, B.J.** (2015). Linking energetics and overwintering in temperate insects. *Journal of Thermal Biology* **54**, 5-11.
- Staples, J.F., Buck, L.T.** (2009). Matching cellular metabolic supply and demand in energy-stressed animals. *Comparative Biochemistry and Physiology A* **153**, 95-105.
- Stegwee, D.** (1964). Respiratory chain metabolism in the Colorado potato beetle – II. Respiration and oxidative phosphorylation in ‘sarcosomes’ from diapausing beetles. *Journal of Insect Physiology* **10**, 97-102.
- Stegwee, D., Kimmel, E., De Boer, J., Henstra, S.** (1963). Hormonal control of reversible degeneration of flight muscle in the Colorado potato beetle, *Leptinotarsa decemlineata* Say (Coleoptera). *Journal of Cell Biology* **19**, 519-527.

- Sun, B.J., Huebner, C., Treidel, L.A., Clark, R.M., Roberts, K.T., Kenagy, G., Williams, C.M.** (2020). Nocturnal dispersal flight of crickets: Behavioural and physiological responses to cool environmental temperatures. *Functional Ecology* **34**, 1907-1920.
- Unnithan, G., Nair, K.** (1977). Ultrastructure of juvenile hormone-induced degenerating flight muscles in a bark beetle, *Ips paraconfusus*. *Cell and Tissue Research* **185**, 481-490.
- Vainshtein, A., Desjardins, E.M., Armani, A., Sandri, M., Hood, D.A.**, (2015). PGC-1 α modulates denervation-induced mitophagy in skeletal muscle. *Skeletal Muscle* **5**, 1-17.
- Villa, E., Marchetti, S., Ricci, J.-E.** (2018). No Parkin zone: mitophagy without Parkin. *Trends in Cell Biology* **28**, 882-895.
- Webb, A.E., Brunet, A.** (2014). FOXO transcription factors: key regulators of cellular quality control. *Trends in Biochemical Sciences* **39**, 159-169.
- White, C.R., Kearney, M.R.** (2013). Determinants of inter-specific variation in basal metabolic rate. *Journal of Comparative Physiology B* **183**, 1-26.
- Williams, C.M., Henry, H.A., Sinclair, B.J.** (2015). Cold truths: how winter drives responses of terrestrial organisms to climate change. *Biological Reviews* **90**, 214-235.
- Williams, C.M., Marshall, K.E., MacMillan, H.A., Dzurisin, J.D.K., Hellmann, J.J., Sinclair, B.J.** (2012). Thermal variability increases the impact of autumnal warming and drives metabolic depression in an overwintering butterfly. *PLoS One* **7**, e34470.
- Wilsterman, K., Ballinger, M.A., Williams, C.M.** (2021). A unifying, eco-physiological framework for animal dormancy. *Functional Ecology* **35**, 11-31.
- Wu, K., Liu, J., Zhuang, N., Wang, T.** (2014). UCP4A protects against mitochondrial dysfunction and degeneration in pink1/parkin models of Parkinson's disease. *FASEB Journal* **28**, 5111-5121.
- Xu, R., Andres-Mateos, E., Mejias, R., MacDonald, E.M., Leinwand, L.A., Merriman, D.K., Fink, R.H., Cohn, R.D.** (2013). Hibernating squirrel muscle activates the endurance exercise pathway despite prolonged immobilization. *Experimental Neurology* **247**, 392-401.
- Yocum, G.D., Buckner, J.S., Fatland, C.L.** (2011). A comparison of internal and external lipids of nondiapausing and diapause initiation phase adult Colorado potato beetles, *Leptinotarsa decemlineata*. *Comparative Biochemistry and Physiology B* **159**, 163-170.

Zhang, A., He, X., Zhang, L., Yang, L., Woodman, P., Li, W. (2014). Biogenesis of lysosome-related organelles complex-1 subunit 1 (BLOS1) interacts with sorting nexin 2 and the endosomal sorting complex required for transport-I (ESCRT-I) component TSG101 to mediate the sorting of epidermal growth factor receptor into endosomal compartments. *Journal of Biological Chemistry* **289**, 29180-29194.

Chapter 4

4 Activation of the chaperone response improves cold tolerance in diapausing Colorado potato beetles

4.1 Introduction

Temperate insects may spend over half their lives overwintering during which they face extended periods below 0 °C, and as ectotherms, risk freezing of their body fluids (Williams et al., 2015; Zachariassen, 1985). Most biological processes are temperature sensitive (Hochachka and Somero, 2002), thus exposure to sub-zero temperatures can cause vital physiological processes to fail and lead to reduced overwinter insect survival. Protein structure and function is particularly vulnerable to changes in temperatures; sub-zero temperatures can cause the dissociation of multimeric enzymes thereby rendering them unable to catalyze important biochemical reactions (D'Amico et al., 2002; Privalov, 1990). Furthermore, proteins can denature at sub-zero-temperatures. Once denatured, proteins form harmful aggregates which compromise protein function (Espinosa et al., 2017; Martin and Hartl, 1997). Thus, many insects have evolved strategies to protect their cells and proteins from the adverse effects of sub-zero temperatures.

Insects employ several biochemical mechanisms to protect their proteins and maintain cell function at sub-zero temperatures. Most cold-tolerant insects accumulate low molecular weight metabolites, such as sugars (*e.g.*, trehalose, Toxopeus et al., 2019b), polyhydroxy alcohols (*e.g.*, glycerol, Crosthwaite et al., 2011; Storey and Storey, 1983; Vesala et al., 2012), or free amino acids (*e.g.*, proline, Košťál et al., 2011; Lefevere et al., 1989; Toxopeus et al., 2019b). At high concentrations these metabolites drive a concentration-dependent decrease in supercooling point (SCP; temperature at which insect body fluids spontaneously freeze), thus preventing freezing (Zachariassen, 1985). At lower concentrations they promote cell survival (Toxopeus et al., 2019b) and probably directly stabilize proteins and membranes at sub-zero temperatures (Toxopeus and Sinclair, 2018). Many cold-tolerant insects increase the proportion of polyunsaturated fatty acids in phospholipid membranes to increase membrane fluidity at lower temperatures (*e.g.*, Lee et al., 2006), and re-organize cytoskeletal components to resist low-temperature induced depolymerization (*e.g.*, Des Marteaux et al.,

2018). Many cold-tolerant insects also often express chaperone proteins such as late embryogenesis abundant proteins and heat shock proteins (King and MacRae, 2015).

Heat shock proteins (HSPs) are a large family of molecular chaperones that play several roles in maintaining protein form and function in animal cells (Hendrick and Hartl, 1993; Kiang and Tsokos, 1998; Sorger, 1991). High and low temperatures induce heat shock protein expression, as do cellular stressors such as hypoxia and desiccation (Becker and Craig, 1994). There are inducible and constitutively expressed forms of HSPs in animal cells, both of which help regulate the cellular chaperone response. At physiologically permissive temperatures, constitutive HSPs in a cell are bound to heat shock factors (HSFs). At extreme high or low temperatures, proteins denature, and HSPs will release HSFs to preferentially bind to denatured proteins. Heat shock factors then diffuse into the nucleus where they bind heat shock elements (promoter sequences upstream of HSP coding regions), and activate the transcription of more HSPs (Sorger, 1991). This newly synthesized pool of HSPs re-folds reversibly denatured proteins to prevent harmful aggregates (Reeg et al., 2016).

Heat shock protein expression patterns are well-documented in insects in the context of winter and sub-zero temperature exposure. Many insects will express a variety of HSPs in anticipation of winter, as part of their diapause; a pre-programmed state of dormancy (King and MacRae, 2015). For example, flesh flies (*Sarcophaga crassipalpis*) increase the expression of HSP60 and HSP70 family proteins at the onset of and throughout their diapause (Rinehart et al., 2007). Some insects will express HSPs in preparation for sub-zero temperature exposure through processes such as cold acclimation or cold hardening. For example, *Drosophila melanogaster* express several HSP20, HSP60, and HSP70 family proteins during cold acclimation (MacMillan et al., 2016; Štětina et al., 2015). Direct exposure to sub-zero temperatures also induces HSP expression in insects, but expression does not peak until after recovery from cold stress, such as after cold shock in the linden bug *Pyrrhocoris apterus* (Tollarová-Borovanská et al., 2009). Regardless of whether they express HSPs in preparation for low temperatures or in response to the cold, insects that express HSPs typically survive better at sub-zero temperatures (Storey and Storey, 2012; Yocum et al., 1998), and also recover faster from any cold-induced injury (Košťál and Tollarová-Borovanská, 2009). Heat shock proteins could protect insect proteins from low temperatures

by promoting re-folding of reversibly cold-denatured proteins and preventing harmful protein aggregates from forming, thereby improving survival at low temperatures. However, whether HSPs protect insect cells from protein damage in the cold is rarely tested and thus we still do not know the mechanistic link between HSP expression at the molecular level and increased cold tolerance at the whole-animal level.

The Colorado potato beetle (CPB; *Leptinotarsa decemlineata*) is an insect pest of potato plants that overwinters in temperate environments across North America, Europe, and Asia (Grapputo et al., 2005). In early autumn, short daylengths initiate diapause in adult CPB (De Wilde, 1960). During this time, beetles feed voraciously, arrest their reproductive development, accumulate lipid energy stores, and eventually burrow into the soil where they overwinter in diapause (De Kort, 1990). During the winter, and under natural conditions, diapausing CPB are more cold-tolerant than their non-diapausing counterparts (Boiteau and Coleman, 1996; Hiiesaar et al., 2014). Diapausing CPB are freeze-avoidant, which means they can survive sub-zero temperatures above their supercooling point (SCP; point at which insect body fluids freeze), but die when they freeze (Zachariassen, 1985). Thus, diapausing CPB often depress their SCP compared to non-overwintering stages (Salt, 1933). Colorado potato beetles express *HSP70* during diapause (Chapter 2; Yocum, 2001), after a cold shock while in diapause (Lyytinen et al., 2012), and after exposure to fluctuating sub-zero temperatures while in diapause (Yocum, 2001). However, these patterns of HSP expression have never been causally linked to increased whole animal cold tolerance or better low temperature survival in CPB.

Diapause and cold tolerance co-occur in overwintering CPB under natural conditions; thus, it is difficult to disentangle the mechanisms driving cold tolerance from those of diapause. In the lab, I can produce CPB with a diapausing phenotype with moderate cold tolerance, and diapausing CPB with a cold-tolerant phenotype with enhanced cold tolerance (Figure 1.1). This approach allows me to investigate mechanisms which drive a cold-tolerant phenotype independently of diapause, and the extent to which HSPs help drive this enhanced cold-tolerant phenotype in CPB. Here, I hypothesized that increased expression of HSPs and activation of the cellular chaperone response drives enhanced cold tolerance in diapausing CPB. To test this, I used RNA-seq to identify biological processes that could be important in

improving cold tolerance of diapausing CPB. I showed that the major change in cold-tolerant CPB compared to diapausing CPB is the activation of the cellular chaperone response; the main transcriptomic shift that separates cold-tolerant beetles from diapausing beetles is driven by the differential expression of chaperone-related transcripts in their fat body. From these data, I then hypothesized that the chaperone response is the main driver of cold tolerance in CPB, and that the function of this activated chaperone response is to protect proteins from the cold. To test this hypothesis, I measured levels of protein damage (using protein ubiquitination as a proxy for damage) in cold-tolerant and diapausing CPB, in cold-tolerant and diapause CPB after a cold shock, and in cold-tolerant and diapausing CPB after recovery from a cold shock. I predicted that cold-tolerant CPB would have fewer damaged proteins compared to diapausing beetles, both after a cold shock and after recovery from a cold shock.

4.2 Materials and Methods

4.2.1 Insect care and diapause induction

I established a colony of *L. decemlineata* in 2015 with individuals originally collected from potato fields at the London Research and Development Centre in London, Ontario, Canada and maintained it in greenhouses at the University of Western Ontario. I supplemented the population annually with c. 50 field-collected individuals to reduce inbreeding. For general rearing (control, non-diapausing CPB), I maintained eggs, larvae, and adults on fresh Kennebec potato plants in Bug Dorms (Megaview science, Talchung, Taiwan, w60 × d60 × d60 cm) at 24 °C under a long daylength (16:8 L:D). I allowed adults to freely mate and lay eggs on plants in the Bug Dorms. I induced diapause following the protocols in Chapter 2. I reared eggs laid by control adults on excised potato leaves in petri dishes lined with moist paper towel in temperature and light-controlled incubators (Sanyo Scientific, Bensenville, IL, USA) at 24 °C and short days (8:16 L:D). I transferred newly hatched larvae to 500 mL plastic containers lined with moistened paper towels and fed them daily with fresh potato leaves. I maintained larvae in groups of c. 20 in these containers. I transferred 4th instar larvae to 14 L plastic pupation bins filled with sandy soil and provided them fresh leaves daily until larvae burrowed into the soil to pupate. Once adults emerged from the soil, I transferred them to fresh plastic 500 mL containers filled with soil and kept them at 15 °C

(8:16 L:D), which I refer to as diapause-inducing conditions. I kept 20-30 beetles in each bin of diapause-destined adults and fed these diapause-destined adults fresh potato leaves daily for 3-4 weeks after which they stopped eating and burrowed into the soil. I did not observe any females laying eggs in these diapause-destined populations. I used adults nine weeks after emergence (*i.e.*, nine weeks after transfer to diapause-inducing conditions as adults) because these individuals are in a state of maximal metabolic suppression and therefore most likely in the maintenance stage of their diapause program (Chapter 3).

4.2.2 Cold tolerance induction

To improve cold tolerance of diapausing beetles, I exposed diapausing (at nine weeks in “diapause-inducing” conditions) individuals to a fluctuating thermal regime (Figure 4.1). For all experiments where I refer to “cold-tolerant” beetles, I am describing diapausing beetles that have been exposed to a fluctuating thermal regime and sampled immediately upon return to 15 °C. Briefly, I placed diapausing beetles in 1.7 mL microcentrifuge tubes and placed each tube in an aluminum block cooled by a solution of 50 % methanol circulated from a programmable refrigerated bath (Lauda Proline 3530, Wurzburg, Germany). I used preliminary supercooling data to determine a low temperature where they would not freeze, because beetles are freeze-avoidant, and will die upon ice formation (Boiteau and Coleman, 1996; Sinclair et al., 2015). I cycled the temperature between +5 °C and –8 °C three times (ramping between temperatures at a rate of 0.1 °C min⁻¹), and then returned it to 15 °C.

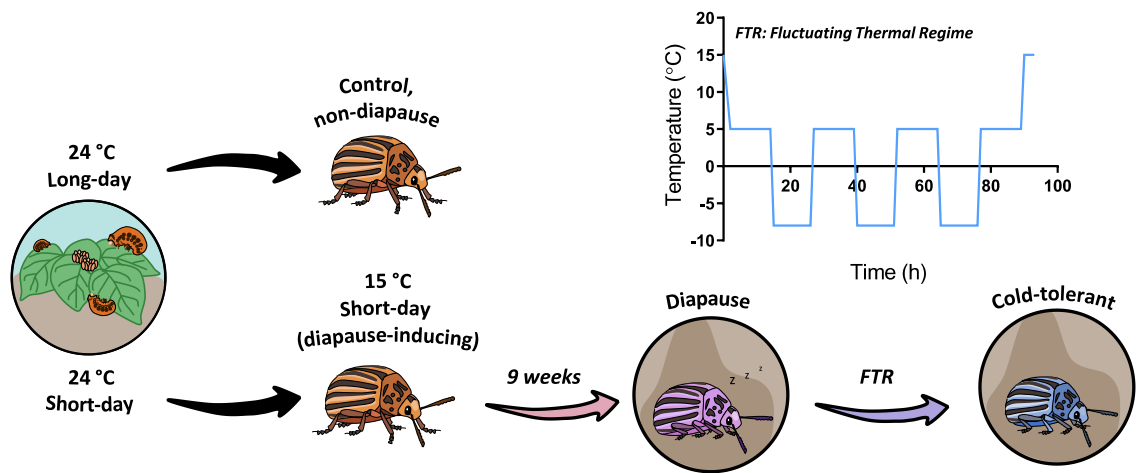


Figure 4.1. Inducing diapausing and cold tolerance in the Colorado potato beetle. To induce diapause in the Colorado potato beetle, I exposed eggs and larvae to short day conditions and then transferred adults to “diapause-inducing” conditions. To induce cold tolerance in diapausing Colorado potato beetles, I exposed them to a three-day fluctuating thermal regime, cycling between +5 °C and -8 °C.

4.2.3 Cold tolerance measurements

I measured supercooling points, hemolymph osmolality, and survival after sub-zero temperature exposure in control, diapausing, and cold-tolerant CPB to determine whether a fluctuating thermal regime improved their cold tolerance. To measure supercooling points, I placed control, diapausing, and cold-tolerant beetles in 1.7 mL microcentrifuge tubes into the same aluminum blocks cooled by circulating methanol mentioned above, and cooled beetles at 0.25 °C min^{-1} , during which each beetle was in constant contact with a type-T copper-constantan thermocouple (Omega, Laval, QC, Canada). I recorded temperature at 2 Hz using Picolog v5.24.1. software (Pico Technology, Cambridge, UK) using a Pico Technology TC-08 interface. I identified the SCP as the lowest temperature before the appearance of an exotherm caused by the latent heat of crystallization (Sinclair et al., 2015). I compared SCPs of control, diapausing, and cold-tolerant beetles using a one-way ANOVA in R version 4.1.0 (R core team, 2021).

I measured hemolymph osmolality of control, diapausing, and cold-tolerant beetles using a nanolitre osmometer (Otago Osmometers, Dunedin New Zealand) as described previously (Crosthwaite et al. 2011). Briefly, I extracted c. 5 μ l of hemolymph from control, diapausing, and cold-tolerant beetles using a micropipette, diluted it 1:3 in 3 % ascorbic acid, and stored it under a drop of Type B immersion oil in a microcentrifuge tube at -80 °C until analysis. I determined osmolality of the hemolymph from the melting point of hemolymph ice crystals, measured each sample in duplicate, and report the mean osmolality values for each animal. I compared osmolality values of control, diapausing and cold-tolerant beetles using a one-way ANOVA in R version 4.1.0 (R core team, 2021).

To assess survival, I cooled individual beetles (control, diapausing and cold-tolerant) to -10 °C (at 0.1 °C /min) and held the beetles at that temperature for 48 hours. I then transferred beetles to individual 100 mL plastic containers and allowed beetles to recover at room temperature (c. 21 °C) for 24 h, after which I assessed survival. I classified beetles as alive if they were 1) upright and moving and/or 2) responded and moved their legs after I gently probed them with a thin paintbrush. I compared survival of all three treatment groups using a Fisher's exact test in R version 4.1.0 (R core team, 2021).

4.2.4 Transcriptomics

4.2.4.1 Tissue dissection, RNA extraction, cDNA library preparation, and sequencing

I dissected approximately 5 mg of abdominal fat body tissue from diapausing and cold-tolerant beetles. I dissected tissues in phosphate buffered saline, blotted excess liquid, and placed the tissue into a pre-weighed 1.7 mL nuclease-free microcentrifuge tube. I flash-froze these samples in liquid nitrogen vapour and stored the tissue at -80 °C until RNA extraction. I generated mRNA libraries from three biological replicates of each treatment (diapause and cold-tolerant). Each biological replicate consisted of c. 5 mg of pooled tissue from each of eight individuals of mixed sex (c. 45 mg tissue in total). I homogenized each tissue sample with a plastic pestle in 500 μ l of TRIzol reagent (Thermofisher Scientific, Mississauga, Ontario, Canada), and extracted RNA according to the manufacturer's protocol. I sent samples to Génome Québec (Montreal, Quebec, Canada) where they were quality-checked

(2100 Bioanalyzer, Agilent, Santa Clara, California, USA), and cDNA libraries were prepared from mRNA. Libraries were sequenced using 125 bp paired-end sequencing on the Illumina HiSeq 2500 platform (Illumina, San Diego, California, USA).

4.2.4.2 Transcriptome Assembly

I used fastp, a program used to process RNA-seq reads produced from sequencing, (version 0.19.7; Chen et al., 2018) to trim adaptor sequences from the RNA-seq reads and to filter out any sequences with a Phred score below 15. A Phred score below 15 indicates that the reads produced from sequencing are of poor quality. I used the program FastQC (version 0.11.8; Andrews, 2010) to check the quality of all my reads before and after trimming by fastp. I mapped quality-trimmed reads to the reference *L. decemlineata* genome (Schoville et al., 2018; Lepdec_OGSV1.1, Bioproject PRJNA171749, available at <https://www.ncbi.nlm.nih.gov/bioproject/171749>) using the program Hisat2 (version 2.1.0; Kim et al., 2019), and then assembled reads using the program Stringtie (version 2.0; Pertea et al., 2015). I used the program Blast2GO (Götz et al., 2008) to obtain identities for all assembled transcripts, and provide GO (Gene ontology) and KEGG (Kyoto Encyclopedia of Genes and Genomes) annotation information for all assembled transcripts.

4.2.4.3 Differential gene expression and GO enrichment analysis

The program Stringtie assembled RNA-seq reads into transcripts and also provided FPKM expression values (the relative expression of a transcript proportional to the number of cDNA fragments that it originated from), but in order to use expression values in DEseq2 I transformed these FPKM expression values into read counts. To transform these FPKM expression values into read counts, I used prepDE (prepDE.py), a python script provided by the authors of Stringtie. I then used those read counts in DEseq2 (a differential expression analysis program, version 1.24.0; Love et al., 2014) to compare transcript abundance between diapausing and cold-tolerant CPB. To construct differential expression tables, I accepted transcripts as differentially expressed if the adjusted *P*-value was <0.05, and the log₂ fold change was >1.5 (I considered log₂ fold changes below 1.5 to be less likely to be biologically relevant in the context of this study; Love et al., 2014). To identify biological processes that were important in driving cold tolerance, I conducted GO enrichment analysis

using the program Goseq (v3.12; Young et al., 2012) in R on full differentially expressed transcript lists (*i.e.*, not just those with a log₂fold change >1.5). Using full lists of differentially expressed transcripts allowed me to conduct an unbiased analysis of patterns of gene expression. I considered GO terms to be over-represented if the *P*-value from the enrichment analysis was <0.05 (recommended by the goseq authors; Young et al., 2012), and if there were three or more transcripts included in a given GO term (because any GO terms with less than three transcripts would not be biologically relevant). I removed redundant GO terms using REViGO (Supek et al., 2011; <http://revigo.irb.hr/>), using the SimRel algorithm with ‘small’ similarity.

4.2.5 Protein ubiquitination measurements

I measured total ubiquitinated protein abundance as a proxy for protein damage in fat body from diapausing and cold-tolerant beetles, diapausing and cold-tolerant beetles that had been cold shocked for 12 h at –10 °C, and recovered from this cold shock for 24 h at 21 °C. I dissected fat body from beetles into PBS, placed tissue into pre-weighed 1.7 mL microcentrifuge tubes, flash froze tissues in liquid nitrogen vapor, and stored them at –80 °C until protein extraction. To extract protein from fat body samples, I placed 200 µl of lysis buffer (2 % SDS, 50 mM Tris, 1 mM PMSF, protease inhibitor cocktail [Sigma Aldrich, St. Louis, Missouri, USA]) into tubes with tissue, sonicated samples twice, each for 20 s with a handheld sonication probe (LabX, Toronto, ON), and centrifuged samples at 5000 × *g* at 4 °C for 10 min. I reserved a 10 µl aliquot (diluted in 90 µl lysis buffer) for protein quantification using a BCA protein assay kit (Thermo Scientific, Waltham, MA, USA) to determine the volume of extract containing 20 µg of protein, which is the amount I loaded into each well.

I denatured protein extracts in 4X Laemmli Sample buffer at 100 °C for 5 min prior to loading in a 4-20% polyacrylamide TGX Stain-Free Gel (Bio-Rad, Mississauga, ON). I separated protein by electrophoresis at 120 V for 1.5 h in Tris-glycine-SDS running buffer (25 mM Tris, 192 mM glycine, 0.1 % SDS). After electrophoresis, I activated gels on a ChemiDoc imaging system (Bio-Rad, Mississauga, ON) using UV light which allowed for total protein visualization for eventual standardization of total ubiquitinated proteins to total protein abundance. After gel activation, I immediately transferred proteins to a low

fluorescence polyvinylidene fluoride (PVDF) membrane (Bio-rad, Mississauga, ON) at 100 V for 2 h at 4 °C. Immediately after transferring, I imaged the blot for total protein on a ChemiDoc imaging system (Bio-Rad, Mississauga, ON), washed the membranes 3 × 5 min in 1X TBS-T (TBS-T; 20 mM Tris, 143 mM NaCl, 0.05 % Tween-20), and then blocked membranes at room temperature for 2 h with 5 % bovine serum albumin (BSA) in 1X TBS-T under constant agitation (300 rpm). After blocking, I washed each membrane 3 × 5 mins with 1X TBS-T, and probed membranes with a mono and poly-ubiquitinated protein antibody (1:1000 in 0.05 % BSA in TBS-T, Enzo) for 15 h at 4 °C under constant agitation (300 rpm). After primary antibody incubation, I washed membranes 3 × 5 mins in 1X TBS-T, and then incubated membranes with a secondary antibody (goat anti-mouse, 1:10000 in 5 % BSA in TBS-T; Thermofisher, Ontario, Canada) for 1 h at room temperature under constant agitation (300 rpm). Finally, I imaged membranes using the ChemiDoc system (Bio-Rad, Mississauga, ON) after incubating membranes in Pierce ECL Western blot substrate (Bio-Rad, Mississauga, ON). I quantified bands of ubiquitin conjugates (total bands/lane) with densitometry analysis in ImageLab (v6.1; Bio-Rad, Mississauga, ON), and standardized protein abundance to total protein, determined with fluorescence using the TGX stain-free gel. I compared standardized volume intensity values (total band intensity/lane) obtained from densitometry analysis using a Two-way ANOVA in R version 4.1.0 (R core team, 2021).

4.3 Results

4.3.1 Exposure to a fluctuating thermal regime improves cold tolerance of diapausing CPB

More diapausing CPB survived two days at $-10\text{ }^{\circ}\text{C}$ after exposure to a fluctuating thermal regime (FTR) than those that were not exposed to an FTR (Figure 4.2; Fisher's Exact Test, $p < 0.001$). Because of this, I refer to diapausing beetles exposed to an FTR as "cold-tolerant" CPB, and those with no exposure to an FTR as just "diapause" CPB (Figure 4.1). Cold-tolerant CPB had the highest hemolymph osmolality (c. 522 mM; Figure 4.2; $F_{2,6}=17.5$, $p=0.003$) and lowest supercooling point (c. $-13\text{ }^{\circ}\text{C}$; Figure 4.2; $F_{2,24}=70.32$, $p < 0.001$) of the three groups and non-diapausing CPB had the lowest hemolymph osmolality (c. 340 mM; Figure 4.2; $F_{2,6}=17.5$, $p=0.003$) and highest supercooling points (c. $-6\text{ }^{\circ}\text{C}$; Figure 4.2; $F_{2,24}=70.32$, $p < 0.001$) of the three groups.

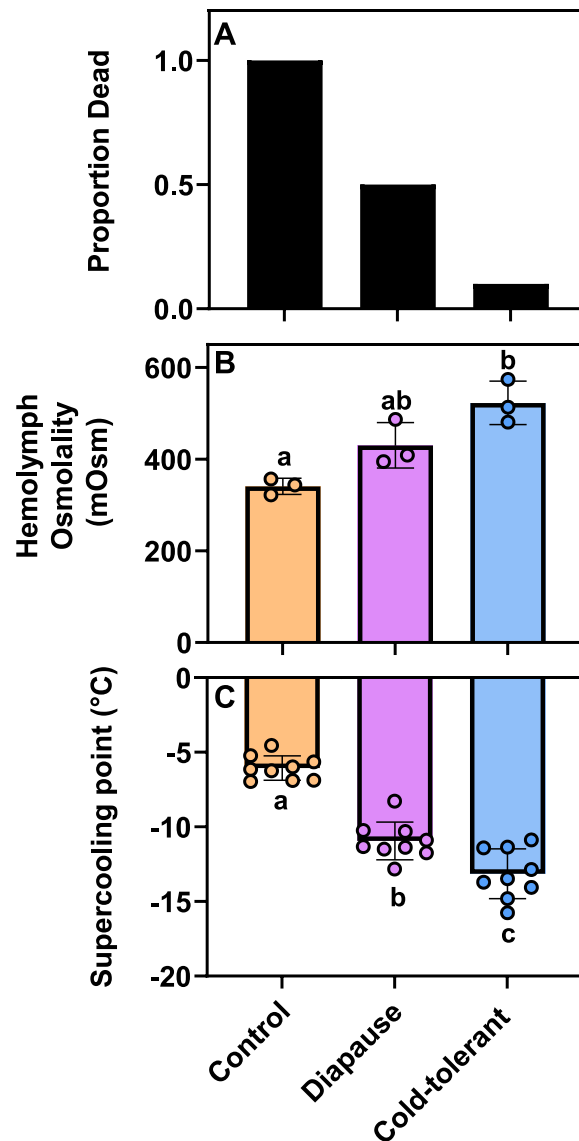


Figure 4.2. Survival at sub-zero temperatures, hemolymph osmolality, and supercooling points of control, diapausing and cold-tolerant Colorado potato beetles. Cold-tolerant CPB (A) survive better after two days at $-10\text{ }^{\circ}\text{C}$ ($n=10/\text{treatment}$), have a higher (B) hemolymph osmolality ($n=3/\text{treatment}$, Mean \pm S.D. osmolality), and a lower (C) supercooling point ($n=9/\text{treatment}$, Mean \pm S.D. SCP) compared to diapausing and control CPB. Different letters denote significant differences among groups ($p < 0.05$).

4.3.2 Transcriptome Summary

I assembled a transcriptome from 12 libraries, each consisting of mRNA from pooled fat body (n=8 beetles/pooled sample) from either diapause or cold-tolerant CPB (Table 4.1). I obtained 68,811,264 – 96,676,338 raw reads per library (average 83,620,460) with an overall alignment rate of 87.03 %. 78.55-81.14 % of reads uniquely mapped to the reference *L. decemlineata* genome (Table 4.1). These values are consistent with other published CPB transcriptomes that report sequence mapping rates (Kaplanoglu et al., 2017; Lebenzon et al., 2021). Of the assembled transcripts, 96 % aligned to sequences in the UniProt database, and of those that aligned, 63 % were annotated (*i.e.*, assigned putative sequence descriptions), and 77 % of those aligned transcripts were assigned to GO terms.

Table 4.1. Summary of the paired-end read libraries mapped to the *L. decemlineata* reference genome.

Biological replicate	Total raw reads after filtering	Mapped reads	Overall alignment rate	Concordant alignment rate (uniquely mapped reads)	%Q30*
<i>Cold-tolerant</i>					
Fat body A	78,582,934	69,787,146	88.07 %	81.14 %	95.14 %
Fat body B	96,676,338	84,427,445	87.33 %	80.04 %	98.05 %
Fat body C	80,372,872	69,458,236	86.42 %	78.55 %	94.50 %
<i>Diapause</i>					
Fat body A	68,811,264	59,459,813	86.41 %	78.79 %	94.38 %
Fat body B	93,066,552	80,474,648	86.47 %	78.70 %	94.32 %
Fat body C	84,212,800	73,029,340	86.72 %	79.05 %	94.38 %
<i>Average</i>	83,620,460	72,772,771	87.03 %	79.38 %	95.13 %

Each treatment and tissue had three biological replicates, and each replicate is represented by a different letter (A, B or C)

*%Q30 = Percent of bases assigned a Phred score of 30 (A Phred score of 30 indicates there is a 99.9 % chance that the correct base was called)

4.3.3 Cold tolerance is driven by a small shift in the fat body transcriptome

Thirty-five transcripts increased in abundance and ten transcripts decreased in abundance in cold-tolerant CPB compared to diapausing CPB (Figure 4.3). This small number of differentially expressed transcripts represents only 0.2 % of the total fat body transcriptome. Among transcripts that were increased in abundance in cold-tolerant CPB relative to diapausing CPB, there was an enrichment of GO terms related to the chaperone response and protein folding (Figure 4.4). Indeed, 15 % of differentially expressed transcripts mapped to a single KEGG pathway: protein processing in the endoplasmic reticulum (ko04141, Figure 4.4). Furthermore, 75 % of the transcripts that increased in abundance >1.5-fold in cold-tolerant CPB were related to the chaperone response. These 13 transcripts encode three heat shock-related proteins: Protein lethal (2) essential for life-like (part of the small heat shock protein 20 family), heat shock protein 68-like (part of the heat shock protein 70 family), and DnaJ (an HSP co-chaperone, part of the heat shock protein 40 family; Table 4.2). The remainder of the transcripts that increased in abundance >1.5-fold in cold-tolerant beetles encode proteins related to signaling (double homeobox protein A, 52 kDa repressor of the inhibitor of the protein kinase-like), regulation of gene expression (AN1-type zinc finger protein 2A-like, Myb-related protein B isoform X1), and lipid digestion (lipase; Table 4.2).

All transcripts that decreased in abundance by more than 1.5-fold in cold-tolerant CPB were of different functional origins (Table 4.2). Two transcripts that encode the 52 kDa repressor of the inhibitor of the protein kinase-like and heat shock protein 68-like were also decreased in abundance and were different transcript variants than those abundance increased (Table 4.2). There were no significantly enriched GO terms among transcripts that decreased in abundance in cold-tolerant beetles, most likely because ten transcripts are not enough for a statistically and biologically relevant enrichment analysis.

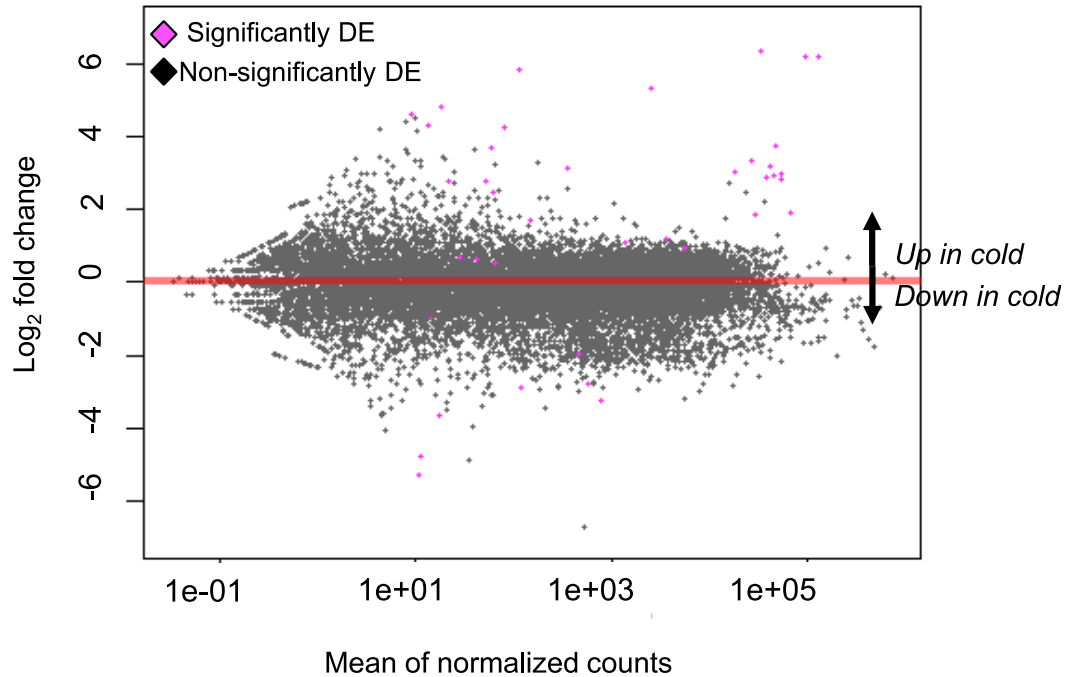


Figure 4.3. Differentially expressed transcripts in the fat body of cold-tolerant Colorado potato beetles compared to diapausing Colorado potato beetles. All data points represent differentially expressed transcripts based on log₂ fold change expression values. Grey points are not significantly differentially expressed, and purple points are significantly differentially expressed based on differential expression analysis with DESeq2 ($p < 0.05$). The red line is plotted to present no change in transcript abundance between cold-tolerant and diapausing CPB. Points above and below the red line represent transcripts increased and decreased in abundance, respectively, in cold-tolerant CPB compared to diapausing CPB.

Table 4.2. Increased expression of chaperone response, signaling, and transcriptional regulation-related transcripts in the fat body of cold-tolerant *L. decemlineata*. Fold change values represent transcripts that are significantly increased in abundance in cold-tolerant beetles compared to diapausing beetles (adjusted *p*-value of <0.05). All transcript IDs that follow a sequence description are variants of the same transcript.

Sequence description	Transcript ID(s)	Log₂ Fold change
<i>Chaperone response</i>		
Protein lethal (2) essential for life-like	LDEC000329-RA	2.9
	LDEC000330-RA	1.9
	LDEC003106-RA	3.8
	LDEC003107-RA	3.0
	LDEC003108-RA	2.9
	LDEC007977-RA	3.4
	LDEC007978-RA	3.0
Heat shock protein 68-like	LDEC008130-RA	3.2
	LDEC001138-RA	6.2
	LDEC001140-RA	6.3
	LDEC016280-RA	2.8
Heat shock protein 70	LDEC016281-RA	2.8
	LDEC016283-RA	2.5
dnaJ protein homolog 1	LDEC001676-RA	1.8
<i>Signaling and transcriptional regulation</i>		
Double homeobox protein A	LDEC001194-RA	1.7
52 kDa repressor of the inhibitor of the protein kinase-like	LDEC019140-RA	3.7
AN1-type zinc finger protein 2A-like	LDEC008440-RA	1.2
Myb-related protein B isoform X1	LDEC010530-RA	3.1
<i>Lipid digestion</i>		
Lipase 3-like	LDEC005770-RA	5.8

Table 4.3. All transcripts that significantly decreased in abundance in cold-tolerant *L.decemlineata* compared to diapause *L. decemlineata*. Fold change values represent transcripts that are significantly decreased in abundance in cold-tolerant beetles compared to diapausing beetles (adjusted *p*-value of <0.05).

Sequence description	Transcript ID	Log₂ Fold Change
gustatory receptor 68a-like	LDEC008803-RC	-5.3
52 kDa repressor of the inhibitor of the protein kinase-like	LDEC018293-RA	-4.8
RNA-binding protein 24-B-like	LDEC020604-RA	-3.6
heat shock protein 68-like	LDEC001410-RA	-3.3
odorant-binding protein	LDEC018115-RA	-2.9
alpha-(1,3)-fucosyltransferase C-like	LDEC006634-RA	-2.8
feline leukemia virus subgroup C receptor-related protein 2	LDEC007842-RA	-1.9

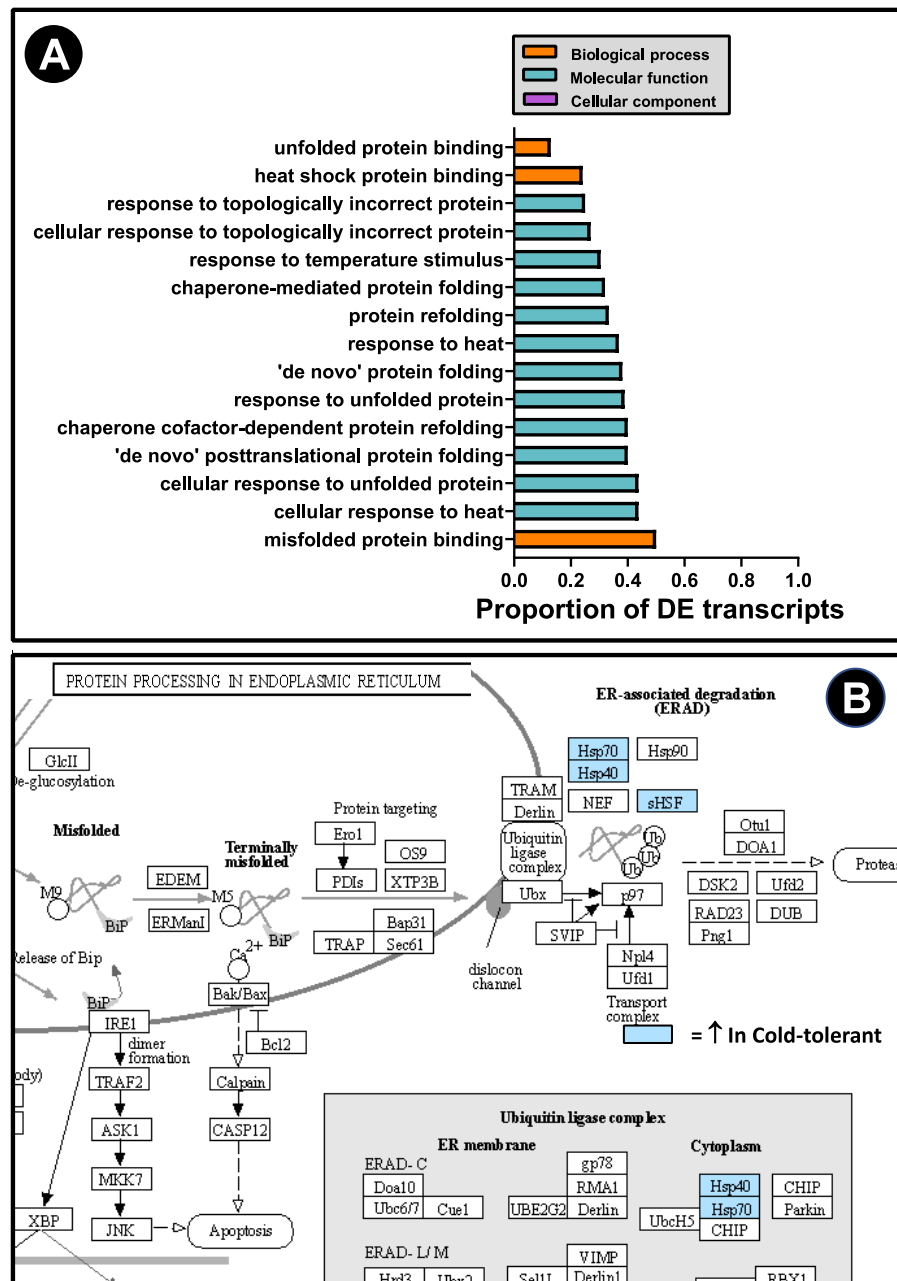


Figure 4.4. (A) Gene Ontology enrichment and (B) KEGG pathway mapping of transcripts that increased in cold-tolerant Colorado potato beetles. All enriched gene ontology (GO) terms among transcripts increased in abundance in the fat body of cold-tolerant beetles are related to proteostasis and the chaperone response, and several of the transcripts are involved in protein processing in the endoplasmic reticulum KEGG pathway. Bars in (A) represent the proportion of differentially expressed transcripts annotated with that specific GO term to total number of genes in that GO category. Blue-highlighted boxes in (B) represent transcripts increased in abundance in cold-tolerant beetles.

4.3.4 Diapausing beetles recover fewer proteins after cold shock

Total ubiquitinated protein levels were similar among diapausing and cold-tolerant CPB (Figure 4.5, Table 4.4). Total protein ubiquitination appeared to be lower in cold-tolerant CPB before a cold shock, although it was not significant. A power analysis based on the observed standardized effect size indicated that a sample size of eight would be required to detect this effect size (the current sample size was four). Cold shock elicited higher levels of protein ubiquitination, but only in cold-tolerant CPB (Figure 4.5, Table 4.4). Cold-tolerant beetles had more ubiquitinated proteins after a cold shock ($p=0.005$) and a nearly significantly lower level of ubiquitinated proteins after recovering from a cold shock ($p=0.060$), whereas the amount of protein ubiquitination did not change in diapausing beetles after a cold shock or after recovery from a cold shock (Figure 4.5).

Table 4.4. Statistical results from a two-way ANOVA comparing protein ubiquitination in diapausing and cold-tolerant Colorado potato beetles with no prior cold shock, a cold shock, and after recovery from a cold shock.

<i>Effect</i>	<i>df</i>	<i>SS</i>	<i>F</i>	<i>P</i>
Phenotype (diapause, cold-tolerant)	1	4.55e+15	0.006	0.94
Treatment (no cold shock, cold shock, cold shock + recovery)	2	9.54e+18	6.43	0.008*
Phenotype × Treatment	2	5.82e+19	3.92	0.04*
Error	18	1.34e+19		

*indicates a significant result

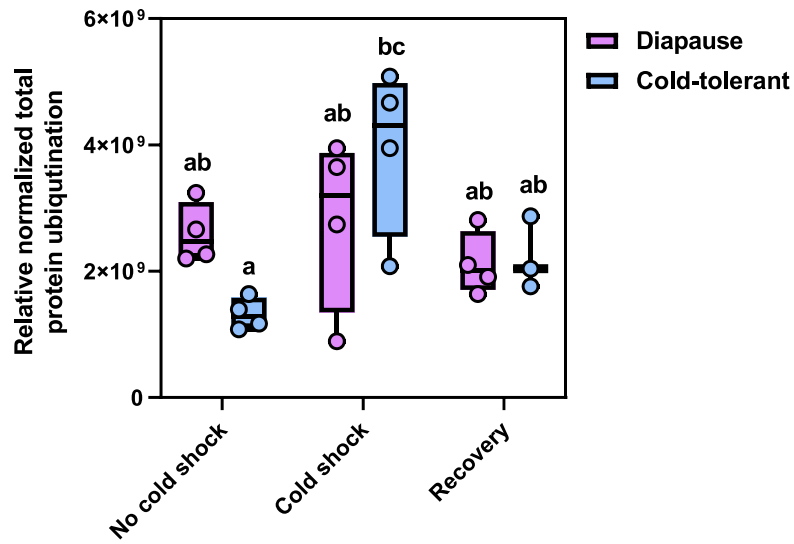


Figure 4.5. Protein ubiquitination in diapausing and cold-tolerant Colorado potato beetles after a cold shock at -10°C and recovery from that cold shock at 21°C . I normalized total protein ubiquitination to protein abundance using Bio-Rad stain-free immunoblots. Boxplots show median, minimum, and maximum values. Each point represents total protein ubiquitination in the fat body of an individual beetle. Different letters denote significant differences among groups ($p < 0.05$).

4.4 Discussion

Many overwintering insects express HSPs either in anticipation of or in response to sub-zero temperature exposure. However, the extent to which HSP expression contributes to protein protection and whole animal survival is unknown. I hypothesized that increased expression of HSPs and activation of the cellular chaperone response plays a role in driving cold tolerance of CPB. My data support this hypothesis because exposure to a fluctuating thermal regime improved cold tolerance of diapausing CPB, and these cold-tolerant CPB increased the abundance of heat shock-related transcripts to a greater extent compared to just diapausing beetles. This suggests that the chaperone response is only activated in cold-tolerant phenotypes, and not as part of the CPB diapause programme. I also hypothesized that the function of this activated chaperone response is to protect proteins from the cold. I provide a putative role for heat shock-related proteins in cold-tolerant beetles; increased expression of HSPs in cold-tolerant CPB is associated with slightly lower levels of protein

damage, and a higher capacity for protein repair. Taken together this suggests that activation of the chaperone response may protect fat body proteins in cold-tolerant CPB from cold-induced damage.

4.4.1 Putative role of the chaperone response in CPB cold tolerance

Cold-tolerant CPB had insignificantly lower levels of protein ubiquitination compared to diapausing beetles, which provides some indirect evidence that HSPs are re-folding denatured proteins in cold-tolerant CPB to restore their function. When proteins are reversibly denatured, HSPs can re-fold them such that they remain functional and are able to carry out important biological processes (Fernández-Fernández et al., 2017). However, if proteins are irreversibly denatured, HSPs are unable to re-fold them into a functional native conformation, and these denatured proteins are ubiquitinated and sent to the proteasome for degradation (Kandasamy and Andréasson, 2018). Thus, high levels of protein ubiquitination in a cell often indicate high levels of protein damage (Hofmann and Somero, 1995).

Increased expression of HSPs in cold-tolerant beetles may be sufficient to prevent irreversible protein denaturation, thus improving their survival at sub-zero temperatures.

CPB could increase the expression of HSPs after exposure to a fluctuating thermal regime as an anticipatory response to prepare for future cold exposures. As I showed in Chapter 2, diapausing CPB do not increase the abundance of *HSP68*, *protein lethal (2) essential for life*, and *DnaJ* compared to non-diapausing CPB, thus the expression of these chaperone proteins do not appear to be part of the CPB diapause programme but rather a result of their acquisition of cold tolerance. Diapausing CPB in my study had no prior sub-zero temperature exposure, thus I propose that fluctuating sub-zero temperatures induced the initial expression of heat shock-related transcripts, thereby increasing the overall intracellular levels of chaperone proteins to allow for faster protein repair after future cold exposures. Indeed, high basal intracellular levels of *HSP70* are associated with faster induction of the heat shock response (Wang and Lindquist, 1998), and many organisms increase the expression of HSPs in anticipation of exposure to environmental stressors (Arad et al., 2010; Rinehart et al., 2007b). Furthermore, cold-tolerant CPB potentially reduce protein damage after recovery from a cold shock to a greater extent than diapausing CPB. Taken together, this suggests that HSP expression improves CPB low temperature survival by increasing their capacity for

protein repair. To further test this hypothesis, I suggest using a manipulative tool such as RNA interference (RNAi) to knock down *HSP68* and/or *DnaJ* in diapausing CPB. If HSPs are indeed increasing CPB's capacity for protein repair, I predict that knocking down these heat shock-related transcripts in diapausing CPB before exposure to a fluctuating thermal regime would prevent protein re-folding and thus prevent CPB from becoming more cold-tolerant.

Protein re-folding by *HSP68* and *DnaJ* is ATP-dependent. For example, the *Escherichia coli* heat shock protein, GroEL, requires c. 100 ATP molecules to re-fold one rhodanase protein (Martin et al., 1991). Thus, rescuing denatured proteins requires both the induction of HSPs, and a sufficient ATP supply to fuel refolding. Cold-tolerant CPB increase the abundance of *lipase-3*, which encodes a lipolysis enzyme that could mobilize fuel for ATP production in fat body cells and provide energy for protein folding reactions. Further, cold-tolerant CPB accumulate proline in their fat body (J.E. Lebenzon, unpublished data) which could also provide energy for HSP re-folding reactions by oxidizing proline *via* mitochondrial proline dehydrogenase, thereby driving ATP synthesis (Teulier et al. 2016). Taken together, I hypothesize that cold-tolerant CPB mobilize lipid stores upon induction of the chaperone response, and in anticipation of the increased energy demand required for protein folding. I predict that cold-tolerant CPB will have slightly higher metabolic rates than diapausing CPB during recovery from a cold shock to meet these energy demands, and that fat body [ATP] increases upon exposure to the cold. To test this, I suggest using RNA interference (RNAi) to knock down *HSP68* and/or *DnaJ* in cold-tolerant CPB and predict that knocking down heat shock-related proteins would prevent lipid mobilization and ATP production, and decrease the metabolic rate of cold-tolerant CPB during recovery from cold shock.

4.4.2 Regulation of cold tolerance in CPB by other biological processes

Although I found that chaperone-related transcripts made up the majority (74 %) of differentially expressed transcripts in cold-tolerant CPB, c. 20 % of differentially expressed transcripts were related to transcriptional regulation. Cold-tolerant CPB increased the abundance of transcripts that encode several transcription factors; Double homeobox protein A, myb-related protein B isoform X1, and AN1-type zinc finger protein 2A-like.

Interestingly, these transcription factors are differentially expressed in other cold-tolerant insects. For example, Alfalfa leafcutting bees (*Megachile rotundata*) increase the abundance of transcripts encoding homeobox proteins and myb-related proteins in response to a fluctuating thermal regime (Melicher et al., 2019; Torson et al., 2017), and *Gryllis veletis* crickets increase the abundance of transcripts encoding homeobox proteins and zinc-finger proteins in response to cold acclimation (Toxopeus et al., 2019a). Although the precise physiological processes that these transcription factors regulate are still unknown (especially in insects), they could play a role in activating/repressing the expression of genes encoding proteins important for driving cellular survival at low temperatures. In Chapter 2, I did not find any evidence that CPB increase the abundance of these transcription factors during diapause alone (in Chapter 2), providing evidence that homeobox proteins, myb-related proteins, and zinc-finger type transcripts factors are necessary for cold tolerance independent of diapause.

Because there were so few transcription factors differentially expressed in cold-tolerant CPB, it would be fairly straightforward to identify which genes the transcription factors regulate and determine their function in improving cold tolerance. I suggest using chromatin immunoprecipitation (ChIP) sequencing (Mundade et al., 2014) to identify DNA binding regions of these transcription factors. Furthermore, increasing the abundance of transcription factors after a fluctuating thermal regime could prepare CPB for future cold exposures. To test this, I suggest using RNAi to knock down expression of these transcription factors in diapausing CPB before exposing them to a fluctuating thermal regime. If transcription factors help prime CPB for future cold exposures, then knocking them down should prevent diapausing CPB from becoming cold-tolerant.

4.4.3 Cold activation of the chaperone response independently of diapause in CPB

The extent to which HSPs and the chaperone response confer cold tolerance independently of diapause is currently unknown. Previously, I found that diapause alone does not induce *HSP70* or other chaperone-related transcript expression in the fat body (Chapter 2). Here I report that diapausing CPB only increase *HSP* expression and activate the chaperone response in their fat body after the acquisition of cold tolerance. Taken together, this suggests

that the chaperone response is important for conferring cold tolerance (and protecting proteins in the fat body), independent of diapause. Because CPB suppress their metabolic rate during diapause (Chapter 3), perhaps it is only adaptive for CPB to activate the ATP-dependent chaperone response in direct anticipation of a cold exposure, rather than constitutively express HSPs throughout their diapause programme.

These data build on earlier work which showed that CPB increase HSP70 both during diapause and after exposure to a fluctuating thermal regime (Yocum, 2001). A major caveat of this previous work is that HSP expression was measured in whole body homogenates, rather than specific tissues. This approach could have masked important tissue-specific differences in HSP expression and explain why I did not observe any diapause-driven HSP expression in CPB fat body (Chapter 2). Fat body is the major site of intermediary metabolism in insects, thus I propose that CPB activate the chaperone response in their fat body to protect the function of metabolically important proteins, such as key enzymes involved in lipid and energy metabolism, but only when there is a low temperature exposure. I suggest using co-immunoprecipitation and mass spectrometry to isolate heat shock protein/substrate interactions and identify which protein substrates HSPs are re-folding in cold-tolerant CPB.

4.5 Conclusions and future directions

I show that improved cold tolerance in CPB coincides with activation of the chaperone response and provide some evidence that HSPs play a major role in protein repair. Cold-tolerant CPB appear to have fewer damaged proteins, and a greater capacity for protein repair after exposure to a sub-zero temperature exposure compared to diapausing CPB, but more data is required to confirm this. Because the majority of transcriptomic shifts I observed in cold-tolerant CPB were related to the chaperone response, the ability to protect proteins is clearly important for overwinter survival in CPB. The ability to enhance mechanisms of protein protection in response to fluctuating temperatures is likely adaptive because CPB experience similar temperature fluctuations in nature (Yocum, 2001). In the future, I suggest measuring other metrics of protein and cell damage in diapausing and cold-tolerant CPB (*e.g.*, cell survival, levels of protein aggregation, rates of protein folding), to build a more complete picture of protein processing in cells before and after sub-zero temperature

exposure. Further, the energetic costs of the chaperone response merit further investigation, especially since overwintering CPB are in diapause, where resources are limited, and their metabolism is suppressed. I also suggest using manipulative tools such as RNA interference to alter levels of chaperone proteins to better understand how the activation of the chaperone response drives increased cold tolerance and low temperature survival in insects.

4.6 References

- Arad, Z., Mizrahi, T., Goldenberg, S., Heller, J.** (2010). Natural annual cycle of heat shock protein expression in land snails: desert versus Mediterranean species of *Sphincterochila*. *Journal of Experimental Biology* **213**, 3487-3495.
- Becker, J., Craig, E.A.** (1994). Heat-shock proteins as molecular chaperones. *European Journal of Biochemistry* **219**, 11-23.
- Boiteau, G., Coleman, W.** (1996). Cold tolerance in the Colorado potato beetle, *Leptinotarsa decemlineata* (Say)(Coleoptera: Chrysomelidae). *Canadian Entomologist* **128**, 1087-1099.
- Crosthwaite, J.C., Sobek, S., Lyons, D.B., Bernards, M.A., Sinclair, B.J.** (2011). The overwintering physiology of the emerald ash borer, *Agrilus planipennis* Fairmaire (Coleoptera: Buprestidae). *Journal of Insect Physiology* **57**, 166-173.
- D'Amico, S., Claverie, P., Collins, T., Georlette, D., Gratia, E., Hoyoux, A., Meuwis, M.-A., Feller, G., Gerday, C.** (2002). Molecular basis of cold adaptation. *Philosophical Transactions of the Royal Society of London B* **357**, 917-925.
- De Kort, C.** (1990). Thirty-five years of diapause research with the Colorado potato beetle. *Entomologia Experimentalis et Applicata* **56**, 1-13.
- De Wilde, J.** (1960). Diapause in the Colorado beetle (*Leptinotarsa decemlineata* Say) as an endocrine deficiency syndrome of the *corpora allata*. *Acta Physiologica et Pharmacologica Neerlandica*. **11**, 93.
- Des Marteaux, L.E., Stinziano, J.R., Sinclair, B.J.** (2018). Effects of cold acclimation on rectal macromorphology, ultrastructure, and cytoskeletal stability in *Gryllus pennsylvanicus* crickets. *Journal of Insect Physiology* **104**, 15-24.
- Espinosa, Y.R., Grigera, J.R., Caffarena, E.R.** (2017). Essential dynamics of the cold denaturation: pressure and temperature effects in yeast frataxin. *Proteins: Structure, Function, and Bioinformatics* **85**, 125-136.
- Fernández-Fernández, M.R., Gragera, M., Ochoa-Ibarrola, L., Quintana-Gallardo, L., Valpuesta, J.M.** (2017). Hsp70—a master regulator in protein degradation. *FEBS Letters* **591**, 2648-2660.
- Grapputo, A., Boman, S., Lindstroem, L., Lyytinen, A., Mappes, J.** (2005). The voyage of an invasive species across continents: genetic diversity of North American and European Colorado potato beetle populations. *Molecular Ecology* **14**, 4207-4219.
- Hendrick, J.P., Hartl, F.U.** (1993). Molecular chaperone functions of heat-shock proteins. *Annual Review of Biochemistry* **62**, 349-384.

- Hiisaar, K., Karise, R., Williams, I.H., Luik, A., Metspalu, L., Jogar, K., Ereemeev, V., Ploomi, A., Kruus, E., Mand, M.** (2014). Cold tolerance of Colorado potato beetle (*Leptinotarsa decemlineata* Say) adults and eggs. *Zemdirbyste-Agriculture* 101.
- Hofmann, G., Somero, G.** (1995). Evidence for protein damage at environmental temperatures: seasonal changes in levels of ubiquitin conjugates and hsp70 in the intertidal mussel *Mytilus trossulus*. *Journal of Experimental Biology* **198**, 1509-1518.
- Kandasamy, G., Andréasson, C.** (2018). Hsp70–Hsp110 chaperones deliver ubiquitin-dependent and-independent substrates to the 26S proteasome for proteolysis in yeast. *Journal of Cell Science* 131.
- Kaplanoglu, E., Chapman, P., Scott, I.M., Donly, C.** (2017). Overexpression of a cytochrome P450 and a UDP-glycosyltransferase is associated with imidacloprid resistance in the Colorado potato beetle, *Leptinotarsa decemlineata*. *Scientific Reports* **7**, 1-10.
- Kiang, J.G., Tsokos, G.C.** (1998). Heat shock protein 70 kDa: molecular biology, biochemistry, and physiology. *Pharmacology & Therapeutics* **80**, 183-201.
- King, A.M., MacRae, T.H.** (2015). Insect heat shock proteins during stress and diapause. *Annual Review of Entomology* **60**, 59-75.
- Košťál, V., Tollarová-Borovanská, M.** (2009). The 70 kDa heat shock protein assists during the repair of chilling injury in the insect, *Pyrrhocoris apterus*. *PLoS One* **4**, e4546.
- Košťál, V., Zahradníčková, H., Šimek, P.** (2011). Hyperprolinemic larvae of the drosophilid fly, *Chymomyza costata*, survive cryopreservation in liquid nitrogen. *Proceedings of the National Academy of Sciences of the U.S.A.* **108**, 13041-13046.
- Lebenzon, J.E., Torson, A.S., Sinclair, B.J.** (2021). Diapause differentially modulates the transcriptomes of fat body and flight muscle in the Colorado potato beetle. *Comparative Biochemistry and Physiology D*, 100906.
- Lee, R.E., Damodaran, K., Yi, S.-X., Lorigan, G.A.** (2006). Rapid cold-hardening increases membrane fluidity and cold tolerance of insect cells. *Cryobiology* **52**, 459-463.
- Lefevre, K., Koopmanschap, A., De Kort, C.** (1989). Changes in the concentrations of metabolites in haemolymph during and after diapause in female Colorado potato beetle, *Leptinotarsa decemlineata*. *Journal of Insect Physiology* **35**, 121-128.
- Lyytinen, A., Mappes, J., Lindström, L.** (2012). Variation in Hsp70 levels after cold shock: signs of evolutionary responses to thermal selection among *Leptinotarsa decemlineata* populations. *PLoS One* **7**, e31446.

- MacMillan, H.A., Knee, J.M., Dennis, A.B., Udaka, H., Marshall, K.E., Merritt, T.J.S., Sinclair, B.J.** (2016). Cold acclimation wholly reorganizes the *Drosophila melanogaster* transcriptome and metabolome. *Scientific Reports* **6**, 28999.
- Martin, J., Hartl, F.U.** (1997). Chaperone-assisted protein folding. *Current Opinion in Structural Biology* **7**, 41-52.
- Martin, J., Langer, T., Boteva, R., Schramel, A., Horwich, A.L., Hartl, F.-U.** (1991). Chaperonin-mediated protein folding at the surface of groEL through a molten globule-like intermediate. *Nature* **352**, 36-42.
- Melicher, D., Torson, A.S., Anderson, T.J., Yocum, G.D., Rinehart, J.P., Bowsher, J.H.** (2019). Immediate transcriptional response to a temperature pulse under a fluctuating thermal regime. *Integrative and Comparative Biology* **59**, 320-337.
- Mundade, R., Ozer, H.G., Wei, H., Prabhu, L., Lu, T.** (2014). Role of ChIP-seq in the discovery of transcription factor binding sites, differential gene regulation mechanism, epigenetic marks and beyond. *Cell Cycle* **13**, 2847-2852.
- Privalov, P.L.** (1990). Cold denaturation of protein. *Critical Reviews in Biochemistry and Molecular Biology* **25**, 281-306.
- Reeg, S., Jung, T., Castro, J.P., Davies, K.J., Henze, A., Grune, T.** (2016). The molecular chaperone Hsp70 promotes the proteolytic removal of oxidatively damaged proteins by the proteasome. *Free Radical Biology and Medicine* **99**, 153-166.
- Rinehart, J.P., Li, A., Yocum, G.D., Robich, R.M., Hayward, S.A., Denlinger, D.L.** (2007). Up-regulation of heat shock proteins is essential for cold survival during insect diapause. *Proceedings of the National Academy of Sciences of the U.S.A* **104**, 11130-11137.
- Salt, R.W.** (1933). Some experiments on the freezing and hardening of the adults of the Colorado potato beetle, *Leptinotarsa decemlineata* Say. PhD Thesis. Bozeman, Montana, U.S.A: Montana State University.
- Sinclair, B.J., Alvarado, L.E.C., Ferguson, L.V.** (2015). An invitation to measure insect cold tolerance: methods, approaches, and workflow. *Journal of Thermal Biology* **53**, 180-197.
- Sorger, P.K.** (1991). Heat shock factor and the heat shock response. *Cell* **65**, 363-366.
- Štětina, T., Košťál, V., Korbelová, J.** (2015). The role of inducible Hsp70, and other heat shock proteins, in adaptive complex of cold tolerance of the fruit fly (*Drosophila melanogaster*). *PLoS One* **10**, e0128976.
- Storey, J.M., Storey, K.B.** (1983). Regulation of cryoprotectant metabolism in the overwintering gall fly larva, *Eurosta solidaginis*: temperature control of glycerol and sorbitol levels. *Journal of Comparative Physiology* **149**, 495-502.

- Storey, K.B., Storey, J.M.** (2012). Insect cold hardiness: metabolic, gene, and protein adaptation. *Canadian Journal of Zoology* **90**, 456-475.
- Tollarová-Borovanská, M., Lalouette, L., Košťál, V.** (2009). Insect cold tolerance and repair of chill-injury at fluctuating thermal regimes: Role of 70 kDa heat shock protein expression. *CryoLetters* **30**, 312-319.
- Torson, A.S., Yocum, G.D., Rinehart, J.P., Nash, S.A., Kvidera, K.M., Bowsher, J.H.** (2017). Physiological responses to fluctuating temperatures are characterized by distinct transcriptional profiles in a solitary bee. *Journal of Experimental Biology* **220**, 3372-3380.
- Toxopeus, J., Des Marteaux, L.E., Sinclair, B.J.** (2019a). How crickets become freeze tolerant: The transcriptomic underpinnings of acclimation in *Gryllus veletis*. *Comparative Biochemistry and Physiology D* **29**, 55-66.
- Toxopeus, J., Košťál, V., Sinclair, B.J.** (2019b). Evidence for non-colligative function of small cryoprotectants in a freeze-tolerant insect. *Proceedings of the Royal Society B* **286**, 20190050.
- Vesala, L., Salminen, T.S., Košťál, V., Zahradníčková, H., Hoikkala, A.** (2012). Myo-inositol as a main metabolite in overwintering flies: seasonal metabolomic profiles and cold stress tolerance in a northern drosophilid fly. *Journal of Experimental Biology* **215**, 2891-2897.
- Wang, Z., Lindquist, S.** (1998). Developmentally regulated nuclear transport of transcription factors in *Drosophila* embryos enable the heat shock response. *Development* **125**, 4841-4850.
- Williams, C.M., Henry, H.A., Sinclair, B.J.** (2015). Cold truths: how winter drives responses of terrestrial organisms to climate change. *Biological Reviews* **90**, 214-235.
- Yocum, G.** (2001). Differential expression of two HSP70 transcripts in response to cold shock, thermoperiod, and adult diapause in the Colorado potato beetle. *Journal of Insect Physiology* **47**, 1139-1145.
- Yocum, G., Joplin, K., Denlinger, D.** (1998). Upregulation of a 23kDa small heat shock protein transcript during pupal diapause in the flesh fly, *Sarcophaga crassipalpis*. *Insect Biochemistry and Molecular Biology* **28**, 677-682.
- Zachariassen, K.E.** (1985). Physiology of cold tolerance in insects. *Physiological Reviews* **65**, 799-832.

Chapter 5

5 General discussion

In my thesis, I used the Colorado potato beetle (CPB) to fill gaps in our understanding of some of the most widely observed phenotypes in diapausing and cold-tolerant insects, metabolic suppression and chaperone protein expression. I demonstrated tissue-specific roles for fat body and flight muscle in driving diapause phenotypes and generated several novel hypotheses about the biological processes underlying metabolic suppression and stress tolerance during diapause in CPB (Chapter 2). One of the hypotheses that I postulated is that flight muscle mitochondria modulate energy homeostasis and therefore metabolic suppression during diapause in CPB. I test this hypothesis in Chapter 3 and find that metabolic suppression during diapause in CPB is driven, in part, by Parkin-mediated mitophagy of flight muscle mitochondria. Further, CPB reverse this mitophagy and activate mitochondrial biogenesis in anticipation of their emergence from diapause, which leads to the re-establishment of their metabolic rate (Chapter 3). Finally, I show that the chaperone response is important for sub-zero temperature survival in diapausing CPB, but only in cold-tolerant phenotypes (Chapter 4). In this chapter, I aim to synthesize my findings and place them in the broader context of an updated framework for diapause and cold tolerance in CPB and other temperate insects.

5.1 An updated framework for insect diapause: The role of mitochondrial homeostasis in metabolic suppression

Insect diapause has been extensively studied since the early 1900s (Tauber and Tauber, 1976) and since then we have developed a deep understanding of the events that trigger diapause initiation, and the phenotypes and physiological changes associated with insect diapause (Chapter 1). In particular, we knew that diapausing insects suppress their metabolic rate, and that some adults (including CPB) appeared to histolyze their flight muscle during the winter. What we lacked is a mechanistic explanation for metabolic suppression and an adaptive explanation for the phenomenon of adult flight muscle histolysis. In Chapters 2 and 3 I show that whole-animal metabolic suppression during diapause in CPB is linked to this observed flight muscle histolysis. Further, I reveal that the apparent flight muscle degeneration and

regeneration we observe in diapausing CPB is associated with shifts in flight muscle mitochondrial homeostasis.

5.1.1 A conceptual model of metabolic suppression during diapause in CPB

To create a conceptual model of metabolic suppression, I need to explain my data in the context of upstream activation of mitophagy and how CPB shift between mitophagy and mitochondrial homeostasis during diapause. This is the first time (to my knowledge) that altering mitochondrial homeostasis has been implicated in metabolic suppression during animal dormancy, and (if mitophagy-based metabolic suppression is widespread), this conceptual model can serve as an overarching hypothesis for future work on metabolic regulation in diapausing insects.

5.1.1.1 Upstream activation of mitophagy

Mitophagy is activated during diapause maintenance in CPB, however I did not address how Parkin-mediated mitophagy is initiated at the start of diapause. There must be molecules/pathways upstream of Parkin that help initiate mitochondrial degradation, and I propose that mitophagy is activated by changes in FOXO/Juvenile hormone signaling (Figure 5.1). I have two reasons to expect that FOXO/JH signaling regulates mitophagy during diapause. First, low levels of circulating JH in diapause-destined insects can activate FOXO activity. As a transcription factor, FOXO activation then leads to the transcription of genes that drive many physiological changes during diapause, such as cell cycle arrest and lipid accumulation (Sim and Denlinger, 2008; Sim et al., 2015). Indeed, CPB decrease JH titre during diapause initiation (De Kort et al., 1982) and FOXO is expressed in the thorax and fat body of pre-diapausing CPB (Lehmann et al., 2014). Second, FOXO can activate the transcription of mitophagy related genes, including *PINK1*, *ATG5*, and *ATG10* (Audesse et al., 2019; Mei et al., 2009), and could thus help initiate mitophagy in CPB. Taken together, I suggest that in diapausing CPB, FOXO is activated by decreased JH levels, which leads to the transcription of genes required for mitophagy (Figure 5.1). To test this model, I suggest using chromatin immunoprecipitation (ChIP) sequencing to identify FOXO DNA binding sites in CPB entering diapause (Sim et al., 2015), and predict that mitophagy-related genes are targets for FOXO in diapausing CPB. I also suggest using RNAi to knock down *FOXO*

expression in beetles entering diapause. If FOXO plays a role in activating mitophagy gene transcription, then I predict that knocking down *FOXO* expression will prevent the expression of mitophagy-related genes, and ultimately prevent mitophagy-mediated metabolic suppression in diapausing CPB.

Initiating mitophagy requires both the expression of mitophagy-related genes, and a stimulus to stabilize PINK1 and Parkin to the outer mitochondrial membrane. Thus, although I predict that FOXO activates the transcription of genes related to mitophagy, I suggest there are other mechanisms that activate the process of mitophagy once the proteins required for mitophagy are expressed. Mitophagy is normally activated in response to decreased membrane potential in damaged mitochondria; decreased mitochondrial membrane potential destabilizes PINK1 from the outer mitochondrial membrane, recruits Parkin, and activates Parkin-mediated mitophagy (Jin and Youle, 2012). Mitochondrial membrane potential can be decreased when cells express uncoupling proteins (UCPs) which are situated in the inner mitochondrial membrane and dissipate proton gradients, thereby decreasing membrane potential. I observed a c. 5-fold increase in *UCP4* abundance in flight muscle of diapausing CPB in Chapter 2, and thus propose that CPB use *UCP4* to decrease mitochondrial membrane potential and drive activation of Parkin-mediated mitophagy in otherwise healthy mitochondria (Figure 5.1). Indeed, UCP overexpression in dauer larvae of *C. elegans* stimulates mitophagy by decreasing mitochondrial membrane potential (Cho et al., 2017). To test this hypothesis, I suggest measuring the membrane potential of flight muscle mitochondria using fluorescent probes such as safranin (Krumshnabel et al., 2014), and predict that membrane potential will decrease as CPB enter diapause. Further, if *UCP4* is indeed triggering Parkin mediated mitophagy, then I predict that RNAi knockdown of *UCP4* in the early stages of diapause in CPB will prevent changes in mitochondrial membrane potential in diapausing CPB, and ultimately prevent mitophagy-mediated metabolic suppression.

If *UCP4* is involved in the initiation of mitophagy, the question of how *UCP4* expression is stimulated still remains. The expression and function of uncoupling proteins is relatively understudied in insects compared to vertebrates (Sokolova and Sokolov, 2005), but there is some evidence that reactive oxygen species (ROS) can initiate the expression of *UCP4* in insects (Alves-Bezerra et al., 2014). Although ROS are often perceived as damaging

molecules to cells, low levels of ROS can act as signaling molecules and regulate changes in metabolic pathways (Reczek and Chandel, 2015). Oxidative stress pathways were enriched in both the fat body and flight muscle of diapausing CPB according to my GO enrichment analysis in Chapter 2, and ROS regulates metabolic suppression in another diapausing insect (Chen et al., 2020). Thus, in CPB, physiologically relevant levels of ROS in flight muscle could initiate *UCP4* expression, thereby decreasing mitochondrial membrane potential, and triggering mitophagy-mediated metabolic suppression.

5.1.1.2 Interplay between mitophagy and mitochondrial homeostasis during diapause

During early diapause, CPB activate mitophagy in their flight muscle which leads to an imbalance in mitochondrial homeostasis. They appear to shift towards mitochondrial biogenesis and re-establish mitochondrial homeostasis during late diapause, which leads to the recovery of their metabolic rate. Here, I propose a pathway for the shift in mitochondrial homeostasis I observed in diapausing beetles and describe future manipulative experiments to further elucidate this pathway (Figure 5.1, 5.2).

After stimulation of mitophagy by some unknown upstream regulator (*e.g.*, UCP4-driven decreases in membrane potential, Section 5.1.1.1), I propose that CPB stabilize PINK1 to the outer mitochondrial membrane of flight muscle mitochondria through the TOM/TIM complex, a multi-subunit complex of proteins in the outer and inner mitochondrial membrane (increased *TIM* transcript abundance, Chapter 2; Figure 5.1). Once PINK1 is stabilized to the outer membrane in flight muscle of diapausing CPB, Parkin ubiquitinates mitochondria thereby tagging them for removal (Chapter 3). I observed an increase in expression of *Parkin* but did not observe any changes in *PINK1* gene expression during diapause, either using RNA-seq in Chapter 2 or using qPCR in Chapter 3. PINK1 is primarily regulated by reversible protein phosphorylation (Vives-Bauza et al., 2010), and muscle cells tend to constitutively express PINK1 protein (Narendra et al., 2010). Thus, I suggest measuring levels of phosphorylated PINK1 in diapausing CPB to confirm the activation of mitophagy by both PINK1 and Parkin and expect to observe increased levels of phosphorylated PINK1. Furthermore, because *Parkin* expression increased by a little less than 2-fold (which is not a substantial increase in expression) in Chapter 3, and only just above 1-fold from RNA-seq

data in Chapter 2, it is clear that subtle changes in gene expression during diapause can still have large effects on tissue and whole-animal phenotypes.

After mitochondria are ubiquitinated, autophagy-related proteins regulate the expansion of isolation membranes and autophagosome formation in flight muscle cells of diapausing CPB (Chapter 3; Figure 5.1). Several dynein and microtubule-related transcripts increased in abundance, and GO terms related to dynein-based microtubule movement were enriched in flight muscle of diapausing CPB (Chapter 2). During mitophagy, mitochondria, lysosomes, and autophagosomes must be able to move towards each other in flight muscle cells.

Microtubules facilitate the movement of organelles and structures within the cell (Reck-Peterson et al., 2018). For example, microtubules and their associated motor proteins, such as dynein, direct the movement of isolation membranes and autophagosomes towards lysosomes during mitophagy in mammalian and *Drosophila* muscle cells (Batlevi et al., 2010; Ravikumar et al., 2005). In diapausing CPB, I propose that dynein-based microtubule movement is involved in the transport of tagged mitochondria towards isolation membranes and transport of autophagosomes towards lysosomes (Figure 5.1). To test this, I propose using RNAi to knock down dynein-related transcripts in diapausing CPB. If dynein-based microtubule movement is necessary for mitophagy, then I predict that knocking down *dynein* expression would prevent proper fusing of autophagosomes with lysosomes, thereby preventing mitochondrial breakdown.

Once autophagosomes containing mitochondria fuse with lysosomes (which I show in Chapter 3), mitochondria are degraded by lysosomal proteases and this mass degradation of mitochondria in CPB flight muscle is then accompanied by metabolic suppression at the whole-animal level (Figure 5.1). With reduced mitochondrial density, flight muscle mitochondrial respiration is lowered (Chapter 3) and there are fewer sites for ATP production.

Because reducing Parkin-mediated mitophagy (with RNAi knockdown of *Parkin*) did not fully restore whole-animal metabolic rate and mitochondrial function (Chapter 3), I speculate that there are additional mechanisms of metabolic suppression which limit the metabolism of mitochondria that remain in diapausing CPB flight muscle (Figure 5.1). Colorado potato

beetles spend several months in diapause with suppressed metabolism, thus employing additional mechanisms, other than Parkin-mediated mitophagy, to lower their metabolic rate could maximize their energy savings until they emerge from diapause in the spring. Diapausing CPB could 1) reduce mitochondrial ATP production by lowering activities of electron transport system enzymes in remaining mitochondria, possibly *via* post translational modifications (Staples, 2016), or 2) shift to anaerobic metabolism in their flight muscle in the absence of aerobic metabolic machinery (Chen et al., 2020). To test 1), I suggest investigating whether there are changes in the amounts and activities of electron transport enzymes that remain in the flight muscle of diapausing CPB, and measure whether those electron transport enzymes are phosphorylated and/or acetylated. If electron transport enzyme activity is regulated by post-translational modification, I would expect to see changes in enzyme activity alongside changes in phosphorylation and/or acetylation state of the enzymes (Mathers and Staples, 2019). To test 2), I suggest using liquid or gas chromatography coupled to mass spectrometry (metabolomics) to measure the abundance of metabolic intermediates in flight muscle of diapausing CPB (Chen et al., 2020). If CPB shift to anaerobic metabolism, I expect that anaerobic by-products such as lactate or alanine would increase later in diapause, during periods of maximal metabolic suppression.

To recover their metabolic rate, diapausing CPB re-grow their flight muscle mitochondria through transcriptionally mediated mitochondrial biogenesis. Interestingly, CPB activate this mitochondrial biogenesis in anticipation of an increased energy demand because increased abundance of *PGC1 α* and *NRF1* directly precedes the appearance of flight muscle mitochondria, and this occurs when beetles are still beneath the soil without any changes in external stimuli (Figure 5.1). Because CPB increase mitochondrial biogenesis without any external cues, I propose that mitochondrial biogenesis is initiated in response to internal physiological cues, such as cellular energy status (Figure 5.1). AMP-activated kinase (AMPK) is considered to be a master regulator of energy cellular status because it responds to changing AMP: ATP levels in a cell; When AMP: ATP levels increase, AMPK is activated and can restore energy balance by switching on ATP-generating pathways. Specifically, increased AMP: ATP ratios often stimulate mitochondrial biogenesis through the AMPK pathway to increase mitochondrial pools and ATP production (Hardie et al., 2012). If AMP: ATP levels increase towards later stages of diapause in CPB (which could

ultimately happen in the absence of mitochondrial ATP production), AMPK could activate *PGC1 α* (cf. Jäger et al., 2007), and stimulate mitochondrial biogenesis (Figure 5.1).

Therefore, I suggest measuring AMP and ATP levels and AMPK activity in flight muscle cells of diapausing CPB and predict that high AMP:ATP ratios would be associated with increased AMPK activity, and thus initiation of mitochondrial biogenesis.

During diapause, CPB appear to uncouple mitophagy and mitochondrial biogenesis such that mitochondria are removed from flight muscle faster than new mitochondria are synthesized. Mitophagy and mitochondrial biogenesis are normally tightly regulated in cells (Palikaras et al., 2014), and to circumvent this tight regulation and achieve metabolic suppression, CPB must be able to differentially regulate molecules involved in both pathways. In Chapter 3 I present Parkin as a mitophagy-related protein, however Parkin can also regulate mitochondrial biogenesis, and thus plays an important role in modulating overall mitochondrial homeostasis in animal cells. When mitophagy exceeds mitochondrial biogenesis in a cell, Parkin can interact with a protein called PARIS (Parkin interacting substrate), which is a transcriptional repressor of *PGC1 α* (Figure 5.2; Shin et al., 2011). Under these conditions, Parkin ubiquitinates PARIS, sending it for proteasomal degradation, which concomitantly activates the expression of *PGC1 α* and therefore mitochondrial biogenesis (Figure 5.2). Because *Parkin* expression is sustained towards the end of diapause (Chapter 3), I propose that it can stimulate mitochondrial biogenesis (Figure 5.2). Furthermore, AMPK can also stimulate mitophagy through Parkin-independent pathways, so it is possible that Parkin and AMPK cooperate to regulate shifts in mitochondrial homeostasis during diapause (Figure 5.2).

5.1.2 Remaining questions about mitophagy-mediated metabolic suppression

I provide strong evidence that Parkin-mediated mitophagy drives metabolic suppression during diapause and therefore contributes to energy savings over the winter. However, there are still gaps in this model, and I identify three compelling questions about mitophagy-mediated metabolic suppression during diapause. First, did over-active mitophagy in the flight muscle of diapausing CPB evolve specifically for metabolic suppression, or is metabolic suppression just a consequence of flight muscle disuse during diapause? Second,

are there other benefits for enhanced mitophagy in diapausing CPB that extend beyond lowering metabolic rate to save energy? Third, do other diapausing insects also employ mitophagy to lower their metabolic rate during the winter?

To address my first question, I must discuss the possibility that metabolic suppression is just a consequence of flight muscle disuse. Mitophagy can be triggered by muscle disuse (Romanello and Sandri, 2015), therefore it is possible that when CPB do not fly during diapause, mitophagy is activated in their flight muscle, which results in a consequential reduction in metabolic rate. Indeed, long periods without flying can induce muscle atrophy in *Drosophila* (who have similar indirect flight muscles to Coleoptera; Lane et al., 2014), and *Drosophila* with experimentally induced flight muscle disuse atrophy have slightly lower metabolic rates than individuals of the same age with fully active flight muscles (Lane et al., 2014). This suggests that muscle disuse atrophy could lead to metabolic suppression in diapausing CPB that do not fly. However, in my laboratory culture of CPB, non-diapausing beetles do not fly because they have constant access to host potato plants and mates, yet I have never observed any signs of flight muscle atrophy in non-diapausing CPB (personal observations). Thus, it is unlikely that metabolic suppression during diapause is simply a consequence of flight muscle disuse. Rather, I posit that over-active mitophagy is a regulated mechanism that lowers metabolic rate in CPB to contribute to energy savings during the winter when resources are scarce.

There may be other benefits of enhanced mitophagy in flight muscle of diapausing CPB other than lowering metabolic rate to save energy, especially since maintaining mitochondrial homeostasis is integral for cellular function (Palikaras et al., 2014). Recently, mitophagy and the maintenance of mitochondrial homeostasis have been implicated in ageing; decreased rates of cellular mitophagy over time can lead to the build-up of dysfunctional mitochondria and result in ageing phenotypes at the whole animal level (Bakula and Scheibye-Knudsen, 2014). Thus, the capacity to clear damaged mitochondria *via* mitophagy can determine an organism's lifespan. Diapause extends the lifespan of insects (Hand et al., 2016), including CPB (Perferoen et al., 1981). Thus, I propose that enhanced mitophagy in diapausing CPB could promote longevity. Indeed, enhanced mitophagy is required for longevity in dauer formation of *C. elegans* (Palikaras et al., 2015), and enhanced mitophagy *via* Parkin

overexpression can extend *Drosophila* lifespan (Rana et al., 2013). It would be difficult to disentangle the effects of mitophagy on metabolic suppression from effects on longevity, especially because longevity is often associated with lower metabolic rates (Speakman et al., 2002). Regardless, it would be an interesting concept to explore given the importance of mitochondrial homeostasis on protecting cells from the adverse effects of aging.

Because my model of mitophagy-mediated metabolic suppression only applies to CPB, it remains unclear whether other diapausing species employ similar mechanisms to lower their metabolic rate. The majority of diapausing adult insects do not fly during diapause, and at least two orders of adult insects reversibly histolyze their flight muscle during diapause, including Coleoptera and Hemiptera (Harada et al., 2013; Hodek, 2012; Unnithan and Nair, 1977). Thus, it is likely that degrading flight muscle mitochondria during the winter is widespread among other adult diapausing insects. To my knowledge, there are no studies showing metabolic suppression in these other species that appear to degrade flight muscle during diapause. Thus, to test if mitophagy mediates metabolic suppression in other species, we must 1) determine whether other adult insects with apparent flight muscle histolysis also lower their metabolic rate during diapause and 2) identify whether they enhance mitophagy in their flight muscle.

Hypothesis **Shown in Chapter 2** **Shown in Chapter 3**

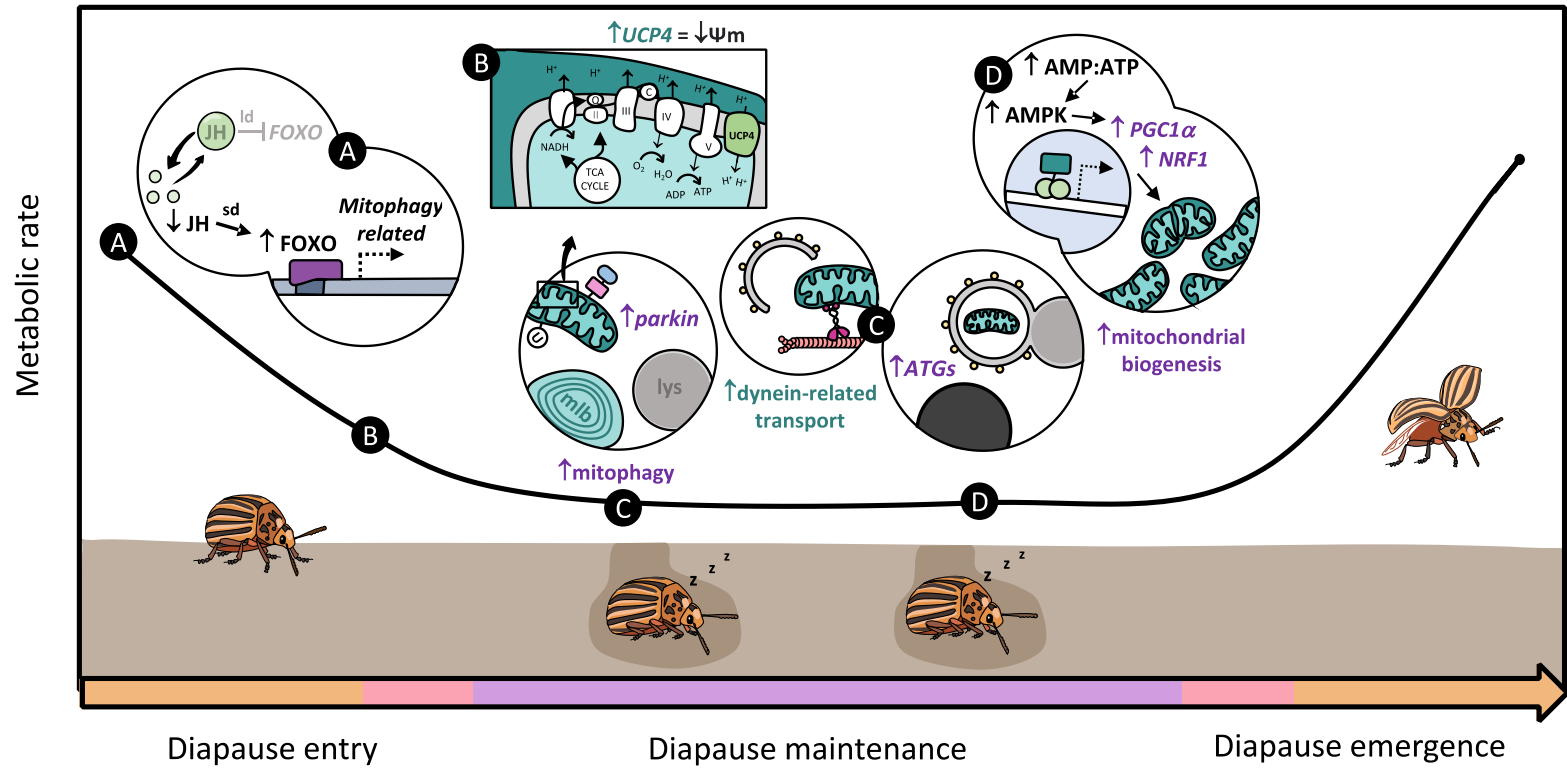


Figure 5.1. Conceptual model of mitophagy-mediated metabolic suppression and reversal of this suppression during diapause in the Colorado potato beetle.

Processes/transcript abundance shown in black are hypotheses, processes/transcript abundance in blue are based on evidence from Chapter 2, and processes/transcript abundance in purple are based on evidence from Chapter 3. (A) In response to short day (sd) conditions, diapause-destined CPB decrease JH signaling which activates FOXO, leading to the transcription of mitophagy-related genes in their flight muscle. (B) In response to an unknown upstream signal, diapause destined CPB increase the expression of *UCP4* in their flight muscle, which decreases the membrane potential of flight muscle mitochondria thus stabilizing PINK1 and Parkin to the outer mitochondrial membrane and initiating mitophagy. (C) During diapause, mitochondria that are tagged for removal are transported to autophagosomes *via* dynein and microtubule-based movement. When autophagosomes fuse with lysosomes (lys), mitochondria are degraded, which results in whole-animal metabolic suppression. (D) Towards the end of diapause (before CPB emerge from their diapause), a lack of mitochondrial ATP production leads to increased AMP: ATP ratios, stimulating AMPK, which activates the transcription of *PGC1 α* and results in mitochondrial biogenesis and the concomitant recovery of metabolic rate.

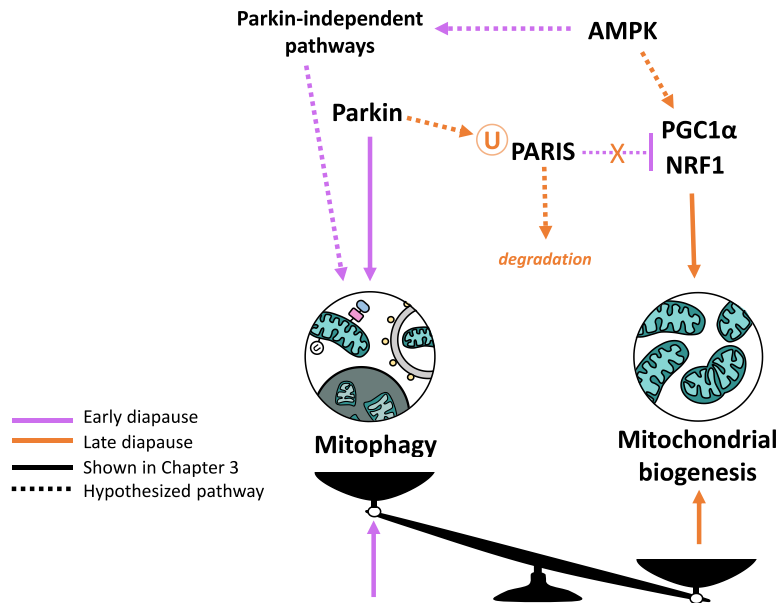


Figure 5.2. Hypothesized regulation of mitochondrial mitophagy and mitochondrial biogenesis by Parkin and AMPK in flight muscle of diapausing Colorado potato beetles. Conceptualized pathway based on information from Chapter 3 and Hang et al. 2015. During early diapause, Parkin initiates mitophagy by tagging mitochondria for autophagic removal. During this time, mitochondrial biogenesis is inhibited by PARIS, a transcription factor which represses the transcription of *PGC1α*. Towards the later stages of diapause, Parkin ubiquitinates PARIS, thereby sending it for proteasomal degradation. *PGC1α* transcription is no longer repressed and can drive the activation of mitochondrial biogenesis and re-establishment of mitochondrial homeostasis. Similarly, AMPK activation of *PGC1α* expression can lead to the activation of mitochondrial biogenesis during late diapause and can also activate mitophagy *via* Parkin-independent pathways in early diapause.

5.1.3 Other testable hypotheses about the mechanisms underlying CPB diapause

In Chapter 2, I presented several hypotheses about how changes in physiology at the tissue level drive whole animal diapause phenotypes. In Chapter 3 I followed up on one of these hypotheses, that flight muscle mitochondria modulate energy metabolism and drive metabolic suppression during diapause. However, I did not have the opportunity to experimentally follow up on any of the other hypotheses that I suggested, and thus there are many outstanding questions about how CPB change their physiology during their diapause maintenance stage, mainly about the role that cell cycle, immunity, and antioxidant-related transcripts play in conferring diapause phenotypes.

For example, we still have a limited understanding of how CPB (and other adult diapausing insects) halt cell cycle progression to arrest their development (Košťál et al., 2009; Tammariello and Denlinger, 1998), and why insects arrest their cell cycles at specific stages (*i.e.*, G1 arrest vs. G2/M arrest). In Chapter 2, I found increased abundance of cell-cycle related transcripts and evidence that CPB arrest their cell cycles at the G2/M transition. I suggest identifying the cell cycle stage at which cells are arrested using flow cytometry (Košťál et al., 2009), and investigate the adaptive mechanisms behind cell cycle arrest at specific stages (Table 5.1). We also do not know how CPB (and other adult diapausing insects) reconfigure their immune system during diapause in anticipation of pathogen stress (Ferguson et al., 2018). In Chapter 2, I found that immunity-related processes were enriched in the fat body of diapausing CPB. Thus, I suggest investigating how CPB immune function changes throughout diapause and use manipulative tools such as RNAi to knockdown immunity-related enzymes and determine the extent to which immunity confers overwinter survival (Table 5.1). I also found that CPB increase the abundance of antioxidant transcripts during diapause (Chapter 2), however there is little evidence showing that CPB (or other diapausing insects) are indeed oxidatively stressed (MacRae, 2010). Thus, we need to determine whether antioxidants mitigate oxidative stress during diapause or help protect insects from ROS damage upon resumption of metabolic rates during diapause termination, when an influx of cellular oxygen is likely to produce ROS and thus damage macromolecules (Table 5.1; Harrison et al., 2018).

Table 5.1. Experiments that test hypothesized mechanisms underlying cell cycle arrest, changes in immunity, and antioxidant capacity in diapausing Colorado potato beetles.

Diapause phenotype	Observation(s) during diapause from Chapter 2	Hypothesis(es)	Experiments	Predictions
Developmental Arrest	↓ <i>cyclin A</i> in fat body ↑ <i>Rad51</i> in fat body	CPB arrest fat body cells at G2 to mitigate and repair DNA damage during diapause	Flow cytometry analysis of fat body cells to determine which cell cycle stage they are arrested at (Košťál et al., 2009)	Fat body cells arrested at G2
			Measure levels of DNA damage in fat body cells throughout diapause using a Comet assay (Lubawy et al. 2019)	↑ DNA damage in non-diapausing fat body cells
			RNAi knockdown of <i>Rad51</i> in diapausing CPB	↑ DNA damage in fat body cells of <i>Rad51</i> knockdown cells
Stress tolerance	↑ <i>Serine proteases</i> in fat body	CPB activate immune responses during diapause to enhance their survival of pathogen stress	Measure phenoloxidase (PO) activity, humoral antimicrobial activity, survival of fungal infections in diapausing CPB (Ferguson and Sinclair, 2017)	↑ PO activity in fat body, ↑ antimicrobial activity in fat body, ↑ survival of fungal infections in diapausing CPB
			RNAi knockdown of <i>Serine protease(s)</i> in diapausing CPB	Compromised immune response in <i>Serine protease</i> knockdown CPB
Stress tolerance	↑ Antioxidants in fat body and flight muscle	Antioxidants repair oxidative damage during diapause/are there for when oxidative damage arises upon resumption of metabolic rate	Measure antioxidant enzyme activity and levels of oxidative stress (<i>i.e.</i> , using MitoB) throughout diapause and upon diapause termination when metabolic rate increases (Torson et al., 2019; Lalouette et al., 2011; Cochemé et al., 2012)	If for oxidative damage during? ↑ oxidative damage in knockdown CPB during diapause
			RNAi knockdown of antioxidants in diapausing CPB, and just before diapause termination	If for oxidative damage upon termination? ↑ oxidative damage in knockdown CPB before termination

5.2 An updated framework for insect cold tolerance: Defining the functional role of the chaperone response

In Chapter 4, I used transcriptomics to investigate the mechanisms underlying cold tolerance in CPB. I expected to find many transcripts differentially expressed, and multiple pathways enriched in cold-tolerant CPB compared to diapausing CPB because there are many physiological changes associated with the acquisition of cold tolerance in insects (Chapter 1). Thus, I was surprised that the major transcriptomic shift I observed between cold-tolerant and diapausing CPB was driven by the differential expression of transcripts related to the chaperone response (Chapter 4). The small transcriptomic shift I observed in Chapter 4 suggests that the chaperone response is essential for sub-zero temperature survival in CPB, and perhaps takes precedence over other physiological changes that could improve their cold tolerance.

5.2.1 A role for chaperone proteins in preparation for and recovery from cold exposure

Based on my observations that cold-tolerant CPB activate the chaperone response, have slightly lower levels of protein damage, appear to repair proteins to a greater extent than diapausing CPB, and can survive better at sub-zero temperatures than less cold-tolerant diapausing CPB (Chapter 4), I propose that the chaperone response plays two roles in conferring cold tolerance in CPB. First, I suggest that the chaperone response prepares cold-tolerant CPB for future cold exposures. Second, I propose that the chaperone response helps cold-tolerant CPB repair fat body proteins after a cold shock. I only measured levels of protein damage in CPB fat body, thus my hypotheses and predictions in this section are based on protein repair in the fat body. However, it is likely that protein repair is important for other tissues in cold-tolerant CPB.

To address my first hypothesis, that the chaperone response prepares cold-tolerant CPB for future cold exposures, we need to consider how fluctuating thermal regimes (FTR) could improve cold tolerance in insects. Exposure to FTRs improves low temperature survival in at least six orders of insects (Colinet et al., 2018), however the mechanisms underlying the beneficial effects of FTRs are not completely understood. The prevailing hypothesis is that insects can use periods of warm temperatures during an FTR to recover from any damage

accrued during cold temperature cycles, which would physiologically prepare them for any subsequent cold exposures (Colinet et al., 2018). I hypothesize that exposure to an FTR in CPB activates the chaperone response so that HSPs can mitigate any protein damage (*via* protein folding) that accrues during early sub-zero temperature phases of the FTR, and thus prepares them for a future sub-zero temperature exposure (Figure 5.3). To further test this hypothesis, I would need to investigate how protein damage changes throughout an FTR exposure. Specifically, I suggest measuring levels of protein damage after each sub-zero temperature cycle. If fluctuating temperatures help drive protein protection in CPB fat body, then I would predict there would be more damage after the first sub-zero temperature cycle compared to the second or third cycle. Further, if activation of the chaperone response is necessary for preparation for cold exposure, then knocking down HSPs before exposure to an FTR using RNAi should prevent CPB from becoming more cold-tolerant.

The second role that the chaperone response could be playing in cold-tolerant CPB is to repair fat body proteins after a cold shock. Proteins risk denaturation when they are exposed to sub-zero temperatures (*i.e.*, during a cold shock) due to the instability of intramolecular hydrophobic interactions at temperatures below 0 °C (Hochachka and Somero, 2002). When proteins are cold-denatured and therefore damaged, cells can initiate protein repair by either re-folding proteins back to their functional conformation *via* HSP-mediated protein folding (reversible protein damage) or disposing of irreversibly damaged proteins through the ubiquitin/proteasome system (Kandasamy and Andreasson, 2018). Because I observed that cold-tolerant CPB lowered protein damage back to pre-cold shock levels, and diapausing CPB had a high level of protein damage throughout exposure to the cold (Chapter 4), I suggest that cold-tolerant CPB have an enhanced capacity to repair proteins from cold-induced damage, compared to diapausing CPB (Figure 5.3). Further, because cold-tolerant CPB activated their chaperone response to a greater extent than diapausing CPB (Chapter 4), I suggest that the role of this activated chaperone response is to repair proteins during recovery from cold shock and facilitate survival.

There are two routes for CPB to deal with protein damage after a cold shock; they can either re-fold reversibly damaged proteins *via* HSP folding or increase their capacity to degrade proteins *via* proteolysis. Indeed, although the primary role of HSPs is to re-fold proteins, HSPs can also stabilize the 26S proteasome thereby enhancing the capacity of cells to

degrade proteins (Reeg et al., 2016). I cannot necessarily distinguish between CPB's capacity to re-fold proteins and their capacity for proteolytic degradation using protein ubiquitination as a proxy for damage, so I suggest conducting further experiments to tease apart the exact mechanisms of protein repair during recovery from a cold shock. I suggest measuring proteasomal activity (*i.e.*, the rate of proteasomal degradation) in fat body of cold-tolerant CPB and predict that if HSPs are indeed stabilizing the proteasome, then cold-tolerant CPB would have higher proteasomal activity during recovery from a cold shock, compared to diapausing CPB (Bartelt et al., 2018). Although it would be difficult to measure rates of protein folding inside fat body cells, I suggest using co-immunoprecipitation and mass spectrometry (Falsone et al., 2005) to try and identify important functional proteins that might be associated with HSPs during recovery. If specific enzymes are associated with HSPs during recovery, then it is likely that HSPs are re-folding them and thus activation of the chaperone response is associated with the repair of unfolded proteins.

In my thesis, I update the current framework of insect cold tolerance by providing some evidence that repairing protein damage improves cold tolerance in insects, something which very few papers investigating HSPs, and insect cold tolerance do. To my knowledge, there is only one study in the last 20 years that has measured how HSPs can prevent protein damage in overwintering insects: increased HSP expression in the Antarctic midge (*Belgica antarctica*) is associated with lower protein aggregation (and thus less protein damage; Rinehart et al., 2006). Moving forward, we need to measure other aspects of protein damage such as protein aggregation, proteolytic capacity, and which proteins HSPs are protecting to fully elucidate how the chaperone response moderates proteostasis and the protection of functionally important proteins at sub-zero temperatures.

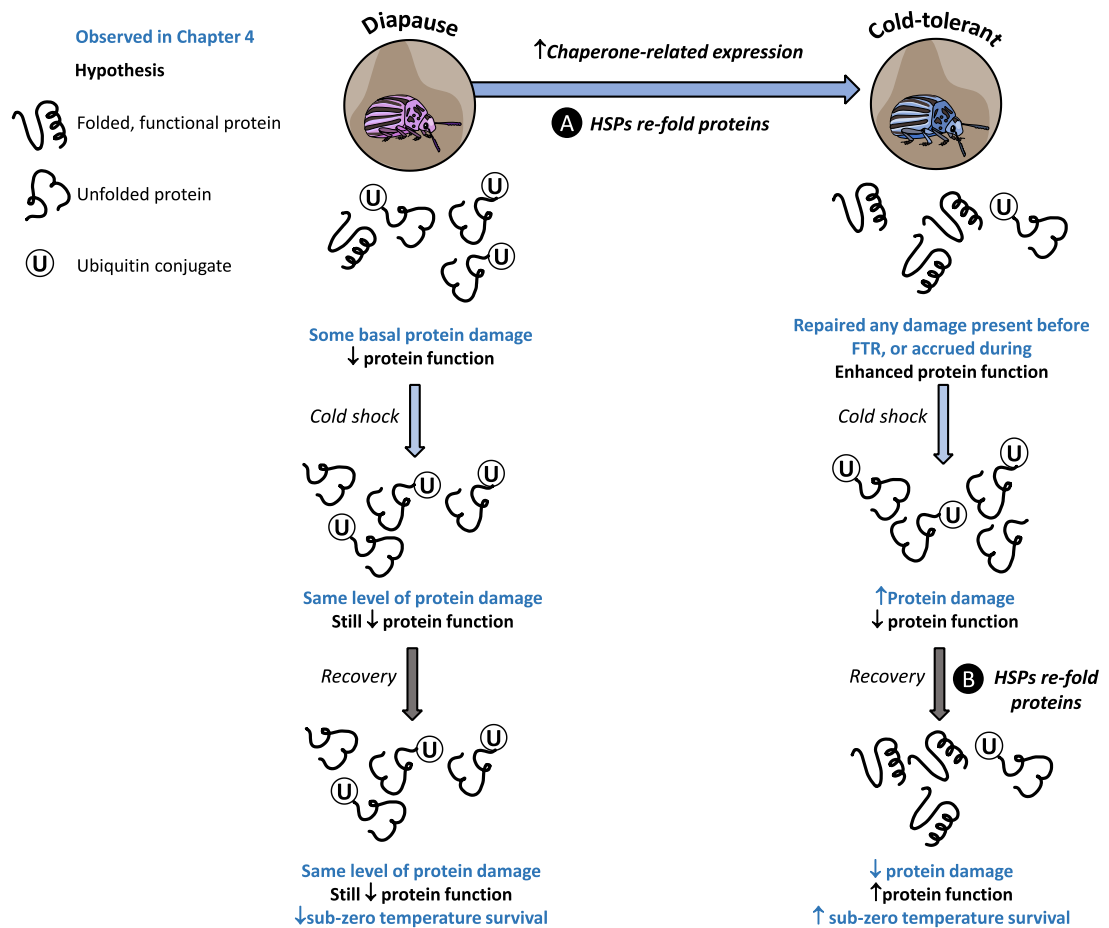


Figure 5.3. Schematic of protein protection by heat shock proteins in cold-tolerant Colorado potato beetles. Cold-tolerant CPB increase the expression of chaperone-related transcripts and based on observations from Chapter 4 I hypothesize that this activation of the chaperone response helps prepare CPB for subsequent cold exposure (A) and helps them repair proteins during recovery from a cold shock (B).

5.3 Disentangling diapause from cold tolerance in CPB

Together, my thesis gives me the opportunity to disentangle the relationship between diapause and cold tolerance in overwintering CPB. Because diapause and cold tolerance coincide in overwintering CPB, CPB are an ideal system for investigating which physiological changes drive diapause, which drive their cold tolerance, and which are shared between the two strategies (Figure 1.1). I primarily used RNA-seq as a broad approach to identify processes that could differ or are shared between diapausing and cold-tolerant CPB. The advantage of using this ‘omics approach is that it allowed me to generate several novel, testable hypotheses about how diapause and cold tolerance are related in CPB. Although I found a large suite of genes and processes that were differentially expressed between diapausing and non-diapausing CPB (Chapter 2), the only biological process separating cold-tolerant CPB from diapausing CPB was activation of the chaperone response (Chapter 4), suggesting that the chaperone response is necessary for cold tolerance but not necessarily part of CPB’s diapause programme. Here I will synthesize my findings and attempt to disentangle the mechanisms of diapause from cold tolerance in the context of the chaperone response.

5.3.1 Differential roles of the chaperone response in diapausing and cold-tolerant CPB

I found that CPB differentially express different families of HSPs in their fat body and flight muscle depending on their physiological state (*i.e.*, during diapause or after acquisition of cold tolerance; Chapters 2 and 4). Specifically, in Chapter 2 I observed that diapausing CPB increase the abundance of *HSP70* in their flight muscle, whereas diapausing CPB do not increase the abundance of any HSPs in their fat body. In Chapter 4 I found that after becoming more cold-tolerant, CPB increased the abundance of several HSPs (*HSP68*, *HSP70*, *DnaJ*, and *protein (2) lethal essential for life*) in their fat body and activated their chaperone response as a result. Given that HSPs are differentially expressed in the flight muscle and fat body, I posit that HSPs therefore play different roles in the flight muscle during diapause, and in the fat body to prepare for cold exposure.

Colorado potato beetle flight muscle shifts its mitochondrial homeostasis during diapause (Chapter 3), and as a result proteostasis, because most mitochondrial proteins are degraded.

To my knowledge, mitochondrial proteins are not degraded in fat body to the same extent as flight muscle. For example, there were no major changes in mitochondrial-related transcript abundance in the fat body during diapause (Chapter 2), thus it is unlikely that fat body undergoes mitophagy to the same extent as flight muscle during diapause. Because *HSP70* was only differentially expressed in CPB flight muscle (and not the fat body) during diapause I suggest that *HSP70* is involved in this shift in mitochondrial homeostasis, rather than expressed to mitigate cold-induced damage during diapause. Indeed, HSP70 has many functions, some of which are not directly involved in refolding proteins damaged by temperature stress (Rosenzweig et al., 2019). Heat shock protein 70 can help regulate mitophagy; HSP70 is part of a complex of proteins which stabilize PINK1 to the outer mitochondrial membrane, which leads to Parkin recruitment and activation of the mitophagy pathway (Zheng et al., 2018). Thus, I hypothesize that in CPB flight muscle during diapause, HSP70 is involved in the initiation of mitophagy. To test this, I suggest using co-immunoprecipitation to identify whether HSP70 and PINK1 interact in diapausing CPB flight muscle (Zheng et al., 2018). Further, if HSP70 helps stabilize PINK1 and is necessary for mitophagy initiation, then knocking down HSP70 using RNAi should prevent or reduce mitophagy in diapausing CPB flight muscle.

After becoming more cold-tolerant, diapausing CPB increased the abundance of several *HSPs* and activated the chaperone response (Chapter 4). Because activation of the chaperone response coincides with reduced protein damage in cold-tolerant CPB, I suggest that (in the context of cold tolerance) *HSPs* rescue proteins from cold-induced damage (Section 5.2.1). Colorado potato beetles did not increase the abundance of any *HSPs* or activate their chaperone response in their fat body during diapause (Chapter 2). Taken together, this suggests that the chaperone response is only important for fat body cells after a cold exposure and in preparation for future exposure, and not necessary for diapause. The importance of the chaperone response in cold tolerance independently of diapause has been similarly observed in other diapausing insects; for example, *S. crassipalpis* increase the abundance of HSP23 and HSP70 over the winter, but *HSPs* are only necessary for their low-temperature survival, not for regulating their decision to enter diapause, or the duration of their diapause (Rinehart et al., 2007). My work adds to this body of literature and provides evidence that *HSPs* can

play a larger role in protecting cells from the cold rather than conferring diapause phenotypes, at least in the fat body.

I suggest that HSPs play a more diverse role in diapause and cold tolerance than just re-folding proteins that have been denatured at low temperatures. HSPs are involved in several cellular processes that do not necessarily involve the direct repair and protection of proteins. For example, HSPs can help translocate polypeptides across cell membranes (Gambill et al., 1993), regulate conformational changes of signaling proteins (Martin and Hartl, 1997), and help clear cell waste through chaperone-mediated autophagy (Arndt et al., 2010). To my knowledge, these alternative roles of chaperone proteins (that do not involve re-folding of cold-denatured proteins) have never been investigated in diapausing and cold-tolerant insects. Here, I show that HSPs can exhibit different functions based on the physiological state of the organism; During diapause when CPB are energetically stressed, any chaperone-related expression could help initiate mitophagy and therefore drive metabolic suppression (Chapter 2, 3). Alternatively, when exposed to sub-zero temperatures, chaperone-related expression could help protect proteins and repair cold-induced damage (Chapter 4). Thus, although I cannot fully disentangle the mechanisms driving diapause and cold tolerance during diapause in CPB, I provide evidence that activation of the chaperone response in CPB fat body is only necessary for cold tolerance, and not for diapause.

5.4 Concluding remarks

In my thesis, I provide answers for two outstanding questions about insect diapause and cold tolerance: 1) how diapausing insects modulate their metabolism during diapause and 2) how cold-tolerant insects protect their cells from sub-zero temperatures.

First, metabolic suppression, and reversal of this suppression, can be achieved in a diapausing insect by degrading and re-growing flight muscle mitochondria. While most other dormant animals “turn down” their mitochondria, diapausing CPB appear to “turn off” their mitochondria by degrading them altogether. Furthermore, CPB have the ability to re-grow their flight muscle mitochondrial pools in anticipation of increased energy demand in the spring, which shows that some insects have a remarkable capacity to modulate their mitochondrial homeostasis in the face of energetic stress during the winter.

Second, CPB appear to protect their cells from sub-zero temperatures by activating the chaperone response and inducing HSP expression. This is the first study linking increased HSP expression to reduced protein damage in a metabolically important tissue in insects and raises new questions about the relative importance of the chaperone response in conferring insect cold tolerance.

Lastly, although my thesis provides new and exciting insights into the mechanisms of overwinter survival in CPB and other temperate insects, it is clear that there is plenty of work to be done to gain a clearer understanding of diapause and cold tolerance. In particular, my work sheds light on some of the cellular aspects of diapause and cold tolerance. I hope that the field of insect overwintering physiology can move towards using cell systems to address questions about diapause and cold tolerance (*i.e.*, Teets et al., 2008; Zhang et al., 2017), to understand how changes at the cellular level drive whole animal overwinter survival.

5.5 References

- Alves-Bezerra, M., Cosentino-Gomes, D., Vieira, L.P., Rocco-Machado, N., Gondim, K.C., Meyer-Fernandes, J.R.** (2014). Identification of uncoupling protein 4 from the blood-sucking insect *Rhodnius prolixus* and its possible role on protection against oxidative stress. *Insect Biochemistry and Molecular Biology* **50**, 24-33.
- Arndt, V., Dick, N., Tawo, R., Dreiseidler, M., Wenzel, D., Hesse, M., Fürst, D.O., Saftig, P., Saint, R., Fleischmann, B.K.** (2010). Chaperone-assisted selective autophagy is essential for muscle maintenance. *Current Biology* **20**, 143-148.
- Audesse, A.J., Dhakal, S., Hassell, L.-A., Gardell, Z., Nemtsova, Y., Webb, A.E.** (2019). FOXO3 directly regulates an autophagy network to functionally regulate proteostasis in adult neural stem cells. *PLoS Genetics* **15**, e1008097.
- Bakula, D., Scheibye-Knudsen, M.** (2020). MitophAging: Mitophagy in aging and disease. *Frontiers in Cell and Developmental Biology* **8**, 239.
- Bartelt, A., Widenmaier, S.B., Schlein, C., Johann, K., Goncalves, R.L.S., Eguchi, K., Fischer, A.W., Parlakgöl, G., Snyder, N.A., Nguyen, T.B.** (2018) Brown adipose tissue thermogenic adaptation requires Nrf1-mediated proteasomal activity. *Nature Medicine* **24**, 292-303.
- Batlevi, Y., Martin, D.N., Pandey, U.B., Simon, C.R., Powers, C.M., Taylor, J.P., Baehrecke, E.H.** (2010). Dynein light chain 1 is required for autophagy, protein clearance, and cell death in *Drosophila*. *Proceedings of the National Academy of Sciences of the U.S.A.* **107**, 742-747.
- Chen, C., Mahar, R., Merritt, M.E., Denlinger, D.L., Hahn, D.A.** (2020). ROS and hypoxia signaling regulate periodic metabolic arousal during insect dormancy to coordinate glucose, amino acid, and lipid metabolism. *Proceedings of the National Academy of Sciences of the U.S.A.* **118**, e2017603118.
- Cho, I., Song, H.-O., Cho, J.H.** (2017). Mitochondrial uncoupling attenuates age-dependent neurodegeneration in *C. elegans*. *Molecules and Cells* **40**, 864.
- Cochemé, H.M., Logan, A., Prime, T.A., Abakumova, I., Quin, C., McQuaker, S.J., Patel, J.V., Fearnley, I.M., James, A.M., Porteous, C.M., Smith, R.A.J., Hartley, R.C., Partridge, L., Murphy, M.P.** (2012). Using the mitochondria-targeted radiometric mass spectrometry probe MitoB to measure H₂O₂ in living *Drosophila*. *Nature Protocols* **7**, 946-958.
- Colinet, H., Rinhart, J.P., Yocum, G.D., Greenlee, K.J.** (2018). mechanisms underpinning the beneficial effects of fluctuating thermal regimes in insect cold tolerance. *Journal of Experimental Biology* **221**, jeb164806.
- De Kort, C., Bergot, B., Schooley, D.** (1982). The nature and titre of juvenile hormone in the Colorado potato beetle, *Leptinotarsa decemlineata*. *Journal of Insect Physiology* **28**, 471-474.

- Falsone, S.F., Gesslbauer, D., Tirk, F., Piccinini, A.-M., Kungl, A.J.** (2005). A proteomic snapshot of the human heat shock protein 90 interactome. *FEBS Letters* **579**, 6350-6354.
- Ferguson, L.V., Kortet, R., Sinclair, B.J.** (2018). Eco-immunology in the cold: the role of immunity in shaping the overwintering survival of ectotherms. *Journal of Experimental Biology* **221**, jeb163873.
- Ferguson, L.V., Sinclair, B.J.** (2017). Insect immunity varies idiosyncratically during overwintering. *Journal of Experimental Zoology Part A: Ecological and Integrative Physiology* **327**, 222-234.
- Gambill, B.D., Voos, W., Kang, P.J., Miao, B., Langer, T., Craig, E.A., Pfanner, N.** (1993). A dual role for mitochondrial heat shock protein 70 in membrane translocation of preproteins. *Journal of Cell Biology* **123**, 109-117.
- Harada, T., Inoue, S., Watanabe, M.** (2013). Effects of low temperature on the condition of flight muscles and flight propensity in a water strider, *Aquarius paludum* (Heteroptera: Gerridae). *European Journal of Entomology* **100**, 481-484.
- Hardie, D.G., Ross, F.A., Hawley, S.A.** (2012). AMPK: a nutrient and energy sensor that maintains energy homeostasis. *Nature Reviews Molecular Cell Biology* **13**, 251-262.
- Harrison, J.F., Greenlee, K.J., Verberk, W.C.** (2018). Functional hypoxia in insects: definition, assessment, and consequences for physiology, ecology, and evolution. *Annual Review of Entomology* **63**, 303-325.
- Hochachka, P.W., Somero, G.N.** (2002). Temperature. In *Biochemical adaptation: mechanism and process in physiological evolution*. pp. 290-451. Oxford university press.
- Hodek, I.** (2011). Adult diapause in Coleoptera. *Psyche: A Journal of Entomology* **2012**, 10111011.
- Jäger, S., Handschin, C., Pierre, J.S.-., Spiegelman, B.M.** (2007). AMP-activated protein kinase (AMPK) action in skeletal muscle via direct phosphorylation of PGC-1 α . *Proceedings of the National Academy of Sciences of the U.S.A* **104**, 12017-12022.
- Jin, S.M., Youle, R.J.** (2012). PINK1-and Parkin-mediated mitophagy at a glance. *Journal of Cell Science* **125**, 795-799.
- Kandasamy, G. and Andreasson, C.** (2018). Hsp70-Hsp110 chaperones deliver ubiquitin-dependent and independent substrates to the 26s proteasome for proteolysis in yeast. *Journal of Cell Science* **131**, jsc10948.
- Košťál, V., Šimůnková, P., Kobelková, A., Shimada, K.** (2009). Cell cycle arrest as a hallmark of insect diapause: changes in gene transcription during diapause induction in the drosophilid fly, *Chymomyza costata*. *Insect Biochemistry and Molecular Biology* **39**, 875-883.

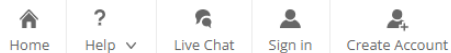
- Krumschnabel, G., Eigentler, A., Fasching, M., Gnaiger, E.** (2014). Use of safranin for the assessment of mitochondrial membrane potential by high-resolution respirometry and fluorometry. *Methods in Enzymology* **542**, 163-181.
- Lane, S.J., Frankino, W.A., Elekonich, M.W., Roberst, S.P.** (2014). The effects of age and lifetime light behaviour on flight capacity in *Drosophila melanogaster*. *Journal of Experimental Biology*, **217**, 1437-1443.
- Lehmann, P., Piironen, S., Kankare, M., Lyytinen, A., Paljakka, M., Lindström, L.** (2014). Photoperiodic effects on diapause-associated gene expression trajectories in European *Leptinotarsa decemlineata* populations. *Insect Molecular Biology* **23**, 566-578.
- Lubawy, J., Daburon, V., Chowański, S., Słocińska, M., Colinet, H.** (2019). Thermal stress causes DNA damage and mortality in a tropical insect. *Journal of Experimental Biology* **23**, jeb213744.
- MacRae, T.H.** (2010). Gene expression, metabolic regulation and stress tolerance during diapause. *Cellular and Molecular Life Sciences* **67**, 2405-2424.
- Mathers, K.E., Staples, J.F.** (2019). Differential posttranslational modification of mitochondrial enzymes corresponds with metabolic suppression during hibernation. *American Journal of Physiology* **317**, R262-R269.
- Martin, J., Hartl, F.U.** (1997). Chaperone-assisted protein folding. *Current Opinion in Structural Biology* **7**, 41-52.
- Mei, Y., Zhang, Y., Yamamoto, K., Xie, W., Mak, T.W., You, H.** (2009). FOXO3a-dependent regulation of Pink1 (Park6) mediates survival signaling in response to cytokine deprivation. *Proceedings of the National Academy of Sciences of the U.S.A.* **106**, 5153-5158.
- Narendra, D.P., Jin, S.M., Tanaka, A., Suen, D.-F., Gautier, C.A., Shen, J., Cookson, M.R., Youle, R.J.** (2010). PINK1 is selectively stabilized on impaired mitochondria to activate Parkin. *PLoS Biology* **8**, e1000298.
- Palikaras, K., Lionaki, E., Tavernarakis, N.** (2015). Coordination of mitophagy and mitochondrial biogenesis during ageing in *C. elegans*. *Nature* **521**, 525-528.
- Peferoen, M., Huybrechts, R., De Loof, A.** (1981) Longevity and fecundity in the Colorado potato beetle, *Leptinotarsa decemlineata*. *Entomologia Experimentalis et Applicata* **29**, 321-329.
- Rana, A., Rera, M., Walker, D.W.** (2013). Parkin overexpression during aging reduces proteotoxicity, alters mitochondrial dynamics, and extends lifespan. *Proceedings of the National Academy of Sciences of the U.S.A.* **110**, 8638-8643.

- Ravikumar, B., Acevedo-Arozena, A., Imarisio, S., Berger, Z., Vacher, C., O'Kane, C.J., Brown, S.D., Rubinsztein, D.C.** (2005). Dynein mutations impair autophagic clearance of aggregate-prone proteins. *Nature Genetics* **37**, 771-776.
- Reck-Peterson, S.L., Redwine, W.B., Vale, R.D., Carter, A.P.** (2018). The cytoplasmic dynein transport machinery and its many cargoes. *Nature Reviews Molecular Cell Biology* **19**, 382-398.
- Reczek, C.R., Chandel, N.S.** (2015). ROS-dependent signal transduction. *Current Opinion in Cell Biology* **33**, 8-13.
- Reeg, S., Jung, T., Castro, J.P., Davies, K.J.A., Henze, A., Grune, T.** (2016) The molecular chaperone Hsp70 promotes the proteolytic removal of oxidatively damaged proteins by the proteasome. *Free Radical Biology and Medicine* **99**, 153-166.
- Rinehart, J.P., Li, A., Yocum, G.D., Robich, R.M., Hayward, S.A., Denlinger, D.L.,** (2007). Up-regulation of heat shock proteins is essential for cold survival during insect diapause. *Proceedings of the National Academy of Sciences of the U.S.A.* **104**, 11130-11137.
- Romanello, V., Sandri, M.** (2015). Mitochondrial quality control and muscle mass maintenance. *Frontiers in Physiology* **6**, 42.
- Rosenzweig, R., Nillegoda, N.B., Mayer, M.P., Bukau, B.** (2019). The Hsp70 chaperone network. *Nature Reviews Molecular Cell Biology* **20**, 665-680.
- Sim, C., Denlinger, D.L.** (2008). Insulin signaling and FOXO regulate the overwintering diapause of the mosquito *Culex pipiens*. *Proceedings of the National Academy of Sciences of the U.S.A.* **105**, 6777-6781.
- Sim, C., Kang, D.S., Kim, S., Bai, X., Denlinger, D.L.** (2015). Identification of FOXO targets that generate diverse features of the diapause phenotype in the mosquito *Culex pipiens*. *Proceedings of the National Academy of Sciences of the U.S.A.* **112**, 3811-3816.
- Sokolova, I., Sokolov, E.** (2005). Evolution of mitochondrial uncoupling proteins: novel invertebrate UCP homologues suggest early evolutionary divergence of the UCP family. *FEBS Letters* **579**, 313-317.
- Staples, J.F.** (2016). Metabolic Flexibility: Hibernation, Torpor, and Estivation. *Comprehensive Physiology* **6**, 737-771.
- Tammariello, S.P., Denlinger, D.L.** (1998). G0/G1 cell cycle arrest in the brain of *Sarcophaga crassipalpis* during pupal diapause and the expression pattern of the cell cycle regulator, proliferating cell nuclear antigen. *Insect Biochemistry and Molecular Biology* **28**, 83-89.
- Tauber, M.J., Tauber, C.A.** (1976). Insect seasonality: diapause maintenance, termination, and postdiapause development. *Annual Review of Entomology* **21**, 81-107.

- Unnithan, G., Nair, K.** (1977). Ultrastructure of juvenile hormone-induced degenerating flight muscles in a bark beetle, *Ips paraconfusus*. *Cell and Tissue Research* **185**, 481-490.
- Vives-Bauza, C., Zhou, C., Huang, Y., Cui, M., De Vries, R.L., Kim, J., May, J., Tocilescu, M.A., Liu, W., Ko, H.S.** (2010). PINK1-dependent recruitment of Parkin to mitochondria in mitophagy. *Proceedings of the National Academy of Sciences of the U.S.A.* **107**, 378-383.
- Zhang, X-S., Wang, T., Lin, X-W., Denlinger, D.L., Xu, W-H.** (2017). Reactive oxygen species extend insect life span using components of the insulin signaling pathway. *Proceedings of the National Academy of Sciences of the United States of America* **114**, E7832-E7840.
- Zheng, Q., Huang, C., Guo, J., Tan, J., Wang, C., Tang, B., Zhang, H.** (2018). Hsp70 participates in PINK1-mediated mitophagy by regulating the stability of PINK1. *Neuroscience Letters* **662**, 264-270.

Appendices

Appendix A: Chapter 2 Supplementary Material



Diapause differentially modulates the transcriptomes of fat body and flight muscle in the Colorado potato beetle

Author: Jacqueline E. Lebenzon, Alex S. Torson, Brent J. Sinclair

Publication: Comparative Biochemistry and Physiology Part D: Genomics and Proteomics

Publisher: Elsevier

Date: December 2021

© 2021 Elsevier Inc. All rights reserved.

Journal Author Rights

Please note that, as the author of this Elsevier article, you retain the right to include it in a thesis or dissertation, provided it is not published commercially. Permission is not required, but please ensure that you reference the journal as the original source. For more information on this and on your other retained rights, please visit: <https://www.elsevier.com/about/our-business/policies/copyright#Author-rights>

BACK

CLOSE WINDOW

Table A1. Summary of the paired-end read libraries mapped to the *Leptinotarsa decemlineata* reference genome

Biological replicate	Total raw reads after filtering	Mapped reads	Overall alignment rate	Concordant alignment rate (uniquely mapped reads)
<i>Control</i>				
Fat body A	73,802,496	64,481,241	87.37 %	79.84 %
Fat body B	78,479,262	68,669,354	87.50 %	80.04 %
Fat body C	68,483,160	59,573,501	86.99 %	79.38 %
Flight muscle A	57,241,508	49,428,042	86.35 %	78.67 %
Flight muscle B	78,425,350	68,951,568	87.92 %	80.95 %
Flight muscle C	95,680,314	81,835,363	85.53 %	77.46 %
<i>Diapause</i>				
Fat body A	68,811,264	59,459,813	86.41 %	78.79 %
Fat body B	93,066,552	80,474,648	86.47 %	78.70 %
Fat body C	84,212,800	73,029,340	86.72 %	79.05 %
Flight muscle A	67,631,964	59,428,207	87.87 %	81.17 %
Flight muscle B	111,920,498	97,124,608	86.78 %	78.92 %
Flight muscle C	69,072,388	59,837,410	86.63 %	78.97 %
<i>Average</i>	78,902,296	39,913,605	86.88 %	79.33 %

Each treatment and tissue had three biological replicates, and each replicate is represented by a different letter (A, B or C)

Table A2. Differential expression of selected insulin signaling-related transcripts in body (FB) and flight muscle (FM) tissue of *L. decemlineata* during diapause. Fold change values represent increased or decreased abundance of transcripts (adjusted *p*-value of <0.05) during diapause compared to a non-diapausing control. ns indicates where expression values were deemed non-significant according to differential gene expression analysis in DEseq2.

Sequence ID	Sequence Description	Fat body		Flight muscle	
		Log ₂ fold change	Adjusted <i>p</i> value	Log ₂ fold change	Adjusted <i>p</i> value
LDEC004651-RA	insulin-like peptide 7	ns	ns	ns	ns
LDEC014334-RA	insulin-like peptide receptor	ns	ns	ns	ns
LDEC000139-RA	insulin-like peptide 1b	ns	ns	ns	ns
LDEC004651-RA	insulin-like peptide 7	ns	ns	ns	ns
LDEC014333-RA	insulin-like peptide receptor	ns	ns	ns	ns
LDEC011405-RA	forkhead box protein O isoform X1	ns	ns	ns	ns
LDEC019686-RA	forkhead box protein D3-like	ns	ns	ns	ns
LDEC008079-RA	forkhead box protein K1 isoform X2	ns	ns	ns	ns
LDEC000454-RA	forkhead box protein C1	ns	ns	ns	ns
LDEC012842-RA	forkhead box protein F1-like	ns	ns	ns	ns
LDEC013193-RA	forkhead box protein N3 isoform X1	ns	ns	ns	ns
LDEC022522-RA	fork head domain-containing protein FD2-like	ns	ns	ns	ns
LDEC010990-RA	fork head transcription factor 1	ns	ns	ns	ns
LDEC014040-RA	forkhead box protein N5 isoform X4	ns	ns	ns	ns
LDEC021284-RA	fork head domain-containing protein crocodile	ns	ns	ns	ns
LDEC009460-RA	forkhead box protein P1 isoform X2	ns	ns	ns	ns
LDEC011405-RA	forkhead box protein O isoform X1	ns	ns	ns	ns
LDEC004602-RA	serine/threonine-protein kinase mTOR	ns	ns	ns	ns
LDEC013666-RA	rapamycin-insensitive companion of mTOR	ns	ns	ns	ns
LDEC010448-RA	target of rapamycin complex subunit Ict8	ns	ns	ns	ns
LDEC018254-RA	regulator complex protein LAMTOR4 homolog	ns	ns	ns	ns
LDEC004604-RA	serine/threonine-protein kinase mTOR	ns	ns	ns	ns

Sequence ID	Sequence Description	Fat body		Flight muscle	
		Log ₂ fold change	Adjusted <i>p</i> value	Log ₂ fold change	Adjusted <i>p</i> value
LDEC009167-RA	regulatory-associated protein of mTOR isoform X2	ns	ns	ns	ns
LDEC004603-RA	target of rapamycin	ns	ns	ns	ns
LDEC024369-RA	serine/threonine-protein kinase mTOR	ns	ns	ns	ns
LDEC004022-RA	regulator complex protein LAMTOR3 homolog	ns	ns	ns	ns
LDEC008436-RA	regulator complex protein LAMTOR5	ns	ns	ns	ns
LDEC008936-RA	regulator complex protein LAMTOR2 homolog	ns	ns	ns	ns
LDEC009169-RA	Regulatory-associated protein of mTOR	ns	ns	ns	ns
LDEC004090-RA	regulator complex protein LAMTOR3 homolog	ns	ns	ns	ns
LDEC009168-RA	regulatory-associated protein of mTOR	ns	ns	ns	ns
LDEC014193-RA	fushi tarazu	ns	ns	ns	ns

Table A3. Differential expression of selected juvenile hormone metabolism-related transcripts in body (FB) and flight muscle (FM) tissue of *L. decemlineata* during diapause. Fold change values represent increased or decreased abundance of transcripts (adjusted *p*-value of <0.05) during diapause compared to a non-diapausing control. ns indicates where expression values were deemed non-significant according to differential gene expression analysis in DEseq2

Sequence ID	Sequence Description	Fat body		Flight muscle	
		Log ₂ fold change	Adjusted <i>p</i> value	Log ₂ fold change	Adjusted <i>p</i> value
LDEC020560-RA	juvenile hormone acid O-methyltransferase-like	ns		ns	
LDEC014960-RA	juvenile hormone acid O-methyltransferase-like	ns		ns	
LDEC011641-RA	juvenile hormone esterase-like	ns		ns	
LDEC011293-RA	juvenile hormone binding protein 5p2	ns		ns	
LDEC009486-RA	juvenile hormone binding protein 5p1	ns		ns	
LDEC009487-RA	juvenile hormone binding protein 5p2	ns		ns	
LDEC009488-RA	juvenile hormone binding protein 3p2	ns		-4.5	<0.001
LDEC006589-RA	juvenile hormone acid O-methyltransferase-like	ns		ns	
LDEC006587-RA	juvenile hormone acid O-methyltransferase-like	ns		ns	
LDEC012576-RA	juvenile hormone esterase-like	ns		ns	
LDEC013097-RA	juvenile hormone esterase-like	ns		ns	
LDEC017830-RA	putative juvenile hormone-inducible protein	ns		ns	
LDEC006590-RA	juvenile hormone acid O-methyltransferase-like	ns		ns	
LDEC004294-RA	putative juvenile hormone-inducible protein	ns		ns	
LDEC004291-RA	putative juvenile hormone-inducible protein	ns		ns	
LDEC004293-RA	putative juvenile hormone-inducible protein	ns		-2.53	0.05
LDEC004292-RA	putative juvenile hormone-inducible protein	ns		ns	
LDEC006810-RA	juvenile hormone esterase-like	2.7	0.02		
LDEC004313-RA	putative juvenile hormone-inducible protein	ns		ns	
LDEC009130-RA	juvenile hormone acid O-methyltransferase-like	ns		ns	
LDEC020561-RA	juvenile hormone acid O-methyltransferase-like	ns		ns	
LDEC020562-RA	juvenile hormone acid O-methyltransferase-like	ns		ns	

Sequence ID	Sequence Description	Fat body		Flight muscle	
		Log ₂ fold change	Adjusted <i>p</i> value	Log ₂ fold change	Adjusted <i>p</i> value
LDEC020564-RA	juvenile hormone acid O-methyltransferase-like	-1.8	<0.001	ns	
LDEC020565-RA	juvenile hormone acid O-methyltransferase-like	2.3	0.05	ns	
LDEC020664-RA	juvenile hormone esterase-like	ns		ns	
LDEC015319-RA	juvenile hormone esterase-like	ns		ns	
LDEC010859-RA	juvenile hormone epoxide hydrolase 1-like	ns		ns	
LDEC023596-RA	juvenile hormone acid O-methyltransferase-like	4.1	<0.001	3.56	0.01
LDEC023595-RA	juvenile hormone acid O-methyltransferase-like	ns		ns	
LDEC000210-RA	juvenile hormone esterase-like	ns		ns	

Table A4. Differential expression of selected cell cycle arrest-related transcripts in body (FB) and flight muscle (FM) tissue of *L. decemlineata* during diapause. Fold change values represent increased or decreased abundance of transcripts (adjusted *p*-value of <0.05) during diapause compared to a non-diapausing control. ns indicates where expression values were deemed non-significant according to differential gene expression analysis in DEseq2.

Sequence ID	Sequence description	Fat body		Flight muscle	
		Log ₂ fold change	Adjusted <i>p</i> value	Log ₂ fold change	Adjusted <i>p</i> value
LDEC005366-RA	cyclin-dependent kinases regulatory subunit	ns	ns	ns	ns
LDEC023506-RA	cyclin-dependent kinase 12	ns	ns	ns	ns
LDEC007360-RA	nuclear receptor corepressor 1	ns	ns	ns	ns
LDEC000674-RA	cyclin-dependent kinase 4 isoform X2	ns	ns	ns	ns
LDEC003406-RA	cyclin-Y-like protein 1	ns	ns	ns	ns
LDEC008318-RA	cyclin-dependent kinase 1	ns	ns	ns	ns
LDEC000277-RA	cyclin-dependent kinase inhibitor 1C-like	ns	ns	ns	ns
LDEC000276-RA	cyclin-dependent kinase inhibitor 1-like	ns	ns	ns	ns
LDEC012463-RA	cyclin-dependent kinase 7	ns	ns	ns	ns
LDEC017465-RA	cyclin-dependent kinase 9	ns	ns	ns	ns
LDEC010974-RA	cyclin-dependent kinase 12 isoform X1	ns	ns	ns	ns
LDEC012239-RA	cyclin-dependent kinase 9	ns	ns	ns	ns
LDEC012238-RA	cyclin-dependent kinase 9	ns	ns	ns	ns
LDEC004266-RA	cyclin-dependent kinase 8	ns	ns	ns	ns
LDEC015878-RA	cyclin-dependent kinase 14 isoform X1	ns	ns	ns	ns
LDEC007340-RA	cyclin-J-like protein isoform X2	ns	ns	ns	ns
LDEC007424-RA	G2/mitotic-specific cyclin-B3	ns	ns	ns	ns
LDEC002575-RA	cyclin-L1	-1.3	<0.001	ns	ns
LDEC002574-RA	cyclin-L1 isoform X2	ns	ns	ns	ns
LDEC010973-RA	Cyclin-dependent kinase 12	ns	ns	ns	ns
LDEC012237-RA	cyclin-dependent kinase 9	-1.3	0.008	ns	ns
LDEC015089-RA	cyclin-dependent kinase 2-like	ns	ns	ns	ns

Sequence ID	Sequence description	Fat body		Flight muscle	
		Log ₂ fold change	Adjusted <i>p</i> value	Log ₂ fold change	Adjusted <i>p</i> value
LDEC008225-RA	G2/mitotic-specific cyclin-B-like	ns	ns	ns	ns
LDEC008224-RA	G2/mitotic-specific cyclin-B-like	ns	ns	ns	ns
LDEC016625-RA	cyclin-dependent kinase 2-interacting protein	ns	ns	ns	ns
LDEC008222-RA	G2/mitotic-specific cyclin-B-like	ns	ns	ns	ns
LDEC010264-RA	cyclin-dependent kinases regulatory subunit	ns	ns	ns	ns
LDEC012071-RA	cyclin-T isoform X2	ns	ns	ns	ns
LDEC021255-RA	G1/S-specific cyclin-D2-like	ns	ns	ns	ns
LDEC000073-RA	cyclin-dependent kinase 10	ns	ns	ns	ns
LDEC005984-RA	cyclin-dependent kinase 5 activator 1	ns	ns	ns	ns
LDEC005985-RA	cyclin-dependent kinase 5 activator 1	ns	ns	ns	ns
LDEC003879-RA	G2/mitotic-specific cyclin-B3	ns	ns	ns	ns
LDEC005525-RA	G1/S-specific cyclin-D2	ns	ns	ns	ns
LDEC008989-RA	Cyclin-dependent kinase 1-like Protein	2.2	<0.001	1.7	0.003
LDEC003008-RA	cyclin-like protein	ns	ns	ns	ns
LDEC005524-RA	G1/S-specific cyclin-D2	ns	ns	ns	ns
LDEC020738-RA	cyclin-dependent-like kinase 5	ns	ns	ns	ns
LDEC002786-RA	cyclin-dependent kinase 20	ns	ns	ns	ns
LDEC001498-RA	S phase cyclin A-associated protein in the ER	ns	ns	ns	ns
LDEC001497-RA	S phase cyclin A-associated protein in the ER	ns	ns	ns	ns
LDEC001496-RA	S phase cyclin A-associated protein in the ER isoform X2	ns	ns	ns	ns
LDEC010431-RA	cyclin-G-associated kinase	ns	ns	ns	ns
LDEC008590-RA	G2/mitotic-specific cyclin-A	ns	ns	ns	ns
LDEC014448-RA	cyclin-C	ns	ns	ns	ns
LDEC019776-RA	G2/mitotic-specific cyclin-B-like	ns	ns	ns	ns
LDEC000641-RA	cyclin-related protein FAM58A	ns	ns	ns	ns
LDEC019423-RA	G2/mitotic-specific cyclin-B-like	ns	ns	ns	ns
LDEC021397-RA	G2/mitotic-specific cyclin-B-like	ns	ns	ns	ns

Sequence ID	Sequence description	Fat body		Flight muscle	
		Log ₂ fold change	Adjusted <i>p</i> value	Log ₂ fold change	Adjusted <i>p</i> value
LDEC008226-RA	G2/mitotic-specific cyclin-B-like	ns	ns	ns	ns
LDEC005600-RA	cyclin-dependent kinase 12-like	ns	ns	ns	ns
LDEC007604-RA	G2/mitotic-specific cyclin-B-like	ns	ns	ns	ns
LDEC022714-RA	G2/mitotic-specific cyclin-B-like	ns	ns	ns	ns
LDEC022715-RA	G2/mitotic-specific cyclin-B-like	ns	ns	ns	ns
LDEC001499-RA	S phase cyclin A-associated protein in the ER	ns	ns	ns	ns
LDEC014449-RA	cyclin-C	1.0	0.003	ns	ns
LDEC003103-RA	G2/mitotic-specific cyclin-A	-1.5	0.02	ns	ns
LDEC003104-RA	G2/mitotic-specific cyclin-A	-1.8	0.009	ns	ns
LDEC008957-RA	cyclin-dependent kinase 2-associated protein 1	ns	ns	ns	ns
LDEC014322-RA	proliferating cell nuclear antigen	ns	ns	ns	ns
LDEC012604-RA	proliferating cell nuclear antigen	ns	ns	ns	ns
LDEC000784-RA	TP53-regulating kinase	ns	ns	ns	ns
LDEC000783-RA	TP53-regulating kinase	ns	ns	ns	ns
LDEC004434-RA	TP53-regulated inhibitor of apoptosis 1-like	ns	ns	ns	ns
LDEC018882-RA	tumor protein p53-inducible nuclear protein 2	ns	ns	-0.7	0.01
LDEC001127-RA	cell death-inducing p53-target protein 1	ns	ns	ns	ns
LDEC001126-RA	cell death-inducing p53-target protein 1	ns	ns	ns	ns
LDEC001128-RA	cell death-inducing p53-target protein 1	ns	ns	ns	ns
LDEC001723-RA	apoptosis-stimulating of p53 protein 1 isoform X4	ns	ns	ns	ns
LDEC001727-RA	Apoptosis-stimulating of p53 protein 1	ns	ns	ns	ns
LDEC006855-RA	cellular tumor antigen p53	ns	ns	ns	ns
LDEC001725-RA	apoptosis-stimulating of p53 protein 1 isoform X3	ns	ns	5.8	<0.001
LDEC007199-RA	apoptosis-resistant E3 ubiquitin protein ligase 1 isoform X2	ns	ns	ns	ns
LDEC014206-RA	programmed cell death protein 6	ns	ns	ns	ns
LDEC016796-RA	nuclear apoptosis-inducing factor 1-like	ns	ns	ns	ns

Sequence ID	Sequence description	Fat body		Flight muscle	
		Log ₂ fold change	Adjusted <i>p</i> value	Log ₂ fold change	Adjusted <i>p</i> value
LDEC020746-RA	apoptosis-inducing factor 3 isoform X1	ns	ns	0.8	0.04
LDEC016342-RA	apoptosis-inducing factor 3 isoform X1	ns	ns	ns	ns
LDEC016341-RA	apoptosis-inducing factor 3 isoform X1	ns	ns	ns	ns
LDEC007549-RA	death-associated inhibitor of apoptosis 2	ns	ns	ns	ns
LDEC007550-RA	death-associated inhibitor of apoptosis 2	ns	ns	ns	ns
LDEC004331-RA	cell division cycle and apoptosis regulator protein 1-like	ns	ns	ns	ns
LDEC000144-RA	apoptosis inhibitor 5	ns	ns	ns	ns
LDEC008814-RA	inhibitor of apoptosis 3	ns	ns	ns	ns

Table A5. Differential expression of selected lipid metabolism-related transcripts in body (FB) and flight muscle (FM) tissue of *L. decemlineata* during diapause. Fold change values represent increased or decreased abundance of transcripts (adjusted *p*-value of <0.05) during diapause compared to a non-diapausing control. ns indicates where expression values were deemed non-significant according to differential gene expression analysis in DEseq2.

Sequence ID	Sequence Description	Fat body		Flight muscle	
		Log ₂ fold change	Adjusted <i>p</i> value	Log ₂ fold change	Adjusted <i>p</i> value
LDEC009937-RA	fatty acid synthase-like	ns	ns	ns	ns
LDEC004337-RA	fatty acid-binding protein, liver-like	ns	ns	ns	ns
LDEC004338-RA	fatty acid-binding protein-like	ns	ns	-4.7	<0.001
LDEC002435-RA	fatty acid synthase-like	ns	ns	ns	ns
LDEC002434-RA	fatty acid synthase	ns	ns	ns	ns
LDEC002433-RA	fatty acid synthase-like	ns	ns	ns	ns
LDEC022762-RA	elongation of very long chain fatty acids protein 4-like	-4.7	<0.001	-4.9	<0.001
LDEC002436-RA	fatty acid synthase	ns	ns	ns	ns
LDEC011862-RA	elongation of very long chain fatty acids protein AAEL008004-like	2.7	0.02	ns	ns
LDEC011864-RA	elongation of very long chain fatty acids protein AAEL008004-like	ns	ns	ns	ns
LDEC014617-RA	fatty acid synthase	ns	ns	ns	ns
LDEC004342-RA	fatty acid-binding protein-like	ns	ns	ns	ns
LDEC004340-RA	fatty acid-binding protein-like	ns	ns	ns	ns
LDEC011859-RA	elongation of very long chain fatty acids protein AAEL008004-like	ns	ns	ns	ns
LDEC008992-RA	fatty acid synthase	ns	ns	ns	ns
LDEC011860-RA	elongation of very long chain fatty acids protein AAEL008004-like	ns	ns	ns	ns
LDEC011861-RA	elongation of very long chain fatty acids protein AAEL008004	ns	ns	ns	ns
LDEC004346-RA	fatty acid binding protein 1-B.1-like	ns	ns	ns	ns
LDEC004347-RA	fatty acid-binding protein, liver	ns	ns	ns	ns
LDEC004350-RA	fatty acid synthase-like	ns	ns	ns	ns
LDEC002854-RA	fatty acid synthase-like	ns	ns	ns	ns
LDEC002857-RA	fatty acid synthase-like	ns	ns	ns	ns

Sequence ID	Sequence Description	Fat body		Flight muscle	
		Log ₂ fold change	Adjusted <i>p</i> value	Log ₂ fold change	Adjusted <i>p</i> value
LDEC020615-RA	fatty acid synthase	2.5	0.03	ns	ns
LDEC015064-RA	fatty acid synthase	ns	ns	ns	ns
LDEC015064-RA	fatty acid synthase	ns	ns	ns	ns
LDEC015062-RA	fatty acid synthase	ns	ns	ns	ns
LDEC002855-RA	fatty acid synthase-like	ns	ns	ns	ns
LDEC015584-RA	long-chain fatty acid transport protein 4	ns	ns	ns	ns
LDEC015586-RA	long-chain fatty acid transport protein 4	ns	ns	ns	ns
LDEC008108-RA	elongation of very long chain fatty acids protein 6	ns	ns	-1.4	0.04
LDEC004559-RA	fatty acid-binding protein, brain-like	ns	ns	ns	ns
LDEC015065-RA	fatty acid synthase	ns	ns	ns	ns
LDEC010496-RA	elongation of very long chain fatty acids protein AAEL008004-like	-2.6	<0.001	-2.5	<0.001
LDEC010497-RA	elongation of very long chain fatty acids protein AAEL008004-like	ns	ns	-3.0	<0.001
LDEC010498-RA	elongation of very long chain fatty acids protein AAEL008004-like	ns	ns	ns	ns
LDEC016593-RA	elongation of very long chain fatty acids protein AAEL008004	-1.7	0.03	-1.7	0.04
LDEC011855-RA	elongation of very long chain fatty acids protein AAEL008004-like	ns	ns	ns	ns
LDEC017075-RA	lipase 3	3.3	0.03	ns	ns
LDEC005771-RA	lipase 3-like	3.1	<0.001	ns	ns
LDEC012490-RA	lipase member H-A	3.1	0.01	ns	ns
LDEC010801-RA	lipase 3-like isoform X1	2.9	0.02	2.7	0.03
LDEC006931-RA	pancreatic triacylglycerol lipase	2.2	0.02	-2.04	0.03
LDEC024623-RA	lipase 3-like	1.7	0.05	ns	ns
LDEC005772-RA	lipase 3-like	1.6	0.02	1.5	0.04
LDEC005773-RA	lipase 3-like	ns	ns	2.0	<0.001

Table A6. Differential expression of selected energy metabolism-related transcripts in body (FB) and flight muscle (FM) tissue of *L. decemlineata* during diapause. Fold change values represent increased or decreased abundance of transcripts (adjusted *p*-value of <0.05) during diapause compared to a non-diapausing control. ns indicates where expression values were deemed non-significant according to differential gene expression analysis in DEseq2.

Sequence ID	Sequence description	Fat body		Flight muscle	
		Log ₂ fold change	Adjusted <i>p</i> value	Log ₂ fold change	Adjusted <i>p</i> value
LDEC000163-RA	ATP synthase subunit g, mitochondrial	ns	ns	ns	ns
LDEC000409-RA	succinate dehydrogenase assembly factor 2-A, mitochondrial	ns	ns	ns	ns
LDEC000603-RA	cytochrome c oxidase subunit 6A1, mitochondrial	ns	ns	3.7	0.01
LDEC000689-RA	cytochrome c oxidase subunit 7C, mitochondrial-like	ns	ns	ns	ns
LDEC001083-RA	NADH dehydrogenase [ubiquinone] iron-sulfur protein 3, mitochondrial	ns	ns	ns	ns
LDEC001593-RA	cytochrome b-c1 complex subunit Rieske, mitochondrial-like	ns	ns	ns	ns
LDEC001746-RA	NADH dehydrogenase 1 alpha subcomplex subunit 9, mitochondrial	ns	ns	ns	ns
LDEC001800-RA	succinate dehydrogenase flavoprotein subunit, mitochondrial	ns	ns	4.7	<0.001
LDEC001906-RA	succinate--CoA ligase [GDP-forming] subunit beta, mitochondrial	ns	ns	ns	ns
LDEC001990-RA	cytochrome c oxidase assembly factor 4 homolog, mitochondrial	ns	ns	ns	ns
LDEC002278-RA	NADH dehydrogenase iron-sulfur protein 6, mitochondrial	ns	ns	ns	ns
LDEC002395-RA	ATP synthase subunit e, mitochondrial	ns	ns	4.8	<0.001
LDEC003129-RA	NADH dehydrogenase flavoprotein 3, mitochondrial	ns	ns	ns	ns
LDEC003295-RA	cytochrome c oxidase subunit 4 isoform 1, mitochondrial	ns	ns	ns	ns
LDEC003349-RA	cytochrome c oxidase subunit 4 isoform 1, mitochondrial-like	ns	ns	ns	ns
LDEC003352-RA	ATP synthase subunit gamma, mitochondrial	ns	ns	ns	ns
LDEC003376-RA	cytochrome b-c1 complex subunit 6, mitochondrial	ns	ns	ns	ns
LDEC004142-RA	cytochrome c oxidase assembly protein COX16 homolog, mitochondrial	ns	ns	ns	ns
LDEC004794-RA	ATP synthase subunit b, mitochondrial	ns	ns	4.3	<0.001
LDEC004832-RA	complex I intermediate-associated protein 30, mitochondrial	0.5	0.01	ns	ns
LDEC005582-RA	NADH dehydrogenase [ubiquinone] iron-sulfur protein 4, mitochondrial	ns	ns	ns	ns

Sequence ID	Sequence description	Fat body		Flight muscle	
		Log ₂ fold change	Adjusted <i>p</i> value	Log ₂ fold change	Adjusted <i>p</i> value
LDEC006349-RA	ATP synthase-coupling factor 6, mitochondrial	ns	ns	ns	ns
LDEC006423-RA	ATP synthase mitochondrial F1 complex assembly factor 2	ns	ns	ns	ns
LDEC006705-RA	ATP synthase subunit e, mitochondrial	ns	ns	ns	ns
LDEC006874-RA	NADH dehydrogenase [ubiquinone] iron-sulfur protein 3, mitochondrial	ns	ns	3.9	<0.001
LDEC007508-RA	NADH dehydrogenase [ubiquinone] 1 beta subcomplex subunit 2, mitochondrial-like	ns	ns	ns	ns
LDEC007946-RA	cytochrome c oxidase subunit 5A, mitochondrial	ns	ns	ns	ns
LDEC008450-RA	succinate dehydrogenase [ubiquinone] flavoprotein subunit, mitochondrial	ns	ns	ns	ns
LDEC008722-RA	ATP synthase subunit d, mitochondrial	ns	ns	ns	ns
LDEC009098-RA	succinate-semialdehyde dehydrogenase, mitochondrial	ns	ns	ns	ns
LDEC009790-RA	cytochrome b-c1 complex subunit Rieske, mitochondrial	ns	ns	ns	ns
LDEC009840-RA	succinate dehydrogenase cytochrome b560 subunit, mitochondrial-like	ns	ns	ns	ns
LDEC010568-RA	cytochrome b-c1 complex subunit Rieske, mitochondrial	ns	ns	4.7	<0.001
LDEC010738-RA	cytochrome c1, heme protein, mitochondrial	ns	ns	ns	ns
LDEC010764-RA	ATPase inhibitor mai-2, mitochondrial-like	ns	ns	ns	ns
LDEC011951-RA	succinate dehydrogenase [ubiquinone] cytochrome b small subunit, mitochondrial	ns	ns	ns	ns
LDEC012722-RA	succinate--CoA ligase [ADP/GDP-forming] subunit alpha, mitochondrial	ns	ns	ns	ns
LDEC013584-RA	succinyl-CoA:3-ketoacid coenzyme A transferase 1, mitochondrial	ns	ns	ns	ns
LDEC014295-RA	succinate--CoA ligase [ADP-forming] subunit beta, mitochondrial	-0.6	0.01	ns	ns
LDEC014777-RA	ATP synthase subunit b, mitochondrial	ns	ns	ns	ns
LDEC015150-RA	ATPase inhibitor mai-2, mitochondrial-like	ns	ns	3.4	0.02
LDEC015242-RA	ATP synthase subunit O, mitochondrial	ns	ns	ns	ns
LDEC015272-RA	ATP synthase mitochondrial F1 complex assembly factor 1	ns	ns	ns	ns
LDEC015448-RA	ATP synthase lipid-binding protein, mitochondrial	ns	ns	ns	ns
LDEC015698-RA	succinate dehydrogenase [ubiquinone] iron-sulfur subunit, mitochondrial	ns	ns	ns	ns

Sequence ID	Sequence description	Fat body		Flight muscle	
		Log ₂ fold change	Adjusted <i>p</i> value	Log ₂ fold change	Adjusted <i>p</i> value
LDEC015747-RA	NADH dehydrogenase [ubiquinone] 1 beta subcomplex subunit 8, mitochondrial	ns	ns	ns	ns
LDEC016085-RA	ATP synthase subunit epsilon, mitochondrial-like isoform X2	ns	ns	2.6	<0.001
LDEC016683-RA	NADH dehydrogenase [ubiquinone] flavoprotein 2, mitochondrial	ns	ns	ns	ns
LDEC018071-RA	cytochrome c oxidase subunit 5A, mitochondrial	ns	ns	4.4	<0.001
LDEC018421-RA	NADH dehydrogenase [ubiquinone] 1 beta subcomplex subunit 11, mitochondrial	ns	ns	ns	ns
LDEC018453-RA	ATP synthase subunit alpha, mitochondrial	ns	ns	ns	ns
LDEC018454-RA	ATP synthase subunit alpha, mitochondrial	ns	ns	ns	ns
LDEC018456-RA	ATP synthase subunit alpha, mitochondrial	ns	ns	ns	ns
LDEC018955-RA	cytochrome c oxidase assembly protein COX11, mitochondrial	ns	ns	ns	ns
LDEC019063-RA	NADPH:adrenodoxin oxidoreductase, mitochondrial	ns	ns	ns	ns
LDEC019838-RA	ATP synthase subunit s, mitochondrial	ns	ns	ns	ns
LDEC020201-RA	NADH dehydrogenase [ubiquinone] flavoprotein 1, mitochondrial	ns	ns	ns	ns
LDEC020218-RA	NADH dehydrogenase [ubiquinone] 1 alpha subcomplex subunit 10, mitochondrial	ns	ns	ns	ns
LDEC020219-RA	cytochrome c oxidase subunit 7A2, mitochondrial	ns	ns	ns	ns
LDEC020980-RA	NADH-ubiquinone oxidoreductase 75 kDa subunit, mitochondrial	ns	ns	ns	ns
LDEC021426-RA	ATP synthase subunit beta, mitochondrial	ns	ns	ns	ns
LDEC022005-RA	succinate--CoA ligase [ADP/GDP-forming] subunit alpha, mitochondrial	ns	ns	ns	ns
LDEC022255-RA	cytochrome b-c1 complex subunit Rieske, mitochondrial-like	ns	ns	ns	ns
LDEC022565-RA	succinate dehydrogenase assembly factor 3, mitochondrial	1.5	0.01	ns	ns
LDEC022893-RA	NADH dehydrogenase [ubiquinone] iron-sulfur protein 2, mitochondrial-like	ns	ns	ns	ns
LDEC023898-RA	cytochrome c oxidase subunit 6A, mitochondrial	ns	ns	ns	ns
LDEC024041-RA	NADH dehydrogenase [ubiquinone] iron-sulfur protein 4, mitochondrial	ns	ns	4.3	<0.001
LDEC024744-RA	cytochrome c oxidase subunit 3 (mitochondrion)	ns	ns	ns	ns

Sequence ID	Sequence description	Fat body		Flight muscle	
		Log ₂ fold change	Adjusted <i>p</i> value	Log ₂ fold change	Adjusted <i>p</i> value
LDEC024745-RA	NADH dehydrogenase subunit 3 (mitochondrion)	ns	ns	ns	ns
LDEC024746-RA	NADH deshydrogenase subunit 5 (mitochondrion)	ns	ns	ns	ns
LDEC024747-RA	NADH dehydrogenase subunit 4 (mitochondrion)	ns	ns	ns	ns
LDEC024748-RA	NADH deshydrogenase subunit 4 (mitochondrion)	3.0	0.01	ns	ns
LDEC015148-RA	hexokinase type 2 isoform X5	ns	ns	ns	ns
LDEC015696-RA	6-phosphofructo-2-kinase/fructose-2,6-bisphosphatase 1-like Protein	ns	ns	ns	ns
LDEC012512-RA	6-phosphofructo-2-kinase/fructose-2,6-bisphosphatase-like isoform X1	ns	ns	ns	ns
LDEC003817-RA	ATP-dependent 6-phosphofructokinase isoform X1	ns	ns	ns	ns
LDEC010370-RA	fructose-bisphosphate aldolase	ns	ns	ns	ns
LDEC020943-RA	glyceraldehyde 3-phosphate dehydrogenase	ns	ns	ns	ns
LDEC021153-RA	6-phosphogluconate dehydrogenase, decarboxylating	ns	ns	-1.2	0.01
LDEC010564-RA	phosphoglycerate kinase	ns	ns	ns	ns
LDEC010565-RA	phosphoglycerate kinase	ns	ns	2.8	0.03
LDEC010828-RA	glycerate kinase	ns	ns	-1.6	0.04
LDEC006551-RA	glycerate kinase	-1.8	0.01	-1.6	0.01
LDEC003977-RA	enolase	ns	ns	4.46	<0.001
LDEC007262-RA	enolase	ns	ns	ns	ns
LDEC009823-RA	enolase-phosphatase E1	ns	ns	ns	ns
LDEC009823-RA	enolase-phosphatase E1	-1.0	0.01	-1.2	<0.001
LDEC011617-RA	mitochondrial enolase superfamily member 1-like	ns	ns	ns	ns
LDEC009046-RA	ATP-citrate synthase isoform X1	ns	ns	ns	ns
LDEC009045-RA	ATP-citrate synthase isoform X1	ns	ns	ns	ns
LDEC008025-RA	isocitrate dehydrogenase [NAD] subunit beta, mitochondrial	ns	ns	ns	ns
LDEC012769-RA	isocitrate dehydrogenase [NADP] cytoplasmic-like	ns	ns	ns	ns
LDEC016496-RA	cytoplasmic NADP+-dependent isocitrate dehydrogenase	ns	ns	ns	ns
LDEC016497-RA	cytoplasmic NADP+-dependent isocitrate dehydrogenase	ns	ns	ns	ns

Sequence ID	Sequence description	Fat body		Flight muscle	
		Log ₂ fold change	Adjusted <i>p</i> value	Log ₂ fold change	Adjusted <i>p</i> value
LDEC008025-RA	isocitrate dehydrogenase [NAD] subunit beta, mitochondrial	ns	ns	ns	ns
LDEC013584-RA	succinyl-CoA:3-ketoacid coenzyme A transferase 1, mitochondrial	ns	ns	ns	ns
LDEC014621-RA	dihydrolipoyllysine-residue succinyltransferase component of 2-oxoglutarate dehydrogenase complex, mitochondrial-like	ns	ns	ns	ns
LDEC017645-RA	malate dehydrogenase, mitochondrial	ns	ns	ns	ns
LDEC017289-RA	malate dehydrogenase, mitochondrial-like	ns	ns	5.2	<0.001
LDEC007654-RA	putative malate dehydrogenase 1B	ns	ns	ns	ns
LDEC002299-RA	malate dehydrogenase	ns	ns	4.9	<0.001
LDEC023960-RA	malate dehydrogenase, mitochondrial	ns	ns	2.5	0.04
LDEC006362-RA	pyruvate carboxylase, mitochondrial isoform X2	ns	ns	ns	ns
LDEC006364-RA	pyruvate carboxylase, mitochondrial isoform X1	ns	ns	ns	ns
LDEC014842-RA	probable pyruvate dehydrogenase E1 component subunit alpha, mitochondrial	ns	ns	3.3	0.02
LDEC014843-RA	pyruvate dehydrogenase E1 component, alpha subunit	ns	ns	3.8	0.01
LDEC000613-RA	pyruvate dehydrogenase (acetyl-transferring) kinase, mitochondrial	ns	ns	ns	ns
LDEC011716-RA	pyruvate dehydrogenase [acetyl-transferring]-phosphatase 1, mitochondrial	ns	ns	ns	ns
LDEC008594-RA	dihydrolipoyllysine-residue acetyltransferase component of pyruvate dehydrogenase complex, mitochondrial isoform X1	ns	ns	ns	ns
LDEC001269-RA	dihydrolipoyllysine-residue acetyltransferase component 2 of pyruvate dehydrogenase complex, mitochondrial isoform X1	ns	ns	ns	ns
LDEC005950-RA	pyruvate dehydrogenase E1 component subunit beta, mitochondrial	ns	ns	ns	ns

Table A7. Differential expression of selected stress tolerance-related transcripts in fat body (FB) and flight muscle (FM) tissue of *L. decemlineata* during diapause. Fold change values represent increased or decreased abundance of transcripts (adjusted *p*-value of <0.05) during diapause compared to a non-diapausing control. ns indicates where expression values were deemed non-significant according to differential gene expression analysis in DEseq2.

Sequence ID	Sequence description	Fat body		Flight muscle	
		Log ₂ fold change	Adjusted <i>p</i> value	Log ₂ fold change	Adjusted <i>p</i> value
<i>Hypoxia response</i>					
LDEC003836-RA	thioredoxin domain-containing protein 9	ns	ns	ns	ns
LDEC011015-RA	thioredoxin-like protein 4A	-0.9	0.03	ns	ns
LDEC017665-RA	thioredoxin domain-containing protein 17	ns	ns	4.7	<0.001
LDEC017689-RA	thioredoxin-related transmembrane protein 1-like	ns	ns	ns	ns
LDEC004166-RA	thioredoxin domain-containing protein 17	ns	ns	ns	ns
LDEC004821-RA	thioredoxin-like protein 4A	ns	ns	ns	ns
LDEC006824-RA	thioredoxin, mitochondrial-like	ns	ns	-1.4	<0.001
LDEC018504-RA	thioredoxin domain-containing protein 15	ns	ns	ns	ns
LDEC004034-RA	thioredoxin domain-containing protein 5	ns	ns	ns	ns
LDEC008311-RA	thioredoxin-2	ns	ns	ns	ns
LDEC010064-RA	thioredoxin domain-containing protein 11	ns	ns	ns	ns
LDEC016628-RA	thioredoxin-like protein 1	ns	ns	ns	ns
LDEC005477-RA	thioredoxin domain-containing protein	ns	ns	ns	ns
LDEC019567-RA	catalase-like	ns	ns	ns	ns
LDEC019565-RA	catalase-like	ns	ns	ns	ns
LDEC019566-RA	catalase-like	ns	ns	ns	ns
LDEC012452-RA	catalase	ns	ns	-1.8	0.04
LDEC013875-RA	catalase	ns	ns	ns	ns
LDEC013235-RA	superoxide dismutase [Cu-Zn]-like	ns	ns	ns	ns
LDEC013235-RB	superoxide dismutase [Cu-Zn]-like	ns	ns	ns	ns
LDEC013236-RA	superoxide dismutase [Cu-Zn]-like	1.5	0.03	1.6	0.02
LDEC008432-RA	superoxide dismutase [Mn], mitochondrial	ns	ns	ns	ns
LDEC010000-RA	probable phospholipid hydroperoxide glutathione peroxidase	ns	ns	ns	ns

Sequence ID	Sequence description	Fat body		Flight muscle	
		Log ₂ fold change	Adjusted <i>p</i> value	Log ₂ fold change	Adjusted <i>p</i> value
LDEC006766-RA	glutathione S-transferase	ns	ns	ns	ns
LDEC015216-RA	glutathione S-transferase 1	-2.8	0.04	ns	ns
LDEC020265-RA	glutathione S-transferase 1-like	-2.0	<0.001	-1.8	<0.001
LDEC009779-RA	glutathione S-transferase 1-like	ns	ns	ns	ns
LDEC015615-RA	glutathione synthetase-like isoform X1	1.1	0.009	ns	ns
LDEC001118-RA	glutathione S-transferase 1-like	ns	ns	ns	ns
LDEC001119-RA	glutathione S-transferase 1-like	ns	ns	ns	ns
LDEC001122-RA	glutathione S-transferase 1-like	ns	ns	ns	ns
LDEC001121-RA	glutathione S-transferase 1-like	ns	ns	ns	ns
LDEC001123-RA	glutathione S-transferase 1-like	ns	ns	ns	ns
LDEC019760-RA	glutathione S-transferase 1-like	ns	ns	ns	ns
LDEC001116-RA	glutathione S-transferase 1-like	2.2	0.03	ns	ns
LDEC014129-RA	glutathione S-transferase-like	ns	ns	ns	ns
LDEC020798-RA	glutathione S-transferase theta-1	ns	ns	ns	ns
LDEC003606-RA	glutathione synthetase-like isoform X1	ns	ns	ns	ns
LDEC003607-RA	glutathione synthetase-like isoform X2	ns	ns	ns	ns
LDEC023323-RA	glutathione S-transferase 1	ns	ns	ns	ns
LDEC015214-RA	glutathione S-transferase 1-1	ns	ns	ns	ns
LDEC007489-RA	glutathione S-transferase 1-1-like	ns	ns	ns	ns
LDEC004485-RA	glutathione S-transferase C-terminal domain-containing protein homolog	-0.6	0.03	ns	ns
LDEC011711-RA	hypoxia-inducible factor 1-alpha isoform X2	ns	ns	ns	ns
LDEC010673-RA	putative hypoxia-inducible factor 1 beta	ns	ns	ns	ns
LDEC011710-RA	hypoxia-inducible factor 1-alpha	ns	ns	ns	ns
LDEC016032-RA	hypoxia up-regulated protein 1	ns	ns	ns	ns
LDEC016139-RA	hypoxia-inducible factor 1-alpha inhibitor	-1.7	0.02	ns	ns
LDEC024414-RA	hypoxia-inducible factor 1-alpha inhibitor-like	ns	ns	ns	ns
<i>Immunity</i>					
LDEC009623-RA	serine protease persephone-like	ns	ns	ns	ns
LDEC011425-RA	serine protease 10 precursor	ns	ns	ns	ns

Sequence ID	Sequence description	Fat body		Flight muscle	
		Log ₂ fold change	Adjusted <i>p</i> value	Log ₂ fold change	Adjusted <i>p</i> value
LDEC006903-RA	serine protease snake-like	ns	ns	ns	ns
LDEC024740-RA	putative serine protease K12H4.7	ns	ns	ns	ns
LDEC008820-RA	serine protease nudel	-2.7	<0.001	-2.4	<0.001
LDEC000866-RA	serine protease P153	2.3	0.02	ns	ns
LDEC018942-RA	serine protease 7-like	ns	ns	ns	ns
LDEC018941-RA	serine protease 7-like	2.9	<0.001	ns	ns
LDEC000867-RA	serine protease P153	2.1	0.03	ns	ns
LDEC008818-RA	serine protease nudel	-3.7	<0.001	-3.5	<0.001
LDEC010088-RA	serine protease H57	2.6	<0.001	3.6	<0.001
LDEC010627-RA	modular serine protease-like	ns	ns	ns	ns
LDEC015400-RA	serine protease easter	ns	ns	ns	ns
LDEC009783-RA	serine protease H57	-3.0	0.02	ns	ns
LDEC010628-RA	modular serine protease-like	ns	ns	ns	ns
LDEC003252-RA	serine protease 33-like	ns	ns	ns	ns
LDEC011571-RA	serine protease 33-like isoform X2	ns	ns	ns	ns
LDEC020484-RA	serine protease persephone	2.0	0.02	ns	ns
LDEC021025-RA	serine protease easter-like	2.5	0.01	3.4	<0.001
LDEC008647-RA	serine protease easter-like	ns	ns	ns	ns
LDEC008817-RA	serine protease nudel	-4.2	<0.001	-3.5	0.002
LDEC021885-RA	serine protease easter-like	ns	ns	ns	ns
LDEC003791-RA	serine protease gd-like	ns	ns	ns	ns
LDEC001146-RA	putative serine protease K12H4.7	ns	ns	ns	ns
LDEC001147-RA	putative serine protease K12H4.7	ns	ns	ns	ns
LDEC001146-RA	putative serine protease K12H4.7	ns	ns	ns	ns
LDEC001147-RA	putative serine protease K12H4.7	ns	ns	ns	ns
LDEC018940-RA	serine protease 7-like	2.7	0.006	ns	ns
LDEC003789-RA	serine protease gd-like	-1.7	0.007	ns	ns
LDEC003790-RA	serine protease gd-like	ns	ns	ns	ns
LDEC024229-RA	serine protease gd-like	-1.4	<0.001	ns	ns
LDEC002196-RA	serine protease gd-like	ns	ns	ns	ns

Sequence ID	Sequence description	Fat body		Flight muscle	
		Log ₂ fold change	Adjusted <i>p</i> value	Log ₂ fold change	Adjusted <i>p</i> value
LDEC005500-RA	serine protease easter-like	ns	ns	ns	ns
LDEC005847-RA	serine protease P83	ns	ns	ns	ns
<i>Chaperone response</i>					
LDEC000729-RA	heat-shock protein 90	ns	ns	ns	ns
LDEC005932-RA	heat shock protein 90	ns	ns	ns	ns
LDEC000728-RA	heat shock protein 83	ns	ns	ns	ns
LDEC000387-RA	heat shock protein 83	ns	ns	ns	ns
LDEC017005-RA	heat shock 70 kDa protein-like	ns	ns	ns	ns
LDEC000250-RA	heat shock protein 70	ns	ns	5.2	<0.001
LDEC002760-RA	heat shock 70 kDa protein 4 isoform X1	ns	ns	ns	ns
LDEC017004-RA	heat shock 70 kDa protein-like	ns	ns	ns	ns
LDEC017006-RA	heat shock 70 kDa protein-like	ns	ns	ns	ns
LDEC016283-RA	heat shock protein 70	ns	ns	ns	ns
LDEC010172-RA	heat shock protein 68-like	ns	ns	2.8	0.03
LDEC021981-RA	heat shock protein 67B2-like	0.9	0.005	ns	ns
LDEC001137-RA	heat shock protein 68-like	-4.0	<0.001	-3.8	<0.001
LDEC001140-RA	heat shock protein 68-like	-4.0	<0.001	-3.9	<0.001
LDEC001138-RA	heat shock protein 68-like	-4.0	<0.001	-3.6	<0.001
LDEC016280-RA	heat shock protein 68-like	ns	ns	ns	ns
LDEC016281-RA	heat shock protein 68-like	ns	ns	ns	ns
LDEC016282-RA	heat shock protein 68-like	ns	ns	ns	ns
LDEC009746-RA	heat shock protein 75 kDa, mitochondrial	ns	ns	ns	ns
LDEC009747-RA	heat shock protein 75 kDa, mitochondrial	ns	ns	ns	ns
LDEC009745-RA	heat shock protein 75 kDa, mitochondrial	ns	ns	ns	ns
LDEC005817-RA	10 kDa heat shock protein, mitochondrial	ns	ns	ns	ns
LDEC005807-RA	heat shock factor-binding protein 1	ns	ns	ns	ns
LDEC000022-RA	heat shock factor protein isoform X2	ns	ns	ns	ns
LDEC021135-RA	heat shock protein DDB_G0288861 isoform X1	ns	ns	ns	ns
LDEC010624-RA	heat shock 70 kDa protein cognate 5	ns	ns	ns	ns
LDEC008522-RA	heat shock 70 kDa protein cognate 1-like	ns	ns	ns	ns

Sequence ID	Sequence description	Fat body		Flight muscle	
		Log ₂ fold change	Adjusted <i>p</i> value	Log ₂ fold change	Adjusted <i>p</i> value
LDEC008523-RA	heat shock 70 kDa protein cognate 2	ns	ns	ns	ns
LDEC007545-RA	heat shock 70 kDa protein cognate 4	ns	ns	ns	ns
LDEC000251-RA	heat shock cognate 71 kDa protein-like	ns	ns	-1.5	<0.001
LDEC018987-RA	heat shock 70 kDa protein cognate 3	0.7	0.02	ns	ns
LDEC009961-RA	heat shock 70 kDa protein cognate 4	ns	ns	ns	ns
LDEC009962-RA	heat shock 70 kDa protein cognate 4	1.3	<0.001	ns	ns
LDEC011463-RA	heat shock protein beta-1 isoform X2	ns	ns	ns	ns
LDEC004975-RA	28 kDa heat- and acid-stable phosphoprotein-like	ns	ns	ns	ns
LDEC021831-RA	activator of 90 kDa heat shock protein ATPase homolog 1	-0.9	<0.001	ns	ns
LDEC000968-RA	heat shock factor protein isoform X1	ns	ns	ns	ns
<i>Cell structure and integrity</i>					
LDEC000164-RA	tubulin-specific chaperone C	ns	ns	ns	ns
LDEC000503-RA	actin, alpha skeletal muscle-like	ns	ns	-1.7	0.04
LDEC000622-RA	tubulin--tyrosine ligase-like protein 12	ns	ns	ns	ns
LDEC000761-RA	actin-related protein 6	ns	ns	ns	ns
LDEC001155-RA	tubulin polyglutamylase TTLL6 isoform X2	ns	ns	ns	ns
LDEC001455-RA	gamma-tubulin complex component 5-like	ns	ns	0.8	0.02
LDEC001987-RA	F-actin-uncapping protein LRRC16A isoform X2	ns	ns	ns	ns
LDEC002053-RA	actin-related protein 6	ns	ns	ns	ns
LDEC002785-RA	F-actin-capping protein subunit alpha	ns	ns	ns	ns
LDEC002903-RA	phosphatase and actin regulator 1-like isoform X3	ns	ns	ns	ns
LDEC002904-RA	phosphatase and actin regulator 4 isoform X5	-1.4	0.004	ns	ns
LDEC003006-RA	actin-like protein 6B	ns	ns	ns	ns
LDEC003241-RA	keratin, type I cytoskeletal 9-like	ns	ns	ns	ns
LDEC003627-RA	keratin-3, type I cytoskeletal 51 kDa-like	ns	ns	ns	ns
LDEC004146-RA	phosphatase and actin regulator 2 isoform X3	ns	ns	ns	ns
LDEC004147-RA	phosphatase and actin regulator 2 isoform X1	4.6	<0.001	ns	ns
LDEC004364-RA	tubulin alpha chain-like	ns	ns	ns	ns
LDEC004366-RA	tubulin alpha-3 chain	ns	ns	ns	ns
LDEC004367-RA	tubulin alpha chain-like	ns	ns	ns	ns

Sequence ID	Sequence description	Fat body		Flight muscle	
		Log ₂ fold change	Adjusted <i>p</i> value	Log ₂ fold change	Adjusted <i>p</i> value
LDEC004601-RA	F-actin-capping protein subunit beta isoform X1	ns	ns	ns	ns
LDEC004871-RA	gamma-tubulin complex component 2-like isoform X1	ns	ns	ns	ns
LDEC004872-RA	gamma-tubulin complex component 2-like isoform X2	ns	ns	ns	ns
LDEC005271-RA	actin-related protein 1	-0.6	0.02	-0.6	0.02
LDEC005466-RA	tubulin beta chain	ns	ns	3.9	0.003
LDEC005581-RA	probable actin-related protein 2/3 complex subunit 2	ns	ns	ns	ns
LDEC005699-RA	actin-related protein 2/3 complex subunit 3	ns	ns	ns	ns
LDEC006150-RA	tubulin-folding cofactor B	0.6	0.03	ns	ns
LDEC006156-RA	actin	ns	ns	ns	ns
LDEC006501-RA	actin-binding LIM protein 3 isoform X2	ns	ns	ns	ns
LDEC006706-RA	Tubulin alpha-1 chain	ns	ns	1.3	0.02
LDEC006738-RA	microtubule-actin cross-linking factor 1 isoform X1	ns	ns	ns	ns
LDEC006739-RA	microtubule-actin cross-linking factor 1 isoform X1	ns	ns	ns	ns
LDEC006740-RA	microtubule-actin cross-linking factor 1	ns	ns	ns	ns
LDEC006742-RA	microtubule-actin cross-linking factor 1 isoform X1	ns	ns	ns	ns
LDEC006743-RA	microtubule-actin cross-linking factor 1 isoform X1	ns	ns	ns	ns
LDEC006784-RA	actin-related protein 2/3 complex subunit 1A	ns	ns	ns	ns
LDEC007657-RA	dynactin subunit 4	ns	ns	ns	ns
LDEC008209-RA	tubulin beta chain	ns	ns	ns	ns
LDEC008212-RA	tubulin beta chain	ns	ns	2.0	0.004
LDEC008213-RA	tubulin beta chain isoform X6	ns	ns	1.9	0.02
LDEC008214-RA	tubulin beta-1 chain	ns	ns	1.1	0.01
LDEC008215-RA	tubulin beta-1 chain	ns	ns	1.4	0.03
LDEC008477-RA	F-actin-monooxygenase Mical isoform X1	ns	ns	ns	ns
LDEC008657-RA	Tubulin gamma-2 chain	ns	ns	ns	ns
LDEC008658-RA	tubulin gamma-1 chain-like	ns	ns	ns	ns
LDEC008725-RA	Tubulin beta-1 chain	ns	ns	1.3	0.009
LDEC008966-RA	actin-like protein 6B	ns	ns	ns	ns
LDEC009235-RA	cytoskeleton-associated protein 2-like	ns	ns	ns	ns
LDEC009685-RA	keratin, type I cytoskeletal 9	ns	ns	ns	ns

Sequence ID	Sequence description	Fat body		Flight muscle	
		Log ₂ fold change	Adjusted <i>p</i> value	Log ₂ fold change	Adjusted <i>p</i> value
LDEC009904-RA	actin 2	ns	ns	ns	ns
LDEC009905-RA	actin	ns	ns	ns	ns
LDEC010166-RA	gamma-tubulin complex component 6	ns	ns	ns	ns
LDEC010167-RA	gamma-tubulin complex component 6	ns	ns	ns	ns
LDEC010168-RA	gamma-tubulin complex component 6	ns	ns	ns	ns
LDEC010206-RA	tubulin glycyclase 3A-like isoform X2	ns	ns	3.9	0.002
LDEC010209-RA	tubulin glycyclase 3A-like isoform X1	ns	ns	3.1	0.04
LDEC010268-RA	actin-related protein 3	ns	ns	ns	ns
LDEC010305-RA	actin cytoskeleton-regulatory complex protein PAN1-like	ns	ns	ns	ns
LDEC010305-RA	actin cytoskeleton-regulatory complex protein PAN1-like	ns	ns	ns	ns
LDEC010306-RA	actin cytoskeleton-regulatory complex protein PAN1-like	ns	ns	ns	ns
LDEC010594-RA	tubulin polyglutamylase TTLL4-like isoform X1	ns	ns	ns	ns
LDEC010750-RA	tubulin-specific chaperone E	ns	ns	ns	ns
LDEC011662-RA	afadin- and alpha-actinin-binding protein-like	ns	ns	ns	ns
LDEC011698-RA	probable tubulin polyglutamylase TTLL1	ns	ns	3.6	0.02
LDEC011893-RA	beta-tubulin	ns	ns	3.4	0.01
LDEC011972-RA	actin-related protein 10	ns	ns	ns	ns
LDEC012437-RA	actin-related protein 2/3 complex subunit 4	ns	ns	ns	ns
LDEC012542-RA	actin-binding Rho-activating protein-like	-2.4	<0.001	-1.2	0.01
LDEC012682-RA	actin-related protein 5	ns	ns	ns	ns
LDEC012683-RA	actin-related protein 5	0.3	0.03	ns	ns
LDEC014138-RA	actin cytoskeleton-regulatory complex protein PAN1	ns	ns	ns	ns
LDEC014229-RA	tau-tubulin kinase homolog Asator isoform X3	ns	ns	ns	ns
LDEC014231-RA	tau-tubulin kinase homolog Asator isoform X3	ns	ns	ns	ns
LDEC014257-RA	tubulin alpha-3 chain	ns	ns	3.4	0.008
LDEC014257-RA	tubulin alpha-3 chain	ns	ns	ns	ns
LDEC014369-RA	tubulin beta chain	ns	ns	ns	ns
LDEC014814-RA	actin, cytoplasmic A3a	ns	ns	ns	ns
LDEC014817-RA	actin, cytoplasmic A3a	ns	ns	ns	ns
LDEC014818-RA	actin, clone 302-like	ns	ns	ns	ns

Sequence ID	Sequence description	Fat body		Flight muscle	
		Log ₂ fold change	Adjusted <i>p</i> value	Log ₂ fold change	Adjusted <i>p</i> value
LDEC014819-RA	beta-actin-like protein 2 isoform X2	ns	ns	ns	ns
LDEC016231-RA	actin-related protein 8	ns	ns	ns	ns
LDEC016231-RA	actin-related protein 8	ns	ns	ns	ns
LDEC016311-RA	actin-interacting protein 1	-1.1	0.05	ns	ns
LDEC016312-RA	actin-interacting protein 1	ns	ns	ns	ns
LDEC016447-RA	tubulin alpha-8 chain-like isoform X1	ns	ns	4.5	<0.001
LDEC016448-RA	Tubulin alpha-1 chain	ns	ns	4.2	0.003
LDEC016700-RA	tubulin polyglutamylase complex subunit 2	ns	ns	4.2	0.003
LDEC017200-RA	Tubulin beta-1 chain	ns	ns	ns	ns
LDEC017660-RA	gamma-tubulin complex component 3	ns	ns	ns	ns
LDEC017756-RA	activity-regulated cytoskeleton associated protein 1-like	2.42	0.007	ns	ns
LDEC018670-RA	activity-regulated cytoskeleton associated protein 2-like	ns	ns	ns	ns
LDEC019623-RA	actin, muscle	ns	ns	ns	ns
LDEC019679-RA	tubulin-specific chaperone D	ns	ns	ns	ns
LDEC019752-RA	actin-related protein 2 isoform X2	ns	ns	ns	ns
LDEC021024-RA	tubulin polyglutamylase tll6-like	ns	ns	3.7	0.01
LDEC021533-RA	activity-regulated cytoskeleton associated protein 1-like	ns	ns	ns	ns
LDEC022852-RA	activity-regulated cytoskeleton associated protein 2-like	ns	ns	ns	ns
LDEC022950-RA	activity-regulated cytoskeleton associated protein 2-like	ns	ns	ns	ns
LDEC022959-RA	dynactin subunit 4	ns	ns	ns	ns
LDEC023022-RA	microtubule-actin cross-linking factor 1 isoform X1	ns	ns	ns	ns
LDEC023875-RA	tubulin alpha chain	ns	ns	ns	ns
LDEC023884-RA	keratin, type II cytoskeletal 1	ns	ns	ns	ns
LDEC023952-RA	actin-interacting protein 1	ns	ns	ns	ns
LDEC024322-RA	activity-regulated cytoskeleton associated protein 2-like	ns	ns	ns	ns

Table A8. Differential expression of selected transposable element-related transcripts in body (FB) and flight muscle (FM) tissue of *L. decemlineata* during diapause. Fold change values represent increased or decreased abundance of transcripts (adjusted *p*-value of <0.05) during diapause compared to a non-diapausing control. ns indicates where expression values were deemed non-significant according to differential gene expression analysis in DEseq2.

Sequence ID	Sequence Description	Fat body		Flight muscle	
		Log ₂ fold change	Adjusted <i>p</i> value	Log ₂ fold change	Adjusted <i>p</i> value
LDEC011452-RA	piggyBac transposable element-derived protein 2-like	4.6	<0.001	ns	ns
LDEC011331-RA	tigger transposable element-derived protein 6-like isoform X4	4.1	<0.001	ns	ns
LDEC009727-RA	piggyBac transposable element-derived protein 3-like	3.9	<0.001	ns	ns
LDEC010331-RA	piggyBac transposable element-derived protein 3-like	3.7	<0.001	ns	ns
LDEC022668-RA	piggyBac transposable element-derived protein 4-like	3.6	<0.001	3.75	0.02
LDEC024143-RA	piggyBac transposable element-derived protein 4-like	2.8	<0.001	2.23	0.02
LDEC002328-RA	piggyBac transposable element-derived protein 3-like	2.8	<0.001	ns	ns
LDEC017961-RA	piggyBac transposable element-derived protein 4-like	2.6	<0.001	1.74	0.04
LDEC011630-RA	piggyBac transposable element-derived protein 3-like	2.4	<0.002	ns	ns
LDEC001649-RA	piggyBac transposable element-derived protein 3-like	2.4	<0.001	ns	ns
LDEC021965-RA	Transposable element P transposase	2.2	<0.001	ns	ns
LDEC003176-RA	PiggyBac transposable element-derived protein 4	2.2	<0.001	ns	ns
LDEC018325-RA	RNA-directed DNA polymerase from transposon X	2.1	<0.001	ns	ns
LDEC020990-RA	piggyBac transposable element-derived protein	2.1	<0.001	1.78	<0.001
LDEC020065-RA	piggyBac transposable element-derived protein 3-like	1.9	<0.001	1.99	<0.001
LDEC024288-RA	piggyBac transposable element-derived protein 3-like	1.8	<0.001	ns	Ns
LDEC010475-RA	piggyBac transposable element-derived protein 4-like	1.7	<0.001	ns	ns
LDEC014811-RA	piggyBac transposable element-derived protein 4-like	1.7	<0.001	ns	ns
LDEC002190-RA	piggyBac transposable element-derived protein 3-like	1.7	<0.001	ns	ns
LDEC016603-RA	piggyBac transposable element-derived protein 3-like	1.6	<0.001	ns	ns
LDEC001191-RA	piggyBac transposable element-derived protein 3-like	1.6	<0.001	ns	ns
LDEC010663-RA	piggyBac transposable element-derived protein 4-like	1.5	<0.001	ns	ns
LDEC006297-RA	piggyBac transposable element-derived protein 3-like	1.4	<0.001	ns	ns
LDEC008829-RA	piggyBac transposable element-derived protein 3-like	1.3	<0.001	ns	ns
LDEC010913-RA	piggyBac transposable element-derived protein 4-like	1.3	<0.001	ns	ns

Sequence ID	Sequence description	Fat body		Flight muscle	
		Log ₂ fold change	Adjusted <i>p</i> value	Log ₂ fold change	Adjusted <i>p</i> value
LDEC011387-RA	putative transposase-like protein	1.2	<0.001	ns	ns
LDEC021446-RA	putative RNA-directed DNA polymerase from transposon	-5.3	<0.001	ns	ns
LDEC022021-RA	piggyBac transposable element-derived protein 3-like	-2.0	<0.001	-1.63	0.03
LDEC006892-RA	tigger transposable element-derived protein 6-like protein	-1.7	<0.001	ns	ns
LDEC005258-RA	piggyBac transposable element-derived protein 3-like	ns	ns	4.58	<0.001
LDEC008623-RA	tigger transposable element-derived protein 6-like protein	ns	ns	4.52	<0.001
LDEC003663-RA	tigger transposable element-derived protein 6-like	ns	ns	4.00	0.01
LDEC001492-RA	tigger transposable element-derived protein 6-like	ns	ns	3.97	0.01
LDEC023857-RA	piggyBac transposable element-derived protein 4-like	ns	ns	3.59	0.03
LDEC008607-RA	tigger transposable element-derived protein 1-like	ns	ns	1.68	0.04
LDEC006818-RA	THAP domain-containing protein 9	ns	ns	1.52	0.04
LDEC023604-RA	piggyBac transposable element-derived protein 4-like	ns	ns	-3.92	0.01

Appendix B: Chapter 3 Supplementary Material

Table B1. Forward and reverse primer sequences for all genes of interest from Chapter 3 for *Leptinotarsa decemlineata*.

Primers listed for mitophagy-related, mitochondrial biogenesis-related, and “other” were used for measuring transcript abundance of indicated genes of interest. Primers listed for dsRNA construct synthesis were used to amplify templates for double stranded RNA (dsRNA) synthesis. The 5’ end of each primer used for dsRNA construct synthesis contains a T7 promoter which allowed RNA polymerase to bind to each primer and initiate dsRNA synthesis. Details on cycling conditions for all primers can be found in the methods.

<i>Gene of interest</i>	<i>Forward primer (5’ to 3’)</i>	<i>Reverse primer (5’ to 3’)</i>
Mitophagy-related		
<i>Parkin</i>	AAGCCTTGTCGCAATGTAG	CACCAGTGAAATGCACATCC
<i>PINK1</i>	GTGTACGCGGGGAGATGTAA	GTCTGCCACCTTGGCTTTAT
<i>ATG5</i>	TTGATGGTTCCACGACTCAG	CACATCTCCTGGTCCGATTT
Mitochondrial biogenesis-related		
<i>PGC1a</i>	CAGGTTTGGCCCTATAACGA	CGACCTCCAAAGCTCAAGTC
<i>NRF1</i>	TCATACCGCTGATGCTGAAG	CACCAAGGAGGCCTTGTAGA
Other		
<i>mTOR</i>	TGAGACCACTATGGCTGACG	ACGACAACCAACTTCCAACC
<i>FOXO</i>	TGTCTCGGAAGGTCTCGATT	TTGCCCCAGTCAGGTTCTAC
Reference		
<i>TBP1</i>	ATGTCAAGCAGAAAGTCAAGAATCC	GCCGTAATATCCCTAACTCCCAAG
<i>EF1a</i>	CAGGGCAAGGTTTGAAAGATAA	CGTCTGCTTTGCGATTGAG
dsRNA construct synthesis		
<i>Parkin</i>	TAATACGACTCACTATAGTTTGCAAAAGTGGTG CATTTC	TAATACGACTCACTATAGCTGCCAGAACTGTCT CTCC
<i>GFP</i>	TAATACGACTCACTATAGAGACACATGAAGCA GCACGACTT	TAATACGACTCACTATAGAGAAGTTCACCTTGA TGCCGTTTC

Table B2. Summary of statistics for all relevant figures in Chapter 3.

Experiment	Figure	Statistic	P
Metabolic rate	3.1A		
<i>Treatment</i>		F _{6,34} =107.72	<0.001
<i>Mass</i>		F _{1,34} =35.14	<0.001
Mitochondrial respiration rate	3.1B		
<i>Treatment</i>		F _{6,31} =20.78	<0.001
<i>Mass</i>		F _{1,31} =14.03	0.007
Citrate synthase activity	3.2A		
<i>Treatment</i>		F _{6,44} =21.02	<0.001
<i>Protein content</i>		F ₁₄₄ =0.69	0.41
Gene expression			
<i>Parkin</i>	3.3C	F _{6,14} =5.67	0.026
<i>PINK1</i>	3.3C	F _{6,14} =6.57	<0.001
<i>ATG5</i>	3.3C	F _{6,14} =28.51	<0.001
<i>PGC1a</i>	3.3C	F _{6,14} =3.16	0.036
<i>NRF1</i>	3.3C	F _{6,14} =25.47	<0.001
<i>mTOR</i>	B1A	F _{6,14} =4.45	0.010
<i>FOXO</i>	B1B	F _{6,14} =7.23	0.001
RNAi Knockdown verification	3.4	T ₄ =2.37	0.030
RNAi Metabolic rate	3.6B	T ₇ =1.93	0.040
RNAi Mitochondrial respiration rate	3.6B	T ₆ =1.31	0.240
RNAi Citrate synthase activity	3.5A	T ₆ =5.23	<0.001
RNAi Mitochondrial Density	3.5B	T ₂ =4.34	0.020

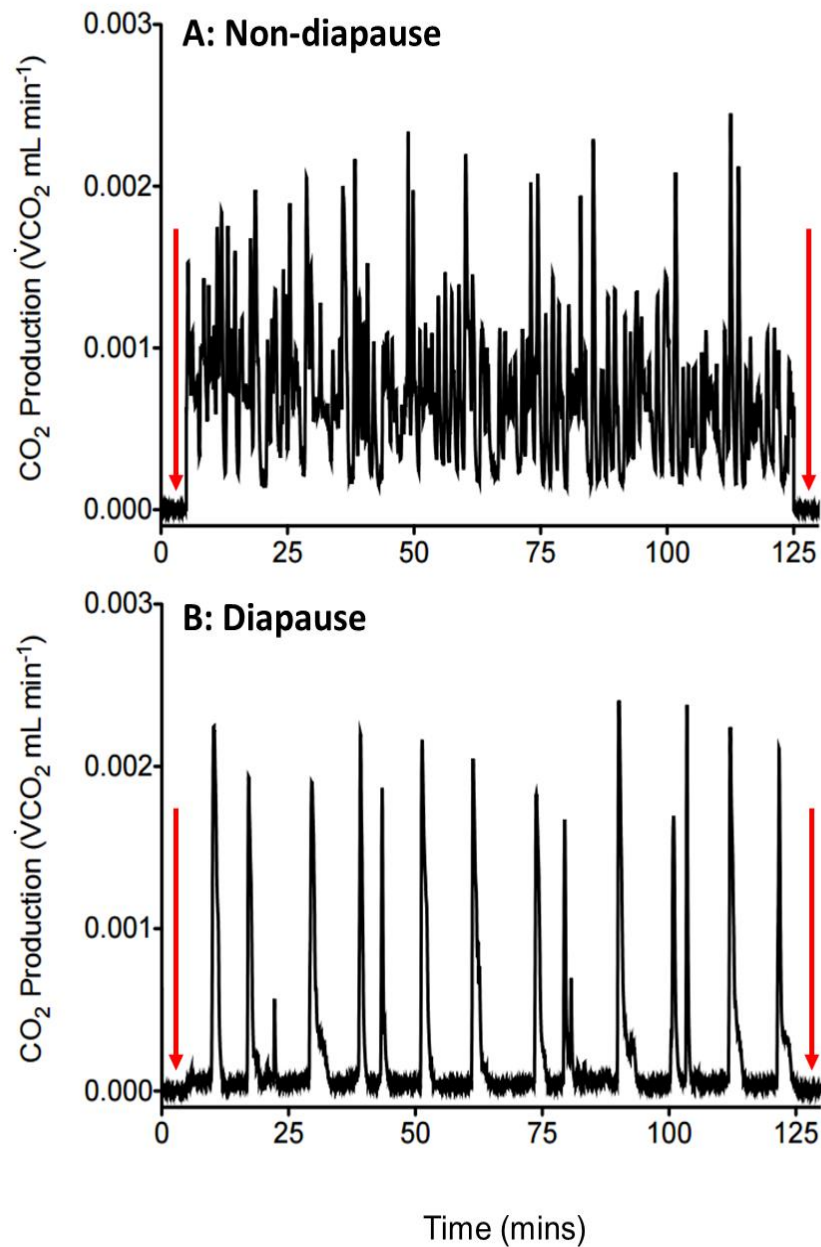


Figure B1. Representative respirometry traces from non-diapausing (A) and diapausing (B) Colorado potato beetles. Rate of CO₂ production in a (A) non-diapausing female (109.16 mg) and a (B) diapausing female (129.70 mg) measured at 15 °C. Non-diapausing beetles show patterns of continuous gas exchange, while diapause beetles show patterns of discontinuous gas exchange. Red arrows indicate baseline measurements taken in the first and last five minutes of the run.

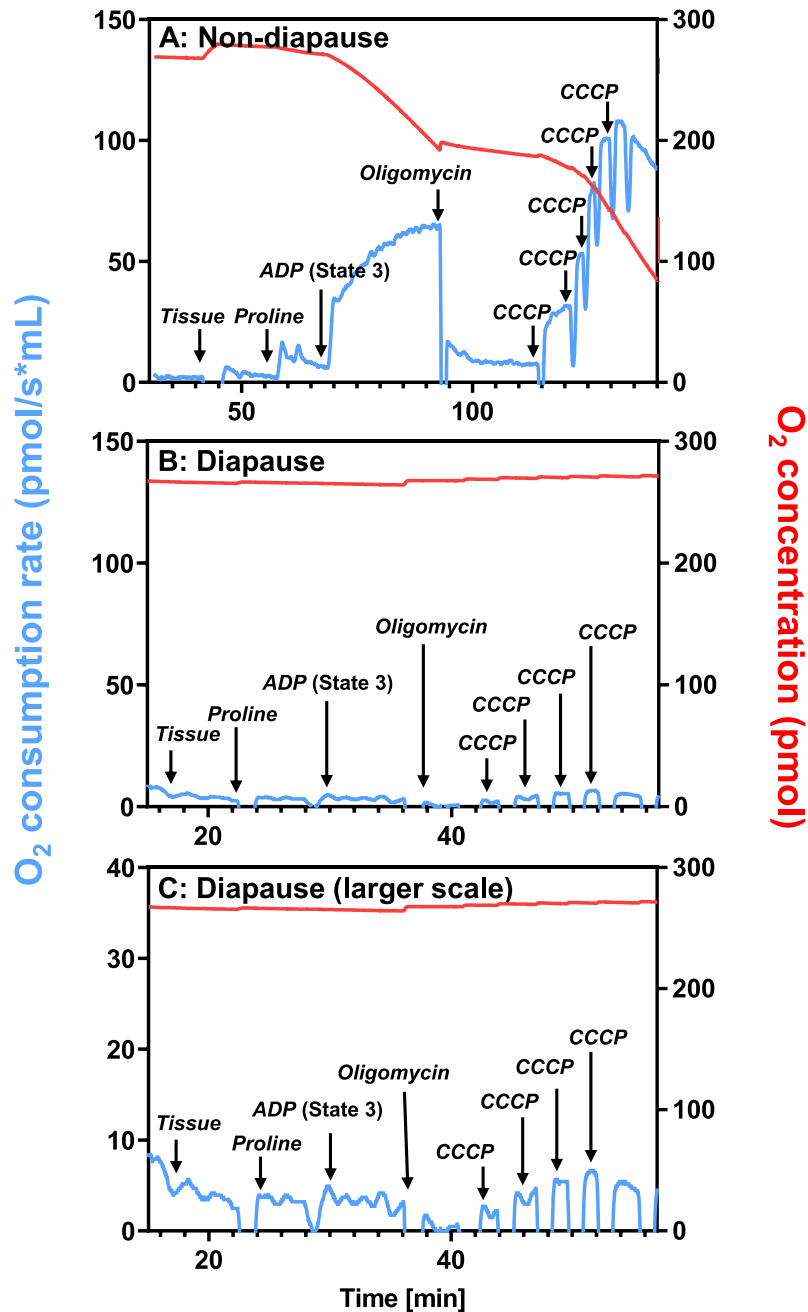


Figure B2. Representative high-resolution respirometry traces from (A) non-diapausing (5.39 mg of tissue) and (B-C) diapausing (2.34 mg of tissue) flight muscle showing O₂ consumption rates (blue line) of permeabilized tissue and O₂ concentrations (red line) in the oxygraph chamber. (B) and (C) are the same trace, (C) is shown with a smaller scale. For details on substrate concentrations and our exact protocols see supplementary methods. First, I added pre-weighed permeabilized tissue into the oxygraph chamber, and waited for rates to stabilize. I then added saturating ADP to stimulate State 3 respiration and waited for those rates to stabilize. Finally, I added oligomycin followed by CCCP to inhibit ATP synthase and uncouple electron transport from ATP synthesis to measure uncoupled

mitochondrial respiration rates. I added CCCP in a step-wise fashion until respiration rates plateaued. These data were collected from two separate runs, therefore the time on the x-axis does not match up.

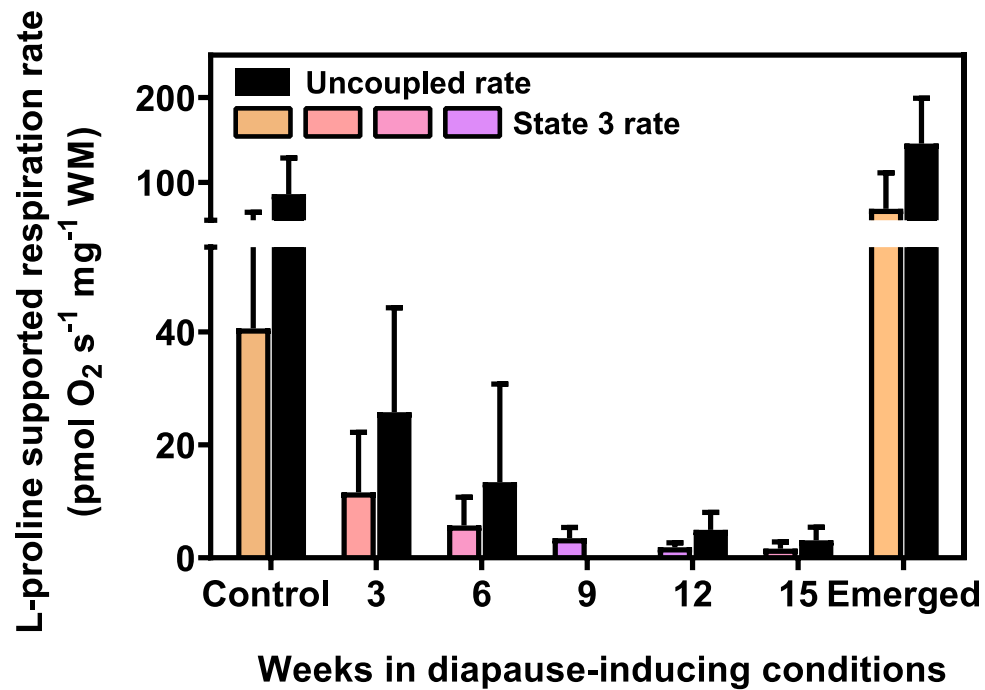


Figure B3.0.3 State 3 (colored bars) and maximal uncoupled (black) mitochondrial respiration rates of Colorado potato beetles entering diapause (3-6), in diapause (9-15), and emerged from diapause. Colored bars are the same values as presented in Figure 1B, and black bars are the maximal uncoupled mitochondrial respiration rates associated with each colored State 3 mitochondrial respiration rate. Data show mean \pm S.D. mitochondrial respiration rates.

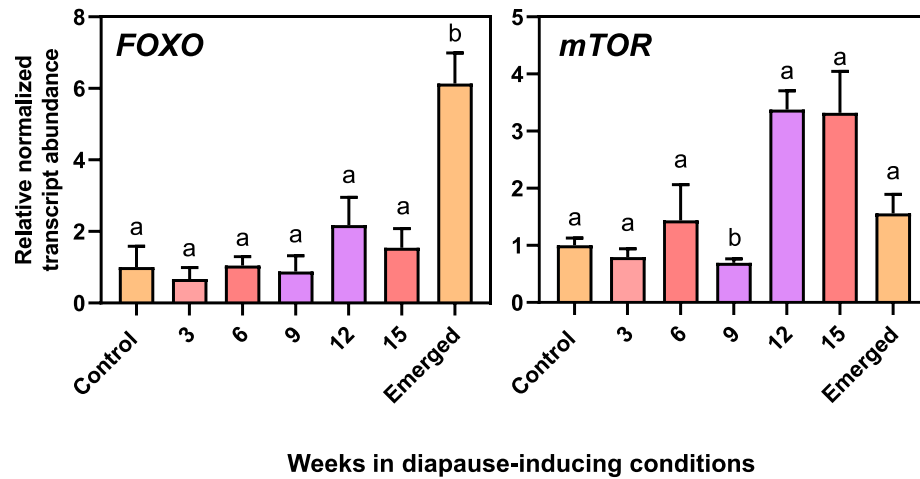
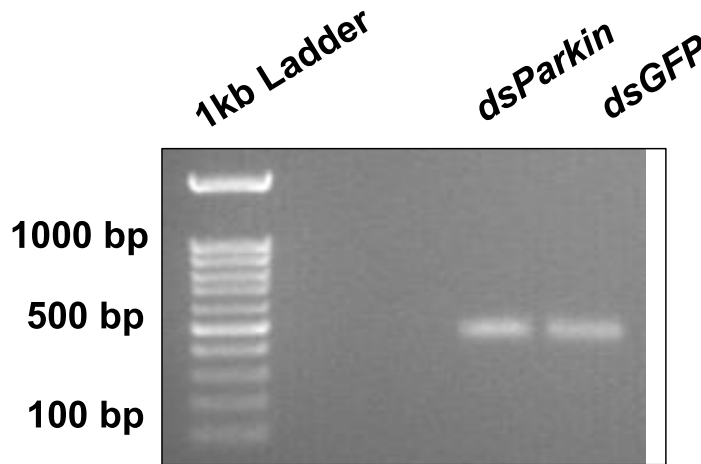


Figure B4. Relative normalized transcript abundance of (A) mTOR and (B) FOXO in flight muscle of control Colorado potato beetles, and beetles exposed to three, six, nine, 12, 15, and 20 weeks of diapause-inducing conditions. Beetles at 20 weeks had emerged from diapause. Expression values are normalized to control values and two reference genes according to the $\Delta\Delta C_t$ method and are plotted as mean \pm S.D. Data were analyzed with a one-way ANOVA and difference letters denote significant differences among treatment groups ($p < 0.05$). Statistics can be found in Table B2.

A: Successful synthesis of *dsParkin* and *dsGFP*



B: Verification of *Parkin* knockdown after 3 days and 5 days post-dsRNA injection

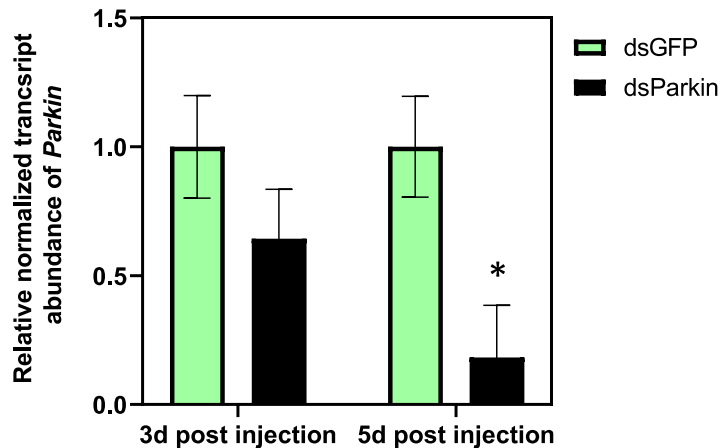


Figure B5. (A) Successful synthesis of parkin and GFP dsRNA products at the expected size of 484 and 411 bp, respectively and (B) verification of *Parkin* transcript knockdown in flight muscle of Colorado potato beetles three- and five-days post-dsRNA injection. I injected beetles exposed to diapause-inducing conditions for seven weeks with 1 μ g of dsRNA complementary to either parking or GFP (n=3/treatment) and compared parkin transcript abundance after three and five days post-injection. Asterisk indicates significant differences between treatments within the same timepoint, statistics can be found in Table B2.

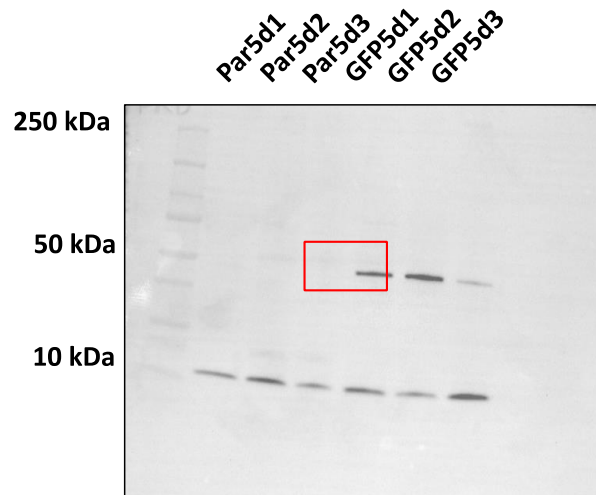


Figure B6. Western blot composite image of colorimetric protein ladder and Parkin protein bands confirming protein knockdown of Parkin in diapausing Colorado potato beetle flight muscle. Each lane contains 20 μ g of protein from flight muscle of the same individuals used for qPCR knockdown verification where the label “Par5d” describes individuals injected with dsParkin (n=3 beetles) and “GFP5d” describes individuals injected with dsGFP (n=3 beetles), and all flight muscle samples were collected 5 days after dsRNA injection; see supplementary data file 1 for qPCR data). The red box outlines lanes displayed in main text Figure 4. There is a non-specific band at ~10 kDa that is stable across all treatment groups.

Appendix C: Chapter 4 Supplementary Material

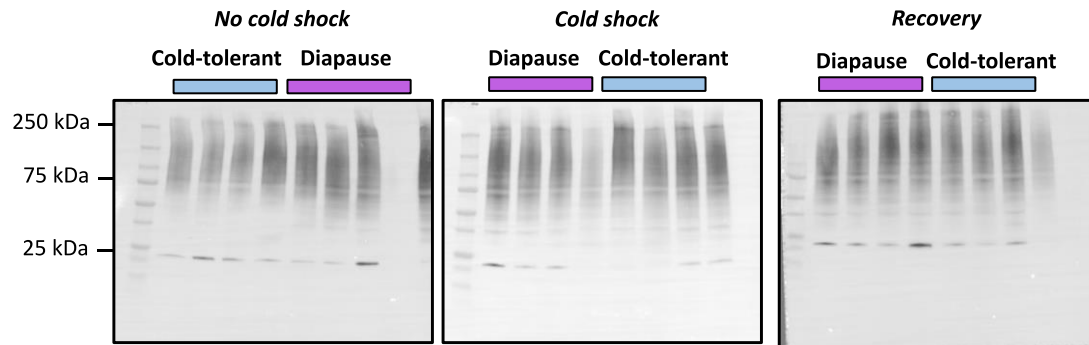


Figure C1. Western blots for data in Figure 4.5. Blots show total protein ubiquitination, with each lane representing fat body from either a diapausing or cold-tolerant CPB.

Curriculum Vitae

Name: Jacqueline Lebenzon

Post-secondary Education and Degrees: The University of Western Ontario
London, Ontario, Canada
2010-2014, BSc (Hons) Biology

The University of Western Ontario
London, Ontario, Canada
2015-2022, PhD Biology

Select Honours and Awards: NSERC Canadian Graduate Scholarship – Master’s, 2016
Company of Biologists JEB Travelling Fellowship, 2017
Province of Ontario Graduate Scholarship, 2017
Canadian Society of Zoologists Helen Battle Award, 2017
NSERC Post Graduate Scholarship – Doctoral, 2018
SICB Best Student Presentation Award, 2019
Entomological Society of Ontario President’s Prize, 2019

Related Work Experience: Biology Instructor
Beat Your Course
2016-2017

Teaching Assistant
The University of Western Ontario
2015-2021

Publications:

- 1) **Lebenzon, J.E.**, Torson, A.S. and Sinclair, B.J. (2021) Diapause differentially modulates the transcriptomes of fat body and flight muscle in the Colorado potato beetle. *Comparative Biochemistry and Physiology D* 40, 100906.
- 2) **Lebenzon, J.E.**, Toxopeus, J., Anthony, S.E. and Sinclair, B.J. (2020) *De novo* assembly and characterization of the Beringian pseudoscorpion transcriptome. *Canadian Entomologist* 153, 301-313
- 3) **Lebenzon, J.E.**, Des Marteaux, L.E. and Sinclair, B.J. (2020) Reversing sodium differentials between the hemolymph and hindgut speeds chill coma recovery, but reduces survival in the fall field cricket, *Gryllus pennsylvanicus*. *Comparative Physiology and Biochemistry A* 244, 110699.

- 4) Karsten, M., **Lebenzon, J.E.**, Sinclair, B.J. and Terblanche, J.S. (2018) Does loss of ion homeostasis explain chill coma and impaired dispersal ability in false codling moth *Thaumatotobia leucotreta* (Lepidoptera: Tortricidae)? *Comparative Biochemistry and Physiology A* 229, 40-44.
- 5) Ferguson, L.V., Dhakal, P., **Lebenzon, J.E.**, Heinrichs, D.E., Bucking, C. and Sinclair, B.J. (2018) Seasonal shifts in the insect gut microbiome are concurrent with changes in cold tolerance and immunity. *Functional Ecology* 32, 2357-2368.
- 6) Toxopeus, J., **Lebenzon, J.E.**, McKinnon, A.H and Sinclair, B.J. (2016) Freeze tolerance of *Cyphoderris monstrosa* (Orthoptera: Prophalangopsidae). *Canadian Entomologist* 148, 668-672.